



**CENTRIFUGAL PUMP DERATING FOR NON-NEWTONIAN SLURRIES: ANALYSIS
OF THE VISCOSITY TO BE USED IN THE HYDRAULIC INSTITUTE METHOD**

by

JEAN-JACQUES NTAMBWE KALOMBO

BSc: Metallurgical Engineering

**Thesis submitted in fulfilment of requirements for the degree
Master of Technology: Chemical Engineering**

in the Faculty of Engineering

at the Cape Peninsula University of Technology

Supervisor: Mr BM Kabamba

**Co-supervisors: Prof. R Haldenwang
Prof. VG Fester**

Cape Town March 13

CPUT Copyright Information

The thesis may not be published either in part (in scholarly, scientific or technical journals), or as a whole (as a monograph), unless permission has been obtained from the university

DECLARATION

I, Jean-Jacques Ntambwe Kalombo, hereby declare that this thesis represents my own work, and that it has not been submitted for academic examination towards any qualification. Furthermore, it represents my own opinions and not necessarily those of the Cape Peninsula University of Technology.

A handwritten signature in black ink, enclosed in a hand-drawn oval. The signature appears to be 'JJN Kalombo' with a stylized flourish extending from the end.

Jean-Jacques Ntambwe Kalombo

Cape Town, April 2012.

ABSTRACT

Centrifugal pumps are the most commonly used pumps in slurry transport systems. The design of pumping systems dealing with liquids more viscous than water requires a reliable method of pump performance prediction for the pump selection. For Newtonian fluids, the Hydraulic Institute method is well established, but there is no generally accepted method for non-Newtonian fluids. Many authors have fallen back on using the Hydraulic Institute method for non-Newtonian fluids. This requires a constant viscosity while non-Newtonian fluid viscosity varies with the shear rate. The question arises: What viscosity should be used in this method for non-Newtonian fluids? Two approaches have been developed: the use of a Bingham plastic viscosity made by Walker and Goulas (1984) and the use of the apparent viscosity calculated using an “equivalent hydraulic pipe” diameter, designed by Pullum *et al.* (2007).

Previous results obtained from these two approaches are not in agreement. Therefore, the aim of this study is to explore a suitable procedure to determine a representative non-Newtonian viscosity to be used in the Hydraulic Institute method to predict the pump performance. To achieve this goal, a set of data was experimentally obtained and the existing data were reused. Test work was conducted using the pump test rig in the Flow Process Research Centre at the Cape Peninsula University of Technology. A Warman 4/3 pump was tested, using four concentrations of kaolin suspension and three concentrations of CMC solution. Five pump speeds were chosen to run these tests: 1200, 1400, 1600, 1800, and 2000 rpm. An additional data set obtained by testing two submersible centrifugal pumps with eight concentrations of sludge, in Stockholm, Sweden, was also analysed. These sets of data were analysed firstly according to the Walker and Goulas (1984) approach and secondly according to the Pullum *et al.* (2007) approach.

The use of the apparent viscosity led to the better pump head prediction. The results of this prediction were close to those obtained in the Pullum *et al.* (2007) work, and even better in some cases. On the other hand, the use of the Bingham plastic viscosity showed better pump efficiency prediction, although the Walker and Goulas (1984) efficiency prediction range was achieved only for one pump out of five. The apparent viscosity reflected the non-Newtonian behaviour but it could not represent alone the non-Newtonian viscosity because of the poor efficiency predictions and the sensitivity of the Pullum *et al.* (2007) approach to a change in viscosity. From the results of this work, it is advisable that the pump performance prediction be done using both apparent and Bingham plastic viscosity, the apparent viscosity for the head prediction and the Bingham plastic viscosity for the efficiency prediction.

DEDICATION

I dedicate this work to:

My God, the Father of my Lord and Saviour, Jesus Christ

My wife, Veronique Ntambwe

My sons, Joel and Samuel Ntambwe

My daughter, Cleda Ntambwe

ACKNOWLEDGEMENTS

I am grateful to:

- Prof. PT Slatter, for the opportunity to be part of the Flow Process Research Centre.
- Mr BM Kabamba, for accepting the responsibility of supervising this work.
- Prof. R Haldenwang, for his supervision, encouragement and sense of responsibility.
- Prof. VG Fester, for her strong assistance, scientific and spiritual support.
- Mr AM Kabwe, for the coaching role played during the completion of this work.
- Mr A Sutherland, for his unfailing support and help.
- All the staff and students of the Flow Process Research Centre for their support and help.

TABLE OF CONTENTS

DECLARATION.....	ii
ABSTRACT	iii
DEDICATION	iv
ACKNOWLEDGEMENTS.....	v
TABLE OF CONTENTS	vi
LIST OF FIGURES.....	x
LIST OF TABLES	xiv
NOMENCLATURE	xv
TERMS AND CONCEPTS CITED.....	xvii
CLARIFICATIONS.....	xvii
Chapter 1 INTRODUCTION.....	1
1.1 BACKGROUND TO THE PROBLEM	1
1.2 STATEMENT OF RESEARCH PROBLEM.....	2
1.3 RESEARCH QUESTION.....	2
1.4 AIM AND OBJECTIVES OF THE STUDY	3
1.5 RESEARCH DESIGN AND METHODOLOGY.....	3
1.6 DELINEATION OF THE STUDY.....	4
1.7 SIGNIFICANCE OF STUDY	4
Chapter 2 THEORY AND LITERATURE REVIEW	5
2.1 INTRODUCTION.....	5
2.2 BASIC CONCEPTS OF FLUID MECHANICS.....	5
2.2.1 Fluid definition	5
2.2.2 Fluid properties.....	5
2.2.3 Viscosity	6
2.2.4 Viscosity calculation	7
2.2.5 Basic equations of fluid motion	8
2.3 RHEOLOGY	9
2.3.1 Introduction.....	9
2.3.2 Newton relationship.....	10
2.3.3 Newtonian fluids	11
2.3.4 Non-Newtonian fluids	11
2.3.5 Time-independent fluid behaviour.....	11
2.3.6 Rheological model of non-Newtonian fluids	12

2.3.7 Choice of rheological model	13
2.3.8 Generalised model	13
2.4 FLOW IN STRAIGHT PIPE	17
2.4.1 Flow regimes and Reynolds number.....	17
2.4.2 Laminar to turbulent transition	17
2.4.3 The shear stress distribution.....	18
2.4.4 Head lost to friction in a pipe	20
2.4.5 Friction factor.....	20
2.4.6 The laminar flow of non-Newtonian fluids	23
2.5 RHEOMETRY OF NON-NEWTONIAN FLUIDS	26
2.5.1 Introduction.....	26
2.5.2 Rotational viscometers	26
2.5.3 Tube viscometers	26
2.5.4 The Rabinowitsch-Mooney relation.....	27
2.5.5 Rheological characterisation.....	27
2.6 OVERVIEW OF PUMPS	28
2.6.1 Introduction.....	28
2.6.2 Centrifugal pump description	29
2.6.3 Working mechanism	30
2.6.4 Theoretical study of a centrifugal pump	31
2.6.5 Flow through the centrifugal pump.....	31
2.6.6 Centrifugal pump performance	34
2.7 CENTRIFUGAL PUMP DERATING.....	36
2.7.1 Pump derating for Newtonian fluid: Hydraulic Institute Method	38
2.7.2 The use of Hydraulic Institute method for non-Newtonian fluids.....	41
2.8 PREVIOUS WORKS AND RESEARCH ASPECTS IDENTIFIED	42
2.8.1 Works using the Walker and Goulas (1984) approach.....	43
2.8.2 Work published using the Pullum <i>et al.</i> (2007) approach	45
2.8.3 Research aspects identified.....	47
2.9 CONCLUSION	47
Chapter 3 EQUIPMENT AND EXPERIMENTAL METHOD	48
3.1 INTRODUCTION.....	48
3.2 EXPERIMENTAL RIG DESCRIPTION AND INSTRUMENTATION	48
3.2.1 Mixing tank	50
3.2.2 Pump test bay	51
3.2.3 Tube viscometer	53

3.2.4 Data acquisition system.....	56
3.2.5 Other apparatus	56
3.3 EXPERIMENTAL PROCEDURES.....	58
3.3.1 Calibration of the instruments	58
3.3.2 Pressure gradient test	62
3.3.3 Pump performance test	63
3.4 MATERIALS TESTED	64
3.4.1 Water.....	64
3.4.2 Kaolin suspension	65
3.4.3 CMC solution.....	65
3.5 EXPERIMENTAL ERRORS.....	65
3.5.1 Error theory	65
3.5.2 Evaluation of errors	67
3.5.3 Errors in measured variables	68
3.5.4 Error of derived variables.....	69
3.5.5 Numerical application of errors	74
3.6 CONCLUSION	77
Chapter 4 PRESENTATION AND ANALYSIS OF RESULTS.....	78
4.1 INTRODUCTION.....	78
4.2 WATER TEST RESULTS.....	78
4.2.1 Water pressure drop test results.....	78
4.2.2 Centrifugal pump performance test results for water.....	79
4.3 FLOW CURVES AND RHEOLOGICAL CHARACTERISATION	81
4.3.1 Pseudo-shear diagrams	81
4.3.2 Rheological characterisation.....	82
4.4 PUMP PERFORMANCE TEST RESULTS	84
4.5 WALKER & GOULAS (1984) APPROACH	87
4.5.1 Bingham plastic viscosity determination	87
4.5.2 Pump performance prediction using the Walker and Goulas (1984) approach.....	90
4.6 PULLUM <i>et al.</i> (2007) APPROACH.....	94
4.6.1 Characteristic dimension w	94
4.6.2 Predicted pump performance	95
4.7 ANALYSIS OF KABAMBA'S (2006) DATA	98
4.7.1 Rheological characterisation.....	98
4.7.2 Pump prediction according to the Walker and Goulas (1984) approach.....	99
4.7.3 Pump prediction using the Pullum <i>et al.</i> (2007) approach	102

4.8 ANALYSIS OF SLUDGE DATA.....	105
4.8.1 Sludge rheology	105
4.8.2 Walker and Goulas (1984) approach	107
4.8.3 Pullum <i>et al.</i> (2007) approach.....	109
4.9 WALKER and GOULAS (1984) APPROACH AND PULLUM <i>et al.</i> (2007) APPROACH COMPARISON.....	110
4.10 CONCLUSIONS.....	111
Chapter 5 DISCUSSION OF RESULTS.....	113
5.1 INTRODUCTION.....	113
5.2 SUMMARY OF NON-NEWTONIAN PUMP DERATION.....	113
5.3 EXPERIMENTAL TEST RIG, EQUIPMENT AND PROCEDURE.....	114
5.4 FLUIDS TESTED	115
5.4.1 Water.....	115
5.4.2 Kaolin	115
5.4.3 CMC.....	116
5.5 HYDRAULIC INSTITUTE METHOD	116
5.5.1 Walker and Goulas (1984) approach	116
5.5.2 Pullum <i>et al.</i> (2007) approach.....	117
5.5.3 Walker and Goulas (1984) approach versus Pullum <i>et al.</i> (2007) approach	118
5.6 ANALYSIS OF VISCOSITY	126
5.6.1 Bingham plastic viscosity versus apparent viscosity	126
5.6.2 Sensitivity of the prediction procedures to a change in viscosity	126
5.7 CONCLUSIONS.....	130
Chapter 6 CONCLUSIONS AND RECOMMENDATIONS.....	131
6.1 INTRODUCTION.....	131
6.2 SUMMARY	131
6.3 CONCLUSIONS	133
6.4 CONTRIBUTIONS.....	133
6.5 RECOMMENDATIONS	134
REFERENCES.....	135
APPENDICES.....	139

LIST OF FIGURES

Figure 2.1: Schematic representation of unidirectional shearing flow (Chhabra & Richardson, 1999)	6
Figure 2.2: Rheogram of Newtonian fluid (Chhabra & Richardson, 1999)	10
Figure 2.3: Pseudoplastic and viscoplastic behaviour (Chhabra & Richardson, 1999)	12
Figure 2.4: Summary of non-Newtonian rheograms (Paterson & Cooke, 1999)	16
Figure 2.5: Stress distribution in horizontal straight pipe (Chhabra & Richardson, 1999)	18
Figure 2.6: Shear stress acting in opposite of flow direction (Slatter, 1994)	19
Figure 2.7: Distribution of shear stress across the pipe cross-section (Chhabra & Richardson, 1999)	19
Figure 2.8: Moody diagram (Munson <i>et al.</i> , 2010).....	22
Figure 2.9: Non-Newtonian shear stress distribution in pipe (Slatter, 1994)	24
Figure 2.10: Illustration of a pseudo-shear diagram for different pipe diameter (Slatter, 1994)..	28
Figure 2.11: Components of centrifugal pump (Perez, 2008).	29
Figure 2.12: Velocity diagrams at the inlet and exit of a centrifugal pump impeller (Munson <i>et al.</i> , 2010)	34
Figure 2.13: Pump performance curve for a single angular speed (Sahdev, 2007)	35
Figure 2.14: Typical published centrifugal pump performance curves (Warman Africa, curve book No. 1564)	36
Figure 2.15: Effect of concentration on the pump performance (Angel & Crisswell, 1997).....	37
Figure 2.16: Hydraulic Institute Chart (Hydraulic Institute, 1983).....	40
Figure 2.17: Experimental HR against calculated values from HI Chart (Walker & Goulas, 1984)	43
Figure 2.18: Experimental ER against calculated values from HI Chart (Walker & Goulas, 1984)	44
Figure 2.19: Calculated head versus experimental head for Warman 4/3 pump (Pullum <i>et al.</i> , 2007)	45
Figure 2.20: Calculated head versus experimental head for GIW 4/3 pump (Pullum <i>et al.</i> , 2007)	46
Figure 2.21: Comparison between the predicted and experimental pump efficiency for the Sery <i>et al.</i> 17% kaolin slurry (Pullum <i>et al.</i> , 2011)	46
Figure 3.1: Layout of the pump test rig (top view of the rig).....	49
Figure 3.2: Mixing tank.....	50
Figure 3.3: Warman 4/3 centrifugal pump	52

Figure 3.4: Point Pressure Transducer (PPT)	53
Figure 3.5: Differential Pressure Transducers (DPTs).....	55
Figure 3.6: Magnetic flow meters	55
Figure 3.7: Hand-Held Communicator (HHC).....	57
Figure 3.8: Tachometer.....	58
Figure 3.9: Calibration graph for the low DPT	59
Figure 3.10: Calibration graph for the high DPT	60
Figure 3.11: Calibration graph for the PPT at the pump outlet.....	60
Figure 3.12: Calibration graph for the PPT at the pump inlet.....	61
Figure 3.13: Example of water pressure gradient test result compared with Colebrook-White curve.....	62
Figure 3.14: Example of pseudo-shear diagram for kaolin 24%	63
Figure 3.15: Example of pump performance results for the Warman 4/3 pump at 1600 rpm	64
Figure 4.1: Water test in 80 mm straight pipe.....	78
Figure 4.2: Water test in 60 mm straight pipe.....	79
Figure 4.3: Warman 4/3 comparison of water test and catalogue curves for the head.....	80
Figure 4.4: Warman 4/3 comparison of water test and catalogue curves for the efficiency.....	80
Figure 4.5: Summary of pseudo-shear diagrams	81
Figure 4.6: Rheograms for kaolin 21%, 24%, 28% and 30%	82
Figure 4.7: Rheograms for CMC 5%, 8% and 9%	83
Figure 4.8: Head curve for the Warman 4/3 pump handling kaolin at 1400 rpm	84
Figure 4.9: Efficiency curve for the Warman 4/3 pump handling kaolin at 1400 rpm.....	85
Figure 4.10: Power curve for the Warman 4/3 pump handling kaolin at 1400 rpm.....	85
Figure 4.11: Head curve for the Warman 4/3 pump handling CMC at 1800 rpm	86
Figure 4.12: Efficiency curve for the Warman 4/3 pump handling CMC at 1800 rpm.....	86
Figure 4.13: Power curve for the Warman 4/3 pump handling CMC at 1900 rpm.....	87
Figure 4.14: Bingham plastic model fitted to kaolin 21, 24, 28, 30% data.....	88
Figure 4.15: Bingham plastic model fitted to CMC 5% data.....	88
Figure 4.16: Bingham plastic model fitted to CMC 8% data.....	89
Figure 4.17: Bingham plastic model fitted to CMC 9% data.....	89
Figure 4.18: Pump performance prediction for the Warman 4/3 handling CMC, using the Walker and Goulas (1984) approach	91
Figure 4.19: Pump performance prediction for the Warman 4/3 handling kaolin, using the Walker and Goulas (1984) approach	92
Figure 4.20: Calculated head versus experimental head for the Walker and Goulas (1984) approach.....	93

Figure 4.21: Calculated efficiency versus experimental efficiency for the Walker and Goulas (1984) approach	94
Figure 4.22: Pump performance prediction for the Warman 4/3 handling CMC, using the Pullum <i>et al.</i> (2007) approach.....	95
Figure 4.23: Pump performance prediction for the Warman 4/3 handling kaolin, using the Pullum <i>et al.</i> (2007) approach.....	96
Figure 4.24: Calculated head versus experimental head for the Pullum <i>et al.</i> (2007) approach.	97
Figure 4.25: Calculated efficiency versus experimental efficiency for the Pullum <i>et al.</i> (2007) approach.....	98
Figure 4.26: Experimental head versus calculated head for the GIW 4/3 using the Walker and Goulas (1984) approach	99
Figure 4.27: Experimental efficiency versus calculated efficiency for the GIW 4/3 using the Walker and Goulas (1984) approach	100
Figure 4.28: Experimental head versus calculated head for the Warman 6/4 using the Walker and Goulas (1984) approach	101
Figure 4.29: Experimental efficiency versus calculated efficiency for the Warman 6/4 using the Walker and Goulas (1984) approach	101
Figure 4.30: Experimental head versus calculated head for the GIW 4/3 in the Pullum <i>et al.</i> (2007) approach	102
Figure 4.31: Experimental efficiency versus calculated efficiency for the GIW 4/3 in the Pullum <i>et al.</i> (2007) approach.....	103
Figure 4.32: Experimental head versus calculated head for the Warman 6/4 in the Pullum <i>et al.</i> (2007) approach	104
Figure 4.33: Experimental efficiency versus calculated efficiency for the Warman 6/4 in the Pullum <i>et al.</i> (2007) approach	104
Figure 4.34: Pseudoplastic model fitted to sludge rheograms	105
Figure 4.35: Bingham plastic model fitted to sludge rheograms	106
Figure 4.36: Yield pseudoplastic model fitted to sludge rheograms.....	106
Figure 4.37: Experimental head (efficiency) versus calculated head (efficiency) for the 135 mm impeller in the Walker and Goulas (1984) approach.....	108
Figure 4.38: Experimental head (efficiency) versus calculated head (efficiency) for the 152 mm impeller in the Walker and Goulas (1984) approach.....	108
Figure 4.39: Experimental head (efficiency) versus calculated head (efficiency) for the 135 mm impeller in the Pullum <i>et al.</i> (2007) approach	109
Figure 4.40: Experimental head (efficiency) versus calculated head (efficiency) for the 152 mm impeller in the Pullum <i>et al.</i> (2007) approach	110

Figure 5.1: Comparison between the results obtained using $w = 0.059$ and $w = 0.023$ for the pump head prediction	117
Figure 5.2: Comparison between the results obtained using $w = 0.084$ and using $w = 0.085$..	118
Figure 5.3: Comparison between Pullum <i>et al.</i> (2007) approach and Walker and Goulas (1984) approach results for the data obtained in this work	120
Figure 5.4: Comparison between Pullum <i>et al.</i> (2007) approach and Walker and Goulas (1984) approach results obtained using existing data for the GIW 4/3 pump.....	121
Figure 5.5: Comparison between Pullum <i>et al.</i> (2007) approach and Walker and Goulas (1984) approach results obtained using existing data for the Warman 6/4 pump.....	122
Figure 5.6: Comparison between Pullum <i>et al.</i> (2007) approach and Walker and Goulas (1984) approach results obtained using submersible centrifugal pump with 135 mm diameter impeller	123
Figure 5.7: Comparison between Pullum <i>et al.</i> (2007) approach and Walker and Goulas (1984) approach results obtained using submersible centrifugal pump with 152 mm diameter impeller	124
Figure 5.8: Sensitivity of the pump performance prediction procedures to a change in viscosity for the Warman 4/3 pump	127
Figure 5.9: Sensitivity of the pump performance prediction procedures to a change in viscosity for the GIW 4/3 pump.....	127
Figure 5.10: Sensitivity of the pump performance prediction procedures to a change in viscosity for the Warman 6/4 pump	128
Figure 5.11: Sensitivity of the pump performance prediction procedures to a change in viscosity for the 135 mm impeller submersible pump	128
Figure 5.12: Sensitivity of the pump performance prediction procedures to a change in viscosity for the 152 mm impeller submersible pump	129

LIST OF TABLES

Table 2.1: Rheological models (Chhabra & Richardson, 1999)	13
Table 2.2: Different models described by the yield pseudoplastic equation	15
Table 3.1: Characteristics of the Warman 4/3 pump (Warman Africa)	51
Table 3.2: Warman 4/3 suction and discharge pipe cross-section relative error	74
Table 3.3: Warman 4/3 suction and discharge pipe cross-section relative error	75
Table 3.4: Errors of computed variables for the Warman 4/3 pump at 1200 rpm	75
Table 3.5: Errors of computed variables for the Warman 4/3 pump at 1400 rpm	76
Table 3.6: Errors of computed variables for the Warman 4/3 pump at 1600 rpm	76
Table 3.7: Errors of computed variables for the Warman 4/3 pump at 1800 rpm	76
Table 3.8: Errors of computed variables for the Warman 4/3 pump at 2000 rpm	77
Table 4.1: Kaolin rheological parameters	83
Table 4.2: CMC rheological parameters	84
Table 4.3: Rheological parameters using the Bingham plastic model	90
Table 4.4: Rheological parameters from Kabamba (2006) data	99
Table 4.5: Rheological parameters of the sludges.	107
Table 4.6: Summary of pump prediction results	111
Table 4.7: Values of characteristic dimension w for different data analysed	111
Table 5.1: Summary of pump deration works using non-Newtonian slurries.	114
Table 5.3: Summary of the results of Walker and Goulas (1984) and Pullum <i>et al.</i> (2007) approaches comparison	125
Table 5.4: Summary of the pump performance prediction procedures sensitivity to a change in viscosity	129
Table 6.1: Summary of the non-Newtonian pump deration results	132

NOMENCLATURE

Symbol	Description	Unit
A	Cross sectional area	m ²
A	True value of a quantity	-
C _H	Head correction factor	-
C _Q	Capacity correction factor	-
C _η	Efficiency correction factor	-
D	Internal pipe diameter	m
dy	Distance between two parallel planes	m
E _R	Efficiency ratio	-
F	Applied shear force	N
F _I	Inertia forces	N
F _V	Viscous forces	N
f	Friction factor	-
g	Gravitational acceleration	m/s ²
H	Head	m
H _R	Head ratio	-
K	Fluid consistency index	Pa.s ⁿ
k	Internal pipe hydraulic roughness	m
L	Pipe length	m
N	Speed of the shaft	rpm.
N	Number of measurements	-
n	Flow behaviour index	-
n'	Slope of logarithmic plot	-
p	Static pressure	Pa
P	Power	w
Q	Volumetric flow rate	m ³ /s
R	Radius	m
R ²	Correlation coefficient	-
r	Radius from the centre line	m
Re	Reynolds number	-
T	Torque on the shaft	N m
U	Impeller blade linear velocity	m/s

V	Velocity	m/s
w	Characteristic dimension	-
W	Relative velocity within blade passage	m/s
X	Single measurement of a quantity	
\bar{X}	Average of all measurements for the same quantity	
Z	Elevation from datum	m

Greek symbols

Δa	Absolute error	-
Δh_f	Friction head loss	m
ΔH_p	Pump head input	m
Δp	Pressure drop	Pa
ΔR^2	Rate of variation of R^2	-
$\% \Delta v$	Percentage of the viscosity variation implemented	-
$\dot{\gamma}$	Shear rate	s^{-1}
η	Pump efficiency	%
μ	Fluid dynamic viscosity	Pa.s
μ_a	Apparent viscosity	Pa.s
μ_{pl}	Bingham plastic viscosity	Pa.s
μ_o	Zero shear viscosity	Pa.s
μ_∞	Infinite shear viscosity	Pa.s
ν	Fluid kinematic viscosity	m^2/s
ρ	Fluid density	kg/m^3
σ	Standard deviation	-
τ	Shear stress	Pa
τ_o	Wall shear stress	Pa
τ_y	Yield stress	Pa
τ_{rz}	Shear stress on the surface of the cylindrical element	Pa
ω	Angular velocity	rad/s

TERMS AND CONCEPTS CITED

BEP	Best efficiency point
CMC	Carboxyl methyl cellulose
DPT	Differential pressure transducer
HHC	Hand-held communicator
HI	Hydraulic Institute
PPT	Point pressure transducer
RD	Relative density
RPM	Rotation per minute
TDH	Total dynamic head
FPRC	Flow Process Research Centre

CLARIFICATIONS

1. Walker and Goulas (1984) approach: The approach using the Bingham plastic viscosity in the Hydraulic Institute method.
2. Pullum *et al.* (2007) approach: The approach using the apparent viscosity calculated using an equivalent hydraulic pipe diameter in the Hydraulic Institute method.
3. For a fluid modelled as Bingham plastic, the Bingham plastic viscosity μ_{pl} is equal to the fluid consistency index K.

Chapter 1 INTRODUCTION

1.1 BACKGROUND TO THE PROBLEM

Centrifugal pumps are selected based on the pump performance curves provided by pump manufacturers (Pullum *et al.*, 2007). These curves are always established experimentally by actual measurement, with water as the reference test liquid (Abulnaga, 2002).

Viscous liquids cause more hydraulic losses in the pump than water (Roco *et al.*, 1986). At greater viscosities, the head and efficiency decrease while the required power increases (Angel & Crisswell, 1997). This alteration of the pump performance is evaluated in comparison with the clear water pump performance curves (Gandhi *et al.*, 2000). It is very important that the hydraulic design of a pipeline for non-Newtonian slurry should be carried out taking into account the reduction of pump performance (Engin & Gur, 2003).

For Newtonian fluids, the Hydraulics Institute (HI) method is exclusively used to predict the centrifugal pump performance (Pullum *et al.*, 2007).

Walker and Goulas (1984) were the first to use the HI method with non-Newtonian fluids. They have used the Bingham plastic viscosity in the HI chart to predict non-Newtonian pump performance. An agreement with $\pm 5\%$ error margin between test data and calculation was obtained.

Pullum *et al.* (2007) stated that the use of the Bingham plastic viscosity has no rheologically-based meaning (though it approximates the high shear rate viscosity). Considering that the pump's rotational speed and the system curve are dictating the flow from which the viscosity can be approximated, Pullum *et al.* (2007) used a totally different approach. They considered that, for most of the flow rates of materials with an appreciable viscosity, the flow regime in the rotor passage is laminar. Therefore, they assumed that the flow throughout the pump is laminar through a conduit called an "equivalent hydraulic pipe". The "equivalent hydraulic pipe" diameter is determined experimentally for each pump used. The flow rate of interest is then used to determine the shear rate at the wall of this pipe from which a viscosity can be determined and applied using the HI method.

Walker and Goulas (1984), Sery and Slatter (2002), Kabamba (2006) and Pullum *et al.* (2007) have used the HI method to correct the viscosity of non-Newtonian materials. In each case, results obtained are still not in agreement.

In this study the emphasis is on the determination of the non-Newtonian viscosity to be used in the HI method. This viscosity can be either the “Bingham plastic viscosity” or the apparent viscosity obtained using the “equivalent hydraulic pipe” diameter.

Non-Newtonian fluids such as kaolin suspensions and CMC solutions were tested to obtain a new data set. Two additional data sets were available: Kabamba (2006) data and submersible centrifugal pump data obtained from testing different concentrations of sludge in Sweden (Haldenwang *et al.*, 2010).

These data were analysed using both approaches. Results from these analyses were compared, and recommendations made.

1.2 STATEMENT OF RESEARCH PROBLEM

The HI method is designed to correct the pump deration for Newtonian fluids (i.e. fluids with constant viscosities). For non-Newtonian fluids the viscosity varies with local shear rate (Pullum *et al.*, 2007). Therefore, to use the HI method for non-Newtonian pump deration requires a viscosity representing the variable non-Newtonian viscosities in the range of the flow rates of interest. Therefore, there is a need to establish a suitable representative viscosity to be used in the HI method to predict the pump performance for non-Newtonian fluids (Pullum *et al.*, 2007). Two approaches have been developed: the first uses the Bingham plastic viscosity in the HI chart while the other uses an apparent viscosity, determined using the equivalent hydraulic pipe diameter, in the HI method.

1.3 RESEARCH QUESTION

Which of the two methods, namely, a) the HI method using a Bingham plastic viscosity (Walker & Goulas, 1984) or b) the HI method using the apparent viscosity obtained from the equivalent hydraulic pipe diameter (Pullum *et al.*, 2007), best predicts the centrifugal pump performance?

1.4 AIM AND OBJECTIVES OF THE STUDY

The aim of this work was to evaluate the procedure to determine a representative non-Newtonian viscosity to be used in the HI method for the pump performance prediction. The objectives of this project are to

- obtain new sets of experimental data for centrifugal pumps handling non-Newtonian fluids, and
- analyse all available datasets (new and existing) using both Walker and Goulas (1984) and Pullum *et al.* (2007) approaches.

1.5 RESEARCH DESIGN AND METHODOLOGY

The test work was conducted in the Flow Process Research Centre laboratory at the Cape Peninsula University of Technology. The test rig encompasses two loops of pipes with inner diameters of 60 mm and 80 mm respectively. A centrifugal pump was used at various speeds to move slurries throughout the rig. Measuring devices such as pressure transducers, magnetic flow meters and torque transducers were used for the reliable collection of pump and pressure drop test data.

Kaolin suspensions and CMC solutions were tested at various concentrations.

Procedures:

- The centrifugal pump was tested at various speeds (1200, 1400, 1600, 1800, and 2000 rpm).
- The flow rates were regulated at constant speed, using a control valve.
- Rheological tests were carried out and plastic viscosities calculated for each material used.
- Bingham plastic viscosity was used in the HI method to predict pump performance.
- The equivalent hydraulic pipe diameter was calculated and the related apparent viscosity was determined.
- The viscosity from the equivalent pipe diameter was used in the HI method for the prediction of the pump performance.
- Results from the two predictions were compared and the conclusion drawn.

In addition, the same procedure was applied to a set of data obtained in Sweden by testing a submersible centrifugal pump with eight concentrations of sludge and two impellers of different diameters (135 mm and 152 mm).

1.6 DELINEATION OF THE STUDY

This study is limited to water and time-independent non-Newtonian fluids being pumped by two types of centrifugal pumps: slurry centrifugal pumps and submersible centrifugal pumps. Larger slurry centrifugal pumps (for which the flow is only a very weak function of the fluid viscosity and the head deration tends to zero) are not considered in this project.

1.7 SIGNIFICANCE OF STUDY

The Mining and minerals industries are now required to operate at higher concentrations, to minimise water consumption. Hence, the resulting slurries are more viscous than water. Most of these materials behave as non-Newtonian fluids (Sellgren *et al.*, 1999). The choice of the best conditions for using a particular centrifugal pump remains a significant practical engineering design and operational challenge. To facilitate this process, we need to accurately predict the pump performance which depends on the viscous properties of the material to be pumped.

This project presents more data and contributes to the evaluation of the two existing non-Newtonian derating procedures.

Chapter 2 THEORY AND LITERATURE REVIEW

2.1 INTRODUCTION

In this chapter, basic concepts of fluid mechanics are reviewed. Important aspects of rheology and the choice of rheological model are discussed. The rheological characterisation is explained. Theoretical concepts related to the centrifugal slurry pump as well as existing methods of centrifugal slurry pump derating are presented. Previous works are reviewed and the research problem identified.

2.2 BASIC CONCEPTS OF FLUID MECHANICS

2.2.1 Fluid definition

A fluid is a physical material which may flow. This means that the constituent elements can continuously change their positions relative to one another when the fluid is subjected to a shear force. Therefore, it offers no lasting resistance to the movement of one layer over another. No shear force is present in the fluid at rest (Massey & Ward-Smith, 1998).

Two types of fluid are distinguished: gases and liquids. This project will deal only with liquids.

2.2.2 Fluid properties

In this project, liquids will be considered as composed of a continuous distribution of matter, with no empty space, called continuum (Massey & Ward-Smith, 1998). Thus, the complete behaviour of a fluid that is accounting for the action of each individual molecule will be avoided (Streeter & Wylie, 1985). Fluids are characterised by a number of properties; the most important of them are given below.

2.2.2.1 Mean and relative density

The fluid mean density is defined as the ratio of the mass of a given quantity of matter to the volume occupied by this quantity of matter. The mean density of water at 4° C is 1000 kg/m³; therefore, water is regarded as a reference fluid.

The relative density of a substance (solid or liquid) is the ratio of its mean density to that of water at 4° C (Massey & Ward-Smith, 1998).

2.2.2.2 Pressure

Pressure of a fluid is the force exerted by the fluid on the inner wall of its container, resulting from all particle collisions and the particle/wall collisions. It can be also considered as the force exerted by the wall of the container on the liquid (Massey & Ward-Smith, 1998).

2.2.3 Viscosity

Under particular conditions, one fluid is described as more viscous than another when it offers greater resistance to flow than the other. This resistance to the displacement of one layer of fluid over an adjacent one is offered only while the movement is taking place and is ascribed to the viscosity of the fluid (Massey & Ward-Smith 1998). Therefore, viscosity is defined as the property which causes a fluid to offer resistance to shear (Streeter & Wylie, 1985).

The viscosity of water at room temperature (20° C) is about 0.001 Pa.s or 1 centipoise.

2.2.3.1 Dynamic viscosity

Consider a thin layer of a liquid held by two parallel planes at a distance dy from each other, as shown in Figure 2.1. If under steady conditions, the liquid undergoes a shear caused by a force F as shown; this will be compensated by a resisting force of the same magnitude and opposite direction to F , acting inside the liquid (Chhabra & Richardson, 1999).

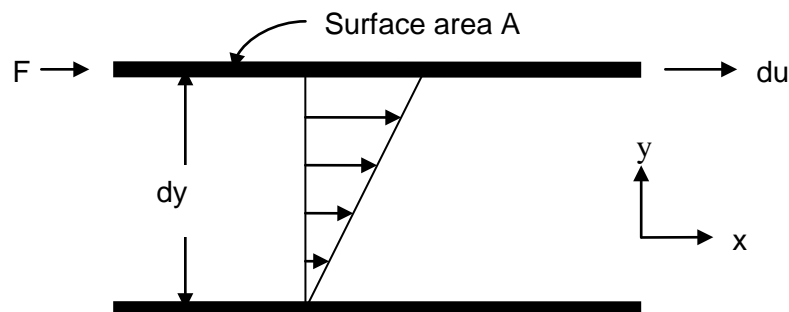


Figure 2.1: Schematic representation of unidirectional shearing flow (Chhabra & Richardson, 1999)

According to Newtonian hypothesis, the resulting shear stress ($\tau = \frac{F}{A}$) is related to the shear rate ($\dot{\gamma} = \frac{du}{dy}$) by simple proportionality stated as follows:

$$\tau = \mu \left(- \frac{du}{dy} \right). \quad \text{Equation 2.1}$$

The coefficient of proportionality μ is known as the dynamic viscosity. By definition, μ depends only on the nature of fluid, temperature and pressure.

The negative sign in Equation 2.1 shows that the shear stress acts in the opposite direction of the motion, i.e., it indicates that the momentum transfer occurs in the direction of decreasing velocity.

When the plot of shear stress against shear rate (called “flow curve” or “rheogram”) of a material is a straight line passing through the origin, the material is said to be Newtonian. The dynamic viscosity μ is the slope (gradient) of this straight line.

When the relationship is non-linear or a straight line which does not pass through the origin, the material is considered to be non-Newtonian.

2.2.3.2 Kinematic viscosity

The kinematic viscosity is the ratio of dynamic viscosity to the density of the fluid. It is given mathematically by the relationship:

$$\nu = \frac{\mu}{\rho}. \quad \text{Equation 2.2}$$

At 20.2° C the kinematic viscosity of water is 1 mm²/s (Massey & Ward-Smith 1998).

2.2.4 Viscosity calculation

For non-Newtonian fluids, a number of different viscosities can be calculated for any particular shear rate value.

2.2.4.1 Apparent viscosity μ_a

The apparent viscosity is defined as the ratio of shear stress to the related shear rate, for each point of the rheogram (Walker & Goulas, 1984):

$$\mu_a = \frac{\tau_o}{\dot{\gamma}} . \quad \text{Equation 2.3}$$

At very low and very high rates of shear, the values of the apparent viscosity are referred to as the zero shear viscosity, μ_o , and the infinite shear viscosity, μ_∞ , respectively (Chhabra & Richardson, 1999).

2.2.4.2 Bingham plastic viscosity μ_{pl}

For any particular shear rate value, the Bingham plastic viscosity μ_{pl} is defined as the slope of the flow curve at that point (Walker & Goulas, 1984). For a Bingham plastic slurry, μ_{pl} is determined by the following relationship:

$$\mu_{pl} = \frac{\tau_o - \tau_y}{\dot{\gamma}} , \quad \text{Equation 2.4}$$

where τ_y = yield stress and $\dot{\gamma}$ = shear rate corresponding the shear stress τ_o .

N.B: When a fluid is modelled as Bingham plastic, the slope μ_{pl} is equal to its consistency index K ($\mu_{pl} = K$). Therefore the Bingham plastic viscosity will be symbolised by K in this work.

2.2.5 Basic equations of fluid motion

When a fluid is in motion, the following basic principles are to be considered.

2.2.5.1 Continuity

The equation of continuity is a mathematical expression of the law of mass conservation. Considering a control volume moving in a short time interval dt , there is no change in the mass. When this control volume passes through cross-section 1 of area A_1 at the velocity V_1 during the time interval dt and then through another cross-section 2 of area A_2 at velocity V_2 during the same time interval dt , the preservation of mass flow rate is expressed by Equation 2.5 (Massey & Ward-Smith, 1998):

$$\rho_1 A_1 V_1 dt = \rho_2 A_2 V_2 dt . \quad \text{Equation 2.5}$$

Fluids being incompressible, the density remains constant ($\rho_1 = \rho_2$). Equation 2.5 above becomes:

$$A_1 V_1 = A_2 V_2 = Q , \quad \text{Equation 2.6}$$

where: A is the cross sectional area [m²].

V is the mean velocity [m/s].

Q is the volumetric flow rate [m³/s].

2.2.5.2 Energy equation

In the control volume, the total energy is conserved. This total energy is the sum of potential, kinetic and pressure energy. The total energy at station 1 (upstream), plus the pump head input, equals the total energy at station 2 (downstream), plus the energy loss due to friction (Liu, 2003). This is simply expressed in the well - known Bernoulli equation:

$$\frac{V_1^2}{2g} + Z_1 + \frac{p_1}{\rho g} + \Delta H_p = \frac{V_2^2}{2g} + Z_2 + \frac{p_2}{\rho g} + \Delta h_f , \quad \text{Equation 2.7}$$

where: ΔH_p is the pump head input (work done per unit weight)

Δh_f is friction head loss (energy loss per unit weight) between stations 1 and 2.

In Equation 2.7 each term is expressed in Joule per Newton [J/N], which corresponds to meter [m] and is referred to as head. Head is related to pressure by the expression:

$$p = \rho g H , \quad \text{Equation 2.8}$$

where H is the head expressed in meter of liquid.

2.3 RHEOLOGY

2.3.1 Introduction

Rheology is the science of flow phenomena. It is defined as the viscous property of a liquid or suspension. It deals particularly with the relationship between the shear stress and shear rate in laminar flow. The mathematical expression of this relationship is given by Equation 2.9

$$\tau = f\left(\frac{du}{dr}\right) . \quad \text{Equation 2.9}$$

2.3.2 Newton relationship

Rheology as science owes its origin to Sir Isaac Newton who postulated the relationship between the magnitude of applied shear stress and the resulting rate of deformation in a fluid, stating (Barr, 1931), "...the resistance which arises from the lack of slipperiness originating in a fluid - other things being equal - is proportional to the velocity by which the parts of the fluid are being separated from each other". Mathematically, this hypothesis is formulated as:

$$\tau = \mu \frac{du}{dy}, \quad \text{Equation 2.10}$$

where: τ = shear stress parallel to the direction of motion,

$\frac{du}{dy}$ = shear rate or the rate at which the velocity u is increasing in the y direction,

μ = coefficient of dynamic viscosity.

In terms of axially symmetric flow of fluid in a pipe, the relationship becomes:

$$\tau = \mu \left(-\frac{du}{dr} \right). \quad \text{Equation 2.11}$$

This relationship is linear, i.e., the plot of shear stress versus shear rate (rheogram) is a straight line passing through the origin (Figure.2.2). The gradient of this line represents the viscosity which is the only parameter required to characterise a Newtonian fluid.

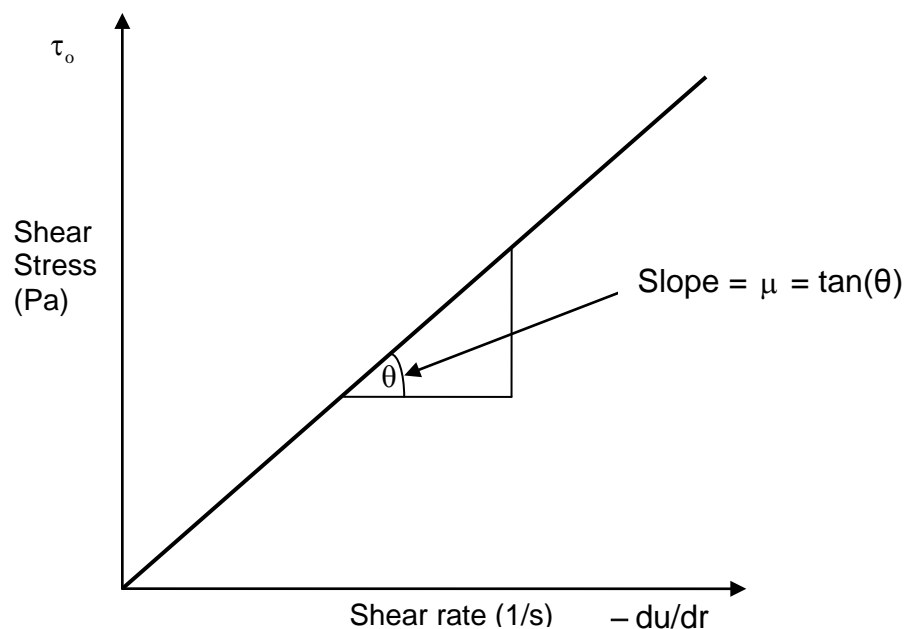


Figure 2.2: Rheogram of Newtonian fluid (Chhabra & Richardson, 1999)

2.3.3 Newtonian fluids

Any fluid which obeys the Newtonian relationship in laminar flow is said to be a Newtonian fluid. Newtonian fluids are characterised by a constant viscosity. Water, oils, honey, glycerine, simple organic liquids, solutions of low molecular weight inorganic salts, molten metals and salts, etc., are examples of Newtonian fluids (Chhabra & Richardson, 1999).

2.3.4 Non-Newtonian fluids

A non-Newtonian fluid is referred to as a fluid whose rheogram is non-linear or a straight line which does not pass through the origin. This fluid is not governed by the Newtonian relationship. Its apparent viscosity changes with temperature, pressure and flow conditions such as flow geometry, rate of shear, etc. (Chhabra & Richardson, 1999).

Non-Newtonian fluids are divided into three general classes:

- Time-independent fluids
- Time-dependent fluids
- Visco-elastic fluids

This project is dealing with the time-independent fluids only.

2.3.5 Time-independent fluid behaviour

The flow behaviour of this class of materials may be described by a relationship of the following form (Chhabra & Richardson, 1999):

$$\tau_{yx} = f(\dot{\gamma}_{yx}). \quad \text{Equation 2.12}$$

These fluids are subdivided into three types: shear-thinning, viscoplastic and shear-thickening. This work is concerned with shear-thinning and viscoplastic fluids.

2.3.5.1 Shear-thinning or pseudoplastic fluids

This type of time-independent non-Newtonian fluid behaviour is characterised by an apparent viscosity which decreases with increasing shear rate (Chhabra & Richardson, 1999).

2.3.5.2 Viscoplastic fluid behaviour

Certain fluids cannot flow until the external applied stress exceeds a certain value called yield stress (τ_y). Below this yield stress, such fluid deforms elastically (Chhabra & Richardson, 1999). The flow curve of such fluid can present a linear or non-linear shape but the graph will never pass through the origin. When this material possesses a linear flow curve on the linear coordinates, it is called Bingham plastic and is characterised by a constant plastic viscosity. When, on the other hand, the flow curve is non-linear on the linear coordinates, it is called yield-pseudoplastic (Chhabra & Richardson, 1999).

Figure 2.3 below gives the flow curves of the time-independent fluid considered in this work.

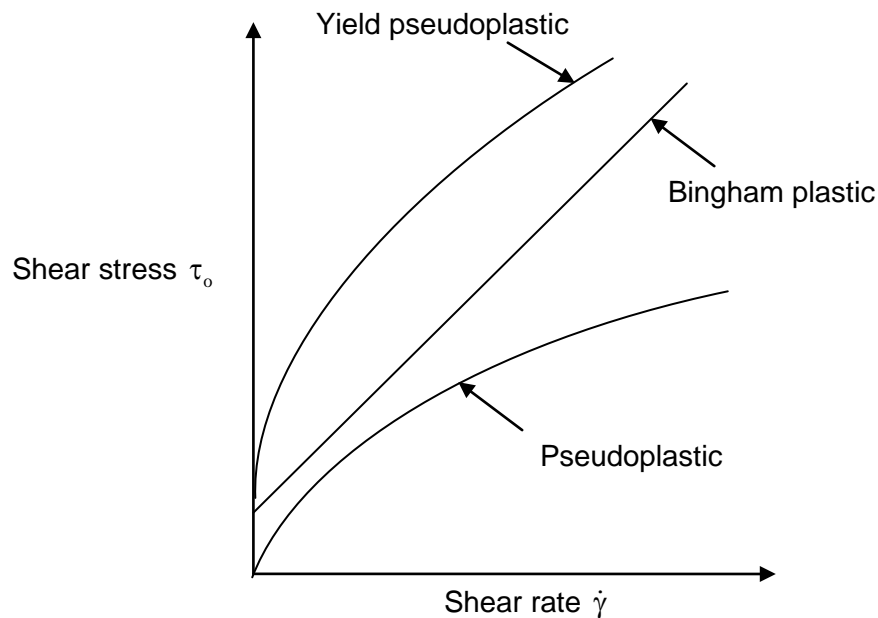


Figure 2.3: Pseudoplastic and viscoplastic behaviour (Chhabra & Richardson, 1999)

2.3.6 Rheological model of non-Newtonian fluids

Many fluid models have been proposed to describe non-Newtonian behaviour. The most common models are depicted in Table 2.1,

Table 2.1: Rheological models (Chhabra & Richardson, 1999)

Fluid model	Constitutive equation	Number of parameters	Parameters
Newtonian	$\tau = \mu \left(-\frac{du}{dr} \right)$	1	μ
Bingham plastic	$\tau = \tau_y + K \left(-\frac{du}{dr} \right)$	2	τ_y and K
Power-law or Ostwald de Waele (pseudoplastic)	$\tau = K \left(-\frac{du}{dr} \right)^n$	2	K and n
Herschel-Bulkley or Yield pseudoplastic	$\tau = \tau_y + K \left(-\frac{du}{dr} \right)^n$	3	τ_y , n and K

where: $(-du/dr)$ = Shear rate.

2.3.7 Choice of rheological model

Both the rheological characterisation in laminar flow and the predictions of turbulent flow rely on the choice of rheological model (Hanks & Ricks, 1975). Being difficult to capture data in turbulent flow, data are measured first in laminar flow (Shook & Roco, 1991), then extrapolated to the high shear stress for turbulent flow prediction (Thomas & Wilson, 1987).

Several rheological models have been developed, and authors have divergent opinions when it comes to the choice of the model to describe non-Newtonian fluids.

The pseudoplastic and Bingham plastic models appear to be the most popular models (Wilson, 1986). The yield pseudoplastic model has the advantages of incorporating the features of the pseudoplastic model (rheogram curvature) and the Bingham plastic model (yield stress). Therefore, it can be used as a generalised model and is often used to describe a number of different fluids (Thomas & Wilson, 1987).

2.3.8 Generalised model

Despite the yield pseudoplastic model being very sensitive to small variations in the rheological parameters, it presents a good reproducibility of the data fit (Al-Fariss & Pinder, 1987). Therefore it remains widely used as a generalised model.

Its constitutive equation is:

$$\tau = \tau_y + K \left(-\frac{du}{dr} \right)^n, \quad \text{Equation 2.13}$$

where: τ_y , K and n are rheological parameters, to be determined by rheological characterisation.

2.3.8.1 Yield stress (τ_y)

A substance is said to possess a yield stress if it does not flow by the external applied stress which is smaller than a certain value. Beyond this value, the material behaves like a fluid. The yield stress is therefore considered as the minimum value of the applied stress required to initiate a sustainable flow.

For real material, it is virtually impossible to ascertain the existence of a true yield stress.

To say whether a fluid has a yield stress or not seems to be related to the choice of a time scale of observation (Chhabra & Richardson, 1999).

2.3.8.2 The fluid consistency index (K)

This parameter is regarded as the value of the fluid apparent viscosity at the shear rate of unity and depends on the unit of time employed (Chhabra & Richardson, 1999). The greater the value of K, the more viscous is the fluid.

Physical properties of particles such as density, shape, roughness, particle size, and size distribution can influence this parameter.

2.3.8.3 The flow behaviour index (n)

This parameter indicates the degree of curvature of the rheogram. For the values of n between 0 and 1, the fluid is shear-thinning. The degree of shear thinning is in inverse proportion to the value of n. This index is greater than unity for a shear-thickening fluid. When $n = 1$ the fluid shows the Newtonian behaviour (Chhabra & Richardson, 1999).

The flow behaviour index, n, is the indication of the rate of increase in shear stress with shear rate. It varies with concentration (Slatter, 1986; Lazarus & Slatter, 1988).

The parameters τ_y , K and n are specific to a given set of slurry conditions and cannot be separated from one another (Chhabra & Richardson, 1999).

The different slurry types that can be described by the generalised yield pseudoplastic equation are given in Table 2.2 below.

Table 2.2: Different models described by the yield pseudoplastic equation

Fluid	Yield stress	Flow behaviour index	Constitutive equation
Newtonian	$\tau_y = 0$	$n = 1$	$\tau = \mu \dot{\gamma}$
Bingham Plastic	$\tau_y > 0$	$n = 1$	$\tau = \tau_y + K \dot{\gamma}$
Pseudoplastic	$\tau_y = 0$	$n < 1$	$\tau = K \dot{\gamma}^n$
Yield Pseudoplastic	$\tau_y > 0$	$n < 1$	$\tau = \tau_y + K \dot{\gamma}^n$
Dilatant	$\tau_y = 0$	$n > 1$	$\tau = K \dot{\gamma}^n$
Yield Dilatant	$\tau_y > 0$	$n > 1$	$\tau = \tau_y + K \dot{\gamma}^n$

Figure 2.4 summarises different shapes of non-Newtonian fluid rheograms.

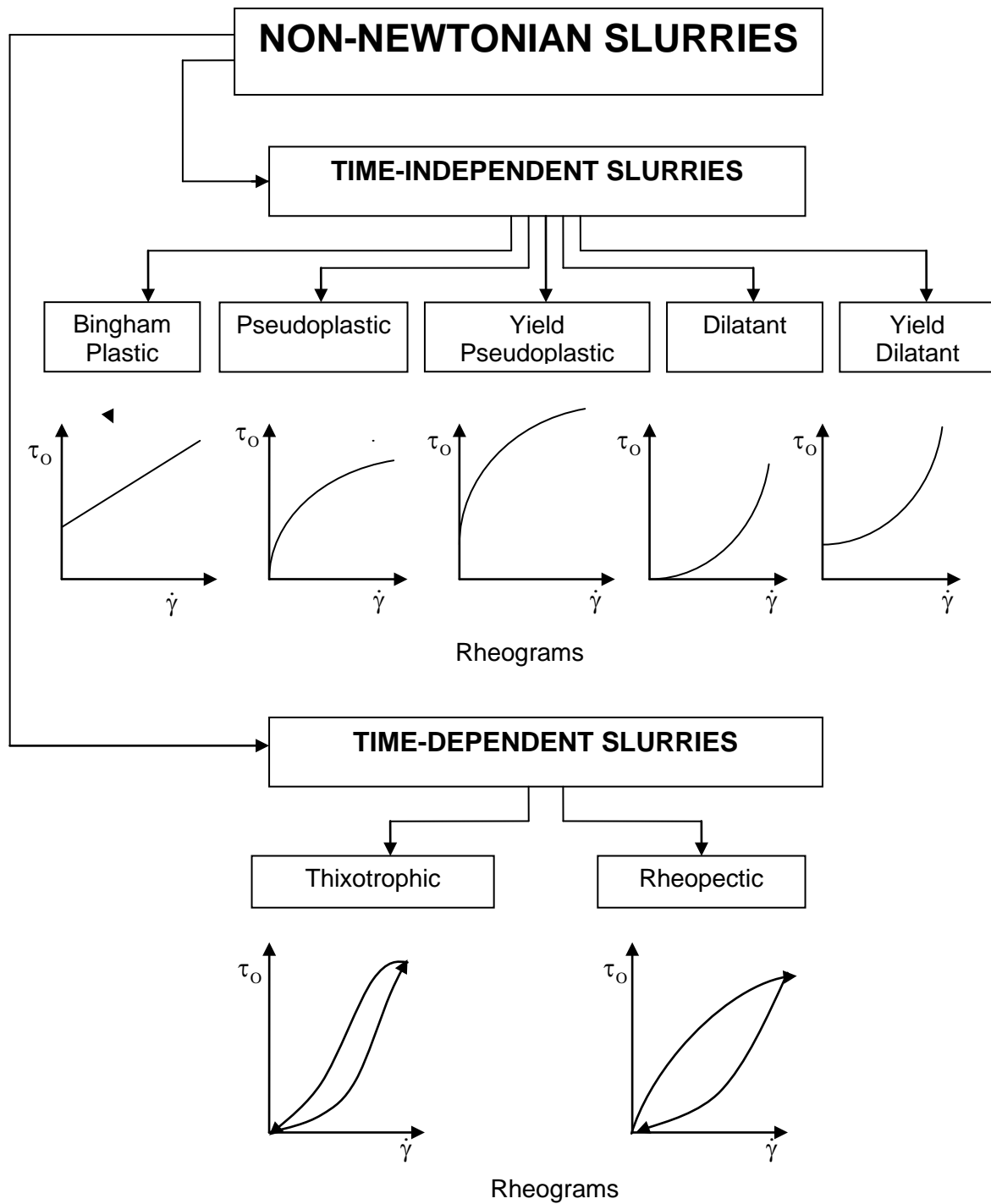


Figure 2.4: Summary of non-Newtonian rheograms (Paterson & Cooke, 1999)

2.4 FLOW IN STRAIGHT PIPE

The fluid flowing through a pipe of constant diameter with a steady and fully developed flow will be considered. The flow may be laminar or turbulent depending on the value of the Reynolds number (Munson *et al.*, 2010).

2.4.1 Flow regimes and Reynolds number

For a steady flow of real fluids, two types of regimes exist: laminar flow and turbulent flow. In the laminar regime, fluid particles move along straight, parallel paths in layers or laminae. Two adjacent layers move with different magnitudes of velocity. Laminar flow is governed by the product of the fluid viscosity and velocity gradient.

$$\tau = \mu \frac{dv}{dy}. \quad \text{Equation 2.14}$$

The forces of viscosity are dominant in laminar flow and suppress any tendency to turbulent conditions (Giles *et al.*, 1994).

In the turbulent regime, fluid particles move randomly in all directions in such a way that it becomes impossible to trace the motion of an individual particle.

To quantify these two regimes, the Reynolds number is used. The Reynolds number (Re) is a dimensionless quantity representing the ratio of inertia forces to viscous forces.

$$\text{Re} = \frac{F_i}{F_v} = \frac{\rho L^2 V^2}{\mu L V} = \frac{\rho V L}{\mu} \quad \text{Equation 2.15}$$

For circular pipes flowing fully the Reynolds number is:

$$\text{Re} = \frac{\rho V D}{\mu}. \quad \text{Equation 2.16}$$

2.4.2 Laminar to turbulent transition

Under normal engineering conditions, transition (laminar-turbulent) occurs at values of Reynolds number between 2000 and 4000 (Massey & Ward-Smith, 1998). There is apparently no upper limit to the value of the Reynolds number at which the transition occurs. There is, however, a definite lower limit below which any disturbances in flow are damped out by the viscous forces (Massey & Ward-Smith, 1998).

For engineering calculations, the generally accepted criterion for the end of stable laminar flow and the beginning of turbulent flow is when the bulk Reynolds number equals 2100. The transition is, therefore, assumed to occur at 2100 (Govier & Aziz, 1972).

2.4.3 The shear stress distribution

When the flow in the pipe of radius R is laminar, the force balance on a cylindrical fluid element of length L and radius r (Figure.2.5) can be written as:

$$\rho(\pi r^2) - (\rho + \Delta\rho)\pi r^2 = \tau_{rz} \cdot 2\pi r L. \quad \text{Equation 2.17}$$

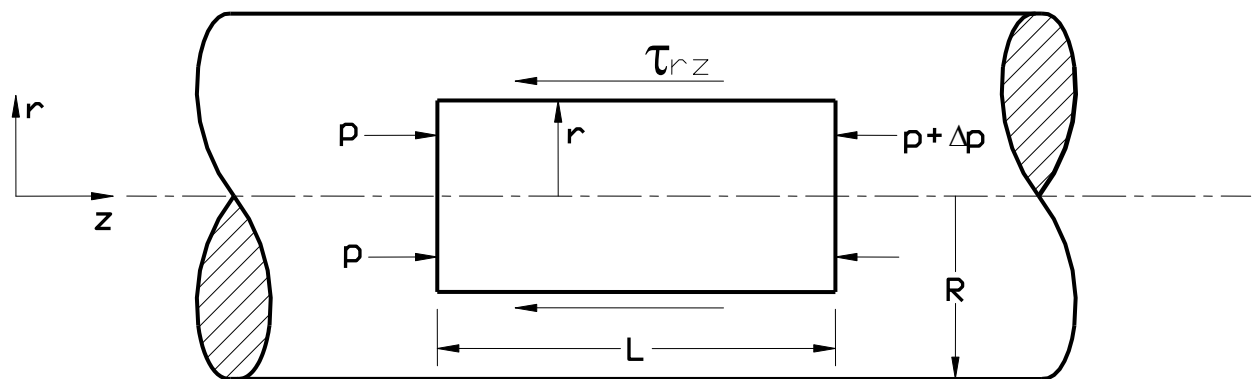


Figure 2.5: Stress distribution in horizontal straight pipe (Chhabra & Richardson, 1999)

This leads to the shear stress acting uniformly on the curved surface of the cylindrical element expressed as:

$$\tau_{rz} = \left(\frac{-\Delta p}{L} \right) \frac{r}{2}. \quad \text{Equation 2.18}$$

This shear stress acts in the opposite direction to the flow motion (Figure 2.6), and is linearly distributed across the pipe cross-section (Figure.2.7). The shear stress is zero at the axis of the tube, where $r = 0$.

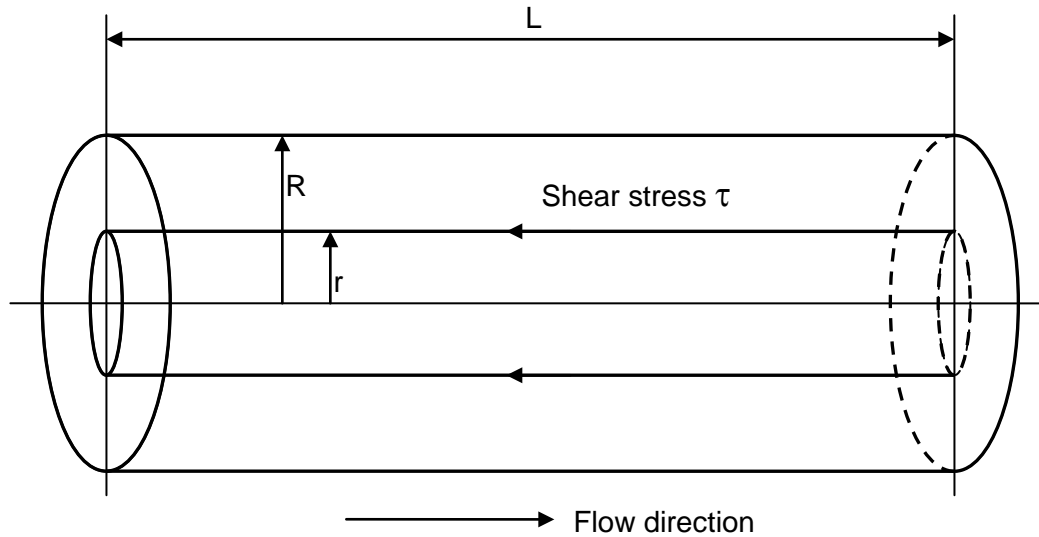


Figure 2.6: Shear stress acting in opposite of flow direction (Slatter, 1994)

At the pipe wall, where $r = R$ the shear stress is maximum and is given by Equation 2.19:

$$\tau_0 = \frac{\Delta p R}{L} \text{ or } \tau_0 = \frac{D\Delta p}{4L}. \quad \text{Equation 2.19}$$

The above Equation 2.19 is applicable in turbulent flow as well (Chhabra & Richardson, 1999).

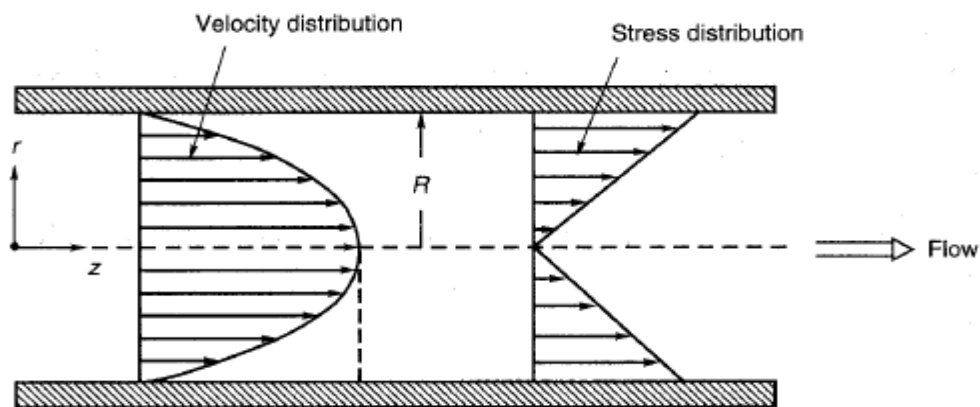


Figure 2.7: Distribution of shear stress across the pipe cross-section (Chhabra & Richardson, 1999)

2.4.4 Head lost to friction in a pipe

The French engineer Henri Darcy (1803 - 1858) investigated the flow of water, under turbulent conditions, in long, unobstructed, straight pipes of uniform diameter and found that the piezometric head was falling uniformly according to the following relationship (Massey & Ward-Smith, 1998):

$$\Delta h = \frac{\Delta p}{\rho g} = \frac{4fL}{D} \frac{V^2}{2g}, \quad \text{Equation 2.20}$$

where: f is the friction factor,

L is the pipe length,

V is the mean velocity,

D is the pipe diameter.

Equation 2.20 is known as the Darcy Weisbach equation in which all quantities, except f , can be measured experimentally.

2.4.5 Friction factor

The friction factor f is the dimensionless factor required to make the Darcy equation produce the correct value of losses (Streeter & Wylie, 1985). It depends on the relative roughness of the pipe surface, the Reynolds number, and the mean stress τ_o at the wall of the pipe (Massey & Ward-Smith, 1998).

2.4.5.1 Newtonian friction factor

Govier and Aziz (1972) define friction factor as the ratio of the wall shear stress (τ_o) to the kinetic energy per unit volume of fluid ($\rho V^2/2$).

The mathematical relationship of this definition is well known as the Fanning friction factor (Massey & Ward-Smith, 1998):

$$f = \frac{2\tau_o}{\rho V^2}. \quad \text{Equation 2.21}$$

In laminar flow for a Newtonian fluid, the flow is governed by the Poiseuille's equation:

$$\Delta p = \frac{8QL\mu}{\pi R^4}. \quad \text{Equation 2.22}$$

Combining the Poiseuille and Darcy equations, the friction factor will be given by:

$$f = \frac{16}{Re}. \quad \text{Equation 2.23}$$

Here the friction factor is independent of the roughness of the pipe walls.

In turbulent flow, the friction factor depends on the pipe roughness and can be obtained from the Colebrook formula:

$$\frac{1}{\sqrt{f}} = -2.0 \log \left(\frac{k}{3.7D} + \frac{2.51}{Re\sqrt{f}} \right), \quad \text{Equation 2.24}$$

where: k is the internal pipe hydraulic roughness (m) (Munson *et al.*, 2010).

For smooth pipes, Blasius proposed the following formula for turbulent regime:

$$f = \frac{0.079}{\sqrt[4]{Re}}. \quad \text{Equation 2.25}$$

For Reynolds numbers between 3000 and 10^5 the Blasius equation leads to a close agreement with experimental results (Massey & Ward-Smith, 1998).

2.4.5.2 Non-Newtonian friction factor

For non-Newtonian fluids, Equations 2.21 and 2.23 can be used if:

- The wall shear stress τ_o is replaced by the chosen rheological model in Equation 2.21.

For a power-law model, f is given by Chhabra and Richardson (1999).

$$f = \frac{2}{\rho V^2} K \left(\frac{8V}{D} \right)^n \quad \text{Equation 2.26}$$

- The Reynolds number Re is considered non-Newtonian in Equation 2.23.

For ordinary commercial pipes, the American engineer Lewis F. Moody prepared a modified diagram (called the Moody diagram) to determine the friction factor (Figure 2.8) (Munson *et al.*, 2010).

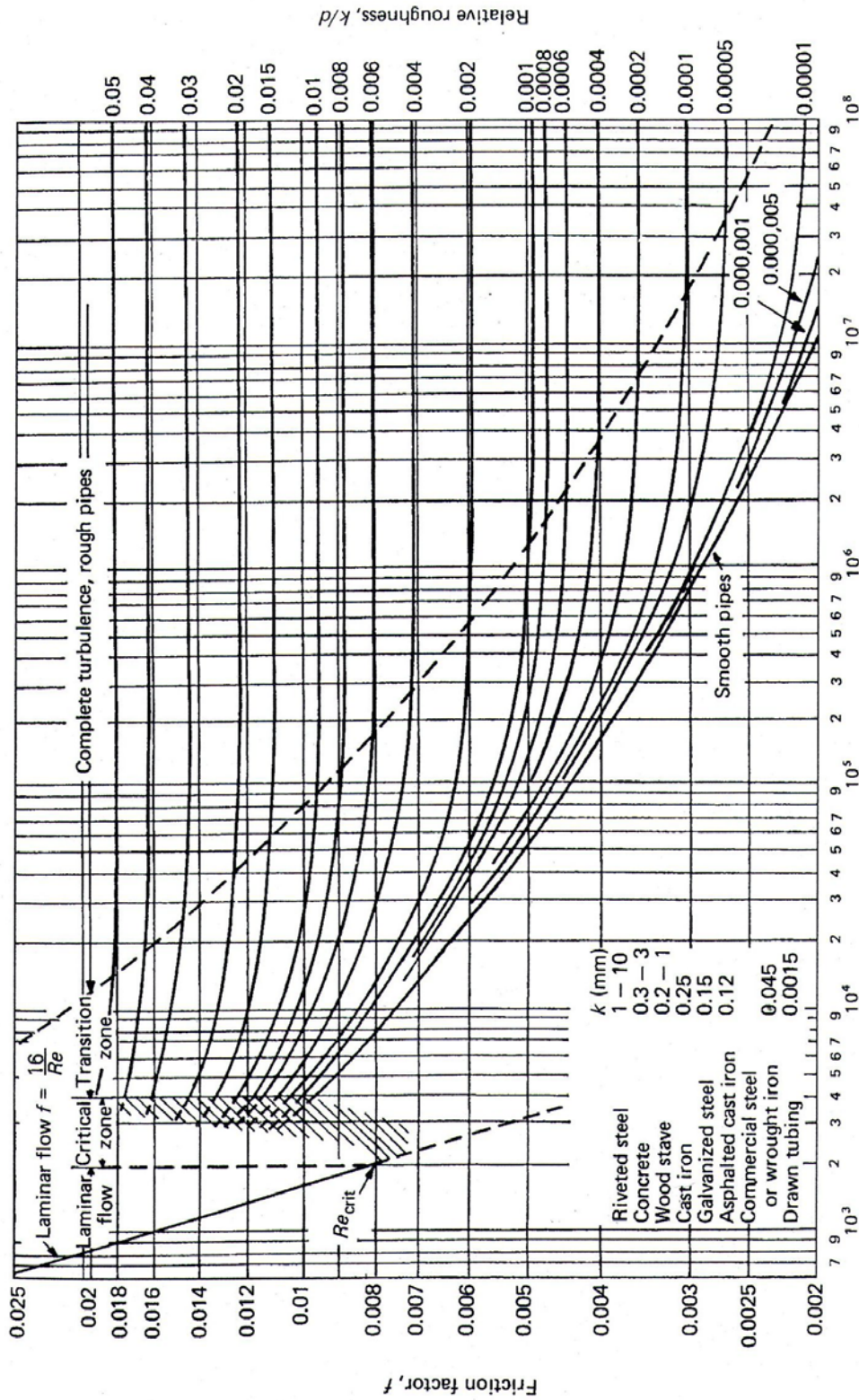


Figure 2.8: Moody diagram (Munson et al., 2010)

2.4.6 The laminar flow of non-Newtonian fluids

2.4.6.1 Introduction

For laminar flow of non-Newtonian fluids, the shear stress due to the friction between layers is not directly proportional to the velocity gradient as for Newtonian fluids. The relationship between the shear stress and velocity gradient is complex.

The yield pseudoplastic will be considered here as a general case.

2.4.6.2 General approach

The general constitutive rheological relationship is given by Equation 2.27 below. It represents a general rheogram.

$$-\frac{du}{dr} = f(\tau). \quad \text{Equation 2.27}$$

The integration of the velocity profile over the pipe cross section gives the flow rate.

$$Q = 2\pi \int_0^R u r dr. \quad \text{Equation 2.28}$$

Integrating by parts and considering that at the pipe wall the velocity $u = 0$ (no slip at the tube wall), Equation 2.28 yields:

$$Q = \pi \int_0^R r^2 \left(-\frac{du}{dr} \right) dr. \quad \text{Equation 2.29}$$

Considering the force balance on a cylindrical element (plug) of radius r and length dL , in the pipe of radius R , the following relationships can be determined:

$$r = \frac{R\tau}{\tau_0}, \text{ and } r^2 = \frac{R^2\tau^2}{\tau_0^2}, \text{ and } dr = \frac{R}{\tau_0} d\tau. \quad \text{Equation 2.30}$$

By substituting the relationships of Equation 2.30 in Equation 2.29, we obtain:

$$Q = \frac{\pi R^3}{\tau_0^3} \int_0^{\tau_0} \tau^2 f(\tau) d\tau. \quad \text{Equation 2.31}$$

Applying the continuity equation $Q = \pi R^2 V$, the expression below can be established:

$$\frac{8V}{D} = \frac{4}{\tau_0^3} \int_0^{\tau_0} \tau^2 f(\tau) d\tau. \quad \text{Equation 2.32}$$

Equation 2.32 is of fundamental importance for the following reasons (Slatter, 1994):

- It shows that in general the pseudo-shear rate ($8V/D$) is a unique function of the rheogram ($f(\tau)$) and the wall shear stress (τ_o), provided that there is no time dependency or slip at the wall and the flow is laminar.
- It shows that relationship between $8V/D$ and τ_o can be obtained by direct numerical integration using data directly from a rheometer, without using a conventional rheological model.
- Since $(8V/D)$ is a unique function of the rheogram ($f(\tau)$) and the wall shear stress (τ_o), it is independent of pipe diameter, and can be used for scale-up and design in laminar flow.

Two regions have to be considered (Figure. 2.9):

In the plug region:

- $0 \leq r \leq r_{\text{plug}}$,
- $0 \leq \tau \leq \tau_y$ and
- $f(\tau) = 0$.

In the sheared region:

- $r_{\text{plug}} \leq r \leq R$,
- $\tau_y \leq \tau \leq \tau_o$ and
- $f(\tau)$ depends on the chosen rheological model.

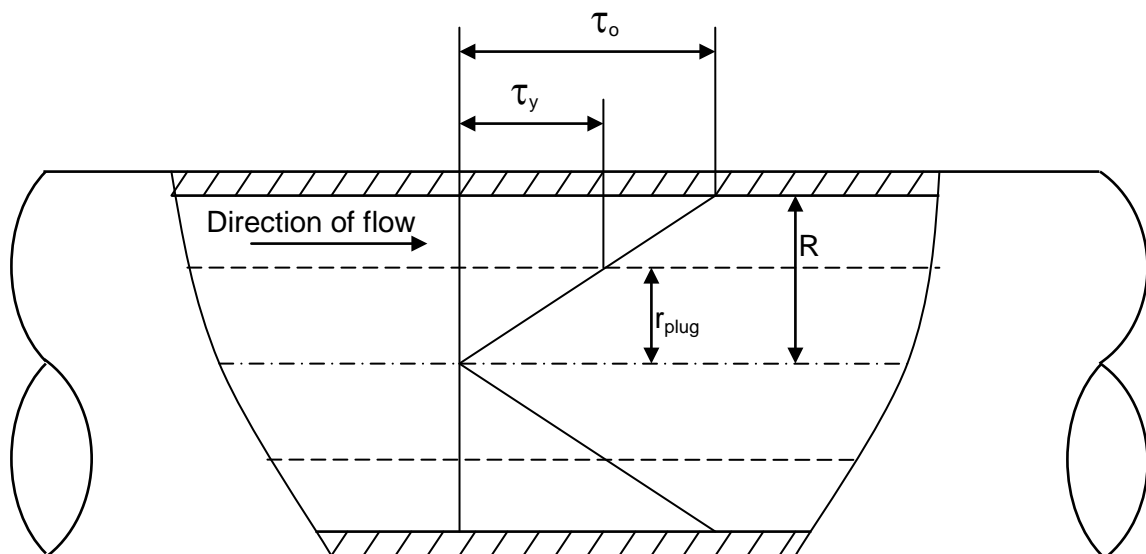


Figure 2.9: Non-Newtonian shear stress distribution in pipe (Slatter, 1994)

2.4.6.3 The yield pseudoplastic model

Non-Newtonian slurries are often best modelled as yield pseudoplastic (Govier & Aziz, 1972).

The constitutive rheological equation is:

$$\tau = \tau_y + K \left(-\frac{du}{dr} \right)^n, \quad \text{Equation 2.33}$$

where: τ_y is the yield stress,

K is the fluid consistency index,

n is the flow behaviour index.

From Equation 2.33 above, the following equation can be derived:

$$f(\tau) = -\frac{du}{dr} = \left(\frac{1}{K} \right)^{\frac{1}{n}} (\tau - \tau_y)^{\frac{1}{n}}. \quad \text{Equation 2.34}$$

Substituting Equation 2.34 in Equation 2.32 yields:

$$\frac{8V}{D} = \frac{4}{\tau_o^3} \int_{\tau_y}^{\tau_o} \tau^2 \left(\frac{1}{K} \right)^{\frac{1}{n}} (\tau - \tau_y)^{\frac{1}{n}} d\tau. \quad \text{Equation 2.35}$$

Integrating by setting $x = \tau - \tau_y$, $dx = d\tau$, and $\tau = x + \tau_y$, the function above yields:

$$\frac{8V}{D} = \frac{4n}{\tau_o^3} \left(\frac{1}{K} \right)^{\frac{1}{n}} (\tau_o - \tau_y)^{n+1} \left[\frac{(\tau_o - \tau_y)^2}{3n+1} + 2\tau_y \frac{(\tau_o - \tau_y)}{2n+1} + \frac{\tau_y^2}{n+1} \right]. \quad \text{Equation 2.36}$$

Equation 2.36 is the form of the generalised yield pseudoplastic model.

The following rheological relationships can be accommodated in this model:

Yield dilatant	$[\tau_y > 0 \text{ and } n > 1]$
Bingham plastic	$[\tau_y > 0 \text{ and } n = 1]$
Yield pseudoplastic	$[\tau_y > 0 \text{ and } n < 1]$
Dilatant	$[\tau_y = 0 \text{ and } n > 1]$
Newtonian	$[\tau_y = 0 \text{ and } n = 1]$
Pseudoplastic	$[\tau_y = 0 \text{ and } n < 1]$

2.5 RHEOMETRY OF NON-NEWTONIAN FLUIDS

2.5.1 Introduction

The aim of viscometry is to establish a qualitative and quantitative relationship between shear rate and shear stress using data from experimental rheological tests performed on a fluid. This helps identify the suitable rheological model to apply to the data (qualitative) and calculate the different rheological parameters required in this model (quantitative). The viscous characteristics of a fluid are obtained by measurement using a device called a viscometer. There are two main types of viscometers: rotational and tube (Slatter, 1994).

2.5.2 Rotational viscometers

Many types of rotational viscometers exist: plate-plate, cone-plate, bob and cup, etc. These viscometers encompass two measuring elements: a fixed and a rotating element. The rotating element induces shear in the test liquid placed between the two elements. The torque of one of the elements is measured to determine the shear stress in the liquid.

This type of viscometer is a highly sophisticated instrument. Besides the torque, it can measure a full range of rheometric phenomena as well (Slatter, 1994). Unfortunately, it presents the following disadvantages: it can reach only a relatively low rate of shear, and centrifugal action can take place between the two measuring elements (Slatter, 1986 and Shook & Roco, 1991). On the other hand, the tube viscometer presents the advantage of being mechanically much simpler than a rotational viscometer, as it is just a smaller pipeline (Lazarus & Slatter, 1988). For these reasons, the tube viscometer is preferred for non-Newtonian fluids (Wilson *et al.*, 2006).

2.5.3 Tube viscometers

A tube viscometer is a pipeline of a relatively small size in which the test fluid is pumped through a straight pipe of known length and inner diameter. The flow rate and pressure drop over a known length of the straight pipe are measured then converted to pseudo-shear rate ($8V/D$) and wall shear stress ($\tau_o = D\Delta p/4L$) respectively. A range of diameters and lengths are necessary to build up an accurate pseudo-shear diagram. The data from a tube viscometer can be analysed using the Rabinowitsch-Mooney relation (Slatter, 1994).

2.5.4 The Rabinowitsch-Mooney relation

The rheological data from a tube viscometer is plotted as wall shear stress ($\tau_o = D\Delta p/4L$) versus pseudo-shear rate ($8V/D$). While for Newtonian fluids $8V/D$ is the true shear rate at the wall, it is only a nominal shear rate, which needs correction to extract the true value of shear rate, for time independent non-Newtonian fluids.

The Rabinowitsch-Mooney relation (Equation 2.37) is recommended to make this correction (Govier & Aziz, 1972 and Chhabra & Richardson, 1999).

$$\left(-\frac{du}{dr}\right)_o = \frac{8V}{D} \left(\frac{3n'+1}{4n'}\right), \quad \text{Equation 2.37}$$

where: n' is obtained as the slope of a double logarithmic plot of $D\Delta p/4L$ versus $8V/D$, i.e.

$$n' = \frac{d\left(\ln \frac{D\Delta p}{4L}\right)}{d\left(\ln \frac{8V}{D}\right)}. \quad \text{Equation 2.38}$$

For Newtonian fluids the value of n' is equal to '1' and Equation 2.37 becomes

$$\left(-\frac{du}{dr}\right)_o = \frac{8V}{D}. \quad \text{Equation 2.39}$$

2.5.5 Rheological characterisation

The output of a tube viscometer is a set of co-ordinates of (V ; Δp). These data are plotted as wall shear stress ($D\Delta p/4L$) versus pseudo-shear rate ($8V/D$) on a diagram called pseudo-shear diagram (Figure 2.10). The data in the laminar region, for different tube diameters, are coincident. These data are extracted and plotted on logarithmic co-ordinates (or the logarithm of both wall shear stress and pseudo-shear rate are calculated and plotted on arithmetic co-ordinates).

A first, second, third or fourth polynomial curve fit function can be fitted to the data at any given $8V/D$ value. The first derivative (n') of the chosen polynomial function describes the slope of this function. The value of n' is used to calculate the Rabinowitsch-Mooney factor which is multiplied by the pseudo-shear rate to obtain the true shear rate.

The wall shear stress is plotted versus true shear rate on linear or logarithmic co-ordinates. Any rheological model (yield pseudoplastic, Bingham plastic or pseudoplastic) which best fits the

data should be chosen and then values of rheological constants (τ_y , K and n) determined (Lazarus & Slatter, 1988).

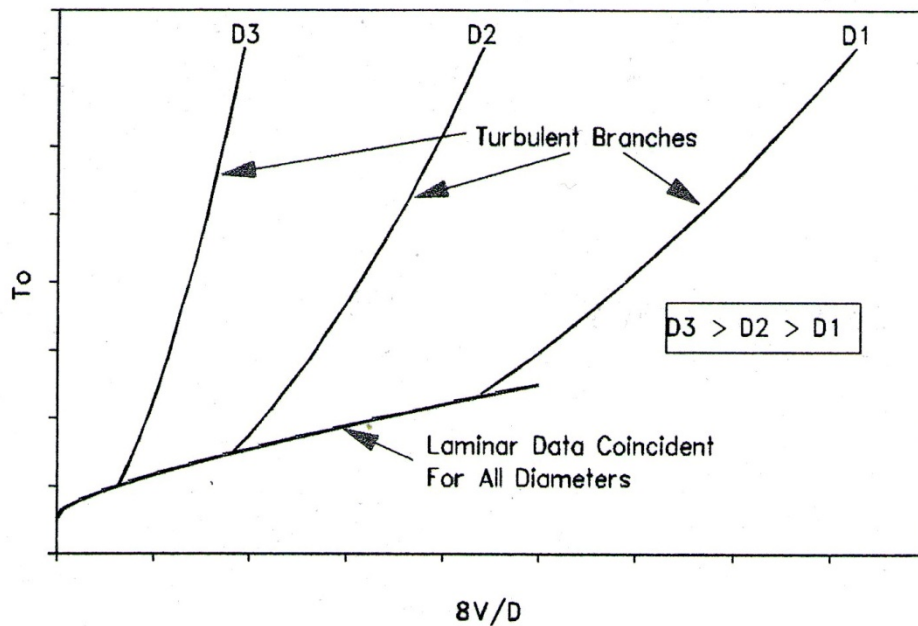


Figure 2.10: Illustration of a pseudo-shear diagram for different pipe diameter (Slatter, 1994).

2.6 OVERVIEW OF PUMPS

2.6.1 Introduction

Many processes in industry rely on the liquid transport or transfer of energy through liquids. Pumps are, therefore, needed in the design of various systems of liquid transport.

The pump description is based on a large number of criteria that make the pump classification a tough exercise (SAPMA, 2005).

Considering the principle by which the energy is imparted to the test liquid, pumps are classified into two main categories (Brown & Heywood, 1991; Wilson *et al.*, 2006): positive displacement pumps and dynamic pumps. The latter category is the major concern for this project. These pumps are based on bladed impellers which rotate within the fluid to impart a tangential acceleration to the fluid and a consequent increase in the energy of the fluid. Their purpose is to convert this energy into pressure energy of the fluid to be used in the associated piping system.

This category encompasses centrifugal pumps, where energy is generated by the centrifugal force of a vortex, and axial pumps (Paterson & Cooke, 1999).

2.6.2 Centrifugal pump description

Pullum *et al.* (2007) described a centrifugal slurry pump as the workhorse of hydraulic conveying systems. They are the most used pumps, partly because they are cheaper than displacement pumps which can develop the same head (Brown & Heywood, 1991), and, because of their versatility and robustness (Paterson & Cooke, 1999).

A centrifugal pump has two main parts:

- The rotating part comprising the shaft and impeller, including the vanes which act on the fluid.
- The stationary part made up of the casing which encloses the impeller, and bearings.

The essential components are depicted in Figure 2.11 below.

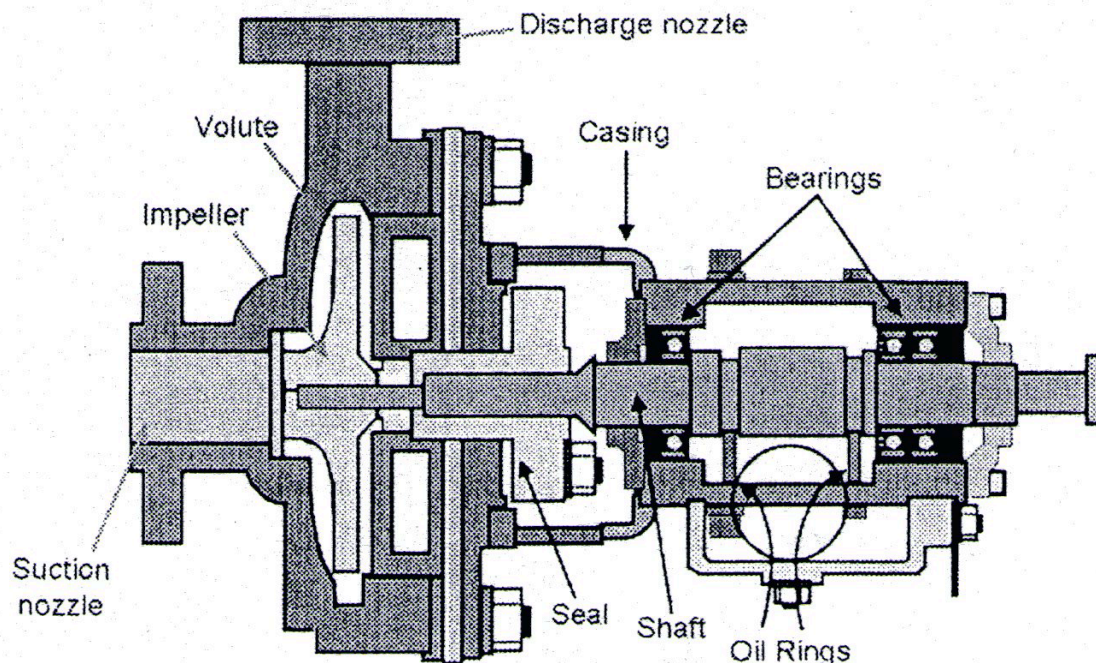


Figure 2.11: Components of centrifugal pump (Perez, 2008).

2.6.2.1 Rotating components

a) Impeller

The impeller is the main rotating part that provides the centrifugal acceleration to the fluid from its suction eye (inlet) to its outer diameter (where the fluid acquires its maximum speed).

Impellers can be classified in many ways (Sahdev, 2007), based on:

- Major direction of flow in reference to the axis of rotation
- Suction type
- Mechanical construction

b) Shaft

The shaft is the component which supports the rotating parts. It transfers the motor rotational motion to the impeller and other rotating parts (Sahdev, 2007).

2.6.2.2 Stationary components

a) Casing

According to their shapes, casings are of two types: volute and circular. The casing has the task of converting the kinetic energy of the fluid leaving the impeller, into pressure energy. The impellers are fitted inside the casings (Sahdev, 2007).

b) Bearings

The bearings maintain a correct alignment between the rotating and the stationary parts under the action of radial and transverse loads (Sahdev, 2007).

2.6.3 Working mechanism

Centrifugal pumps convert the energy of a prime mover (an electric motor) first into velocity or kinetic energy and then into pressure energy of the test fluid. This change of energy is due to the action of the two main parts of the pump. The impeller accelerates the fluid from its suction eye (inlet) to its outer diameter (where the fluid acquires its maximum speed). The increasing cross-sectional area of the volute casing gradually reduces the speed and increases the pressure of the fluid, until full pressure is reached at the pump's outlet (Perez, 2008).

2.6.4 Theoretical study of a centrifugal pump

2.6.4.1 Pump head

Considering a liquid propelled by a centrifugal pump, the dynamic head (H) is the increase in head across the pump. If the pump suction is at section A, the total dynamic head (TDH) is H_A . Similarly, for pump discharge at section B, the TDH is H_B . Using Bernoulli's equation, the TDH is formulated as follows (Wilson *et al.*, 2006):

$$H = H_B - H_A = \frac{V_B^2 - V_A^2}{2g} + \frac{P_B - P_A}{\rho g} + (z_B - z_A). \quad \text{Equation 2.40}$$

2.6.4.2 Pump power

The output power of a centrifugal pump is given by:

$$P_{\text{out}} = \rho g Q H. \quad \text{Equation 2.41}$$

The input power is the actual power delivered to the pump shaft and it is given by Equation 2.42 below:

$$P_{\text{in}} = \frac{2\pi NT}{60}. \quad \text{Equation 2.42}$$

2.6.4.3 Pump efficiency

The pump efficiency is the ratio of the output power to the input power:

$$\eta = \frac{P_{\text{out}}}{P_{\text{in}}}. \quad \text{Equation 2.43}$$

The point of maximum efficiency is called the "Best Efficiency Point (BEP)". This point is very important because many parametric calculations are based on the capacity at BEP. The pump selection is made in such a way that the pump will be running at appropriate speed as close to the BEP as possible. Many users prefer to operate pumps within 80% to 110% of BEP for optimum performance (Wilson *et al.*, 2006).

2.6.5 Flow through the centrifugal pump

2.6.5.1 Flow pathline through the pump

As the impeller rotates, fluid is sucked into the pump through the eye of the casing. Inside the pump, fluid enters the impeller along its axis and flows radially (through blade passage) outward.

As the fluid leaves the impeller, it is collected by the volute casing or diffuser and led to the pump discharge (Munson *et al.*, 2010).

2.6.5.2 Theoretical consideration

The flow through a centrifugal pump is very complex, therefore the basic theory of centrifugal pump operation can be established by considering that the flow of the fluid between the inlet and outlet of the impeller (as the blades rotate), is one-dimensional (Munson *et al.*, 2010).

The blade rotates in a circular path with angular velocity ω , therefore, the linear velocity of the inlet and outlet of the blade is respectively:

$$U_1 = r_1\omega \text{ and } U_2 = r_2\omega. \quad \text{Equation 2.44}$$

For the observer located on the blade, the fluid relative velocity, W , is considered tangential to the blade at both the blade inlet and blade exit.

As shown in Figure 2.12, the fluid absolute velocity, V , is the vector sum of the blade velocity, U , and the relative velocity, W , within the blade passage so that at the entrance and exit we have respectively:

$$V_1 = W_1 + U_1 \text{ and } V_2 = W_2 + U_2. \quad \text{Equation 2.45}$$

Fluid velocities are taken to be average velocities over the inlet and exit sections of the blade passage.

The shaft torque required to rotate the pump impeller is given by:

$$T_{\text{shaft}} = \rho Q(r_2 V_{\theta 2} - r_1 V_{\theta 1}), \quad \text{Equation 2.46}$$

where: $V_{\theta 1}$ and $V_{\theta 2}$ are the tangential components of the absolute velocities, V_1 and V_2 .

Q is the fluid flow rate.

The power transferred to the flowing fluid is given by:

$$P_{\text{out}} = T_{\text{shaft}} \omega = \rho Q \omega (r_2 V_{\theta 2} - r_1 V_{\theta 1}). \quad \text{Equation 2.47}$$

Since $U_1 = r_1\omega$ and $U_2 = r_2\omega$ we obtain

$$P_{\text{out}} = \rho Q (U_2 V_{\theta 2} - U_1 V_{\theta 1}). \quad \text{Equation 2.48}$$

In addition, we know from Equation 2.41 that the ideal or maximum head that a pump adds to the fluid is given by:

$$H = \frac{P_{\text{out}}}{\rho g Q}. \quad \text{Equation 2.49}$$

After replacing P_{out} by Equation 2.48, we get:

$$H = \frac{1}{g}(U_2 V_{\theta 2} - U_1 V_{\theta 1}). \quad \text{Equation 2.50}$$

The actual head rise realised by the fluid is less than the theoretical head.

Often the fluid has no tangential component of velocity, $V_{\theta 1}$ at the blade inlet. It just swirls, as it enters the impeller. Equation 2.50 then becomes:

$$H = \frac{U_2 V_{\theta 2}}{g}. \quad \text{Equation 2.51}$$

From Figure 2.12c,

$$V_{\theta 2} = U_2 - V_{r2} \cot \beta_2, \quad \text{Equation 2.52}$$

the head can be expressed as

$$H = \frac{U_2^2}{g} - \frac{U_2 V_{r2} \cot \beta_2}{g}, \quad \text{Equation 2.53}$$

where: V_{r2} is the radial component of the absolute velocity.

The flow rate Q is related to V_{r2} through Equation 2.54 below.

$$Q = 2\pi \cdot r_2 b_2 V_{r2}, \quad \text{Equation 2.54}$$

where: b_2 is the impeller blade height at the distance r_2 from the axis. Then, the combination of Equations 2.53 and 2.54 yields

$$H = \frac{U_2^2}{g} - \frac{U_2 \cot \beta_2}{2\pi \cdot r_2 b_2 g} Q. \quad \text{Equation 2.55}$$

Equation 2.55 shows that the ideal or maximum head rise for a centrifugal pump is a linear function of Q for a given blade geometry and angular velocity.

The normal range of the blade angles, β_1 and β_2 , are: $20^\circ < \beta_2 < 25^\circ$ and $15^\circ < \beta_1 < 50^\circ$ (Hydraulic Institute, 1983).

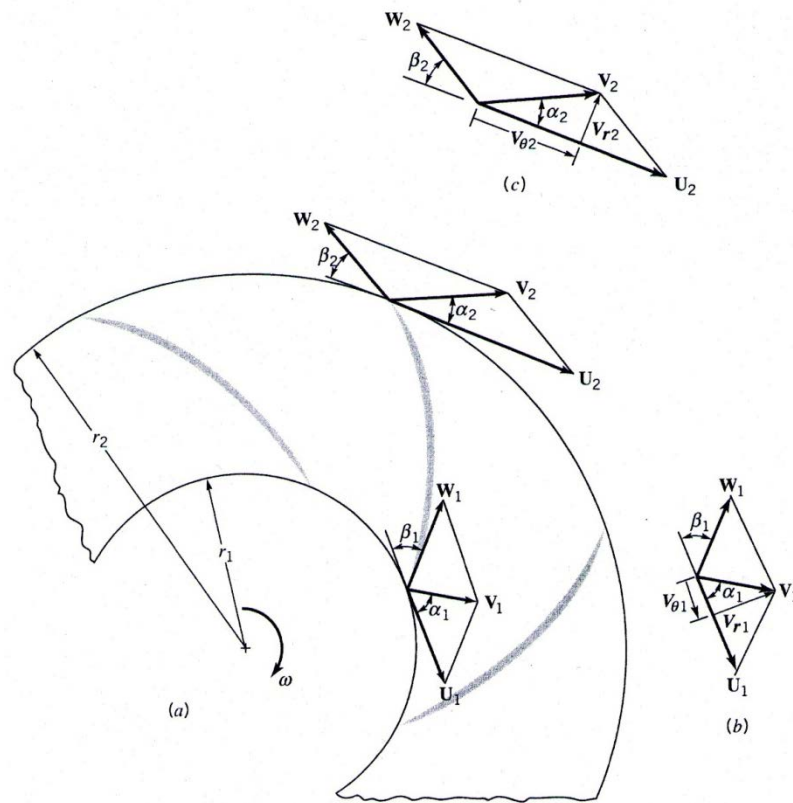


Figure 2.12: Velocity diagrams at the inlet and exit of a centrifugal pump impeller (Munson *et al.*, 2010)

2.6.6 Centrifugal pump performance

The pump performance curves, supplied by the manufacturers, are the only base of centrifugal pumps selection available for plant designers (Pullum *et al.*, 2007).

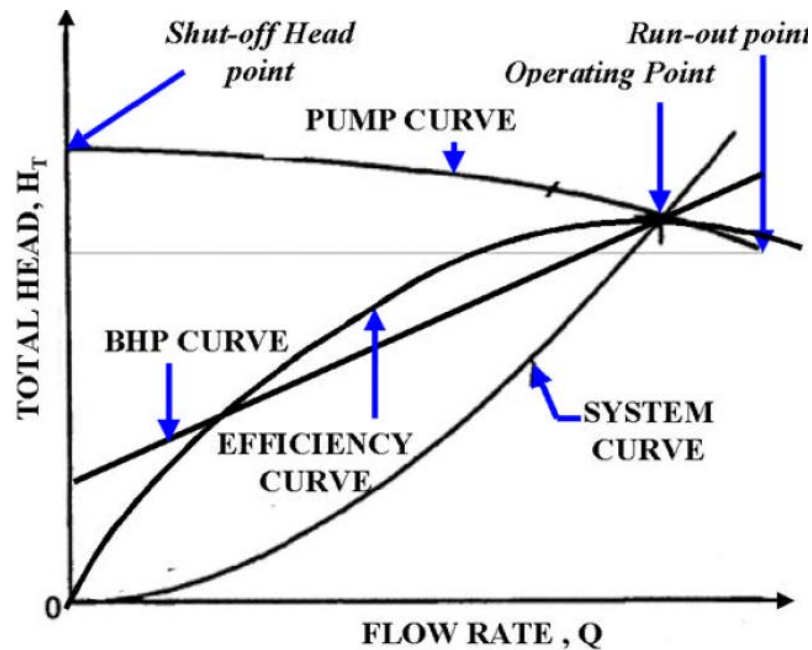


Figure 2.13: Pump performance curve for a single angular speed (Sahdev, 2007)

The performance characteristics for a given pump geometry and operating speed are usually given in the form of a graph encompassing head/flow rate curves, efficiency/flow rate curves and input power/flow rate curves (Figure 2.13). Those curves are established by experimental measurement, using water as reference liquid (Abulnaga, 2002).

The curves shown in Figure 2.13 refer to a single angular velocity, but if the tests are repeated with different values of N , all the points shift. This behaviour can be plotted as a series of $H-Q$ curves for various angular speeds, with contours of efficiency and power added, as shown in Figure 2.14 (Warman Africa).

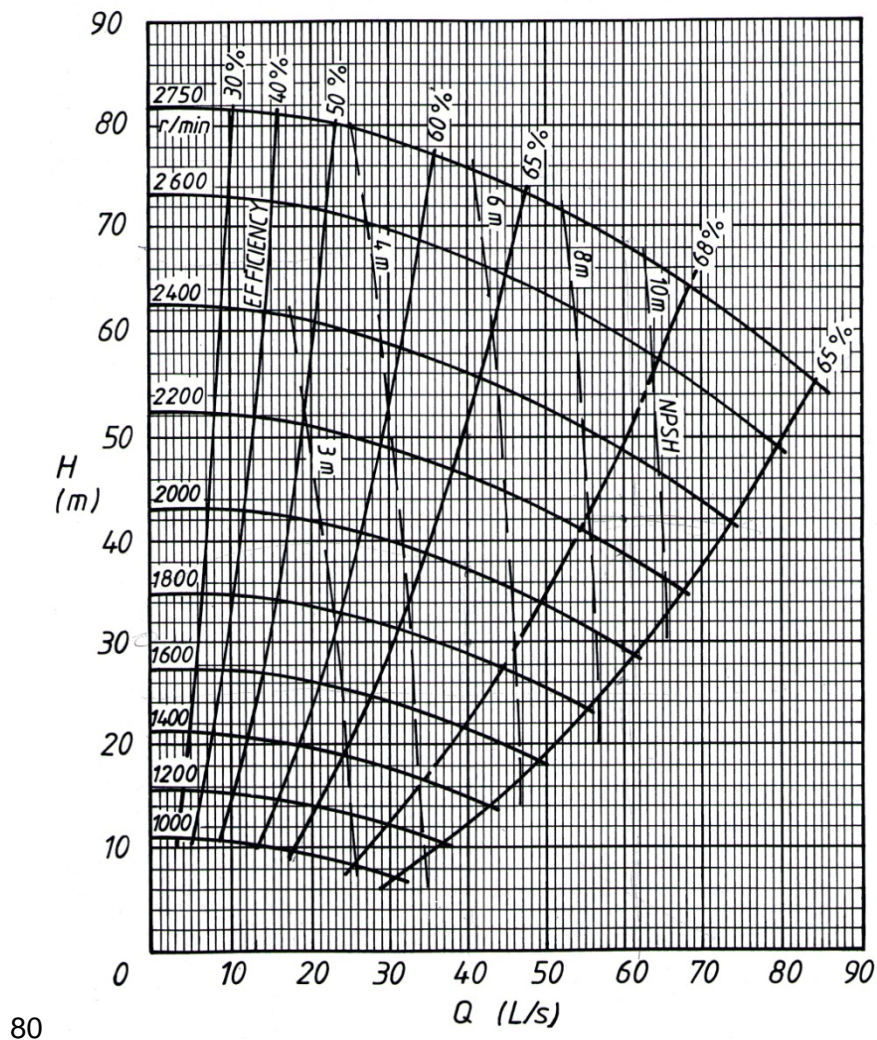


Figure 2.14: Typical published centrifugal pump performance curves (Warman Africa, curve book No. 1564)

2.7 CENTRIFUGAL PUMP DERATING

The performance of centrifugal pumps is affected when handling liquids more viscous than water. An increase in power, a reduction in head and efficiency (and some reduction in capacity) occur with liquids of moderate and high viscosities (Hydraulic Institute, 1983). Figure 2.15 shows the effect of the slurry concentration on the pump performance.

It is critically important that, when designing a pipeline for viscous materials, the corrected pump performance is taken into account.

The reduction in head developed and pump efficiency is quantified by the following ratios, for a given pump speed and flow rate (Sellgren *et al.*, 1999):

Head ratio:

$$H_R = \frac{H_m}{H_w}, \quad \text{Equation 2.56}$$

Efficiency ratio:

$$E_R = \frac{\eta_m}{\eta_w}, \quad \text{Equation 2.57}$$

where: H_m = head generated when pumping slurry

H_w = head generated when pumping water

η_m = efficiency when pumping slurry

η_w = efficiency when pumping water.

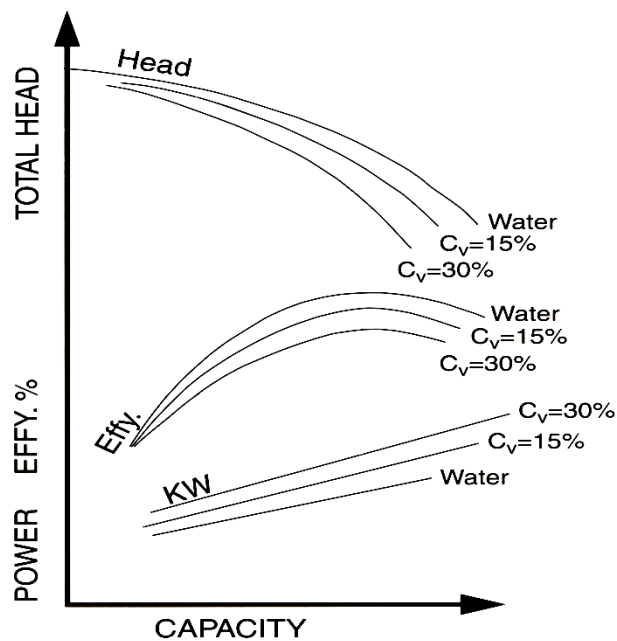


Figure 2.15: Effect of concentration on the pump performance (Angel & Crisswell, 1997)

2.7.1 Pump derating for Newtonian fluid: Hydraulic Institute Method

The HI method is a method used to predict the performance of a conventional centrifugal pump handling a viscous Newtonian fluid, when its performance for water is known (Hydraulic Institute, 1983).

The procedure consists of estimating the pump performance for viscous liquids, using the water pump performance. The correction factors C_Q , C_H and C_η are to be calculated for flow rate, head and efficiency respectively. Equations 2.58 to 2.66 are based on empirical considerations (ANSI/HI 9.6.7. 2004).

The parameter B , based on the water performance best efficiency flow, is determined in the first place, using Equation 2.58 below:

$$B = 16.5 * \frac{(v_{vis})^{0.50} * (H_{BEP-W})^{0.0625}}{(Q_{BEP-W})^{0.375} * N^{0.25}} . \quad \text{Equation 2.58}$$

The factor C_Q is then determined using Equation 2.59:

$$C_Q = (2.71)^{-0.165 * (\log B)^{3.15}} . \quad \text{Equation 2.59}$$

The flow rate of a viscous material is then given by Equation 2.60:

$$Q_{vis} = C_Q * Q_W . \quad \text{Equation 2.60}$$

Equation 2.61 is used to calculate the head correction factor C_H :

$$C_H = 1 - \left[(1 - C_Q) * \left(\frac{Q_W}{Q_{BEP-W}} \right)^{0.75} \right] . \quad \text{Equation 2.61}$$

The head of the viscous material is obtained using Equation 2.62:

$$H_{vis} = C_H * H_W . \quad \text{Equation 2.62}$$

The efficiency correction factor is given by Equation 2.63 for $1.0 < B < 40$ or Equation 2.64 for $B \leq 1.0$.

$$C_{\eta} = B^{-(0.0547 * B^{0.69})}. \quad \text{Equation 2.63}$$

$$C_{\eta} = \frac{1 - \left[(1 - \eta_{\text{BEP-W}}) * \left(\frac{v_{\text{vis}}}{v_{\text{W}}} \right)^{0.07} \right]}{\eta_{\text{BEP-W}}}. \quad \text{Equation 2.64}$$

Therefore, the pump efficiency for viscous materials can be established using Equation 2.65:

$$\eta_{\text{vis}} = C_{\eta} * \eta_{\text{W}}. \quad \text{Equation 2.65}$$

The pump power (P_{vis}) for viscous materials can then be obtained using Equation 2.66:

$$P_{\text{vis}} = \frac{Q_{\text{vis}} * H_{\text{BEP-vis}} * \rho * g}{367 * \eta_{\text{vis}}}. \quad \text{Equation 2.66}$$

Note: - For $B > 40$, $H_{\text{vis}} = H_{\text{W}}$ and $Q_{\text{vis}} = Q_{\text{W}}$

To avoid long calculations, a nomogram called the “Hydraulic Institute Chart” (Figure 2.16) has been compiled to estimate the correction factors. This chart includes two diagrams for correcting liquid viscosity. The first diagram (bottom part) employs the water flow rate at BEP. Using the pumping head at BEP and the kinematic viscosity of the liquid pumped, this diagram provides a rate correlation parameter. This parameter serves as the independent variable in the second diagram (top part) from which the correction factors C_h , C_q , and C_{η} are determined (Hydraulic Institute, 1983). Four different values of C_h corresponding to 60%Q_{bep}, 80%Q_{bep}, 100%Q_{bep} and 120%Q_{bep} respectively are presented.

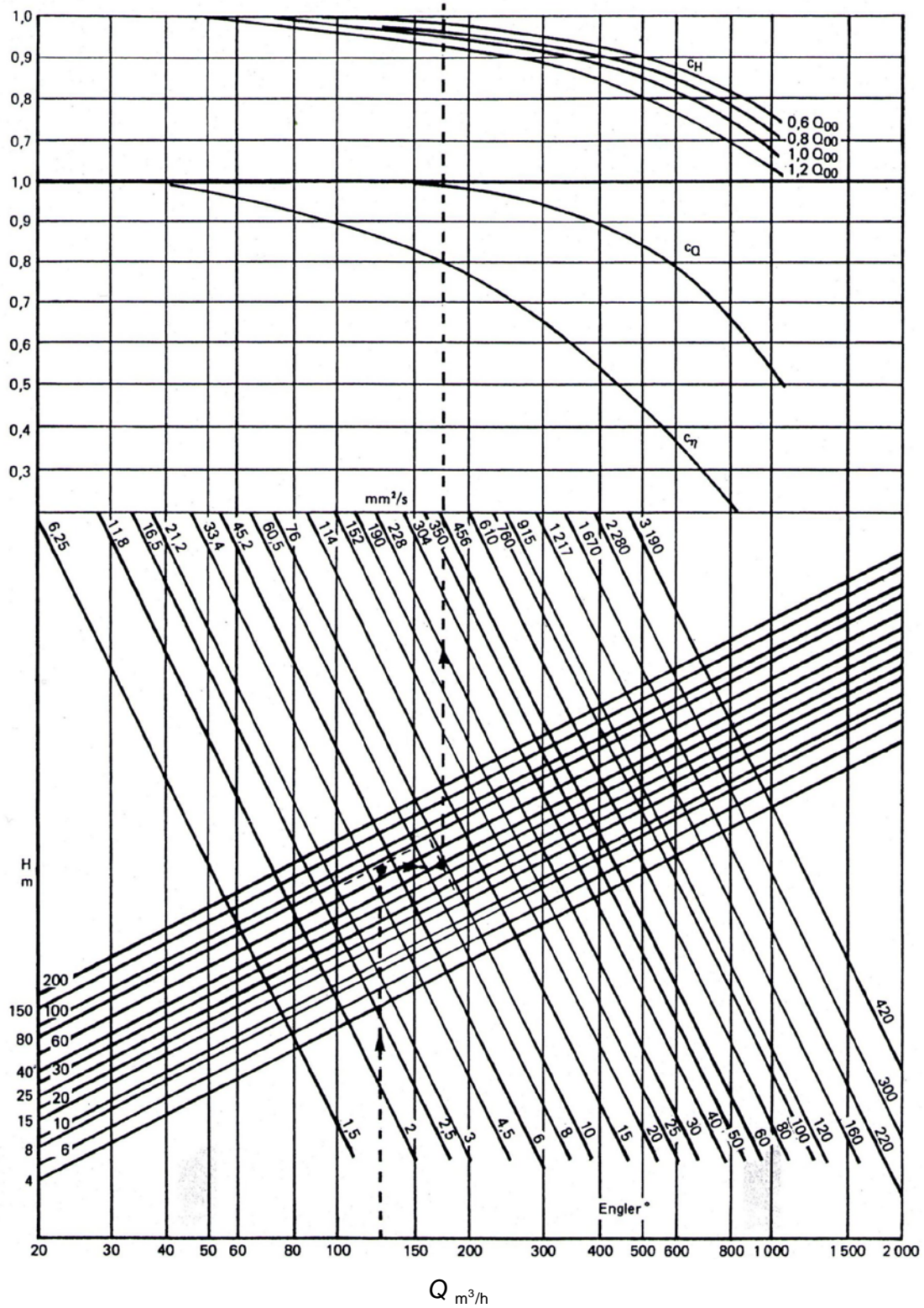


Figure 2.16: Hydraulic Institute Chart (Hydraulic Institute, 1983)

The outcome of the chart is then used to predict the pump performance for viscous Newtonian materials. Equations 2.60, 2.62 and 2.65 will be used to calculate, respectively, the flow rate, the head and efficiency for the viscous materials.

2.7.2 The use of Hydraulic Institute method for non-Newtonian fluids

The pump performance prediction for Newtonian fluids has been well established by using the HI method. For non-Newtonian fluids and complex suspensions, however, there is no generally accepted method to predict the pump performance.

Many authors have fallen back on using the HI method to try to fix the problem of predicting the pump performance for non-Newtonian materials. The question “what viscosity to be used in the nomogram” (Figure 2.16) arises as non-Newtonian fluid viscosity changes with the shear rate. In an attempt to answer this question, the following approaches have been developed.

2.7.2.1 Pump derating using Bingham plastic viscosity

The Walker and Goulas (1984) approach consists of modelling a fluid as a Bingham plastic, by fitting the rheogram with a straight line at high shear rates (above 100 s^{-1}). The gradient of this line is the value of Bingham plastic viscosity to be used in the HI method.

2.7.2.2 Pump derating using an equivalent hydraulic pipe

Pullum *et al.* (2007) state that the use of the Bingham plastic viscosity has no fundamental rheological meaning. They believe that it is the flow of the material through the pump that dictates the fluid viscosity and they noticed that for most of the flow of materials with an appreciable viscosity, the regime in the rotor passages is laminar. Therefore the flow throughout the pump is considered as laminar flow through a conduit called an “equivalent hydraulic pipe”.

a) Pullum *et al.* (2007) approach

The approach adopted was to determine the diameter of the equivalent hydraulic pipe for the pump based on the pump’s main dimensions. The diameter of this pipe was given by Equation 2.67.

$$D_h = \frac{4w\pi D_{imp}}{2(\pi D_{imp} + w)}, \quad \text{Equation 2.67}$$

where w is a characteristic dimension to be determined experimentally.

This diameter and the flow rate of interest were then used to determine the fluid velocity through the equivalent hydraulic pipe.

$$V = \frac{4Q}{\pi D_h^2}. \quad \text{Equation 2.68}$$

For the laminar flow, the true shear rate at the wall of this pipe was then obtained from the Rabinowitsch-Mooney relationship.

$$\dot{\gamma} = \left(\frac{3n'+1}{4n'} \right) \frac{8V}{D_h}, \quad \text{Equation 2.69}$$

where n' is the gradient of the curve $\ln(\tau_o)/\ln(8V/D_h)$ obtained from the rheogram of choice.

The shear stress corresponding to the true shear rate was calculated, using this shear rate in the equation of the fluid rheogram. From these two elements, an apparent viscosity was determined and used in the HI method to predict the pump performance.

b) Determination of the characteristic dimension w

Complete data sets of experimental pump head, for non-Newtonian fluids of the expected range of rheologies, are required to determine the characteristic dimension value for a particular centrifugal pump (Graham *et al.*, 2009). The modified HI procedure is applied to these data sets as detailed above and the corrected pump head data are calculated for all data sets.

The value of w which minimises the error between the experimental data and that calculated is considered as the characteristic dimension w . This characteristic dimension can then be used for other non-Newtonian fluids being pumped by the same pump (Graham *et al.*, 2009).

2.8 PREVIOUS WORKS AND RESEARCH ASPECTS IDENTIFIED

There are only a few papers in the literature which deal with the problem of non-Newtonian pump derating (Pullum *et al.*, 2007). It was observed that pump derating procedures for slurry from its water performance characteristics are at best empirical (Wonnacott, 1993). Works relevant to this project, done in this domain, will be reviewed in this section.

2.8.1 Works using the Walker and Goulas (1984) approach

2.8.1.1 Walker and Goulas (1984)

In their work, Walker and Goulas investigated the change in pump performance characteristics, using two different centrifugal slurry pumps handling a mixture of coal/water and kaolin/water.

The results show that the pump performance is dependent on the slurry's rheological properties. The loss of head and efficiency at higher flow rates seems to depend on the plastic viscosity obtained at high shear rates. Using the Bingham plastic viscosity instead of the dynamic viscosity in the Hydraulics Institute Chart, for the prediction, Walker and Goulas found that most of the tested points lie within $\pm 5\%$ of the predicted values for the head and efficiency (Figures 2.17 and 2.18).

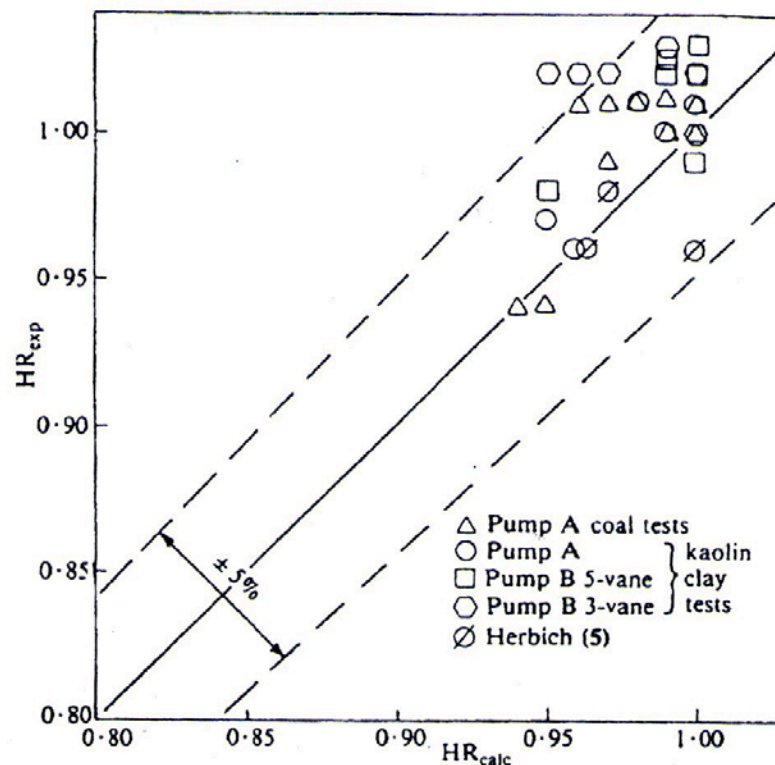


Figure 2.17: Experimental HR against calculated values from HI Chart (Walker & Goulas, 1984)

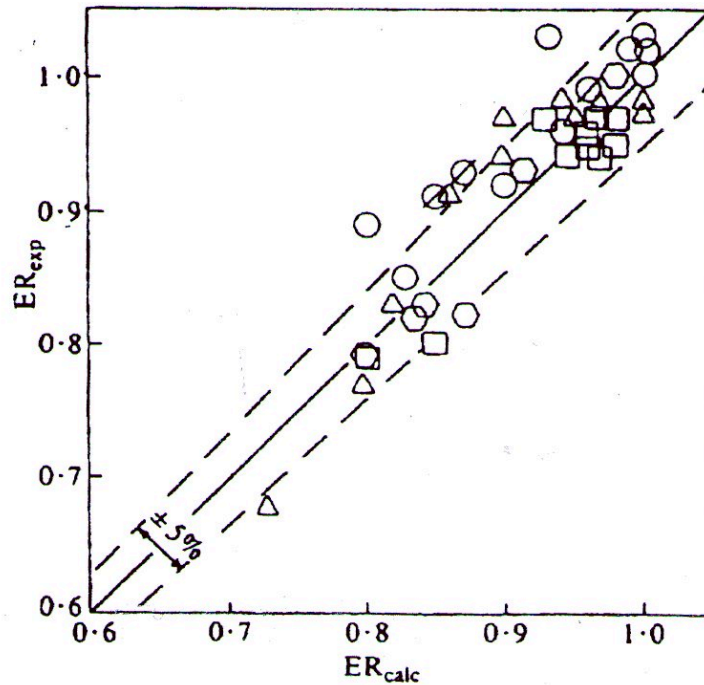


Figure 2.18: Experimental ER against calculated values from HI Chart (Walker & Goulas, 1984)

2.8.1.2 Sery and Slatter (2002)

Sery and Slatter (2002) also presented work on non-Newtonian centrifugal pump derating, using the Bingham plastic viscosity in the HI method. A Warman 4/3 pump was tested using glycerine and kaolin slurries.

The head and efficiency values were predicted within a margin of $\pm 20\%$ and $\pm 10\%$ respectively.

2.8.1.3 Kabamba (2006)

Kabamba (2006) continued with the work started by Sery and Slatter (2002). Two different pumps were used: a GIW 4/3 and a Warman 6/4. Three different materials of different concentrations were used: kaolin and bentonite suspensions, and CMC solution.

Kabamba (2006) used the Bingham plastic viscosity in the HI method to predict the pump performance at high shear rate (around BEP). The head and efficiency were both predicted within a margin of $\pm 15\%$ for the GIW 4/3 pump while for the Warman 6/4 pump, the performance was predicted as follows: $\pm 10\%$ for the head and $\pm 20\%$ for the efficiency.

2.8.2 Work published using the Pullum *et al.* (2007) approach

Pullum *et al.* (2007) conducted centrifugal pump tests on a wide range of highly concentrated non-Newtonian coarse particle suspensions. Two fluids: the aqueous polymer solution of CMC and Ultrez 10 were used as carrier fluids, to test two centrifugal pumps: a GIW 4/3 LCC-M80-30 and a Warman 4/3 AH.

The values of characteristic dimension were $w = 0.059$ for the Warman 4/3 and $w = 0.084$ for the GIW 4/3.

For the fluids and pumps used, Pullum *et al.* (2007) stated that for the test fluids the head developed was generally about 25% less than that of water. In addition, they observed that the ratio of the characteristic dimension to the impeller diameter was similar for both pumps and the average value of this ratio was about 25% ($w/D_{imp} = 25\%$). This ratio was confirmed with many examples by Graham *et al.* (2009).

In their papers, (Pullum *et al.*, 2007) and (Graham *et al.*, 2009) predicted only the head for both pumps. Most of the tested points were within $\pm 10\%$ of the predicted values (see Figures 2.19 and 2.20).

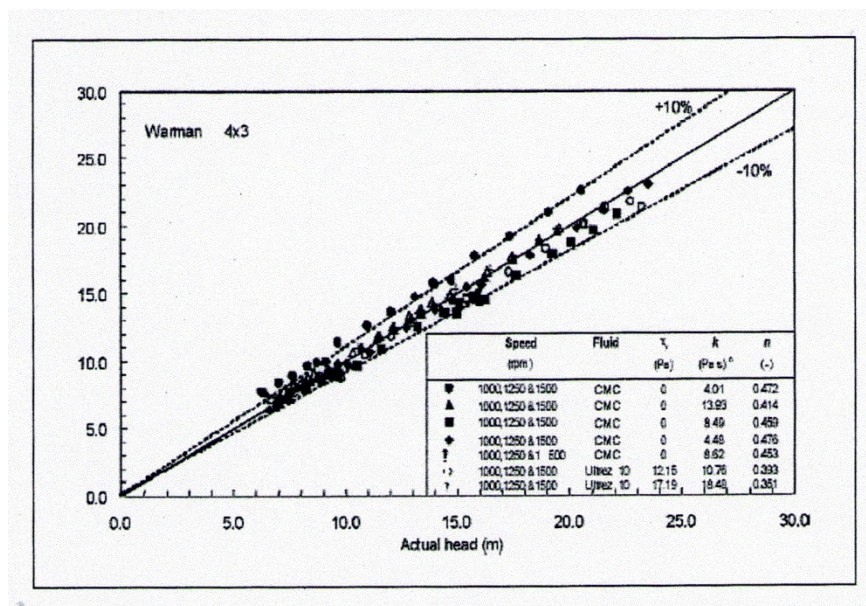


Figure 2.19: Calculated head versus experimental head for Warman 4/3 pump (Pullum *et al.*, 2007)

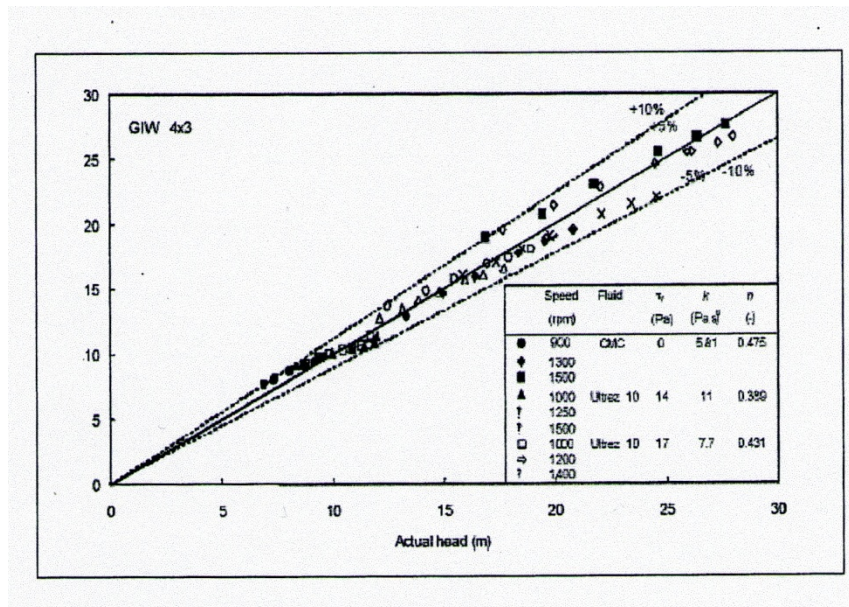


Figure 2.20: Calculated head versus experimental head for GIW 4/3 pump (Pullum *et al.*, 2007)

In their third paper (Pullum *et al.*, 2011), where many more data sets from the open literature were included, the authors stated (in the conclusions) that the pump efficiency was predicted within 10% of the actual values. However, only Figure 2.21 below was presented as efficiency prediction results.

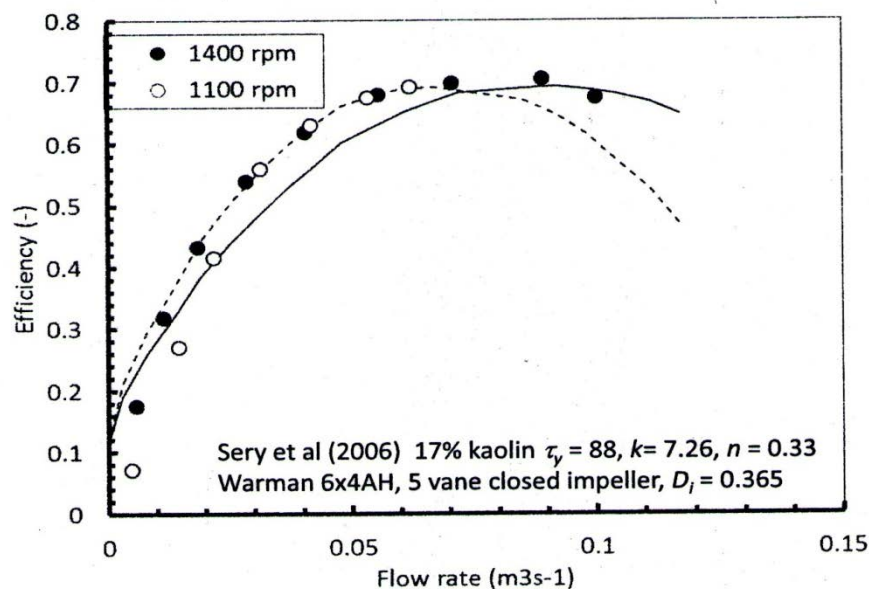


Figure 2.21: Comparison between the predicted and experimental pump efficiency for the Sery *et al.* 17% kaolin slurry (Pullum *et al.*, 2011)

2.8.3 Research aspects identified

From the literature reviewed for the non-Newtonian pump derating, the following can be highlighted:

- There is no agreement in the results obtained in the different works using the Bingham plastic viscosity (Walker & Goulas (1984) approach) to predict the pump performance; furthermore none of these have reached the same results as the Walker and Goulas (1984) work for both head and efficiency prediction.
- On the other hand, the Pullum *et al.* (2007) work, although using the apparent viscosity calculated based on the rotor passage geometry, flow rate and fluid rheology, has still shown results (of $\pm 10\%$ error margin) less accurate than those of the Walker and Goulas (1984) prediction ($\pm 5\%$ error margin) for the pump head. Moreover the efficiency prediction is not clearly established in the Pullum *et al.* (2007) approach.

The above considerations justify the need to compare the two approaches by applying them to the same data sets to predict the non-Newtonian pump performance using the HI method.

2.9 CONCLUSION

In this chapter, some basic concepts of fluid mechanics have been presented. The flow of material through straight pipes has been explained for both Newtonian and non-Newtonian fluids. Basic elements of rheology relative to the behaviour of non-Newtonian materials, including the choice of rheological models and the rheological characterisation, have been reviewed. The description and working principles of a centrifugal pump, as well as viscous material effects on the pump performance have been examined. Important theory and literature relating to centrifugal pump operation and flow of material inside the pump have been presented. An overview of previous works related to the non-Newtonian pump performance prediction has been given and the research aspects prompting this study were identified.

Chapter 3 EQUIPMENT AND EXPERIMENTAL METHOD

3.1 INTRODUCTION

In this chapter, the experimental apparatus, the test procedures and materials tested in this project are described. The calibration procedures and results are presented.

The theory and calculation of different errors involved in the experimental procedures are explained. Results of the error calculation of different variables are presented.

3.2 EXPERIMENTAL RIG DESCRIPTION AND INSTRUMENTATION

The pump test rig consisted of the following:

- A mixing tank
- A pump test bay
- A tube viscometer, and
- A data acquisition system

The layout of the pump test rig is depicted by Figure 3.1 below.

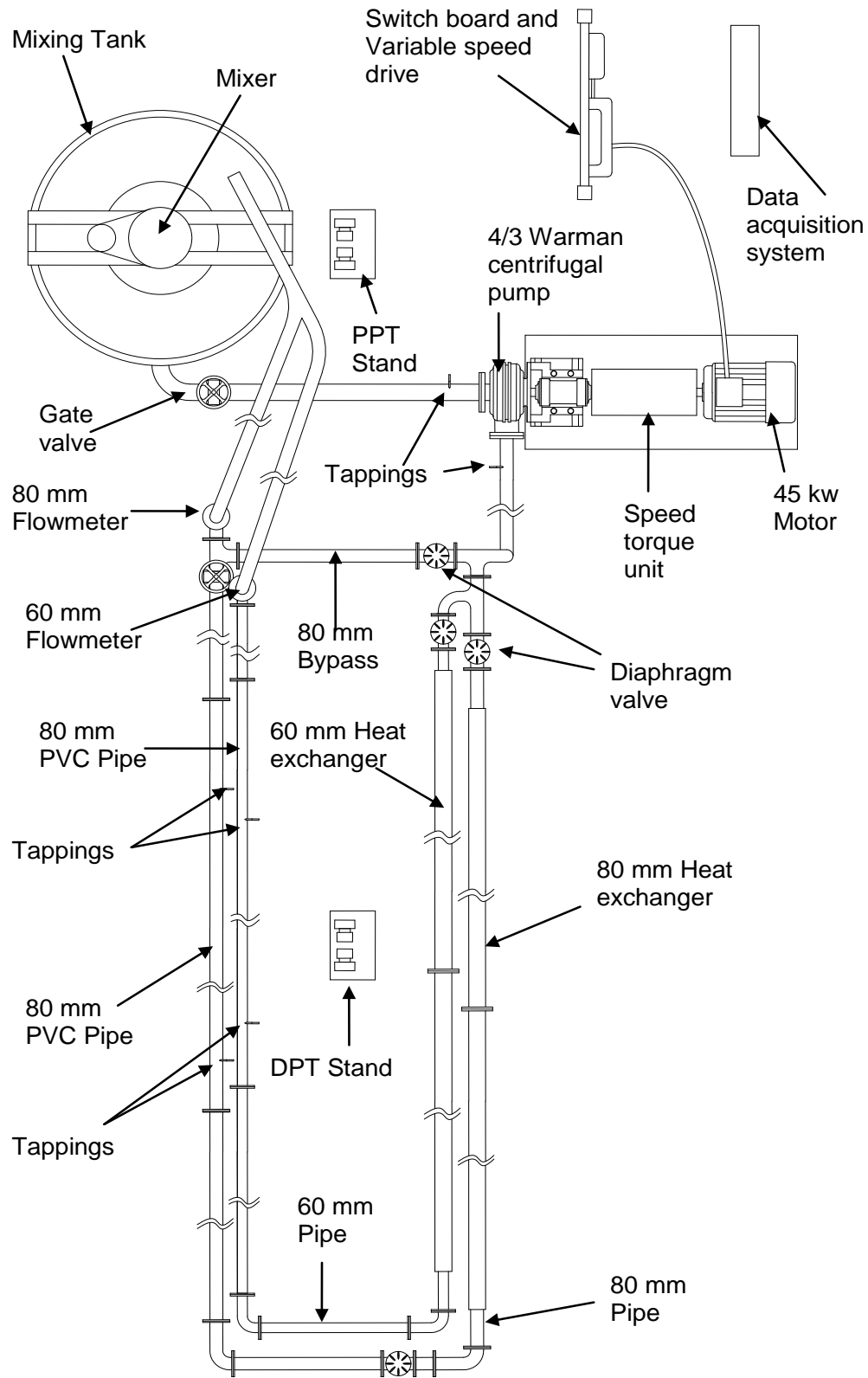


Figure 3.1: Layout of the pump test rig (top view of the rig)

3.2.1 Mixing tank

The mixing tank includes a 3.11 m³ cylindro-conical steel tank used for mixing and storage of slurries (Figure 3.2). This tank is equipped with a mixer, to ensure the homogeneity of the suspensions.

The mixer consists of:

- A squirrel cage electrical motor of 18.5 kW vertically positioned on top of the mixing tank, and
- A wheel-shaped rubber coated stirrer of 0.4 m diameter, equipped with six vanes at both side, fixed at the lower extremity of a shaft measuring 2.70 m long and 0.07m in diameter.

The mixer is run to ensure the mixture homogeneity during the slurry preparation and before and/or during each test.



Figure 3.2: Mixing tank

3.2.2 Pump test bay

This includes a centrifugal pump driven by an electrical motor connected to a speed-torque unit placed between the electrical motor and the pump shaft (Figure 3.3).

A Warman 4/3 centrifugal slurry pump was used in this project. This pump was a metal, single-stage end-suction centrifugal slurry pump.

Details of the characteristics of this pump are given in Table 3.1.

Table 3.1: Characteristics of the Warman 4/3 pump (Warman Africa)

Warman 4/3							
Pump		Impeller				Liner	Pump performance curve
Size	Type	Vanes	Types	Mat'l	Vane \varnothing	Mat'l	WPA 43 A01 Feb 1988
4/3	AH	5	Closed	Metal	245	Metal	
Gland Sealed Pump							
Frame		Norm Max Rpm		Norm Max kw		Max Particle Size (mm)	
D		2750		60		36 Sphere	



Figure 3.3: Warman 4/3 centrifugal pump

A 45 kW squirrel cage motor was used to drive the pump.

To start the motor and vary the speed, an electrical board holding both the main power switch and a 90 kW Klöckner Moeller variable-speed drive was connected to the motor.

To monitor the pump rotational speed, a 1 kN.m Kyowa speed-torque unit was placed between the pump shaft and the electrical motor. The characteristics of this speed-torque unit are as follows:

- Type TP-100K MAB, and
- Serial number 3X0580001

As the pump shaft was coupled with the speed-torque unit, the pump rotational speed was measured by recording the rotational speed (in RPM) of the speed-torque unit, using a digital meter.

The centrifugal pump test requires the measurement of the pressure at the pump inlet and outlet. Therefore, tapings were placed at the pump inlet and outlet at twice the distance of the suction or discharge internal pipe diameter ($2D$) from the flanges, to allow the flow of the tested materials to become steady.

Each tapping was connected to a PPT of the type FHPW03V1-AKCYOY-OY Fuji Electric (Figure 3.4), of maximum pressure 3000 kPa and 0.25 % accuracy. A compound vacuum-positive PPT was connected to the pump inlet, and a positive PPT to the outlet. The range of the inlet PPT was set up from -100 to 200 kPa and that of the outlet from 0 to 1500 kPa.



Figure 3.4: Point Pressure Transducer (PPT)

3.2.3 Tube viscometer

3.2.3.1 Pipe loop

The tube viscometer was composed of two metallic pipe loops of 65 mm and 80 mm inner diameter respectively. These loops were fixed horizontally with a vertical section at the end to discharge the test liquids in the tank. Each pipe loop included:

- A portion of PVC pipe of same diameter on the horizontal return line, with two tapping points connected to the differential pressure transducers (DPT).
- A valve placed at the beginning of the loop to control the flow rate.
- A flow meter mounted in the vertical pipe.

- A jacket made of a bigger diameter metallic pipe surrounding the long straight metallic portion of the loop. This jacket was connected to the cooling system.

For the pump test, a bypass was available, allowing fluid recirculation without feeding the horizontal part of the pipe loop.

3.2.3.2 Differential pressure transducer (DPT)

Two Fuji electric DPTs (Figure 3.5) were used to measure the differential pressure between the two tapping points made on each straight PVC pipe, for the rheology. A type FHKW12V1-AKCYY-AA was used as a low DPT and a type FHKW37V1-AKCYY-AA as a high DPT.

The DPT was supplied with a maximum voltage of 28V DC and the current output was from 4 to 20mA. The experimental range was set from 0 to 130 kPa for the high DPT and from 0 to 6 kPa for the low DPT. The two tapping points on each PVC portion of pipe were made over a fixed distance:

- 2.5 m for the 80 mm diameter pipe and
- 3 m for the 65 mm diameter pipe.

A valve was fixed on the pipe at each tapping to allow the connection with the pressure transducer. The DPT was then connected to the tappings with nylon tubes of 3 mm inner diameter. Each nylon tube was intercepted by a pod, to prevent slurry from reaching and damaging the DPT. Each pod had two valves: a top valve for flushing the line and removing air bubbles and a bottom valve to flush away the collected solids.



Figure 3.5: Differential Pressure Transducers (DPTs)

3.2.3.3 Flow meter

In the vertical return line of each pipe a flow meter was mounted. Krohne IFC 300 OPTIFLUX flow meters (Figure 3.6) were fitted to both the 65 mm and 80 mm pipes. The outputs of these instruments were logged automatically on the computer via the data acquisition unit.



Figure 3.6: Magnetic flow meters

3.2.3.4 Cooling system

The cooling system comprised a cooling tower, metallic pipes and jackets surrounding the metallic straight test pipes from the pumps. The cooling tower fed the jackets with cold water through metallic pipes of 50 mm inner diameter. This water was pumped and recirculated in the opposite direction to that of the tested materials to facilitate the heat exchange between the tested materials (high temperature, around 50°C) and water (low temperature, around 20°C).

3.2.4 Data acquisition system

3.2.4.1 Data acquisition unit (DAU)

An Agilent 34970A data acquisition unit was used to monitor and convert analogue electrical signals, from sensors, into digital signals suitable for processing by the computer. Several channels are available in the DAU to allow it to deal separately with analogue signals from different sensors.

3.2.4.2 Computer

The digital signals from the DAU are recorded, processed and stored in an Intel Celeron 2.40 GHZ, 260 RAM personal computer.

The test programs are written in Visual Basic 6. In these programs, Microsoft Excel spreadsheets are set up to receive and process data. Calculations are made to convert digital numbers, corresponding to the analogue electrical signals, into magnitude (pressure or flow) using calibration values.

3.2.5 Other apparatus

3.2.5.1 Hand-held communicator (HHC)

During the calibration of the DPT or PPT, a FXW 10 AY1-A3 type of multifunction Fuji electric hand-held communicator (Figure 3.7) was used to change the range and double check the pressure readings. The HHC allowed the comparison of data displayed with the values generated by the test program, after calibration.



Figure 3.7: Hand-Held Communicator (HHC)

3.2.5.2 Air pump

When calibrating pressure transducers, an air pump equipped with a digital manometer was used to vary the pressure in the pressure transducer.

3.2.5.3 Tachometer

A tachometer (Figure 3.8) was used to double-check the pump rotational speed.



Figure 3.8: Tachometer

3.3 EXPERIMENTAL PROCEDURES

The experimental procedures required various operations of which the three most important were: the calibration of instruments, the determination of fluid viscous properties, and the determination of pump performance.

3.3.1 Calibration of the instruments

The reliability of the result from this experimental work relies on the accurate calibration of the instruments.

3.3.1.1 DPT calibration

The two DPTs used for the differential pressure measurement were calibrated using an air pump (equipped with a digital manometer) and the hand-held communicator. The low DPT is set to operate in the range from 0 to 6 kPa while the high DPT is set to function in the range from 0 to 130 kPa. Different steps of the calibration procedure are as follows:

- The DAU is switched on to the channel corresponding to the DPT.

- The DPT is set to zero.
- All the nylon tubes are disconnected from the DPT to release any pressure induced by the system and to expose the DPT to the atmospheric pressure.
- The HHC is connected to the DPT and switched on. The DPT is set to the required range of pressure (0 - 6 kPa or 0 - 130 kPa) and then the HHC is set on data recording mode. The reading of the HHC is zero and the voltage recorded by the DAU is considered as the zero mark.
- The air pump is connected to the high pressure side of the DPT and the pressure is applied up to the maximum pressure of the range. The readings of both pressure on the HHC (and/or manometer) and voltage on the DAU are recorded.
- The pressure is decreased progressively and both the pressure and voltage readings are recorded.
- The pressure readings are plotted against the voltage readings.

The calibration values are obtained by performing a linear regression on the plot of pressure versus transducer DC voltage output. The coefficient of correlation R^2 has to be better than 0.999. Figures 3.9 and 3.10 are typical results of the DPT calibration.

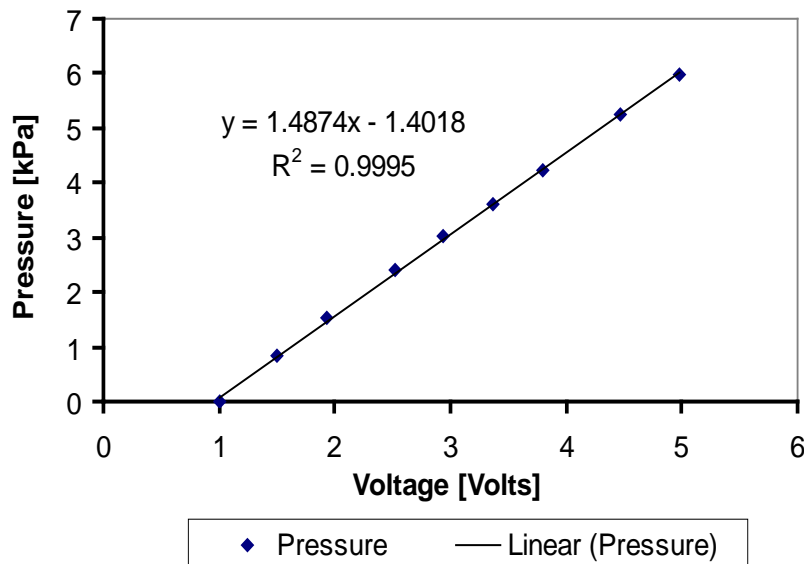


Figure 3.9: Calibration graph for the low DPT

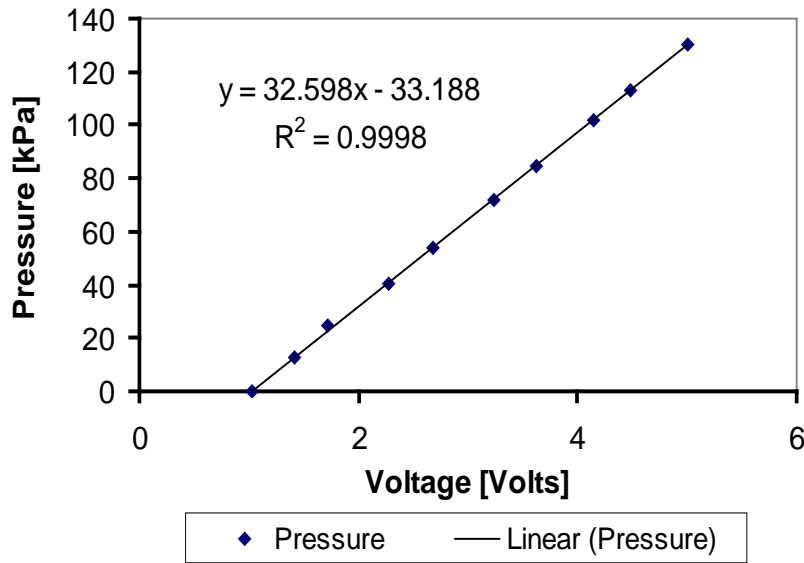


Figure 3.10: Calibration graph for the high DPT

3.3.1.2 PPT calibration

The PPT calibration followed the same steps as for the DPT. The PPT is connected to the pump discharge and calibrated using the HHC and the air compressor capable of supplying the pressure up to 1500 kPa. The plot of the PPT output voltage versus the HHC pressure reading is depicted in Figure 3.11.

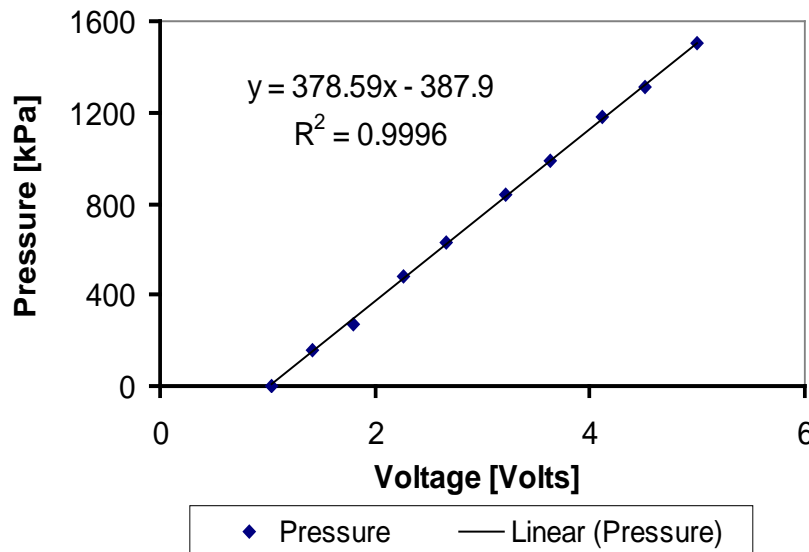


Figure 3.11: Calibration graph for the PPT at the pump outlet

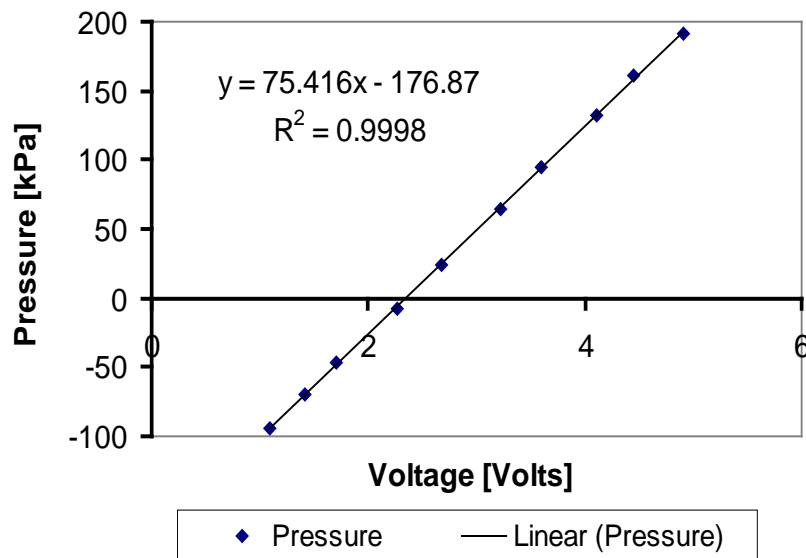


Figure 3.12: Calibration graph for the PPT at the pump inlet

For the PPT connected to the pump suction side, the calibration requires two different operations, as it has to function from negative values (-100 kPa) to positive values (200 kPa). For the positive values, the procedure above is repeated. For the negative values, a vacuum pump is used to apply negative pressure up to -75 kPa. A common plot of the PPT output voltage versus the HHC pressure readings, for the positive and negative values, is compiled to obtain the calibration factors (Figure 3.12).

3.3.1.3 Flow meter calibration

The flow meter accuracy is 0.5% for a velocity < 0.5 m/s and 0.025% of full scale for a velocity > 0.5 m/s according to the manufacturer's catalogue.

The maximum capacity is set at 60 l/s for the 80 mm flow meter and 35 l/s for the 65 mm flow meter. To obtain the calibration values, 0 l/s corresponds to 1 V and the maximum flow rate to 5V.

3.3.1.4 Speed-torque unit calibration

The speed-torque unit calibration consisted of correlating the data logger voltages to the torque displayed. The calibration values are obtained from a linear regression and stored in the computer to be used during the tests. The speed is not calibrated but double-checked using a tachometer.

3.3.2 Pressure gradient test

This test consists of measuring, at the same time, the pressure drop across a known length of straight pipe and the fluid flow rate while the fluid is pumped and recirculated in the pipe loop.

3.3.2.1 Water pressure gradient test

The pressure gradient test is performed first with water to check the equipment and pipe roughness. To ensure the reliability of the measured values, these are compared with the Colebrook-White equation. The experimental points (shear stress versus velocity τ_o -V) are plotted on the same graph with the theoretical Colebrook-White curve. These points must fall in the zone of $\pm 5\%$ margin of the theoretical curve for a reliable pressure gradient test. This test is performed for the two pipes separately.

With this procedure, it is possible to estimate the pipe roughness, which is the value that allows the points to fall in the zone of $\pm 5\%$ margin. An example is presented in Figure 3.13.

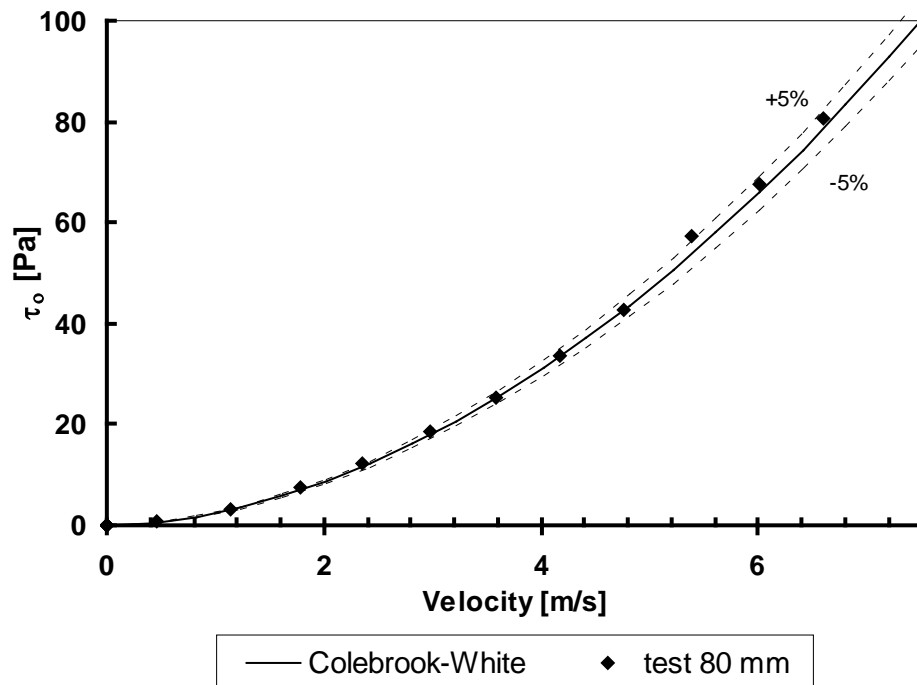


Figure 3.13: Example of water pressure gradient test result compared with Colebrook-White curve

3.3.2.2 Rheological test

This test is exactly the same as the water pressure gradient test but uses slurries. Each concentration of each material is tested in two pipes. Results of the two pipes are plotted on the same graph (shear stress versus pseudo-shear rate) ($\tau_o - 8V/D$) called “pseudo-shear diagram”.

The laminar zone of each pipe test data is used to determine the rheological parameters. Figure 3.14 is an example of a pseudo-shear diagram.

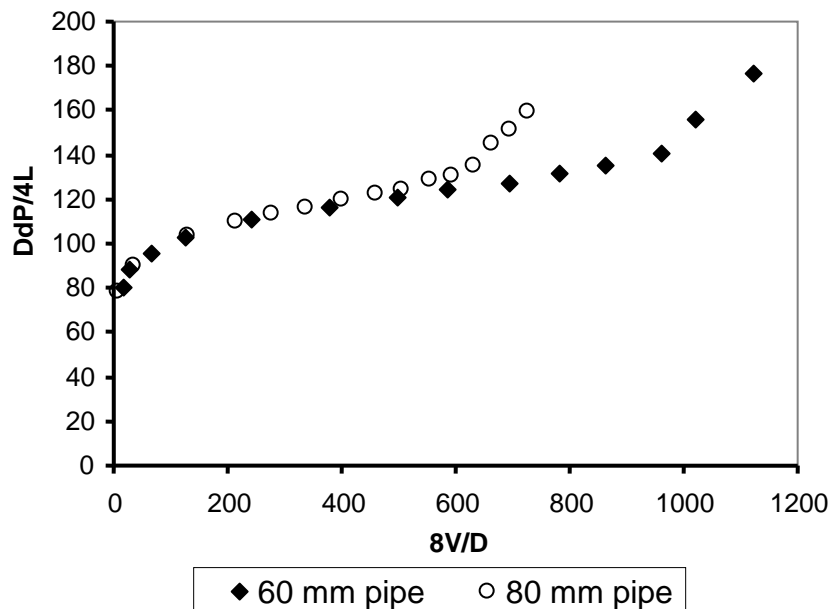


Figure 3.14: Example of pseudo-shear diagram for kaolin 24%

3.3.3 Pump performance test

The purpose of this test is to establish the performance of the pump when pumping different materials. This performance is expressed as the plot of head, efficiency and power versus flow rate. The pump performance test procedure is as follows:

- Warming up of the equipment by pumping and recirculating the fluid tested through the rig for at least 30 minutes to ensure good homogeneity of the mixture.
- A representative sample is taken through a sampling tap to measure the relative density.
- The fluid is then pumped and recirculated using the bypass.
- The reading of measurement starts after flushing the system, setting all the parameters in the computer program and selecting the pump speed. The speed is kept constant

while the flow rate is decreased (from fully open to fully closed) or increased using the valve.

- The speed is changed after accomplishing the cycle of the valve. Five different speeds are used.
- Data are recorded on an Excel spreadsheet and processed to obtain the plot of performance for each speed. The typical example of these plots is show in Figure 3.15.
- The procedure is repeated for the different materials.

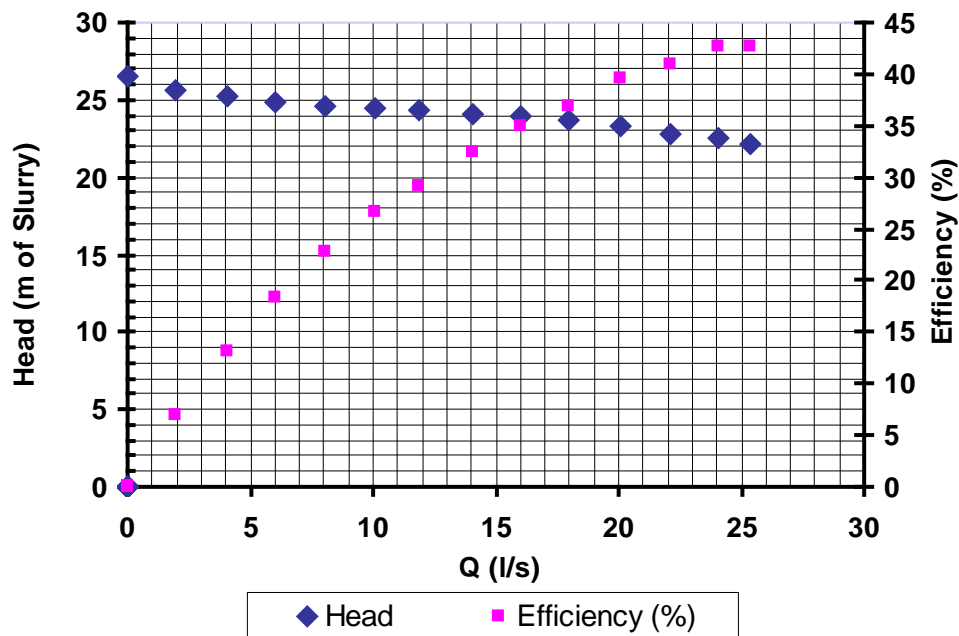


Figure 3.15: Example of pump performance results for the Warman 4/3 pump at 1600 rpm

3.4 MATERIALS TESTED

The following materials were tested to complete this study: water, kaolin in water suspension and CMC in water solution.

3.4.1 Water

Water was used for the calibration test in both the pump and pressure gradient test rig. In the straight pipe water was used for the purpose of the instrumentation calibration and in the pump test for the comparison of pump performance with the catalogue curves supplied by the manufacturer.

3.4.2 Kaolin suspension

The kaolin suspension was prepared by mixing the dry white kaolin powder with the tap water. A mixer was used to obtain a homogenous suspension. Four different volumetric concentrations were tested: 21%, 24%, 28% and 30%.

3.4.3 CMC solution

The CMC was supplied, by Protea Chemicals, in the form of yellowish powder, easily soluble in water at low concentrations.

The CMC solution was prepared by mixing the yellowish powder with tap water. The CMC was spread progressively, in small quantities, over the surface of agitated tap water to avoid the formation of lumps. The concentrations of 5%, 8% and 9% (weight-by-weight) were used in this study. The materials were mixed for at least 48 hours before testing to obtain satisfactory homogeneity. As the material could change with time owing to evaporation, the relative density test was performed before every pump test.

3.5 EXPERIMENTAL ERRORS

Experimental works always involve some degree of uncertainty in the measured and computed variables, when they are carried out. The evaluation of the magnitude of these uncertainties is a very critical task for the reliability of the data obtained. A brief theory of errors is presented in this section, as well as the experimental errors encountered in this study.

3.5.1 Error theory

There is no absolute accuracy whenever measurements are made, except when discrete numbers are dealt with. It is, therefore, necessary to determine the error margins affecting measurements and to evaluate the accuracy and precision of particular measured quantity (Barry, 1991). The first step in evaluating the reliability of experimental measurements is to examine the causes and types of errors. Errors are usually classified by three types (Benzinger & Aksay, 1999).

3.5.1.1 Gross errors

These errors result from blunders, equipment failure and/or power failures. A gross error is immediate cause for rejection of a measurement (Benzinger & Aksay, 1999).

3.5.1.2 Systematic errors

Systematic errors result in a constant bias in an experimental measurement. They are due to known conditions and vary with these conditions. These conditions might be:

- Natural (temperature, moisture, atmospheric pressure...).
- Instrumental (calibration, range, graduation...).
- Personal-physical limitations (poor ability in noting time at the beginning and the end of intervals when using a stopwatch, poor ability of reading correct value of length).

The following precautionary procedures were applied to prevent occurrence of this type of error in this project:

- Only calibration constants obtained with a correlation coefficient of better than $R^2 = 0.999$ were considered.
- Measurements were repeated at least three times.

3.5.1.3 Random errors

Most experiments proceed with minor variations that change from event to event and follow no systematic trends. Random errors are due to these minor variations. These errors make the same quantity, measured many times, to give close but not identical results. They have a tendency to be mutually compensating and are random in occurrence and size. Generally, the distribution of values will be assumed to follow a normal or Gaussian distribution (Benzinger & Aksay, 1999).

This type of error is evaluated only by studying the discrepancies that occur among repeated measurements of the same quantity (Barry, 1991).

3.5.2 Evaluation of errors

3.5.2.1 The standard deviation σ

Whenever it is possible to obtain several measurements for the same quantity, the average is taken as best values. This average is just the arithmetic mean given by:

$$\bar{x} = \frac{\sum x}{N}, \quad \text{Equation 3.1}$$

where: x is a single measurement and N the number of measurements.

The standard deviation is thus expressed by the following relationship:

$$\sigma = \sqrt{\frac{1}{N-1} \sum_{i=1}^N (x - \bar{x})^2}. \quad \text{Equation 3.2}$$

It represents how the measured values spread about the mean, in repeated measurements, and therefore is a good estimate of the statistical error of the experiment. If μ is the true value, the exact meaning of σ can be related to the probability p_t for finding a single measurement of x to be within the range $(\mu - t\sigma, \mu + t\sigma)$. This probability can be 68.3%, 95.5% and 99.7% for $t = 1, 2$ and 3 respectively.

The standard deviation is not defined if only one measurement exists; the errors are measured by repeating the measurement. The standard deviation measures the “width” of the distribution of values about the average (Benzinger & Aksay, 1999).

3.5.2.2 Single errors

The maximum error or absolute error, Δa , is considered to be the smallest subdivision of the measuring instrument, i.e., the smallest value detectable by the measuring instrument (Barry, 1991). It can be calculated using the standard deviation of a set of repeated measurements.

The relationship below gives the maximum error for a confidence interval of 99.9 %.

$$\Delta a = 3.29\sigma. \quad \text{Equation 3.3}$$

For a 95.5% confidence, the absolute error is given by:

$$\Delta a = 2\sigma. \quad \text{Equation 3.4}$$

The uncertainty or error associated with a measurement of a variable X can be therefore expressed as:

$$X = A \pm \Delta a, \quad \text{Equation 3.5}$$

where A is considered as a true value of the quantity.

The relative error is defined as the ratio:

$$\frac{\Delta a}{A}, \quad \text{Equation 3.6}$$

and is generally expressed as a percentage.

3.5.2.3 Combined errors

Frequently one is interested in a physical property that requires the combination of several other physical measurements.

The subsequent errors of independent variables are combined to establish the error of the variable resulting from computation of these independent variables. If the variable X is a function of n other variables, i.e., $X = F(a, b, c, \dots, n)$, the expected highest error can be calculated using Equation 3.7 below (Brinkworth, 1968):

$$\left(\frac{\Delta X}{X}\right)^2 = \sum \left(\frac{\partial X}{\partial n}\right)^2 \left(\frac{n}{X}\right)^2 \left(\frac{\Delta n}{n}\right)^2 \quad \text{Equation 3.7}$$

where: X is the computed result

ΔX is the absolute error of the computed result

n is an independent variable involved

Δn is the absolute error of the independent variable.

3.5.3 Errors in measured variables

3.5.3.1 Flow rate

The flow meter manufacturer gave the maximum measuring error of $\pm 1.5\%$ of measured value ± 1 mm/s.

3.5.3.2 Pressure

The accuracy of the pressure transducers used was $\pm 0.25\%$ of the full scale. Their calibrations were made in such a way that the correlation coefficient reached at least the value of 0.999.

3.5.3.3 Weight

An electronic balance with an accuracy of ± 0.001 g was used to weigh all samples for the RD tests. Thus, a relative error of 0.002 % could be found for a sample of 50 g. This was assumed to be very small for the relative density (RD) test. A representative value of the error was therefore calculated using the standard deviation of different measurements taken. That was found to be 0.35%.

3.5.3.4 Distance between pressure tappings

A tape measure graduated in mm was used to measure the tapping distance. That led to an absolute error of ± 0.001 m (according to section 3.5.2.2). A relative error could, therefore, be calculated by dividing this absolute error by the measured value of the tapping distance.

3.5.4 Error of derived variables

The errors for the principal derived variables related to the pump test are discussed in this section. The accuracy of the derived variables depends on the actual measured values.

3.5.4.1 Pipe cross-section area

The cross-section area, A , of a pipe with diameter, D , is calculated using the following relationship:

$$A = \pi \frac{D^2}{4}. \quad \text{Equation 3.8}$$

The relative error of A is obtained by applying Equation 3.7 to Equation 3.8 as follows:

$$\left(\frac{\Delta A}{A}\right)^2 = \left(\frac{\pi D}{2}\right)^2 \left(\frac{D}{A}\right)^2 \left(\frac{\Delta D}{D}\right)^2. \quad \text{Equation 3.9}$$

After replacing A by Equation 3.8 in Equation 3.9 and simplifying the expression, it becomes:

$$\left(\frac{\Delta A}{A}\right)^2 = 4 \left(\frac{\Delta D}{D}\right)^2. \quad \text{Equation 3.10}$$

Therefore, the relative error is expressed by:

$$\frac{\Delta A}{A} = \pm 2 \left(\frac{\Delta D}{D}\right). \quad \text{Equation 3.11}$$

3.5.4.2 Fluid velocity

The fluid velocity is given by the ratio of the flow rate to the cross-section area:

$$V = \frac{Q}{A}. \quad \text{Equation 3.12}$$

Combining Equation 3.8 and Equation 3.12, the velocity becomes;

$$V = \frac{4Q}{\pi D^2}. \quad \text{Equation 3.13}$$

Equation 3.7 is applied to Equation 3.13 to obtain the velocity relative error:

$$\left(\frac{\Delta V}{V}\right)^2 = \left(\frac{4}{\pi D^2}\right)^2 \left(\frac{Q}{V}\right)^2 \left(\frac{\Delta Q}{Q}\right)^2 + \left(-\frac{8Q}{\pi D^3}\right)^2 \left(\frac{D}{V}\right)^2 \left(\frac{\Delta D}{D}\right)^2. \quad \text{Equation 3.14}$$

After simplification, Equation 3.14 becomes:

$$\left(\frac{\Delta V}{V}\right)^2 = \left(\frac{\Delta Q}{Q}\right)^2 + 4\left(\frac{\Delta D}{D}\right)^2. \quad \text{Equation 3.15}$$

The highest expected velocity error is, therefore,

$$\frac{\Delta V}{V} = \pm \sqrt{\left(\frac{\Delta Q}{Q}\right)^2 + 4\left(\frac{\Delta D}{D}\right)^2}, \quad \text{Equation 3.16}$$

3.5.4.3 Pseudo-shear rate

The pseudo-shear rate is calculated using Equation 3.17 below:

$$\dot{\gamma} = \frac{8V}{D}. \quad \text{Equation 3.17}$$

The application of Equation 3.7 to Equation 3.17 results in:

$$\left(\frac{\Delta \dot{\gamma}}{\dot{\gamma}}\right)^2 = \left(\frac{\Delta V}{V}\right)^2 + \left(\frac{\Delta D}{D}\right)^2. \quad \text{Equation 3.18}$$

After replacing Equation 3.16 in Equation 3.18, the error is:

$$\frac{\Delta \dot{\gamma}}{\dot{\gamma}} = \pm \sqrt{\left(\frac{\Delta Q}{Q}\right)^2 + 5\left(\frac{\Delta D}{D}\right)^2}. \quad \text{Equation 3.19}$$

3.5.4.4 Wall shear stress

The wall shear stress is calculated from the expression:

$$\tau_o = \frac{\Delta p D}{4L}. \quad \text{Equation 3.20}$$

The application of Equation 3.7 to Equation 3.20 gives:

$$\left(\frac{\Delta \tau_o}{\tau_o}\right)^2 = \left(\frac{\Delta(\Delta p)}{\Delta p}\right)^2 + \left(\frac{\Delta D}{D}\right)^2 + \left(\frac{\Delta L}{L}\right)^2. \quad \text{Equation 3.21}$$

The highest shear stress error expected is then given by:

$$\frac{\Delta \tau_o}{\tau_o} = \pm \sqrt{\left(\frac{\Delta(\Delta p)}{\Delta p}\right)^2 + \left(\frac{\Delta D}{D}\right)^2 + \left(\frac{\Delta L}{L}\right)^2}. \quad \text{Equation 3.22}$$

3.5.4.5 Suction pressure p_1 and discharge pressure p_2

If H_{1m} and H_{2m} represent the tapping height above the inlet and the outlet centre line respectively, and H_{1w} and H_{2w} the water column height above the inlet and outlet tapping, the pressure at the suction (P_1) and that at the discharge (P_2) will be determined using Equation 3.23 and Equation 3.24 respectively.

$$p_1 = \rho_1 g H_{1m} + \rho_1 g H_{1w} = \rho_1 g (H_{1m} + H_{1w}). \quad \text{Equation 3.23}$$

$$p_2 = \rho_2 g H_{2m} + \rho_2 g H_{2w} = \rho_2 g (H_{2m} + H_{2w}). \quad \text{Equation 3.24}$$

The application of Equation 3.7 to Equation 3.23 results in:

$$\left(\frac{\Delta p_1}{p_1}\right)^2 = (\rho_1 g)^2 \left(\frac{H_{1m}}{p_1}\right)^2 \left(\frac{\Delta H_{1m}}{H_{1m}}\right)^2 + (\rho_1 g)^2 \left(\frac{H_{1w}}{p_1}\right)^2 \left(\frac{\Delta H_{1w}}{H_{1w}}\right)^2. \quad \text{Equation 3.25}$$

After replacing P_1 by Equation 3.25 and simplifying, the expression of the highest error at the suction side is given by:

$$\frac{\Delta p_1}{p_1} = \pm \sqrt{\left(\frac{H_{1m}}{H_{1m} + H_{1w}}\right)^2 \left(\frac{\Delta H_{1m}}{H_{1m}}\right)^2 + \left(\frac{H_{1w}}{H_{1m} + H_{1w}}\right)^2 \left(\frac{\Delta H_{1w}}{H_{1w}}\right)^2}. \quad \text{Equation 3.26}$$

In the same way, the highest error expected at the discharge side is given by:

$$\frac{\Delta p_2}{p_2} = \pm \sqrt{\left(\frac{H_{2m}}{H_{2m} + H_{2w}}\right)^2 \left(\frac{\Delta H_{2m}}{H_{2m}}\right)^2 + \left(\frac{H_{2w}}{H_{2m} + H_{2w}}\right)^2 \left(\frac{\Delta H_{2w}}{H_{2w}}\right)^2}. \quad \text{Equation 3.27}$$

3.5.4.6 Total pump suction and discharge head

The total head at the suction H_1 and at the discharge H_2 are given by Equation 3.28 and Equation 3.29 respectively.

$$H_1 = \frac{p_1}{\rho_1 g} + Z_1 + \frac{V_1^2}{2g}. \quad \text{Equation 3.28}$$

$$H_2 = \frac{p_2}{\rho_2 g} + Z_2 + \frac{V_2^2}{2g}. \quad \text{Equation 3.29}$$

Equation 3.28 becomes Equation 3.30 after replacing V_1 by Equation 3.13.

$$H_1 = \frac{p_1}{\rho_1 g} + Z_1 + \frac{8Q^2}{g\pi^2 D^4}. \quad \text{Equation 3.30}$$

After application of Equation 3.7 to Equation 3.30, where Z is assumed errorless, it yields:

$$\left(\frac{\Delta H_1}{H_1}\right)^2 = \left(\frac{1}{\rho_1 g}\right)^2 \left(\frac{p_1}{H_1}\right)^2 \left(\frac{\Delta p_1}{p_1}\right)^2 + \left(\frac{16Q}{g\pi^2 D^4}\right)^2 \left(\frac{Q}{H_1}\right)^2 \left(\frac{\Delta Q}{Q}\right)^2 + \left(\frac{-32Q^2}{g\pi^2 D^5}\right)^2 \left(\frac{D}{H_1}\right)^2 \left(\frac{\Delta D}{D}\right)^2. \quad \text{Equation 3.31}$$

Considering Equation 3.31, let:

$$C_1 = \frac{1}{\rho_1 g} \frac{p_1}{H_1} = \frac{p_1}{\rho_1 + \frac{8Q^2 \rho_1}{\pi^2 D^4}}, \quad \text{Equation 3.32}$$

$$C_2 = \frac{16Q}{g\pi^2 D^4} \frac{Q}{H_1} = \frac{16Q^2}{\pi^2 D^4 p_1 + 8Q^2} \quad \text{Equation 3.33}$$

and

$$C_3 = \frac{-32Q^2 D}{g\pi^2 D^5 H_1} = -\frac{32Q^2}{\pi^2 D^4 p_1 + 8Q^2} \quad \text{Equation 3.34}$$

N.B: $C_3 = -2C_2$

Equation 3.31 can be simplified as follows:

$$\left(\frac{\Delta H_1}{H_1}\right)^2 = C_1^2 \left(\frac{\Delta p_1}{p_1}\right)^2 + C_2^2 \left(\frac{\Delta Q}{Q}\right)^2 + 4C_2^2 \left(\frac{\Delta D}{D}\right)^2. \quad \text{Equation 3.35}$$

Thus, the highest error expected is:

$$\frac{\Delta H_1}{H_1} = \pm \sqrt{C_1^2 \left(\frac{\Delta p_1}{p_1}\right)^2 + C_2^2 \left(\frac{\Delta Q}{Q}\right)^2 + 4C_2^2 \left(\frac{\Delta D}{D}\right)^2}. \quad \text{Equation 3.36}$$

Using the same procedure, the highest error expected at the discharge yields:

$$\frac{\Delta H_2}{H_2} = \pm \sqrt{C_1'^2 \left(\frac{\Delta p_2}{p_2} \right)^2 + C_2'^2 \left(\frac{\Delta Q}{Q} \right)^2 + 4C_2'^2 \left(\frac{\Delta D}{D} \right)^2}. \quad \text{Equation 3.37}$$

Where C' is obtained by replacing P_1 , H_1 and ρ_1 by P_2 , H_2 and ρ_2 respectively, in C .

3.5.4.7 Pump input power (P_{in})

The pump input power is obtained using the formula:

$$P_{in} = 2\pi nT. \quad \text{Equation 3.38}$$

The application of Equation 3.7 to Equation 3.38 gives:

$$\left(\frac{\Delta P_{in}}{P_{in}} \right)^2 = (2\pi T)^2 \left(\frac{n}{P_{in}} \right)^2 \left(\frac{\Delta n}{n} \right)^2 + (2\pi n)^2 \left(\frac{T}{P_{in}} \right)^2 \left(\frac{\Delta T}{T} \right)^2. \quad \text{Equation 3.39}$$

After replacing P_{in} , in Equation 3.39, by Equation 3.38 we obtain:

$$\left(\frac{\Delta P_{in}}{P_{in}} \right)^2 = (2\pi T)^2 \left(\frac{n}{2\pi nT} \right)^2 \left(\frac{\Delta n}{n} \right)^2 + (2\pi n)^2 \left(\frac{T}{2\pi nT} \right)^2 \left(\frac{\Delta T}{T} \right)^2. \quad \text{Equation 3.40}$$

After simplification, the highest error is given by:

$$\frac{\Delta P_{in}}{P_{in}} = \pm \sqrt{\left(\frac{\Delta n}{n} \right)^2 + \left(\frac{\Delta T}{T} \right)^2}. \quad \text{Equation 3.41}$$

3.5.4.8 Pump output power (P_{out})

The power developed by the pump is expressed by:

$$P_{out} = \rho_m gQH. \quad \text{Equation 3.42}$$

The application of Equation 3.7 to Equation 3.42 gives:

$$\left(\frac{\Delta P_{out}}{P_{out}} \right)^2 = (\rho_m gH)^2 \left(\frac{Q}{P_{out}} \right)^2 \left(\frac{\Delta Q}{Q} \right)^2 + (\rho_m gQ)^2 \left(\frac{H}{P_{out}} \right)^2 \left(\frac{\Delta H}{H} \right)^2. \quad \text{Equation 3.43}$$

By considering Equation 3.41 in Equation 3.43 and simplifying, the highest error expected is:

$$\frac{\Delta P_{out}}{P_{out}} = \pm \sqrt{\left(\frac{\Delta Q}{Q} \right)^2 + \left(\frac{\Delta H}{H} \right)^2}. \quad \text{Equation 3.44}$$

3.5.4.9 Pump efficiency

The pump efficiency is obtained from the following ratio:

$$\eta = \frac{P_{out}}{P_{in}}. \quad \text{Equation 3.45}$$

Equation 3.7 applied to Equation 3.45 yields:

$$\left(\frac{\Delta\eta}{\eta}\right)^2 = \left(-\frac{P_{out}}{P_{in}^2}\right)^2 \left(\frac{P_{in}}{\eta}\right)^2 \left(\frac{\Delta P_{in}}{P_{in}}\right)^2 + \left(\frac{1}{P_{in}}\right)^2 \left(\frac{P_{out}}{\eta}\right)^2 \left(\frac{\Delta P_{out}}{P_{out}}\right)^2. \quad \text{Equation 3.46}$$

After combination of Equation 3.45 and Equation 3.46, the highest expected error is:

$$\frac{\Delta\eta}{\eta} = \pm \sqrt{\left(\frac{\Delta P_{in}}{P_{in}}\right)^2 + \left(\frac{\Delta P_{out}}{P_{out}}\right)^2}. \quad \text{Equation 3.47}$$

Considering Equation 3.41 and Equation 3.44 in Equation 3.47, the error can be expressed by:

$$\frac{\Delta\eta}{\eta} = \pm \sqrt{\left(\frac{\Delta n}{n}\right)^2 + \left(\frac{\Delta T}{T}\right)^2 + \left(\frac{\Delta Q}{Q}\right)^2 + \left(\frac{\Delta H}{H}\right)^2}. \quad \text{Equation 3.48}$$

3.5.5 Numerical application of errors

In this section, errors in the pipe internal diameter measurement and the cross-section area are calculated using the instruments' accuracy on one hand and the standard deviation of the current measurements, on the other hand, and these are compared.

3.5.5.1 Error calculation using the instrument accuracy

The accuracy of the calliper used to measure the internal diameter was 1/50 mm. This means that the absolute error made when measuring the pipe internal diameter was $\Delta a = 0.020$ mm.

Table 3.2: Warman 4/3 suction and discharge pipe cross-section relative error

Warman 4/3				
	Pipe internal diameter [mm]	Absolute error [mm]	Internal diameter relative error [±%]	Expected highest error on the cross-section [±%]
Inlet	102.5	0.02	0.02	0.04
Outlet	78.5	0.02	0.03	0.05

Table 3.2 shows the average value of the diameter from 35 random readings, the relative error on the diameter and cross-section area for both the inlet and outlet pipes of the pump. These

calculations are made using the absolute error obtained from the instrument accuracy as stated in section 3.5.4.1.

3.5.5.2 Error calculation using the standard deviation

The values shown in Table 3.3 were obtained by considering the measurement at 95% confidence level. The expected highest error for the cross-section was calculated using Equation 3.11.

Table 3.3: Warman 4/3 suction and discharge pipe cross-section relative error

Warman 4/3					
	Pipe internal diameter [mm]	Standard deviation (σ)	Absolute error at 95% confidence [mm]	Internal diameter relative error [$\pm\%$]	Expected highest error on the cross-section [$\pm\%$]
Inlet	102.5	0.29	0.58	0.57	1.13
Outlet	78.5	0.30	0.61	0.77	1.55

3.5.5.3 Error of principal computed variables

The following five variables were recorded more than 100 times while running the pump at a constant speed: flow rate – pump shaft torque – pump speed – suction pressure – discharge pressure. The mean value and standard deviation were calculated for each variable; hence the relative error was calculated at 95% of confidence level according to Equation 3.4. The highest expected errors were then calculated for velocity, head, power and efficiency.

Table 3.4: Errors of computed variables for the Warman 4/3 pump at 1200 rpm

Warman 4/3 at 1200 rpm									
Variables	Average value	Standard deviation	Absolute error at 95% conf.	Relative error	Expected highest error [$\pm\%$]				
					Velocity	Head	Power out	Power in	Efficiency
Pump speed [rpm]	1206.770	0.052	0.105	0.009	-	-	-	-	-
Pump flow rate [l/s]	13.314	0.016	0.032	0.244	-	-	-	-	-
Pump Inlet [kPa]	-3.625	0.023	0.046	-1.271	1.160	1.271	-	1.618	-
Pump Outlet [kPa]	134.628	0.209	0.418	0.311	1.567	0.311	0.395	-	-
Pump shaft torque [Nm]	27.220	0.220	0.440	1.618	-	-	-	-	1.665

Table 3.5: Errors of computed variables for the Warman 4/3 pump at 1400 rpm

Warman 4/3 at 1400 rpm									
Variables	Average value	Standard deviation	Absolute error at 95% conf.	Relative error	Expected highest error [±%]				
					Velocity	Head	Power out	Power in	Efficiency
Pump speed [rpm]	1404.824	0.055	0.111	0.008	-	-	-	-	-
Pump flow rate [l/s]	16.101	0.176	0.352	2.189	-	-	-	-	-
Pump Inlet [kPa]	-5.301	0.072	0.144	-2.724	2.465	2.725	-	1.979	-
Pump Outlet [kPa]	180.196	0.336	0.672	0.373	2.681	0.373	2.220	-	-
Pump shaft torque [Nm]	36.643	0.363	0.725	1.979	-	-	-	-	2.974

Table 3.6: Errors of computed variables for the Warman 4/3 pump at 1600 rpm

Warman 4/3 at 1600 rpm									
Variables	Average value	Standard deviation	Absolute error at 95% conf.	Relative error	Expected highest error [±%]				
					Velocity	Head	Power out	Power in	Efficiency
Pump speed [rpm]	1607.642	0.014	0.028	0.002	-	-	-	-	-
Pump flow rate [l/s]	18.396	0.022	0.044	0.239	-	-	-	-	-
Pump Inlet [kPa]	-7.048	0.032	0.063	-0.896	1.159	0.896	-	0.983	-
Pump Outlet [kPa]	235.563	0.345	0.690	0.293	1.566	0.293	0.378	-	-
Pump shaft torque [Nm]	48.059	0.236	0.472	0.983	-	-	-	-	1.053

Table 3.7: Errors of computed variables for the Warman 4/3 pump at 1800 rpm

Warman 4/3 at 1800 rpm									
Variables	Average value	Standard deviation	Absolute error at 95% conf.	Relative error	Expected highest error [±%]				
					Velocity	Head	Power out	Power in	Efficiency
Pump speed [rpm]	1808.156	0.059	0.118	0.007	-	-	-	-	-
Pump flow rate [l/s]	22.549	0.022	0.044	0.195	-	-	-	-	-
Pump Inlet [kPa]	-10.330	0.043	0.086	-0.829	1.150	0.829	-	0.663	-
Pump Outlet [kPa]	290.100	0.301	0.602	0.208	1.560	0.208	0.285	-	-
Pump shaft torque [Nm]	63.855	0.212	0.424	0.663	-	-	-	-	0.722

Table 3.8: Errors of computed variables for the Warman 4/3 pump at 2000 rpm

Warman 4/3 at 2000 rpm									
Variables	Average value	Standard deviation	Absolute error at 95% conf.	Relative error	Expected highest error [±%]				
					Velocity	Head	Power out	Power in	Efficiency
Pump speed [rpm]	2007.091	0.073	0.145	0.007	-	-	-	-	-
Pump flow rate [l/s]	25.879	0.021	0.042	0.163	-	-	-	-	-
Pump Inlet [kPa]	-14.070	0.056	0.112	-0.793	1.145	0.794	-	0.834	-
Pump Outlet [kPa]	351.223	0.479	0.958	0.273	1.556	0.273	0.318	-	-
Pump shaft torque [Nm]	77.537	0.323	0.647	0.834	-	-	-	-	0.893

3.6 CONCLUSION

The experimental rig and all instrumentation have been described. The rig was commissioned using water.

The calibration procedure of different experimental equipment has been presented including the experimental procedures. The calibration results have shown that data from this experimental rig would be reliable.

Materials tested have been described.

The theory of errors has been explained as well as the error calculation on measured and computed variables. Results have been analysed and the magnitudes are deemed to be within acceptable margins.

The results of the experimental work are displayed and analysed in Chapter 4.

Chapter 4 PRESENTATION AND ANALYSIS OF RESULTS

4.1 INTRODUCTION

The results of the centrifugal pump performance tests, using two types of material, are presented in this chapter, as well as the results of water tests. The water pressure drop test results are compared with the Colebrook-White prediction to ensure the correct operation of the system. In the same way, the water pump performance test results are compared with the catalogue pump curves to ensure the reliability of pump performance tests for the viscous materials. These results are then analysed according to the two approaches as stated in Chapter 2. The Bingham plastic viscosity determination is presented as well.

4.2 WATER TEST RESULTS

4.2.1 Water pressure drop test results

The results of the water pressure drop tests for the two pipes are correlated with the Colebrook-White equation to determine the roughness of the pipe and ascertain the accuracy and the credibility of the flow meter and DPT. This correlation is shown in Figures 4.1 and 4.2 for the 80 mm and 60 mm pipes respectively.

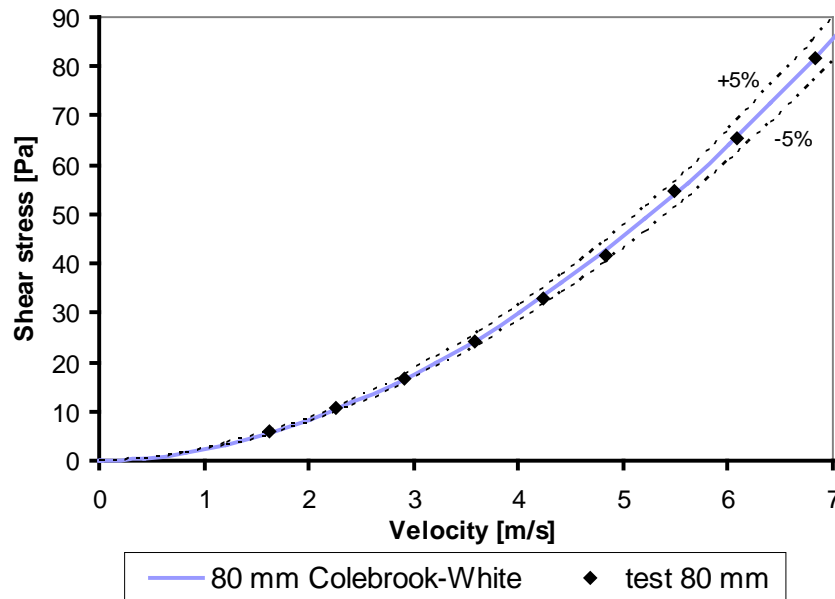


Figure 4.1: Water test in 80 mm straight pipe

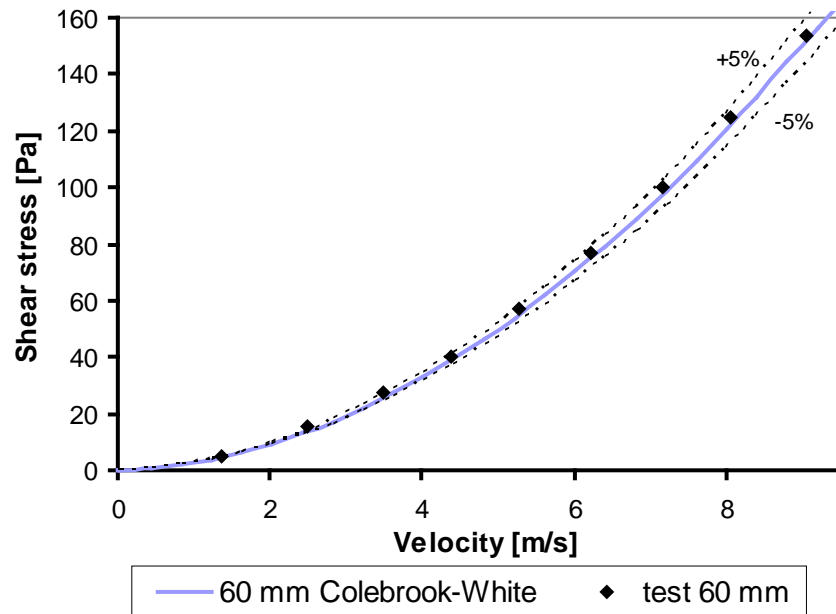


Figure 4.2: Water test in 60 mm straight pipe

From Figures 4.1 and 4.2, a good agreement between experimental data and the theoretical Colebrook-White curve can be noticed. Such an agreement implies the validity and degree of accuracy of the experimental procedure and tube viscometer used in this investigation.

4.2.2 Centrifugal pump performance test results for water

The centrifugal pump performance test was first conducted with water. The results were compared with the catalogue pump curves supplied by the pump manufacturer to ascertain the reliability and accuracy of the experimental apparatus used in the pump section. The water pump curves were then used as reference for the pump performance calculations.

Results obtained for the pump head and efficiency at the different speeds considered in this work are summarised in Figures 4.3 and 4.4 respectively.

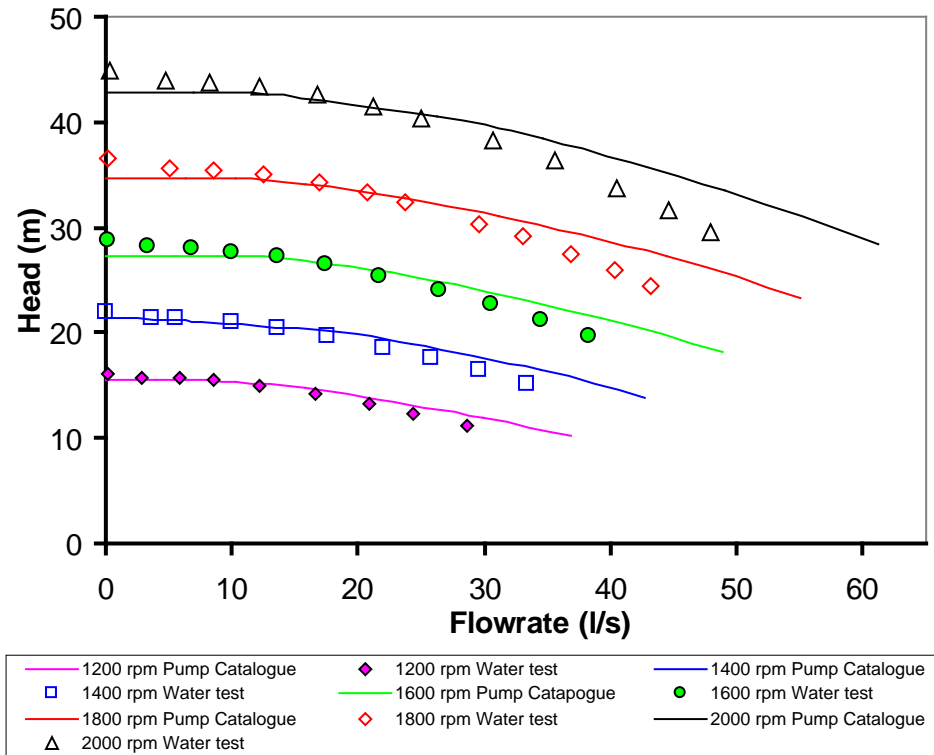


Figure 4.3: Warman 4/3 comparison of water test and catalogue curves for the head

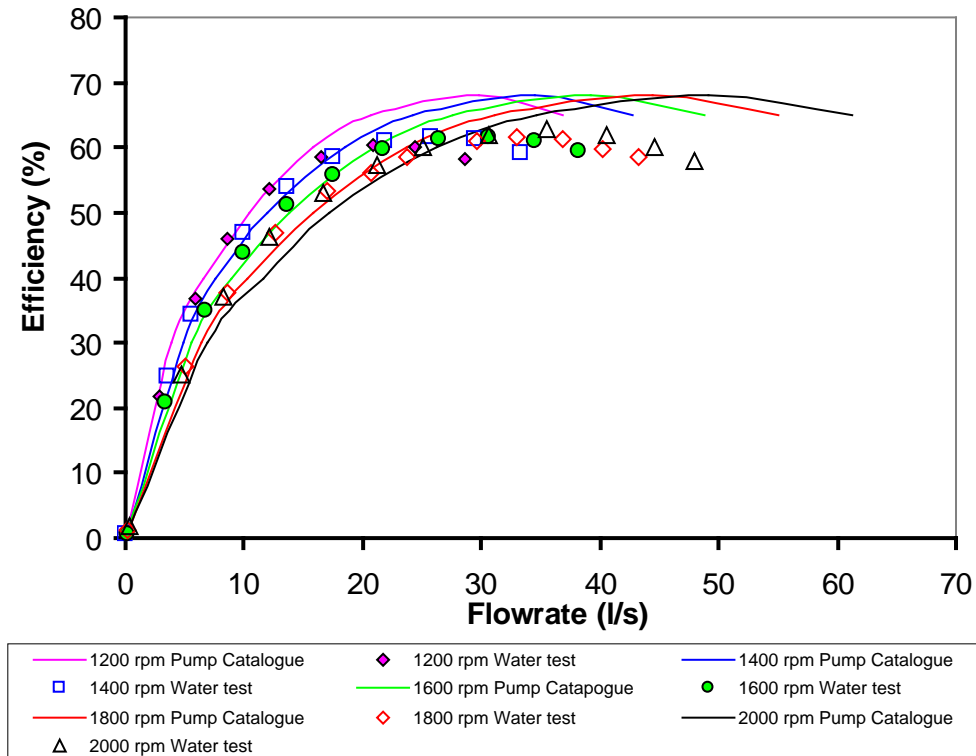


Figure 4.4: Warman 4/3 comparison of water test and catalogue curves for the efficiency

According to the international standard (ISO 9906), tolerances are allowed when comparing the test results with the guaranteed values (catalogue). The values of tolerance factors are $\pm 5\%$ and -5% for pump head and efficiency respectively for the accuracy of Grade 2. This requirement was met for the water pump test results above. This reveals that the calibration and experimental apparatus can be considered accurate and reliable.

4.3 FLOW CURVES AND RHEOLOGICAL CHARACTERISATION

The pressure drop test was performed to determine the viscous properties of different materials used. The results of this test are presented in this section, as well as the rheological characterisation results.

4.3.1 Pseudo-shear diagrams

Figure 4.5 shows the typical results of the pseudo-shear diagrams for the materials tested.

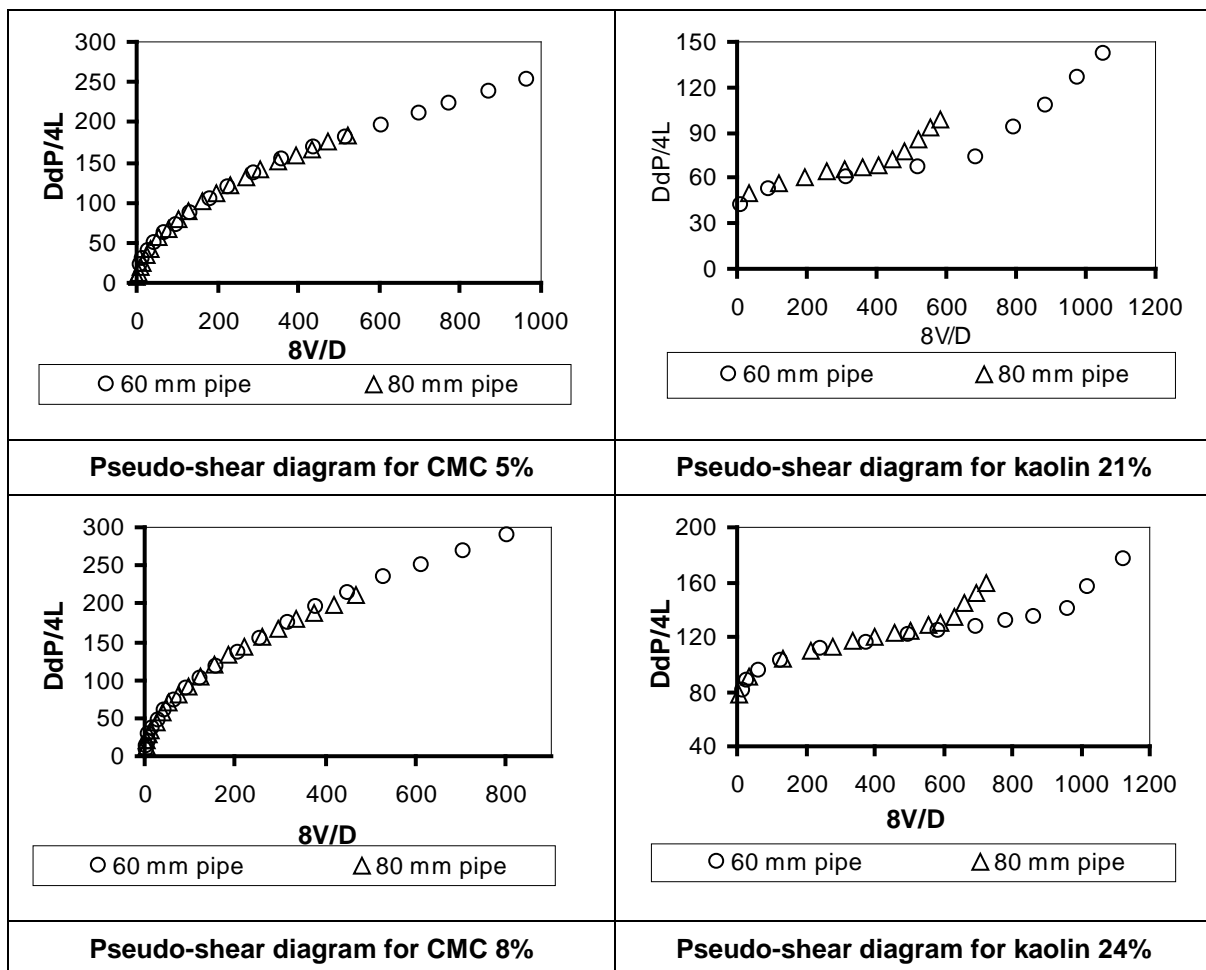


Figure 4.5: Summary of pseudo-shear diagrams

4.3.2 Rheological characterisation

Both the CMC solutions and kaolin suspensions typically display pseudoplastic and yield pseudoplastic behaviour respectively. This section will show how the rheological constants were determined by fitting the rheological models to the experimental data. Results obtained for the different concentrations tested will also be presented.

4.3.2.1 Kaolin

As explained earlier in section 2.5.5., a third order polynomial Excel curve fit function was chosen to fit the laminar data for kaolin, therefore the slope n' was a second order polynomial.

The Herschel-Bulkley model was used to model the flow behaviour of kaolin. The rheological constants were then determined by fitting the model to the plot of wall shear rate versus true shear rate. Figure 4.6 shows how the rheogram fits the experimental data in the laminar zone, for different concentrations of kaolin.

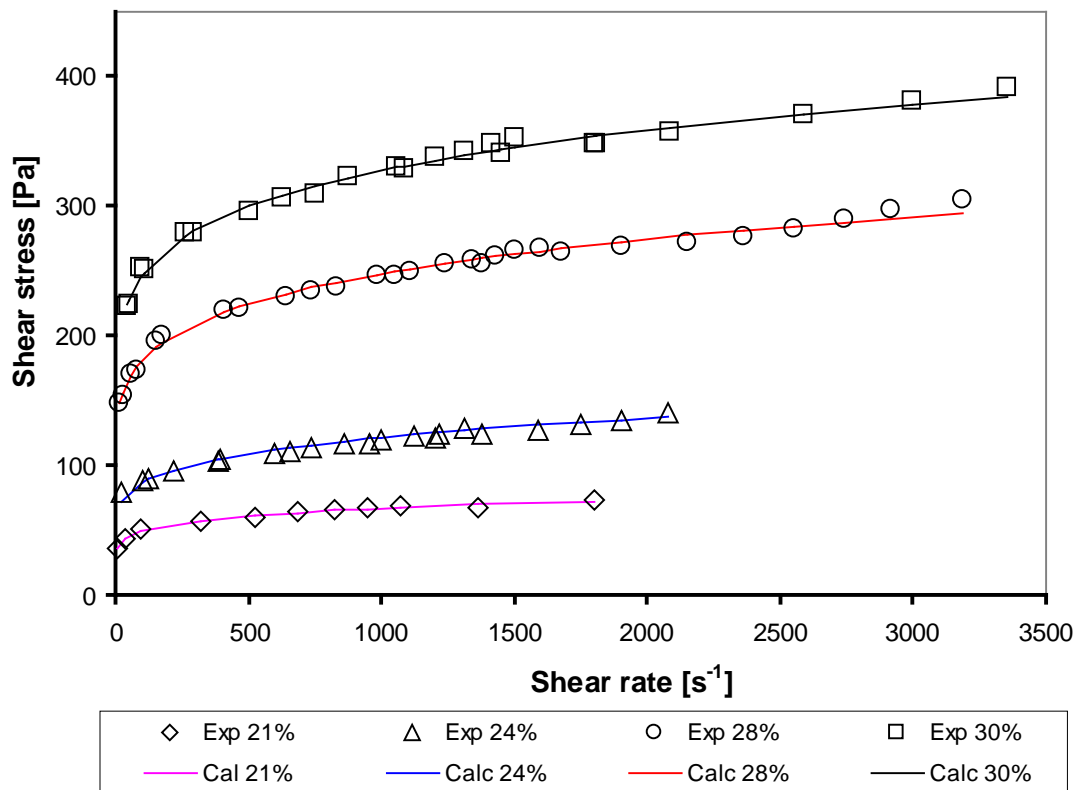


Figure 4.6: Rheograms for kaolin 21%, 24%, 28% and 30%

Using the data from Figure 4.6, a summary of different rheological parameters for different concentrations of kaolin, is given in Table 4.1.

Table 4.1: Kaolin rheological parameters

Concentrations	Density [kg/m^3]	τ_y [Pa]	K [$\text{Pa}\cdot\text{s}^n$]	n
Kaolin 21%	1348.1	7.02	21.21	0.150
Kaolin 24%	1400.6	35.00	18.02	0.227
Kaolin 28%	1461.7	68.02	45.23	0.200
Kaolin 30%	1490.2	78.02	76.72	0.171

4.3.2.2 Carboxyl methyl cellulose (CMC)

The power-law model was used to describe the flow behaviour of the CMC solution. The rheological constants were then determined using the same procedure as for kaolin. The power-law trend was fitted to the experimental data in the laminar zone for different concentrations of CMC. Figure 4.7 shows the results for the three concentrations of CMC.

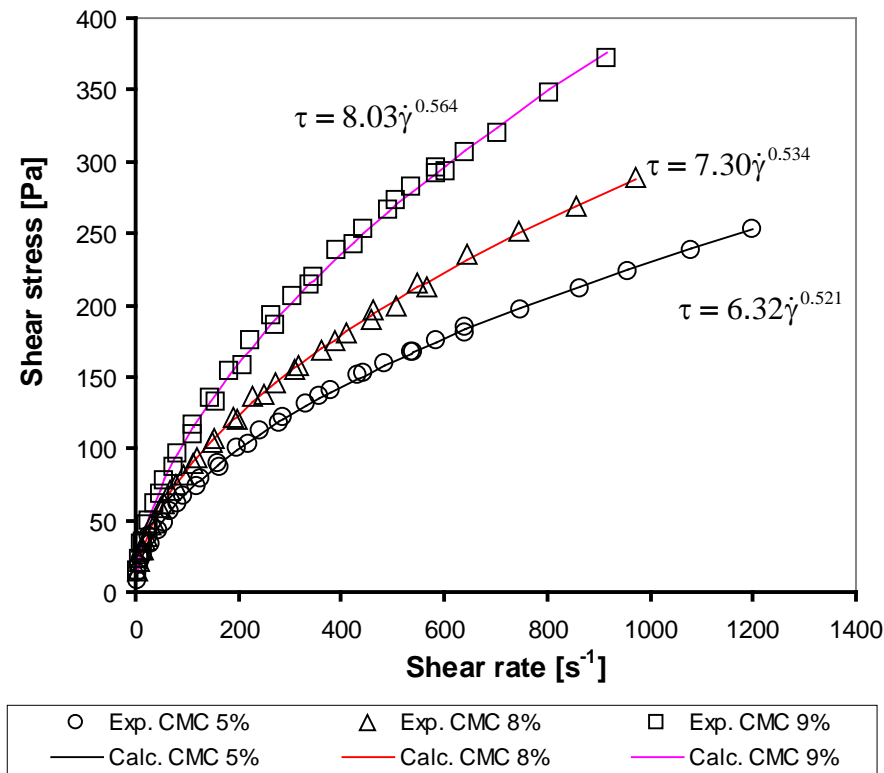


Figure 4.7: Rheograms for CMC 5%, 8% and 9%

The different rheological parameters obtained for CMC are depicted in Table 4.2 below.

Table 4.2: CMC rheological parameters

Material	Density [kg/m^3]	K [$\text{Pa}\cdot\text{s}^n$]	n
CMC 5%	1030.3	6.32	0.521
CMC 8%	1046.2	7.30	0.534
CMC 9%	1057.9	8.03	0.564

4.4 PUMP PERFORMANCE TEST RESULTS

Using the water test results as a reference, various concentrations of the viscous materials were tested to assess the pump deration. Figures 4.8 to 4.13 represent typical results obtained for both kaolin and CMC.

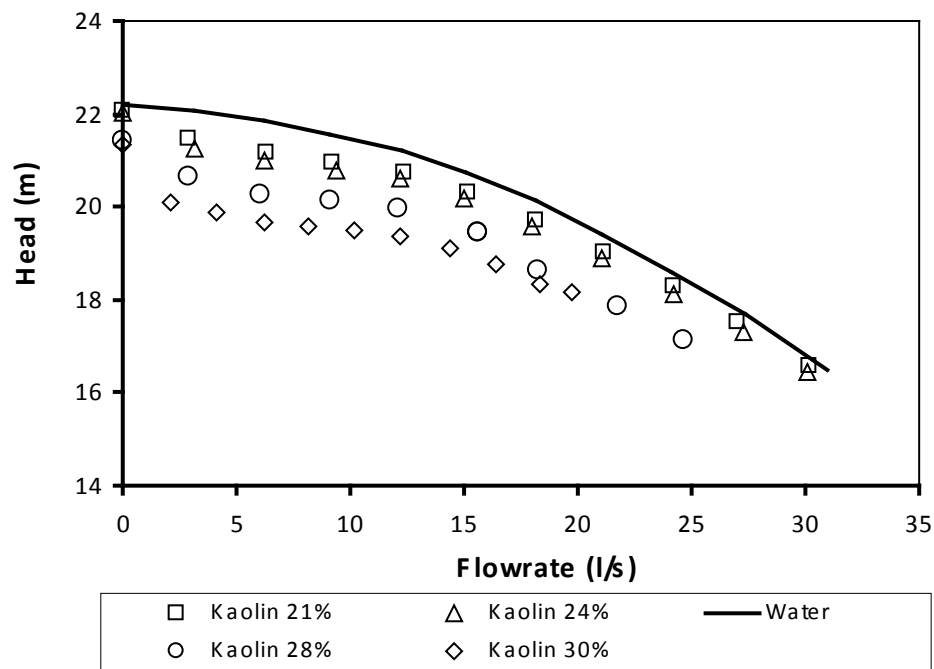


Figure 4.8: Head curve for the Warman 4/3 pump handling kaolin at 1400 rpm

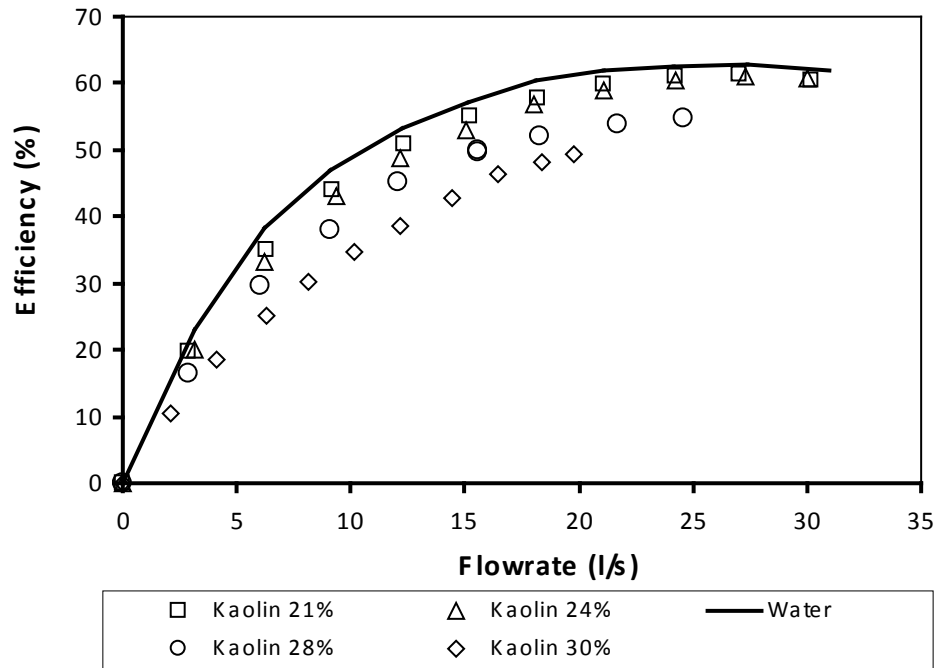


Figure 4.9: Efficiency curve for the Warman 4/3 pump handling kaolin at 1400 rpm

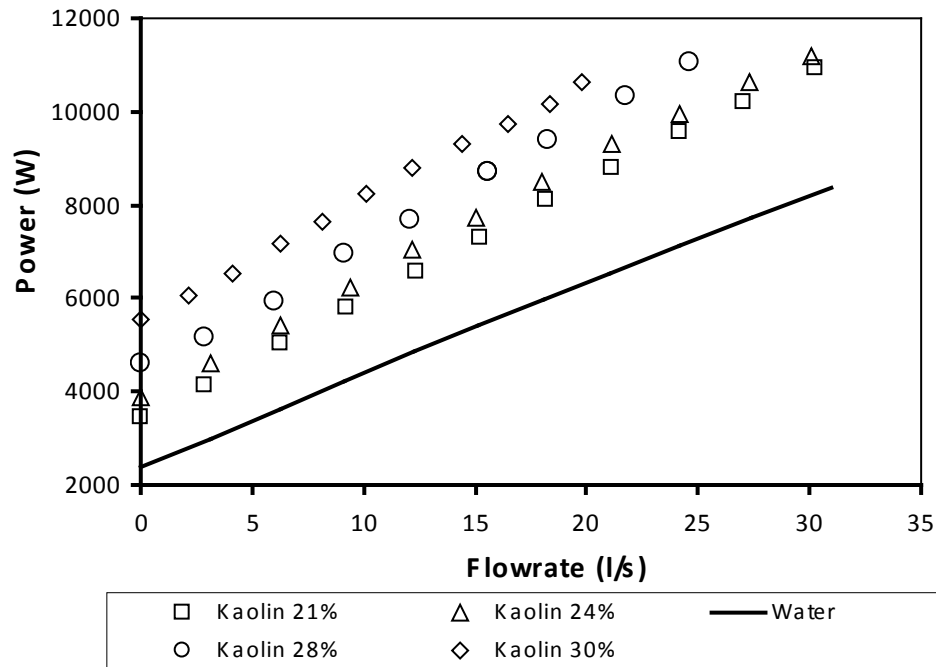


Figure 4.10: Power curve for the Warman 4/3 pump handling kaolin at 1400 rpm

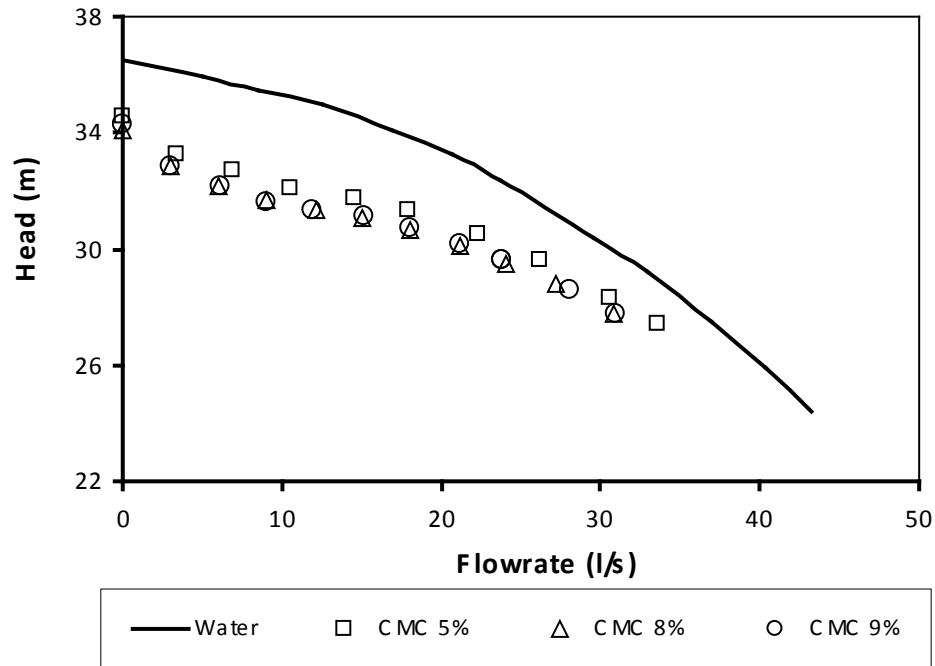


Figure 4.11: Head curve for the Warman 4/3 pump handling CMC at 1800 rpm

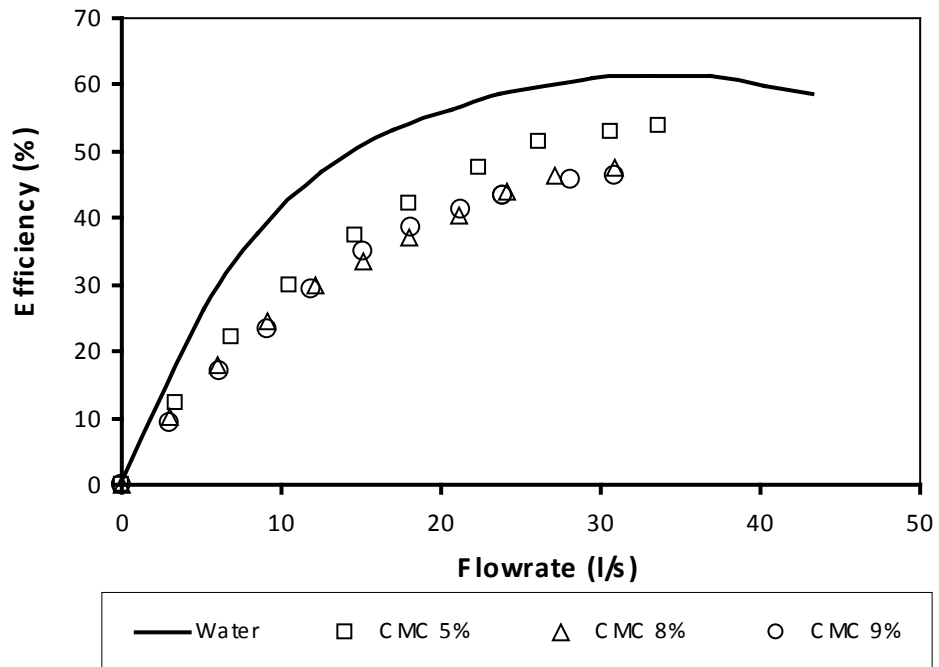


Figure 4.12: Efficiency curve for the Warman 4/3 pump handling CMC at 1800 rpm

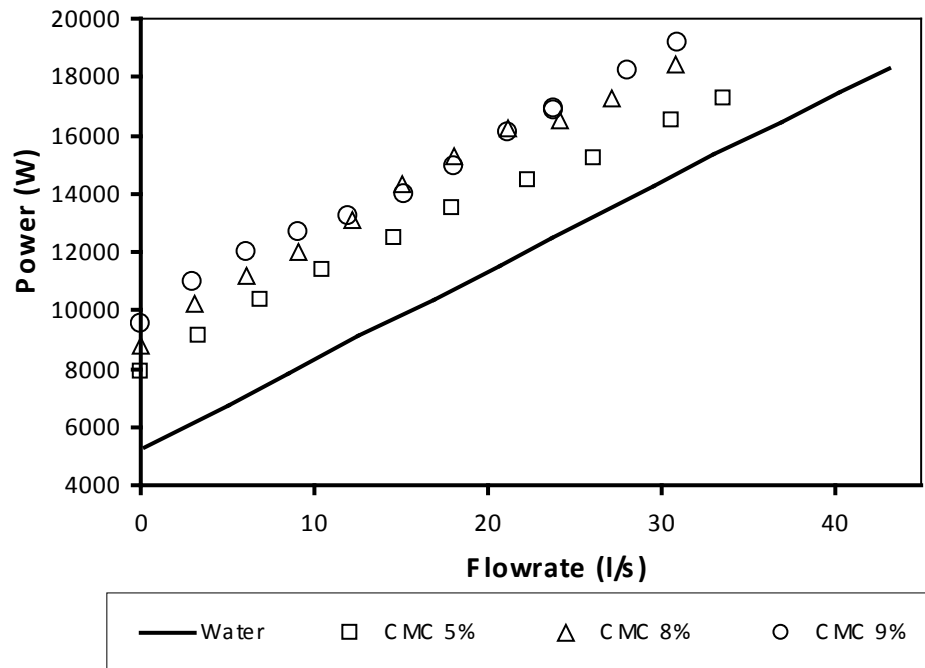


Figure 4.13: Power curve for the Warman 4/3 pump handling CMC at 1900 rpm

These results show that, for both materials, the pump decreases in performance. The deration appears to be greater for CMC than kaolin.

4.5 WALKER & GOULAS (1984) APPROACH

As stated in Chapter 2, the Walker and Goulas (1984) approach uses the Bingham plastic viscosity in the HI method to predict the pump performance for non-Newtonian slurries. Therefore, this section will cover firstly the results of the Bingham plastic viscosity determination and then the results of pump performance prediction.

4.5.1 Bingham plastic viscosity determination

The Bingham plastic viscosity is determined by forcing the fluid to be modelled as Bingham plastic. The result of this process is displayed in Figures 4.14 to 4.17. In these diagrams, the gradient of the straight line represents the plastic viscosity K .

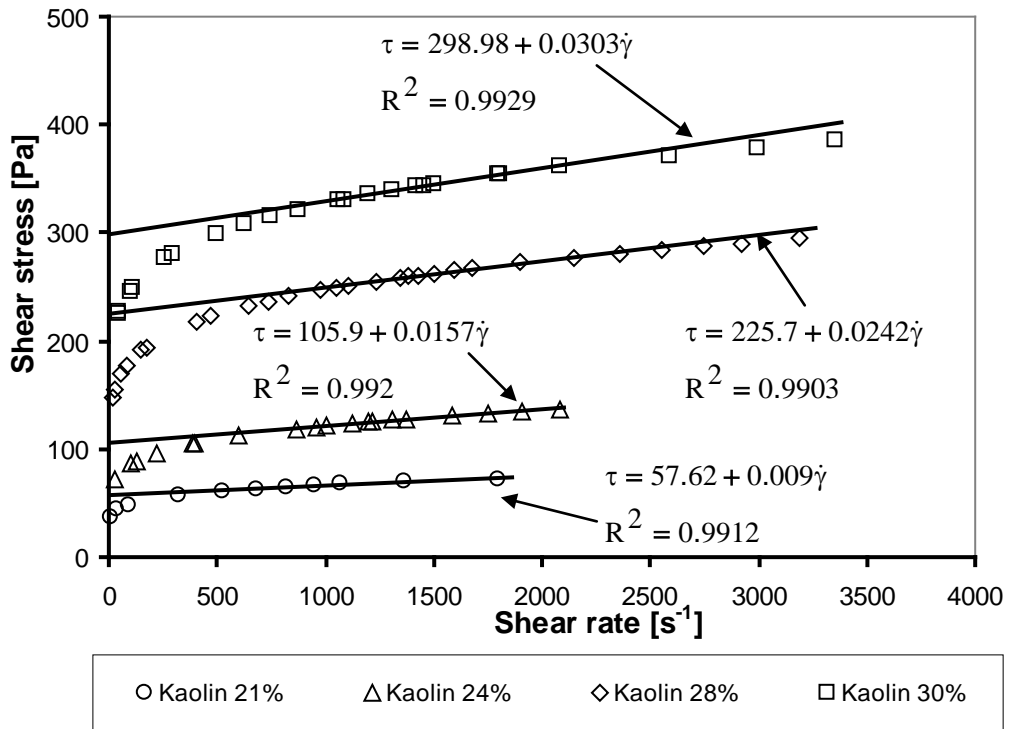


Figure 4.14: Bingham plastic model fitted to kaolin 21, 24, 28, 30% data

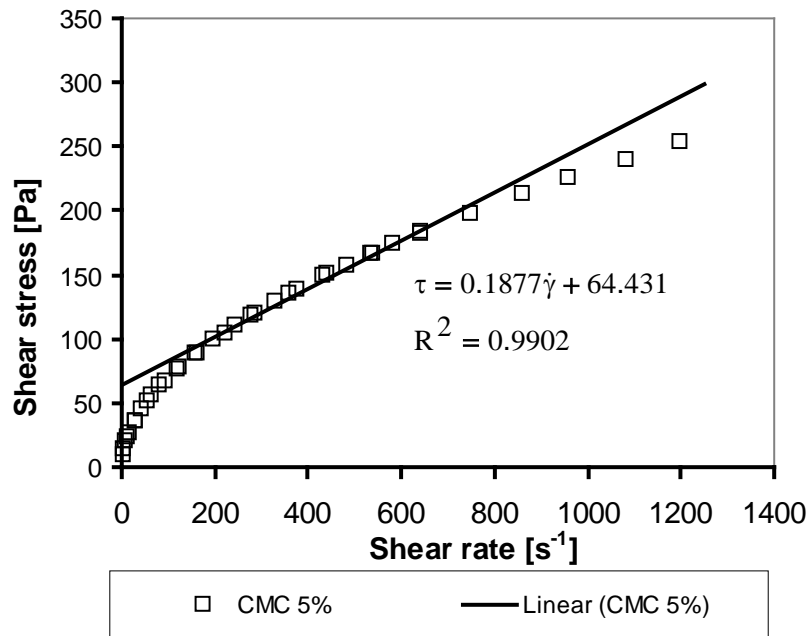


Figure 4.15: Bingham plastic model fitted to CMC 5% data

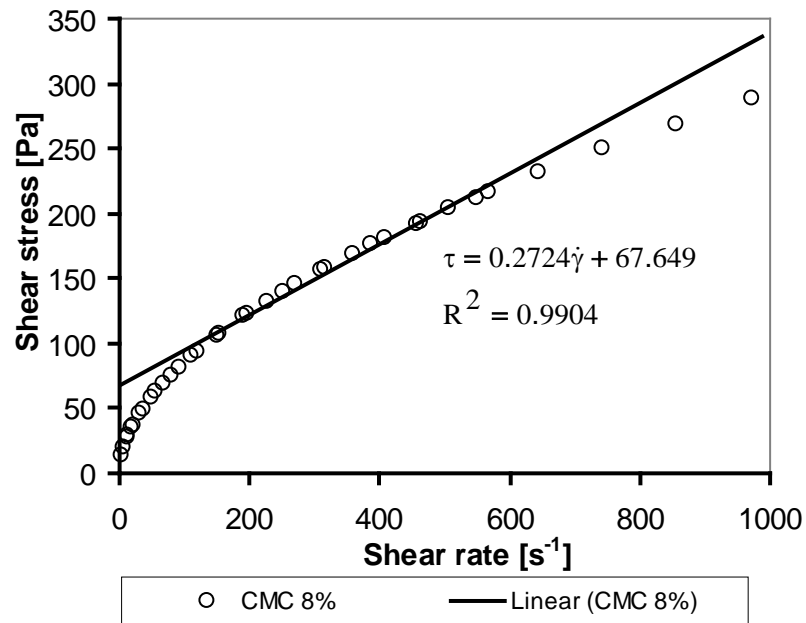


Figure 4.16: Bingham plastic model fitted to CMC 8% data

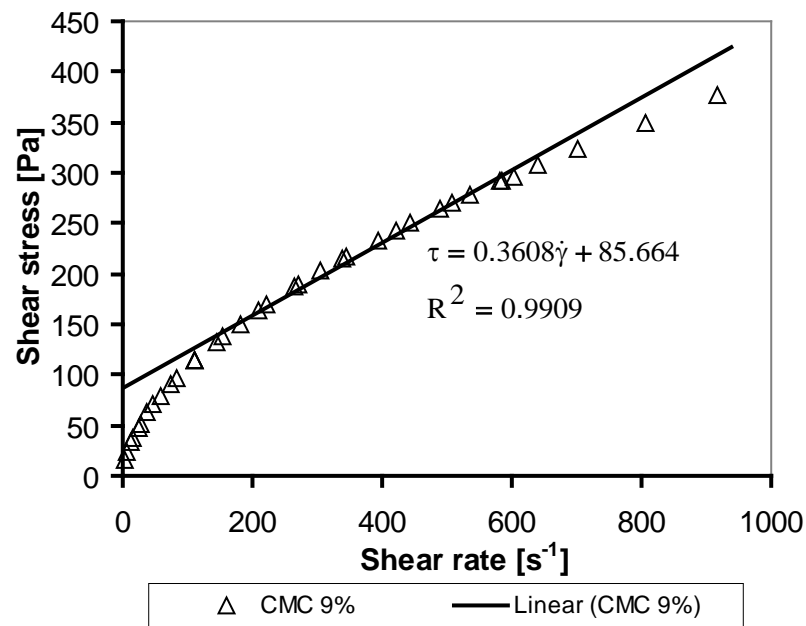


Figure 4.17: Bingham plastic model fitted to CMC 9% data

The Table 4.3 summarises the plastic viscosities for the different materials tested.

Table 4.3: Rheological parameters using the Bingham plastic model

Materials		Density [kg/m ³]	Bingham model		
			τ_y [Pa]	K [Pa.s ⁿ]	n
Kaolin	21%	1348.1	57.62	0.009	1
	24%	1400.6	105.90	0.016	1
	28%	1461.7	225.70	0.024	1
	30%	1490.2	298.98	0.030	1
CMC	5%	1030.3	64.43	0.188	1
	8%	1046.2	67.65	0.272	1
	9%	1057.9	85.66	0.361	1

4.5.2 Pump performance prediction using the Walker and Goulas (1984) approach

The Bingham plastic viscosities obtained are used in the HI method to determine the predicted performance, according to Equations 2.58 to 2.66. Calculated and experimental performance is then plotted on the same graph and compared with the water performance. Figures 4.18 and 4.19 below are typical results obtained.

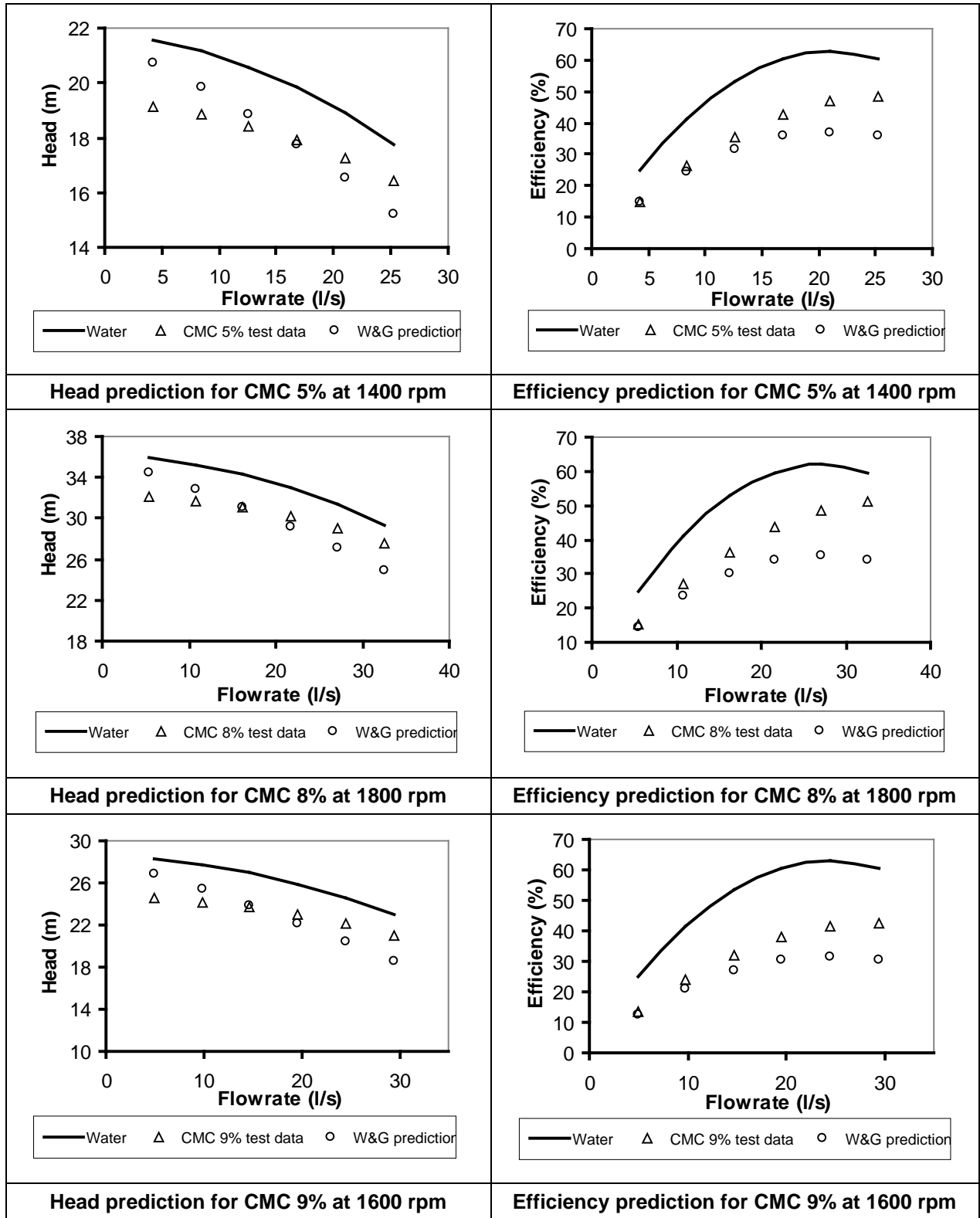


Figure 4.18: Pump performance prediction for the Warman 4/3 handling CMC, using the Walker and Goulas (1984) approach

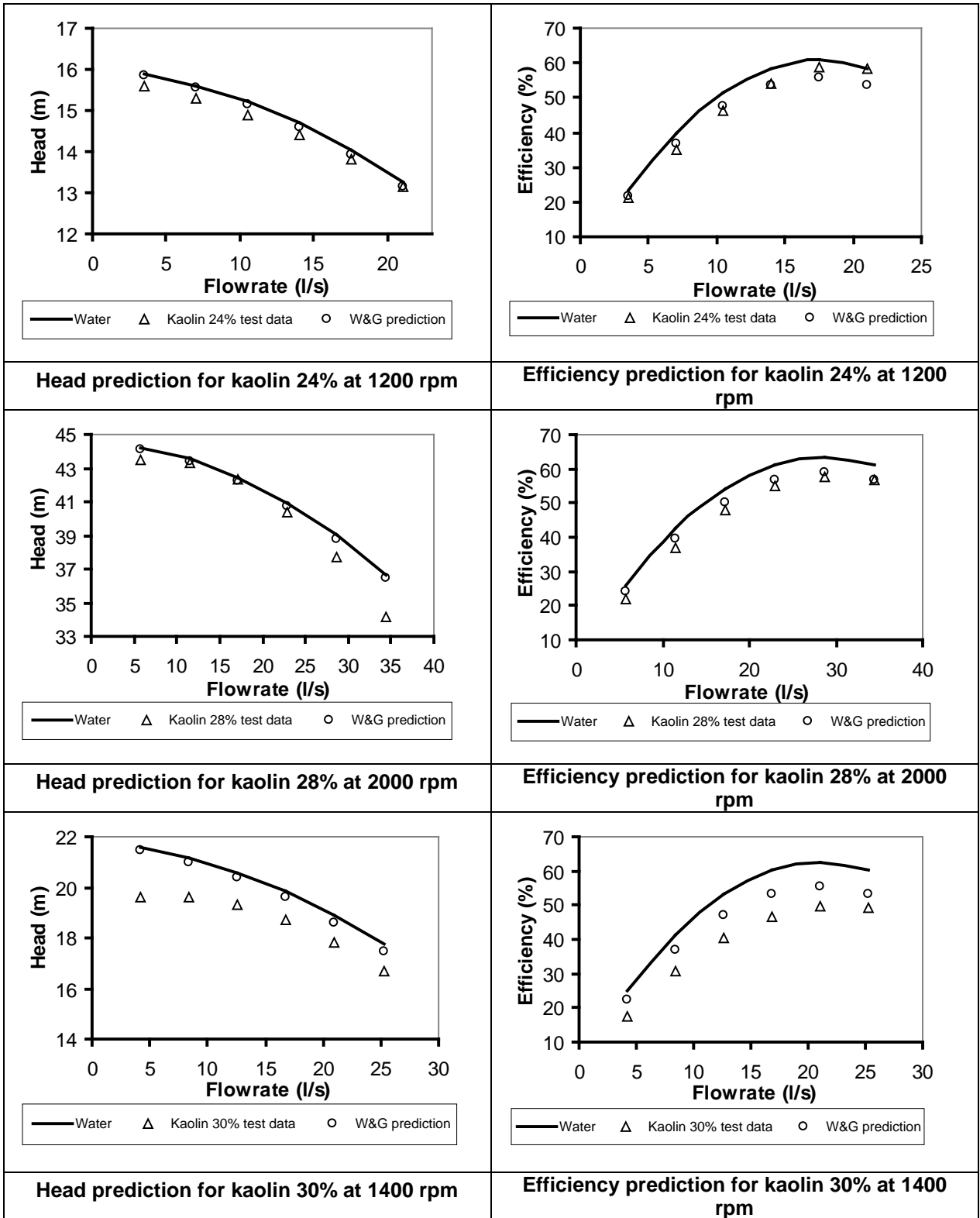


Figure 4.19: Pump performance prediction for the Warman 4/3 handling kaolin, using the Walker and Goulas (1984) approach

The comparison of experimental and calculated data indicates that 93% of the points fall into the zone of $\pm 10\%$ for the head prediction and 90% of the points into the zone of $\pm 18\%$ for the efficiency prediction (see Figures 4.20 and 4.21).

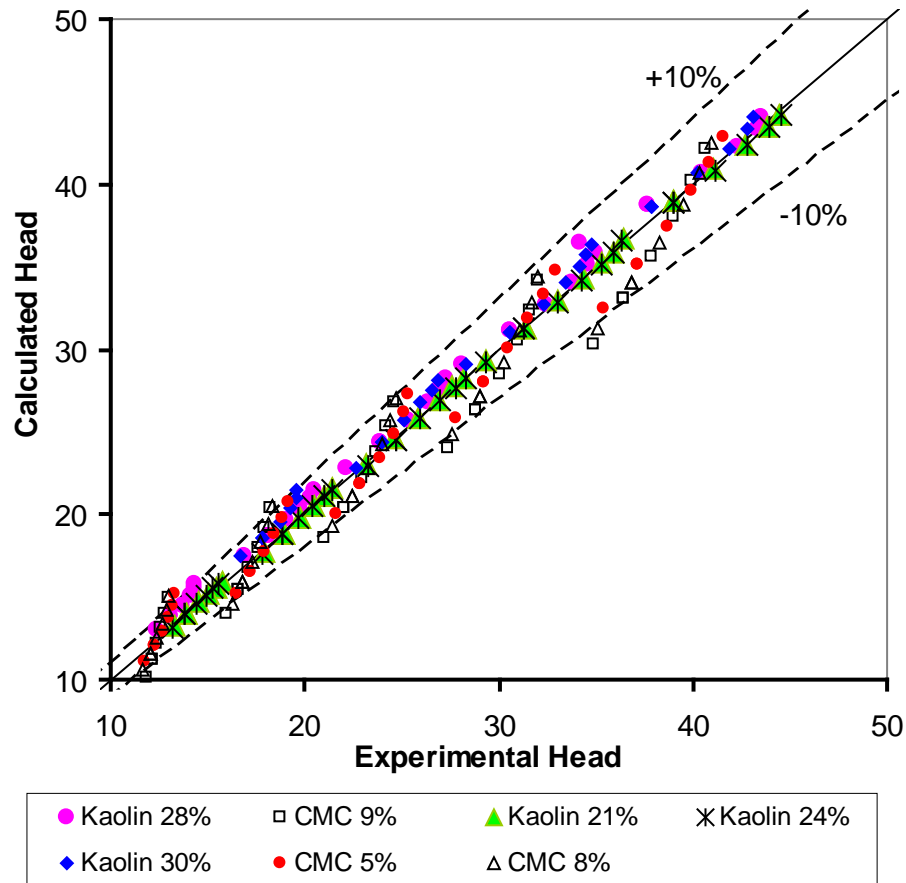


Figure 4.20: Calculated head versus experimental head for the Walker and Goulas (1984) approach

Note: To establish the same reference for comparison, a range in the correlation graph was considered as error margin only when it contains at least 90% of points.

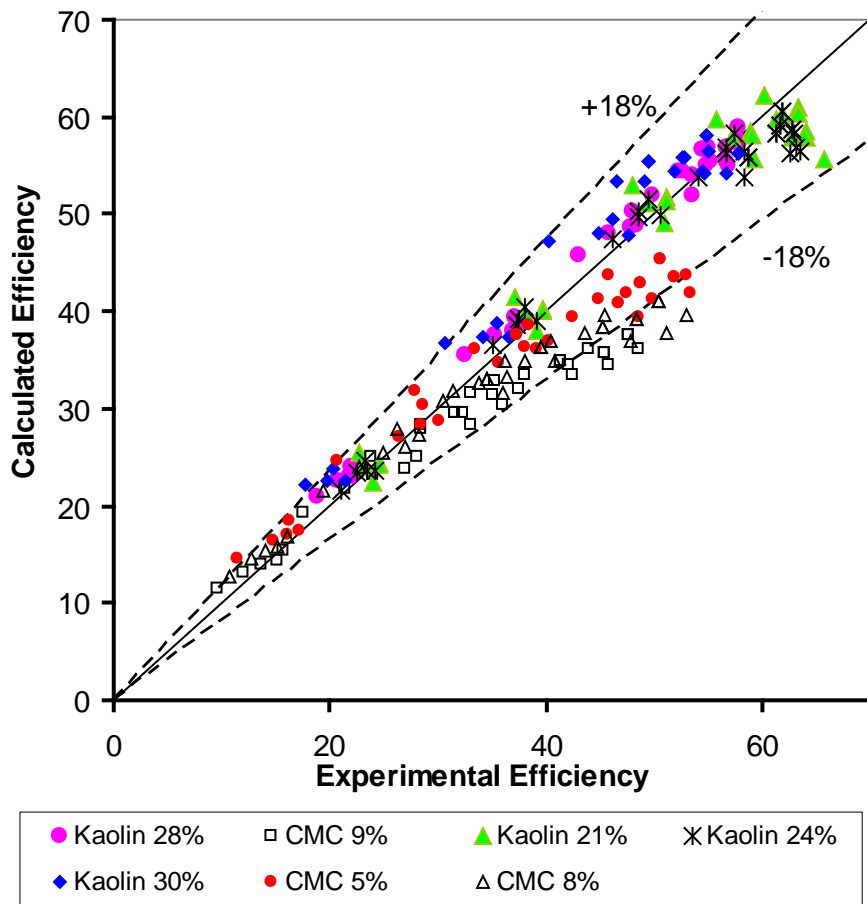


Figure 4.21: Calculated efficiency versus experimental efficiency for the Walker and Goulas (1984) approach

4.6 PULLUM *et al.* (2007) APPROACH

To predict the pump performance, Pullum *et al.* (2007) used the apparent viscosity in the HI method, as explained in section 2.7.2.2. To determine this apparent viscosity, a value of the characteristic dimension w should be fixed. Then the prediction is made using this value of w . The results for this prediction are presented in this section.

4.6.1 Characteristic dimension w

As stated in section 2.7.2.2.b, to determine the value of the characteristic dimension w , the Pullum *et al.* (2007) approach was applied to the sets of data available. Considering that Graham *et al.* (2009) pointed out that the average value of the ratio $w/D_{imp} = 25\%$, a value of $w = 0.25 * D_{imp}$ (or $w = 0.061$ for the Warman 4/3 used in this work) was chosen as first estimate of w . This first estimate led to the calculation of the intermediate predicted pump head data. The error between these intermediate predicted head data and experimental data was determined.

An iterative process was then applied and “a least square error method” was used for the optimisation of w .

The value of the characteristic dimension $w = 0.023$ was established for the Warman 4/3 pump.

4.6.2 Predicted pump performance

The pump performance prediction obtained using $w = 0.023$ was compared with the experimental pump performance and water pump performance. Figures 4.22 and 4.23 depict the results of this prediction for different motor speeds and concentrations of the materials used.

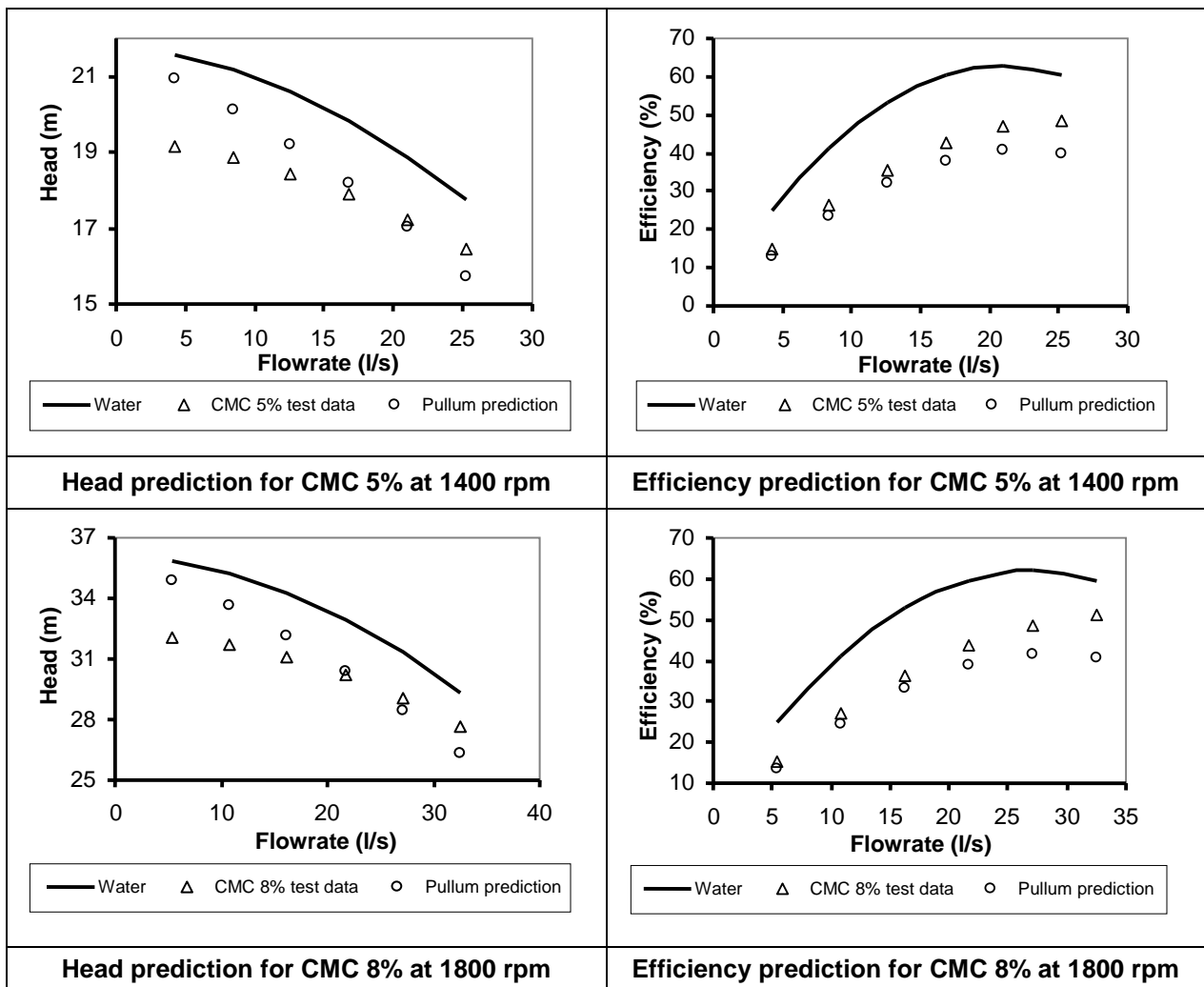


Figure 4.22: Pump performance prediction for the Warman 4/3 handling CMC, using the Pullum *et al.* (2007) approach

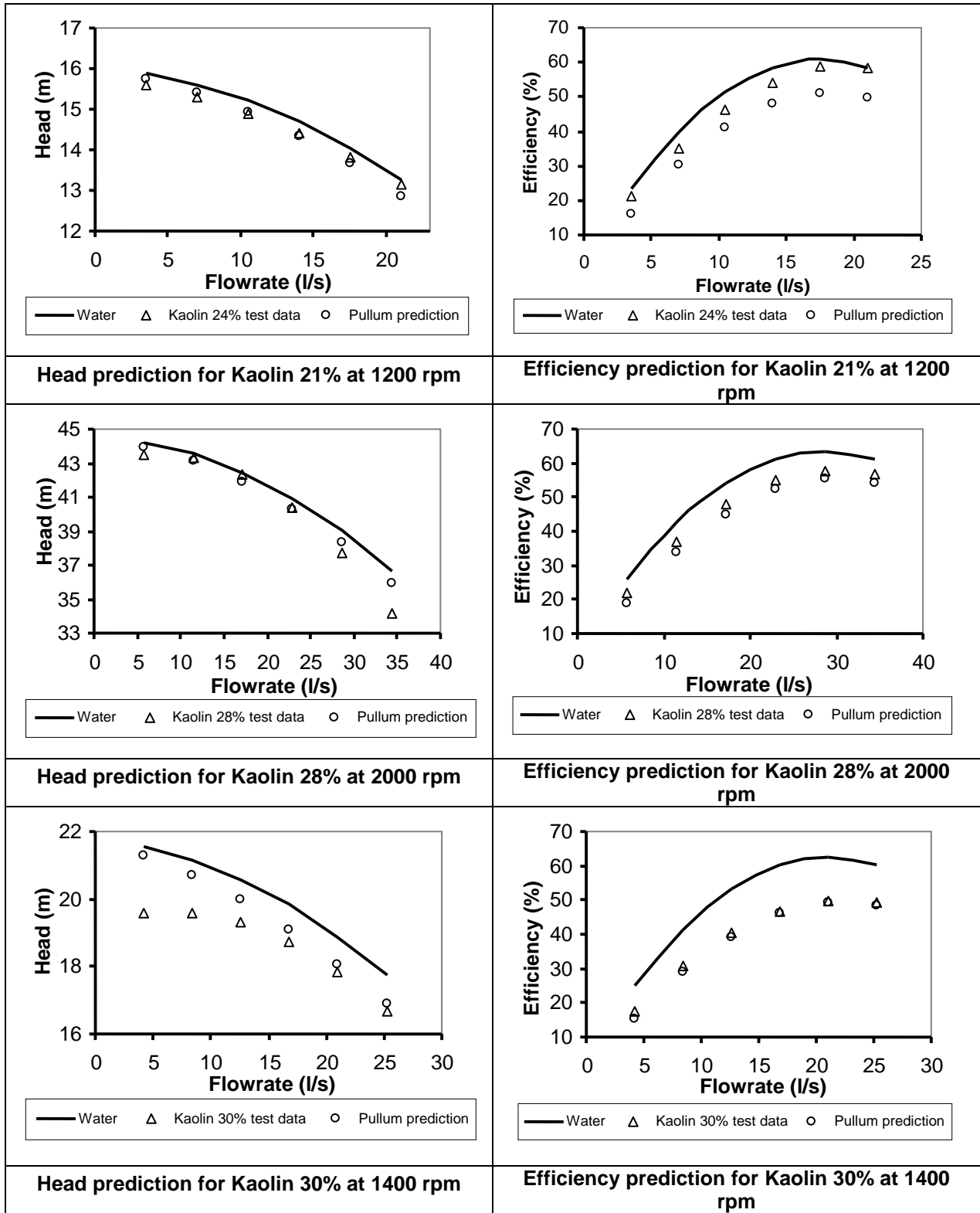


Figure 4.23: Pump performance prediction for the Warman 4/3 handling kaolin, using the Pullum et al. (2007) approach

In Figures 4.24 and 4.25, plots of experimental data against calculated data (using the Pullum *et al.* (2007) approach) reveal that 91% of the points for the head prediction are within $\pm 8\%$ and 92% within -20% for the efficiency.

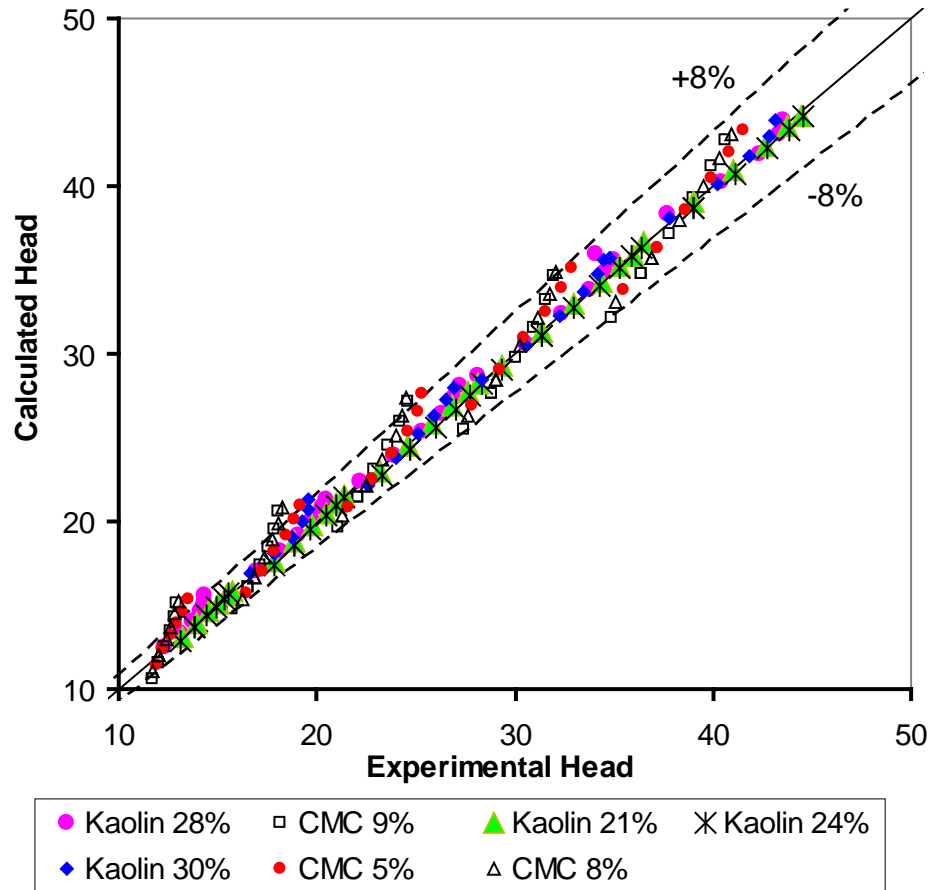


Figure 4.24: Calculated head versus experimental head for the Pullum *et al.* (2007) approach.

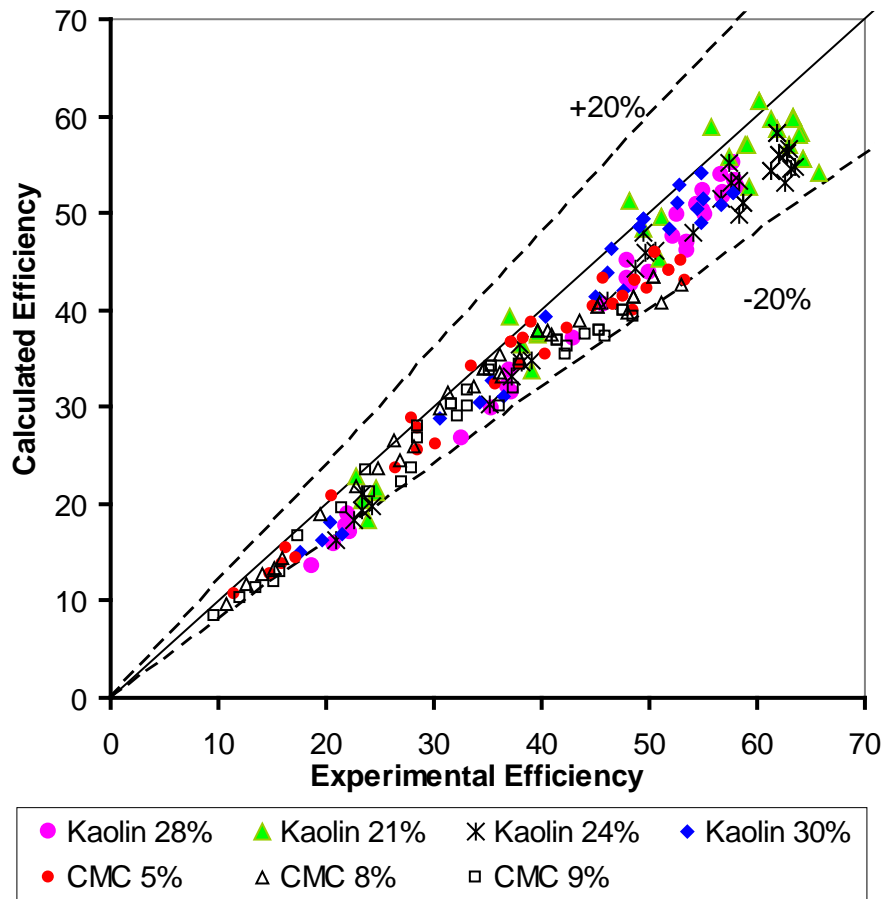


Figure 4.25: Calculated efficiency versus experimental efficiency for the Pullum *et al.* (2007) approach

4.7 ANALYSIS OF KABAMBA'S (2006) DATA

Data obtained by Kabamba (2006) were analysed, using the two approaches and the results are presented in this section.

4.7.1 Rheological characterisation

The results of the rheological characterisation and Bingham plastic viscosity determination for existing data are summarised in Table 4.4.

Table 4.4: Rheological parameters from Kabamba (2006) data

Materials		Herschel-Bulkley model			Bingham model		
		τ_y [Pa]	K [Pa.s ⁿ]	n	τ_y [Pa]	K [Pa.s ⁿ]	n
CMC	5%	0.0	1.299	0.650	17.6	0.114	1
	6%	0.0	2.039	0.650	31.0	0.167	1
	7%	0.0	3.875	0.589	54.4	0.187	1
Kaolin	17%	115.6	0.240	0.704	125.2	0.020	1
	19%	156.8	0.933	0.531	190.3	0.010	1
	21%	207.7	3.626	0.403	246.6	0.019	1
Bentonite	7%	5.7	0.016	1.000	5.7	0.016	1
	9%	28.9	0.017	1.000	28.9	0.017	1

4.7.2 Pump prediction according to the Walker and Goulas (1984) approach

4.7.2.1 Prediction for the GIW 4/3

The pump head, for the GIW 4/3 pump, was predicted with an error margin of +15% (Figure 4.26) and efficiency was predicted with $\pm 18\%$ error margin as shown in Figure 4.27.

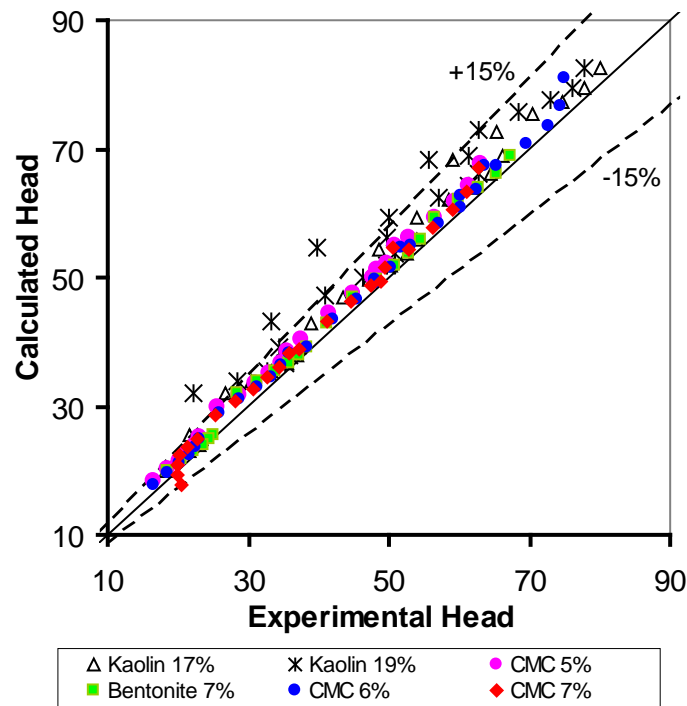


Figure 4.26: Experimental head versus calculated head for the GIW 4/3 using the Walker and Goulas (1984) approach

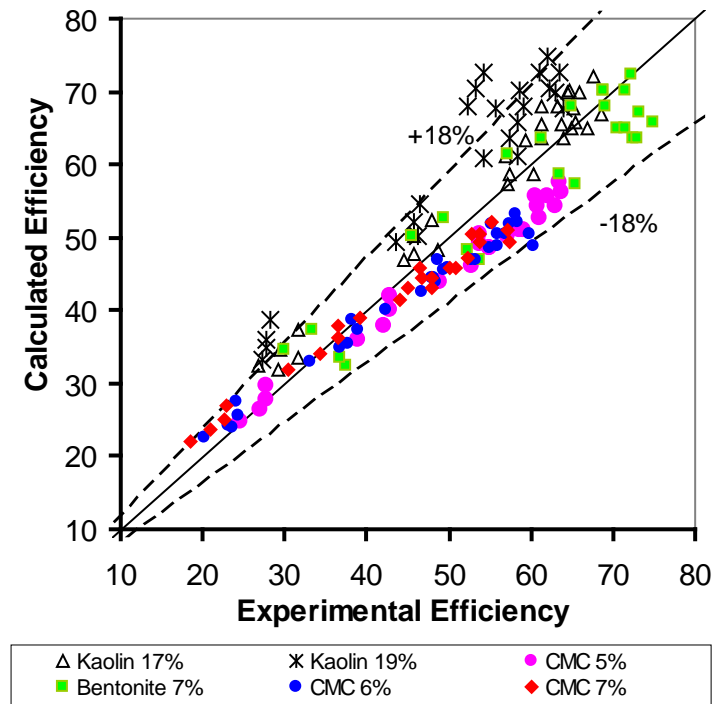


Figure 4.27: Experimental efficiency versus calculated efficiency for the GIW 4/3 using the Walker and Goulas (1984) approach

4.7.2.2 Prediction for the Warman 6/4

The pump head, for the Warman 6/4 pump, was within the error margin between -3 and +27% (Figure 4.23) and the efficiency was predicted with $\pm 26\%$ error margin as shown in Figure 4.29.

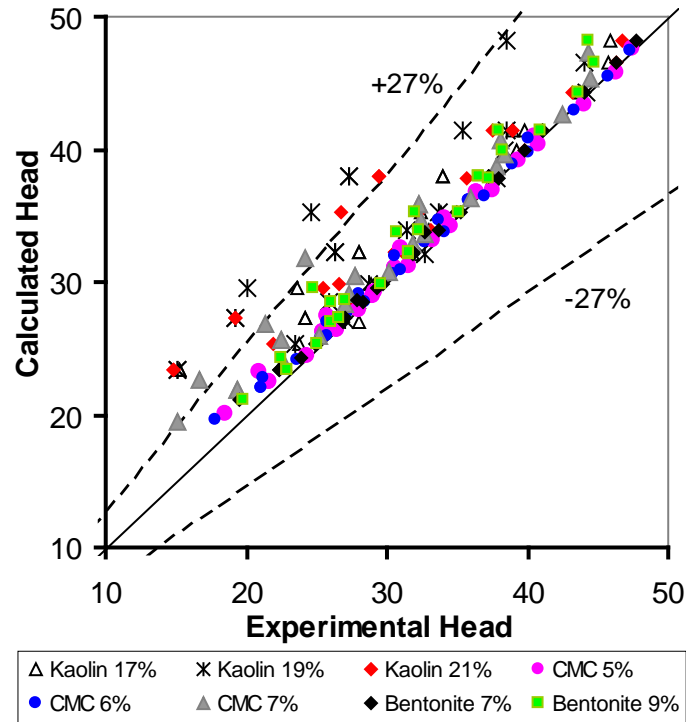


Figure 4.28: Experimental head versus calculated head for the Warman 6/4 using the Walker and Goulas (1984) approach

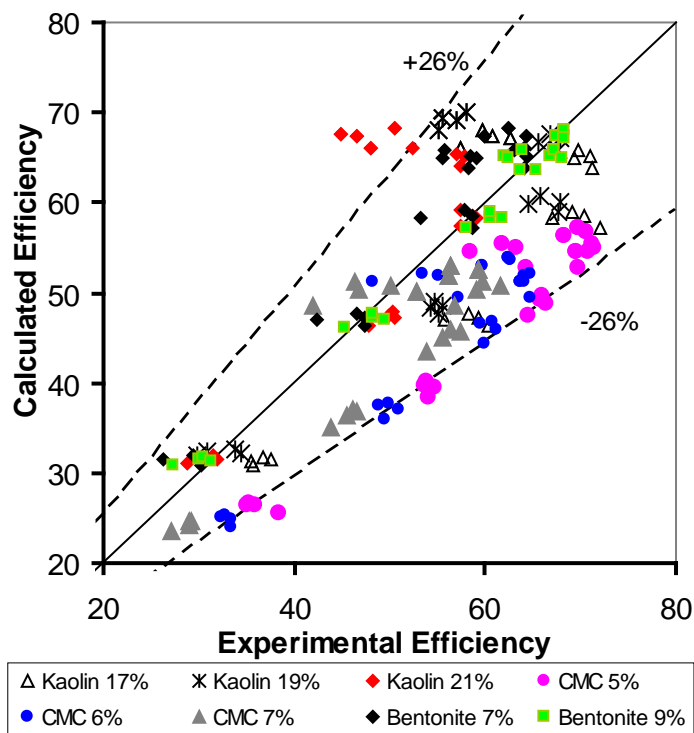


Figure 4.29: Experimental efficiency versus calculated efficiency for the Warman 6/4 using the Walker and Goulas (1984) approach

4.7.3 Pump prediction using the Pullum *et al.* (2007) approach

4.7.3.1 Prediction for the GIW 4/3

Using the existing data for the GIW 4/3 in the Pullum *et al.* (2007) approach, the characteristic dimension was found to be $w = 0.085$. No difference was noticed between the correlation obtained using $w = 0.085$ and that obtained using $w = 0.084$ (value obtained by Pullum *et al.* (2007) for the GIW 4/3 pump). The pump head was predicted with an error margin of $\pm 8\%$ but the efficiency could not be predicted satisfactorily (see Figures 4.30 and 4.31).

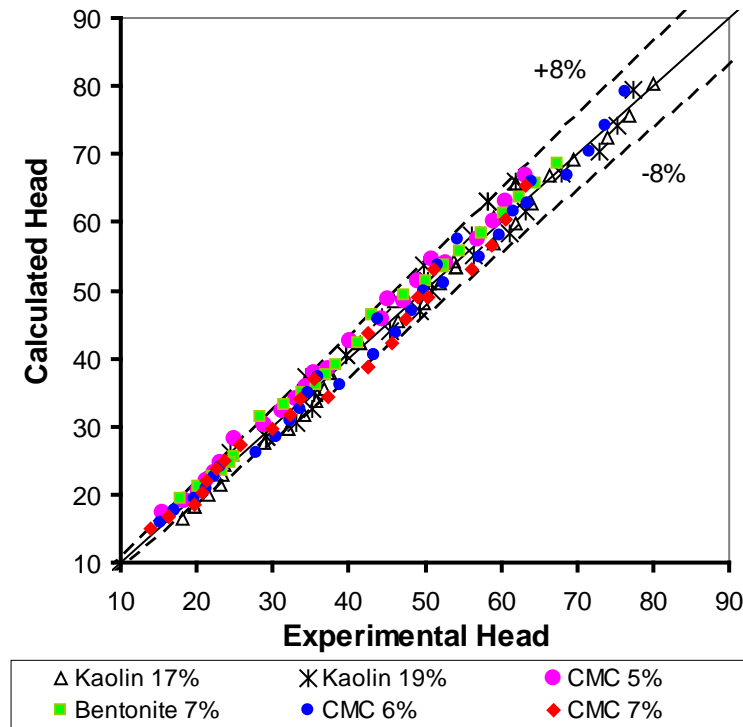


Figure 4.30: Experimental head versus calculated head for the GIW 4/3 in the Pullum *et al.* (2007) approach

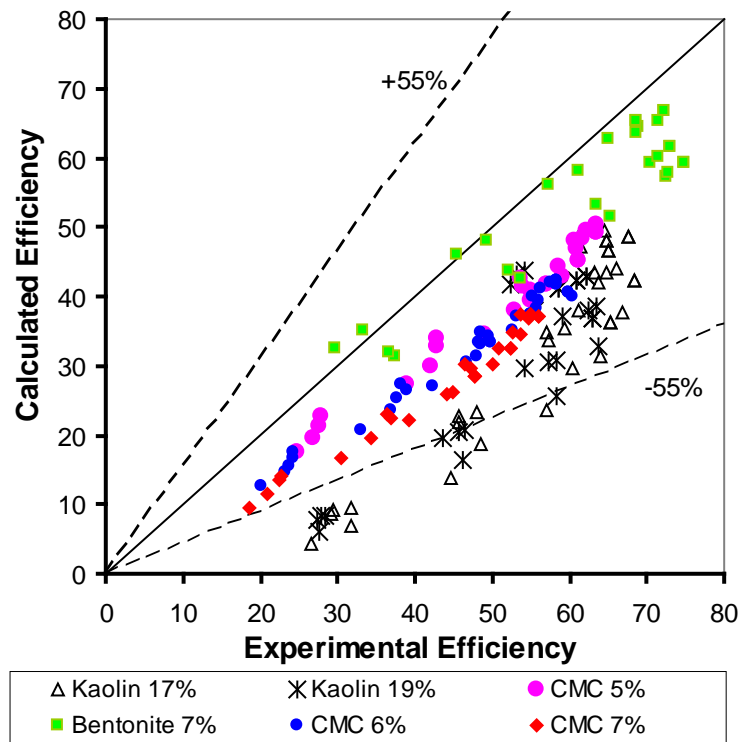


Figure 4.31: Experimental efficiency versus calculated efficiency for the GIW 4/3 in the Pullum *et al.* (2007) approach

4.7.3.2 Prediction for the Warman 6/4

The analysis of the existing data for the Warman 6/4 pump gave the characteristic dimension $w = 0.160$. For the pump head, 90% of the points fall in a $\pm 13\%$ error margin. Once again the efficiency could not be predicted in a satisfactory way (see Figures 4.32 and 4.33).

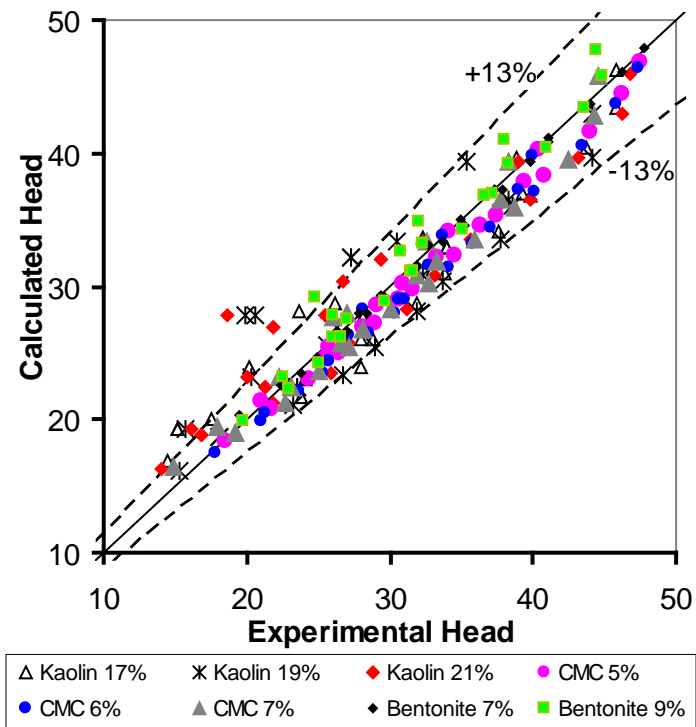


Figure 4.32: Experimental head versus calculated head for the Warman 6/4 in the Pullum *et al.* (2007) approach

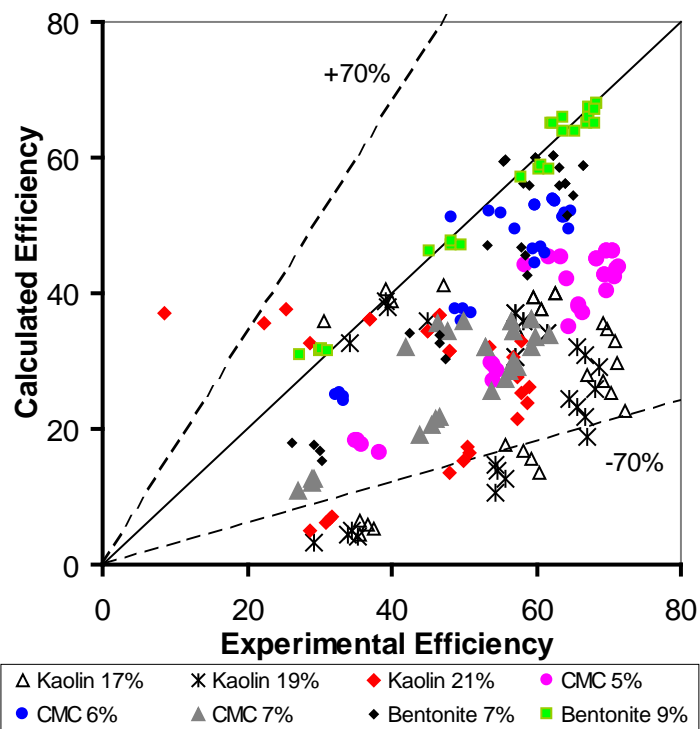


Figure 4.33: Experimental efficiency versus calculated efficiency for the Warman 6/4 in the Pullum *et al.* (2007) approach

4.8 ANALYSIS OF SLUDGE DATA

The same procedure of analysis was applied to a complete set of data obtained by testing two Flygt NZ3102.181 submersible centrifugal pumps of different size impellers (135 mm and 152 mm diameter), pumping eight concentrations of sludge. These tests were conducted in Stockholm, Sweden, by researchers from the FPRC. Figures 4.34 to 4.40 show the results obtained.

4.8.1 Sludge rheology

The sludge rheological characterisation was made considering the three rheological models: the pseudoplastic, the Bingham plastic and the yield pseudoplastic. Figures 4.34 to 4.36 show the rheological characterisation results.

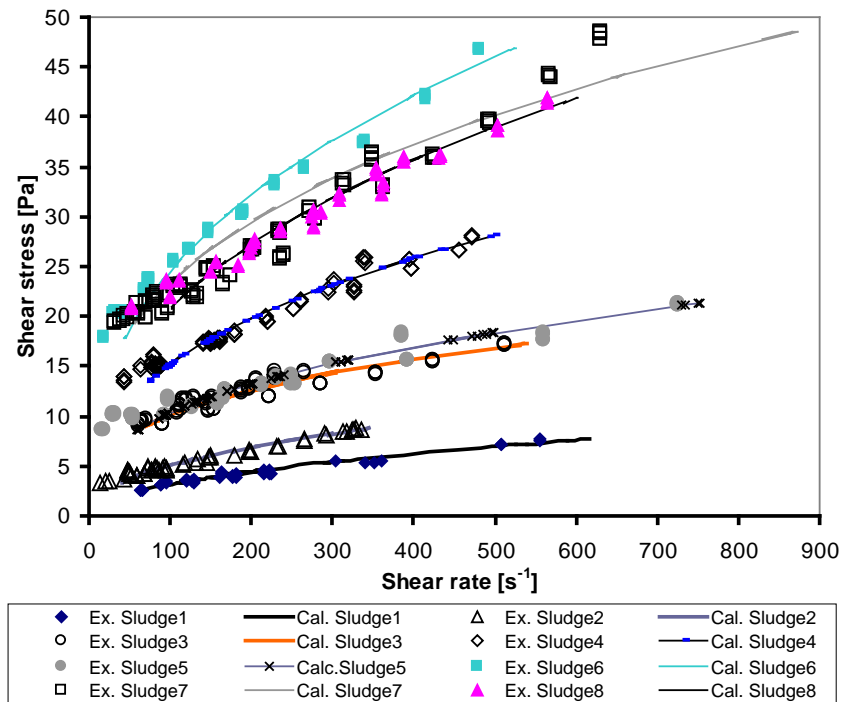


Figure 4.34: Pseudoplastic model fitted to sludge rheograms

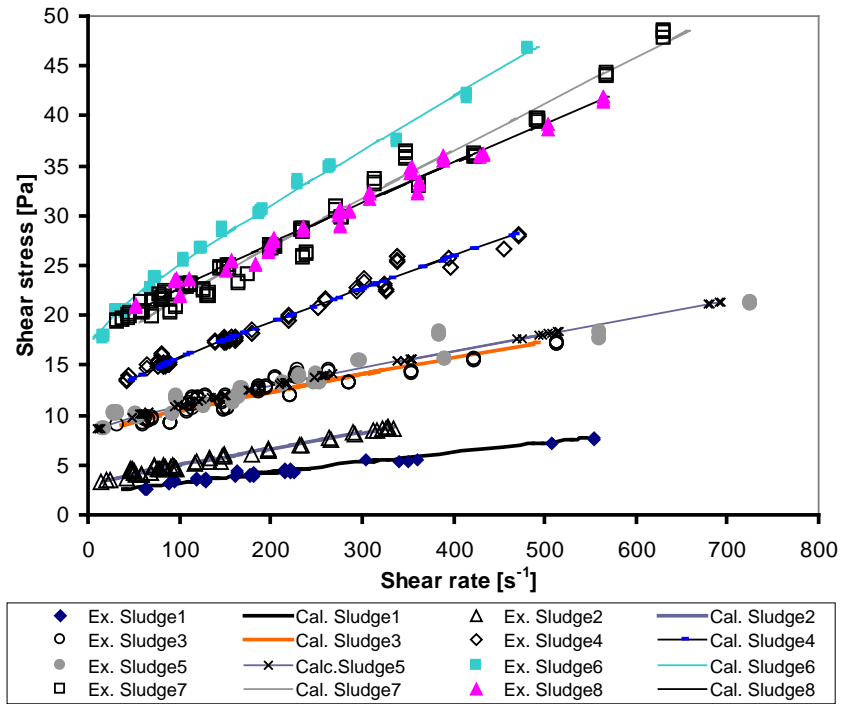


Figure 4.35: Bingham plastic model fitted to sludge rheograms

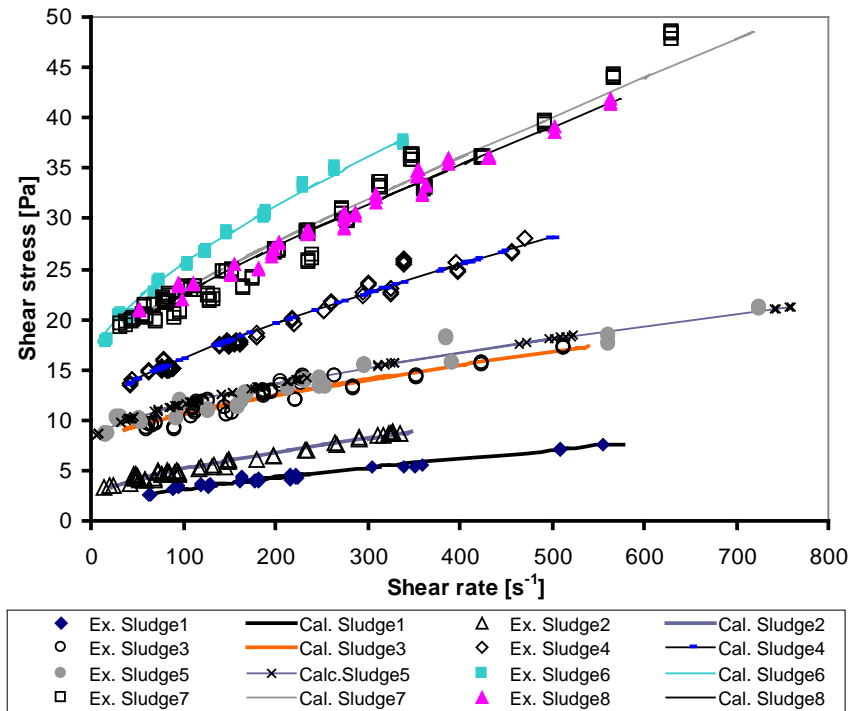


Figure 4.36: Yield pseudoplastic model fitted to sludge rheograms

Table 4.5 below summarises the results of the rheological characterisation.

Table 4.5: Rheological parameters of the sludges.

		Pseudoplastic	Bingham plastic	Yield pseudoplastic
Sludge 1	K	0.318	0.01	0.07
	n	0.477	1	0.697
	τ_y	0	1.8	1
Sludge 2	K	0.574	0.016	0.102
	n	0.446	1	0.69
	τ_y	0	2.7	2
Sludge 3	K	2.055	0.016	0.051
	n	0.317	1	0.802
	τ_y	0	7.3	7
Sludge 4	K	2.318	0.032	0.07
	n	0.381	1	0.86
	τ_y	0	10.1	10
Sludge 5	K	1.748	0.016	0.077
	n	0.357	1	0.749
	τ_y	0	7.7	7.5
Sludge 6	K	3.571	0.052	0.168
	n	0.391	1	0.8
	τ_y	0	15.9	15
Sludge 7	K	1.599	0.04	0.152
	n	0.49	1	0.8
	τ_y	0	11.1	10
Sludge 8	K	3.015	0.038	0.074
	n	0.391	1	0.9
	τ_y	0	15.4	14.4

4.8.2 Walker and Goulas (1984) approach

Obviously, the rheological parameters obtained with the Bingham plastic model were used for the prediction of pump performance in this approach. For the 135 mm and 152 mm impeller submersible centrifugal pumps, the efficiency is correlated within $\pm 7\%$ and $\pm 5\%$ error margin respectively, while the pump head is over-predicted by 16% and 14% respectively. (See Figures 4.37 and 4.38.)

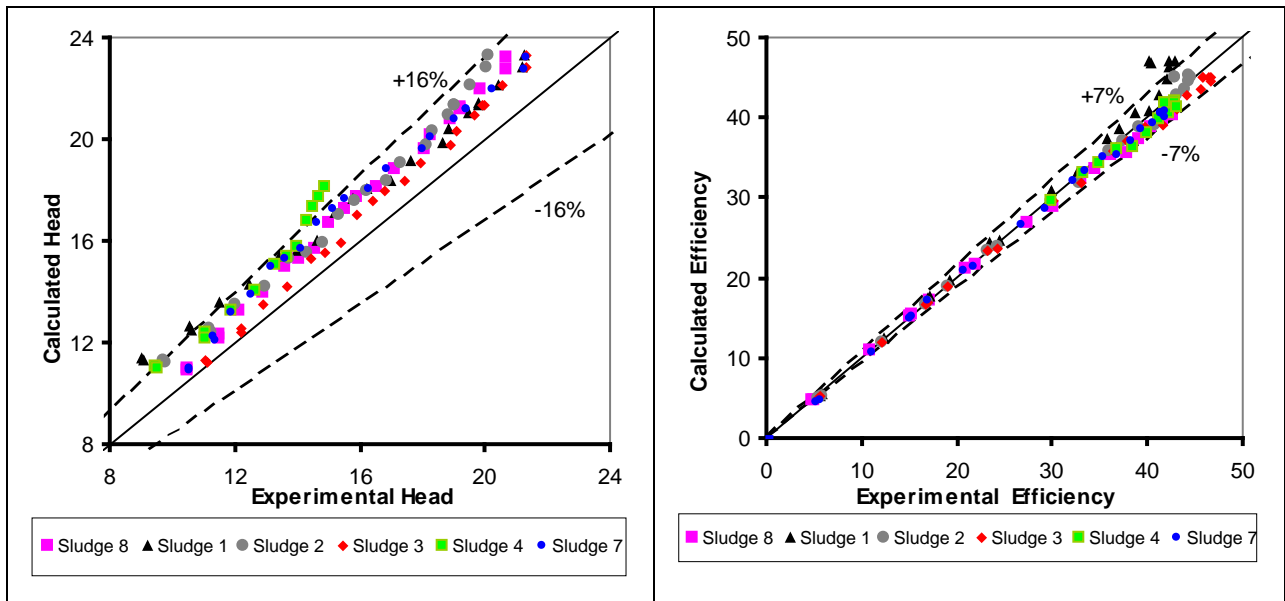


Figure 4.37: Experimental head (efficiency) versus calculated head (efficiency) for the 135 mm impeller in the Walker and Goulas (1984) approach

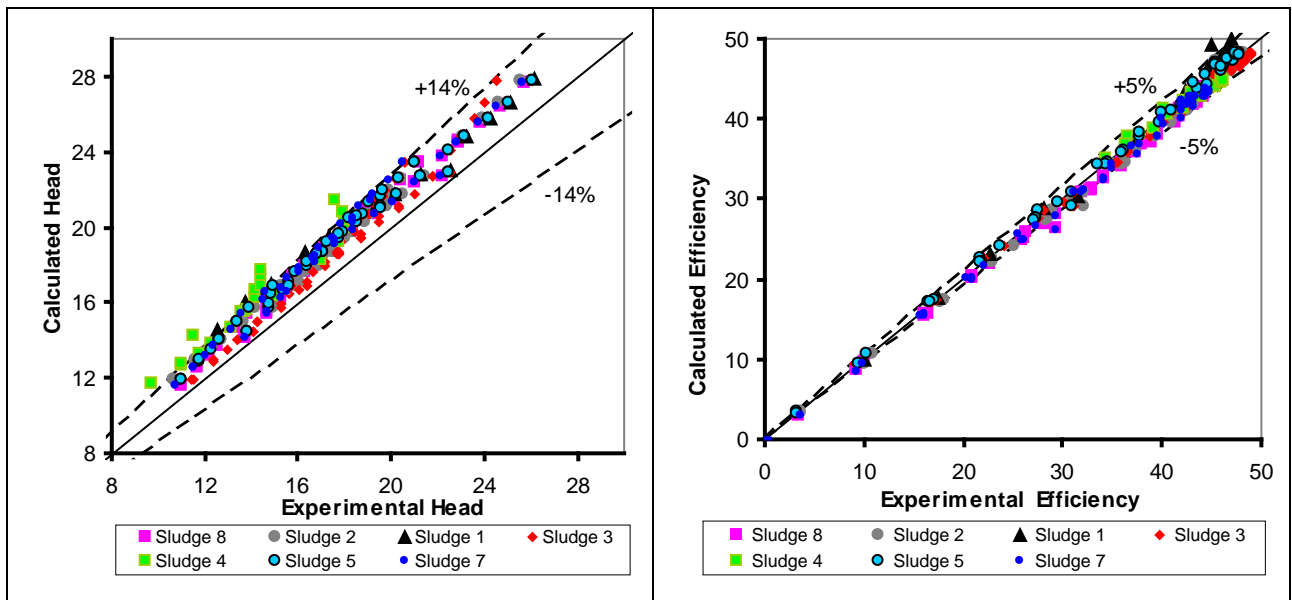


Figure 4.38: Experimental head (efficiency) versus calculated head (efficiency) for the 152 mm impeller in the Walker and Goulas (1984) approach.

4.8.3 Pullum *et al.* (2007) approach

For this approach, the three rheological models were used in the pump performance prediction. The results obtained were so close, but the yield pseudoplastic was selected because of its characteristic of being a general model.

The analysis of the submersible pump data gave the characteristic dimensions $w = 0.071$ and $w = 0.073$ for the 135 mm and 152 mm diameter impeller pumps respectively.

For the two submersible centrifugal pumps, the head is correlated with $\pm 10\%$ error margin for the 135 mm diameter impeller pump and over-predicted by 12% for the 152 mm diameter impeller pump. The efficiency is under-predicted by 32% and 30% for 135 and 152 mm diameter impeller pumps respectively. (See Figures 4.39 and 4.40.)

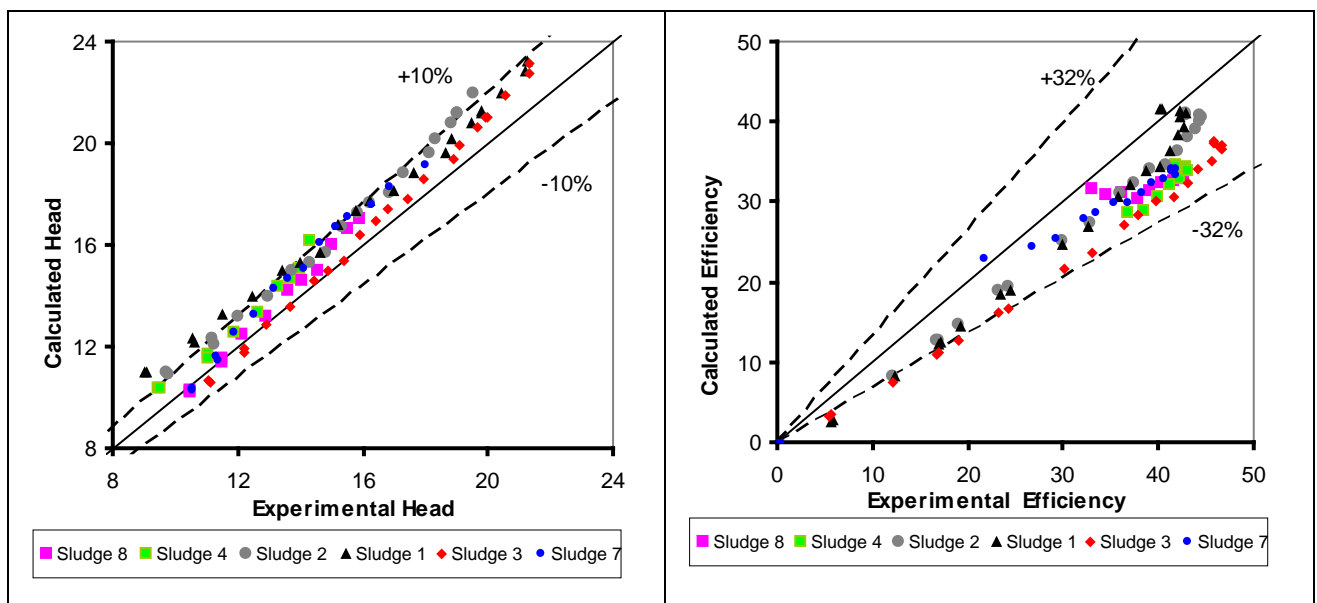


Figure 4.39: Experimental head (efficiency) versus calculated head (efficiency) for the 135 mm impeller in the Pullum *et al.* (2007) approach

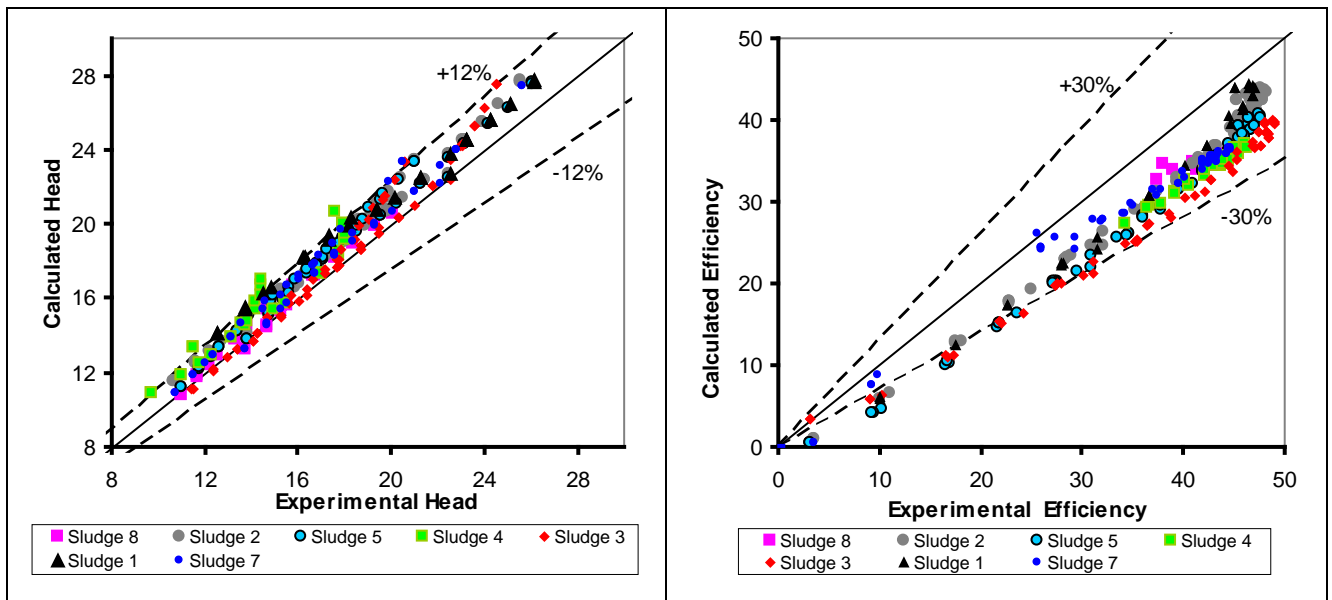


Figure 4.40: Experimental head (efficiency) versus calculated head (efficiency) for the 152 mm impeller in the Pullum *et al.* (2007) approach

4.9 WALKER and GOULAS (1984) APPROACH AND PULLUM *et al.* (2007) APPROACH COMPARISON

For this work's data, Figures 4.20 and 4.24 show that the pump head is well predicted using the Pullum *et al.* (2007) approach ($\pm 8\%$) rather than using the Walker and Goulas (1984) approach ($\pm 10\%$). Figure 4.21 shows the pump efficiency prediction within $\pm 18\%$ for the Walker and Goulas (1984) approach but in Figure 4.25 it can be noticed that the efficiency is under-predicted by 20% for the Pullum *et al.* (2007) approach. For kaolin and CMC data, the pump performance is reasonably well predicted using the Pullum *et al.* (2007) approach.

For the Kabamba (2006) data, using the Pullum *et al.* (2007) approach, the head was predicted within $\pm 8\%$ and $\pm 13\%$ for the GIW 4/3 and Warman 6/4 pumps respectively (Figures 4.30 and 4.32); while it was over-predicted by 15% and 27% using the Walker and Goulas (1984) approach for the two pumps respectively (Figures 4.26 and 4.28). From the previous, the head seems to be better correlated using the Pullum *et al.* (2007) approach than the Walker and Goulas (1984) approach. However, by comparing Figures 4.27 and 4.29 with Figures 4.31 and 4.33 respectively for the two pumps, the efficiency seems to be better predicted by the Walker and Goulas (1984) approach.

For the sludge data, the same observation as for the Kabamba (2006) data can be made by examining Figures 4.37 to 4.40.

Table 4.6 below summarises the results of these correlations.

Table 4.6: Summary of pump prediction results

			Walker & Goulas (1984)		Pullum <i>et al.</i> (2007)	
			Error margin	% Points in error margin	Error margin	% Points in error margin
This work data	Warman 4/3	Head	±10%	93	±8%	91
		Efficiency	±18%	90	-20%	92
Kabamba (2006) data	GIW 4/3	Head	+15%	91	±8%	92
		Efficiency	±18%	91	-	-
	Warman 6/4	Head	-3 to +27%	90	±13%	90
		Efficiency	±26%	92	-	-
Submersible pumps data	135 mm Impeller	Head	+16%	92	±10%	92
		Efficiency	±7%	93	-32 to +6%	90
	152 mm Impeller	Head	+14%	94	-2 to +12%	91
		Efficiency	±5%	92	-30 to +10%	90

Note: Different values of w obtained after analysing all data sets available are presented in Table 4.7 below.

Table 4.7: Values of characteristic dimension w for different data analysed

Pump used	Pullum <i>et al.</i>	This work	Kabamba data	Sludge data
Warman 4/3	0.059	0.023	-	-
Warman 6/4	-	-	0.160	-
GIW 4/3	0.084	-	0.085	-
Flygt (135 mm Ø)	-	-	-	0.071
Flygt (152 mm Ø)	-	-	-	0.073

4.10 CONCLUSIONS

This chapter has outlined the results obtained from the experimental work on the pump rig and the results of the analysis of all available data.

- The water pressure drop test results have been presented and correlated with the Colebrook-White equation to ascertain the accuracy and credibility of the equipment used in the pipe section. Likewise, the pump performance test results for water have

been presented and compared with the catalogue curves to ensure the reliability of the equipment used in the pump section.

- The results of the rheological characterisation and pump performance tests were presented for the various concentrations of kaolin suspensions and CMC solutions tested.
- The experimental data obtained in this work were analysed according to the Walker and Goulas (1984) approach and then again, according to the Pullum *et al.* (2007) approach.
- The databases from Kabamba (2006) were analysed using both approaches.
- Data from the sludge test conducted in Sweden with submersible pumps were analysed using both approaches.

Chapter 5 DISCUSSION OF RESULTS

5.1 INTRODUCTION

The results of the data analysis, presented in Chapter 4, are discussed and evaluated in this chapter. This discussion is articulated with comparisons at two levels:

- Comparison between the results obtained using the values of the characteristic dimension provided in the Pullum *et al.* (2007) work and those obtained using the characteristic dimension established in this work. This is applied only to the Pullum *et al.* (2007) approach.
- Comparison between the overall results in the Walker and Goulas (1984) approach and the overall results in the Pullum *et al.* (2007) approach.

5.2 SUMMARY OF NON-NEWTONIAN PUMP DERATION

Pump users are concerned with finding a procedure for pump performance deration for non-Newtonian material as the HI method is well established for viscous Newtonian materials.

Researchers have therefore used the HI method, meant for Newtonian fluids, to calculate the pump performance deration for non-Newtonian fluids. This was made possible only by defining a unique representative viscosity of the non-Newtonian fluid tested. Two available ways presented in Chapter 2 have been investigated: the Walker and Goulas (1984) approach and the Pullum *et al.* (2007) approach.

Walker and Goulas (1984) were the first to calculate the non-Newtonian pump performance using the Bingham plastic viscosity in the HI Chart. They were able to predict both the head and efficiency of two centrifugal pumps with an error margin of $\pm 5\%$. They dealt only with yield pseudoplastic materials.

Sery and Slatter (2002) used the Walker and Goulas (1984) approach and predicted the head and efficiency of a Warman 4/3 pump, using glycerine and kaolin suspension, with an error margin of $\pm 20\%$ and $\pm 10\%$ respectively.

Kabamba (2006) extended the Walker and Goulas (1984) work to pseudoplastic materials. He predicted both the head and efficiency of a GIW 4/3 pump within a $\pm 15\%$ error margin. He

predicted as well, the head and efficiency of a Warman 6/4 pump within $\pm 10\%$ and $\pm 20\%$ margins respectively.

Pullum *et al.* (2007) used the apparent viscosity, based on the pump geometry, the fluid rheology and flow rate, in the HI method to predict the pump head, as described in section 2.7.2.2. For the two pumps used, the head was predicted within $\pm 10\%$ margin. No efficiency prediction results were presented in their work.

In the present work, the two approaches were used. The pump head was predicted within $\pm 10\%$ and $\pm 8\%$ for the Walker and Goulas (1984) and the Pullum *et al.* (2007) approaches respectively. The efficiency was predicted within $\pm 18\%$ error margin for the Walker and Goulas (1984) approach and under predicted by -20% for the Pullum *et al.* (2007) approach. The summary of the work done on the non-Newtonian pump deration is given in Table 5.1 below.

Table 5.1: Summary of pump deration works using non-Newtonian slurries.

	Walker & Goulas (1984)	Sery & Slatter (2002)	Kabamba (2006)	Pullum <i>et al.</i> (2007)	This work
Centrifugal pumps used	Hazleton 3 in B CTL and Warman 4/3	Warman 4/3	GIW 4/3 and Warman 6/4	GIW 4/3 and Warman 4/3	Warman 4/3
Materials tested	Coal dust and kaolin clay	Glycerine and kaolin	CMC, kaolin and bentonite	CMC and Ultrez 10	CMC and kaolin
Approach used	Walker & Goulas	Walker & Goulas	Walker & Goulas	Pullum <i>et al.</i>	Both approaches
Head correlation	$\pm 5\%$ for both pumps	$\pm 20\%$	$\pm 15\%$ for GIW 4/3 & $\pm 10\%$ for Warman 6/4.	$\pm 10\%$ for both pumps	$\pm 10\%$ for Walker & Goulas and $\pm 8\%$ for Pullum <i>et al.</i>
Efficiency correlation	$\pm 5\%$ for both pumps	$\pm 10\%$	$\pm 15\%$ for GIW 4/3 & $\pm 20\%$ Warman 6/4	-	$\pm 18\%$ for Walker & Goulas and -20% for Pullum <i>et al.</i>

5.3 EXPERIMENTAL TEST RIG, EQUIPMENT AND PROCEDURE

The pump rig was designed and constructed according to the recommendations of the international standard ISO 9906 for rotodynamic pumps and the design conforms to that found in the literature. However, while operating the test rig, the following difficulties were experienced:

- During pump tests, at speeds beyond 1600 rpm, some vibrations were produced by the pump around the pump bay, causing disturbances in the readings of inlet pressure. To fix this problem, the suction tapping and pod were checked (and flushed if necessary) before every single pressure reading.
- When both CMC and kaolin were recirculated in the circuit for a long period of time during the test, they generated heat and consequently raised the temperature. This could be explained by the presence of friction in the pump, pipes and tank. To minimise these effects, the cooling system was used and the pump test times were minimised.

For the reliability of the measurements an average of three sets of readings was used to produce a single experimental point.

5.4 FLUIDS TESTED

Two non-Newtonian materials were tested: various concentrations of CMC solution and kaolin suspension. Water was used for the purpose of apparatus calibration. The CMC solutions and kaolin suspensions were rheologically characterised by the pseudoplastic and yield pseudoplastic models respectively.

5.4.1 Water

Water was used to calibrate the tube viscometer and pump rig. Figures 4.1 and 4.2 show how well the pressure gradient water test results correlated with the theoretical Colebrook-White prediction. This is very important for the pipe section, as it confirms the credibility of the experimental equipment and technique. Likewise the water pump test results correlated well with the catalogue pump curves.

5.4.2 Kaolin

For the range of concentrations used in this work, the material was characterised as a yield pseudoplastic fluid. No significant yield stress could be observed at the concentration below 20%. At that concentration it behaved as a pseudoplastic material. Compared with the kaolin used in previous work (Sery & Slatter, 2002) (Kabamba, 2006), this kaolin showed a different behaviour. High concentrations were required to achieve similar rheological parameters. It could

be pumped at a very high concentration (30%) and yet not include a large head deration compared with the head when pumping water.

5.4.3 CMC

The CMC solution displayed pseudoplastic behaviour as expected. Again some differences were noticed between the CMC used in this work and that used in the previous works. High concentrations (up to 9%) could be mixed and easily pumped, which was not the case in previous works.

5.5 HYDRAULIC INSTITUTE METHOD

This method predicts the performance of a centrifugal pump handling viscous Newtonian materials; this implies a constant viscosity.

When applying this method to non-Newtonian fluids, in the Pullum *et al.* (2007) approach, the formulae are used to allow the minimisation of the error between experimental and calculated data in view of determining the value of a characteristic dimension (w). To allow the same base of comparison, the use of formulae was extended to the Walker and Goulas (1984) approach.

5.5.1 Walker and Goulas (1984) approach

The results obtained by Walker and Goulas (1984), using the HI Chart to predict the non-Newtonian pump performance, are very promising for both head and efficiency prediction. Although the Bingham plastic viscosity gives a good estimate of fluid viscosity at high shear rate and can replace this viscosity for different rheological models, Graham *et al.* (2009) stated that this viscosity has no independent fundamental rheological meaning. Moreover, no experimental work found in the literature using this method has achieved the same accuracies for predictions of head and efficiency.

To obtain the best estimate of the Bingham plastic viscosity, a straight line is fitted to the flow curve with a correlation coefficient of at least $R^2 = 0.99$ in the zone of high shear rate (see Figures 4.14 to 4.17).

5.5.2 Pullum *et al.* (2007) approach

5.5.2.1 Characteristic dimension

The characteristic dimension of $w = 0.059$, obtained in the Pullum *et al.* (2007) work, for the Warman 4/3 pump, did not give a good correlation of the pump head for the data obtained in this work. Only 59% of points fell within $\pm 10\%$ (range obtained by Pullum *et al.* (2007) using $w = 0.059$). For this reason a new characteristic dimension $w = 0.023$, which minimised the error between experimental and calculated head, was adopted. This value of w led to the pump head prediction with more than 94% of points falling within $\pm 10\%$ (see Figure 5.1).

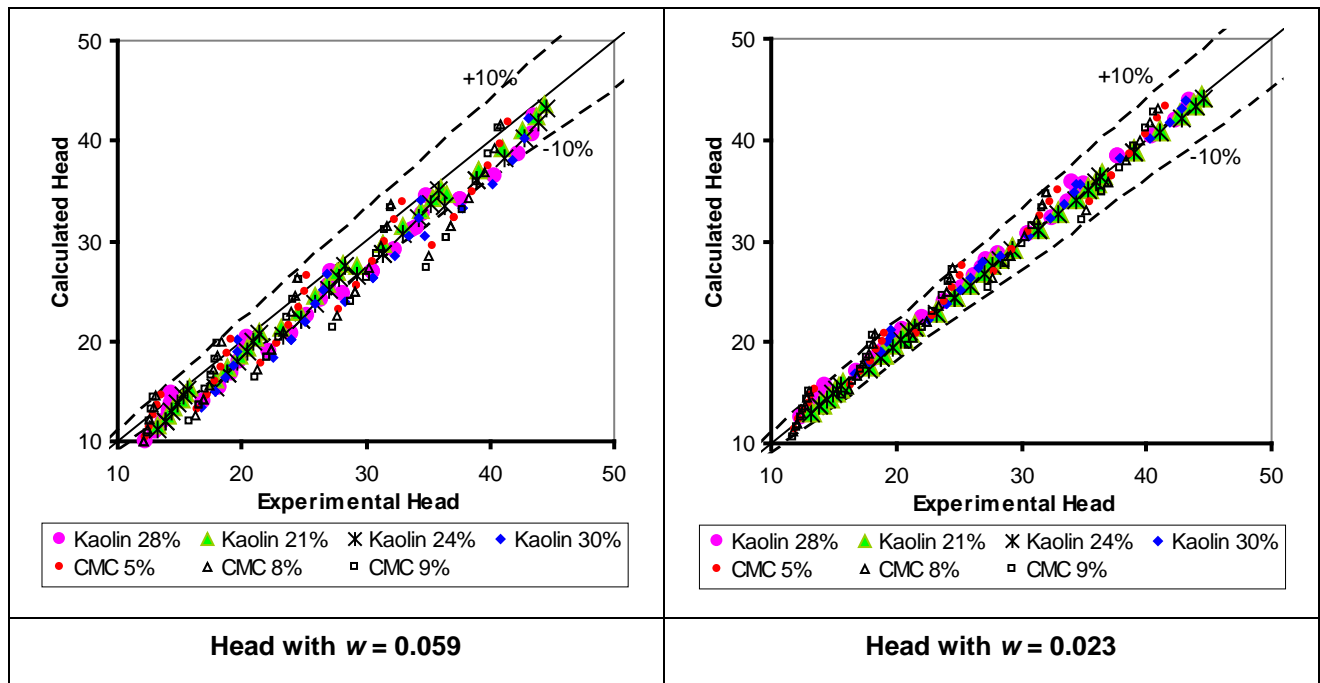


Figure 5.1: Comparison between the results obtained using $w = 0.059$ and $w = 0.023$ for the pump head prediction

The difference of the characteristic dimension values can be justified by the unusual rheological behaviour of the materials tested. In fact, using Kabamba (2006) data and the original value of $w = 0.084$ for the GIW 4/3 pump, the same correlation ranges as the Pullum *et al.* (2007) work were obtained for the pump head. However, for this set of Kabamba (2006) data, it is the value $w = 0.085$ which minimised the error between the experimental and the calculated data. As can be observed in Figure 5.2, there is no significant difference between $w = 0.084$ and $w = 0.085$, and there is also no large difference between the results of the pump head correlation obtained from the two values above (99% and 98% of points fall within $\pm 10\%$ for $w = 0.084$ and $w = 0.085$ respectively).

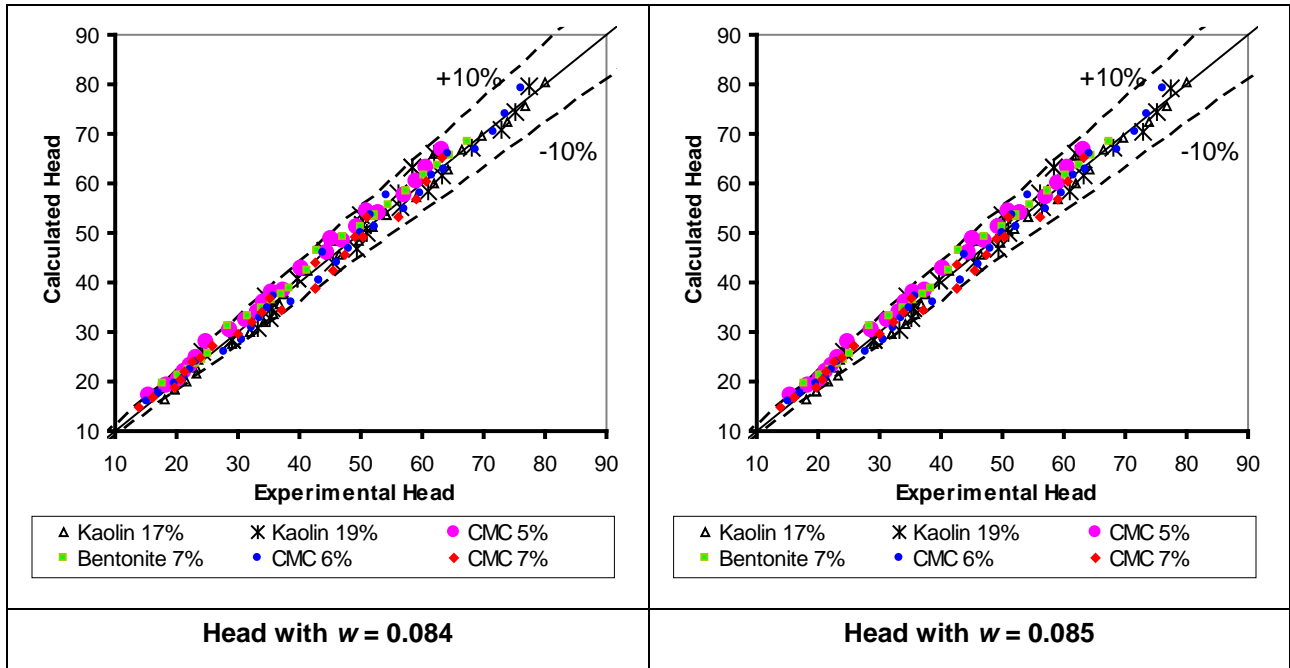


Figure 5.2: Comparison between the results obtained using $w = 0.084$ and using $w = 0.085$

5.5.2.2 Apparent viscosity

Pullum *et al.* (2007) have corrected the HI method by determining a non-Newtonian apparent viscosity which can be used in the HI method (see section 2.7.2.2). The values of this viscosity were very high compared with the corresponding Bingham plastic viscosity values for all datasets except the dataset from the Warman 4/3 pump. The variation of this viscosity with the pump motor speed reflects more the non-Newtonian viscosity behaviour.

5.5.3 Walker and Goulas (1984) approach versus Pullum *et al.* (2007) approach

To compare the results from the two approaches, the same water pump test data were used to predict the pump performance of viscous materials for both approaches. By interpolation, experimental pump test data for viscous materials were expressed in terms of the flow rates of these water pump test data. Then the correlation graphs for head (efficiency) were plotted using as x-coordinate and y-coordinate respectively the experimental head (efficiency) and calculated head (efficiency) corresponding to the same value of flow rate.

A range could be considered as the error margin only if it contains at least 90% of points.

In addition, the correlation coefficient R^2 (expressed by Equations 5.1 and 5.2 for the head and the efficiency respectively) was calculated for each correlation graph. The results of R^2 for the corresponding graphs in the two approaches were compared as well.

$$R^2 = \frac{\sum (H_{\text{pred}} - \text{ave}(H_{\text{exp}}))^2}{\sum (H_{\text{exp}} - H_{\text{pred}})^2 + \sum (H_{\text{pred}} - \text{ave}(H_{\text{exp}}))^2} \quad \text{Equation 5.1}$$

$$R^2 = \frac{\sum (\eta_{\text{pred}} - \text{ave}(\eta_{\text{exp}}))^2}{\sum (\eta_{\text{exp}} - \eta_{\text{pred}})^2 + \sum (\eta_{\text{pred}} - \text{ave}(\eta_{\text{exp}}))^2} \quad \text{Equation 5.2}$$

Figures 5.3 to 5.7 give the comparison of the results obtained using these two approaches.

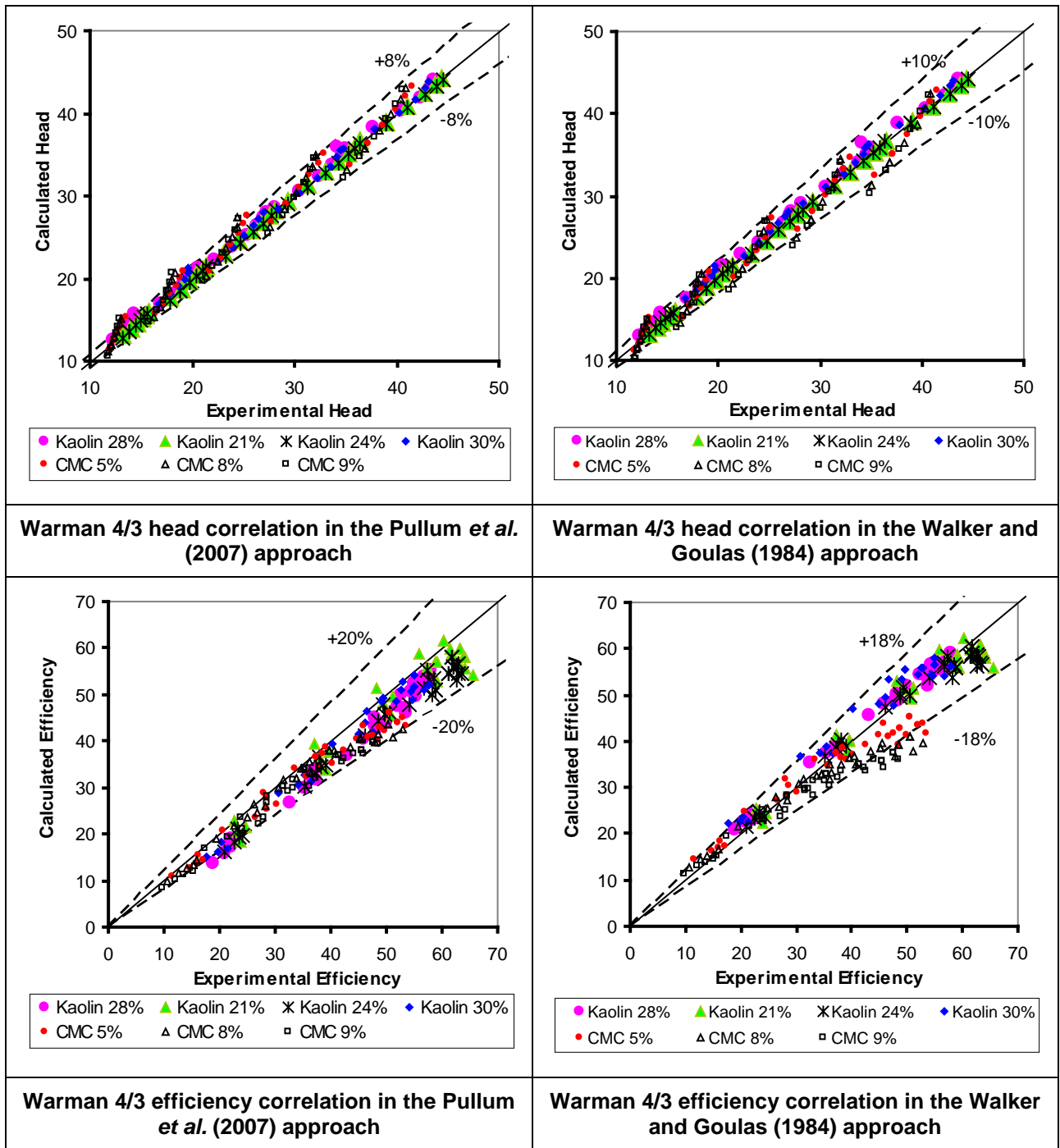


Figure 5.3: Comparison between Pullum et al. (2007) approach and Walker and Goulas (1984) approach results for the data obtained in this work

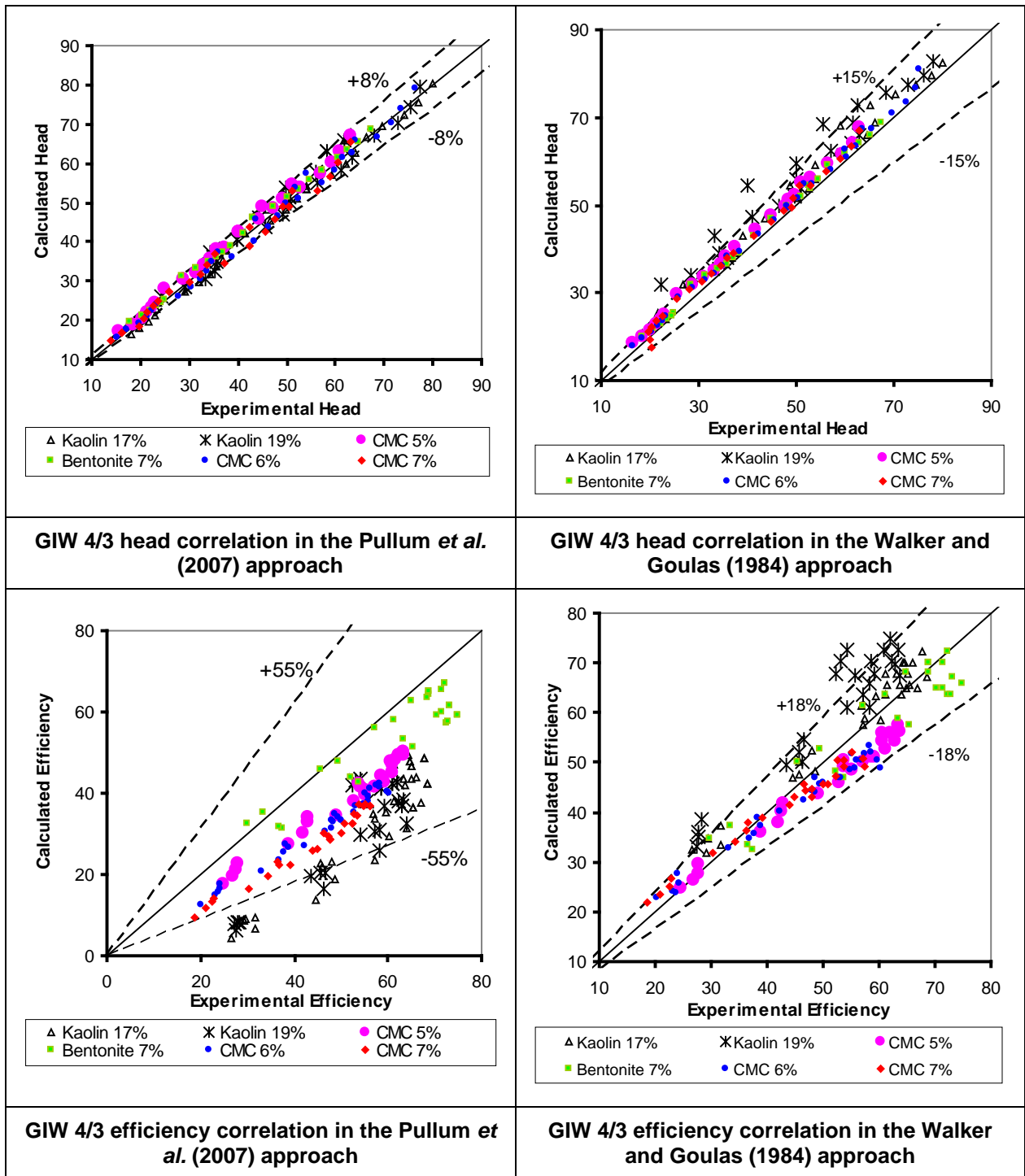


Figure 5.4: Comparison between Pullum *et al.* (2007) approach and Walker and Goulas (1984) approach results obtained using existing data for the GIW 4/3 pump

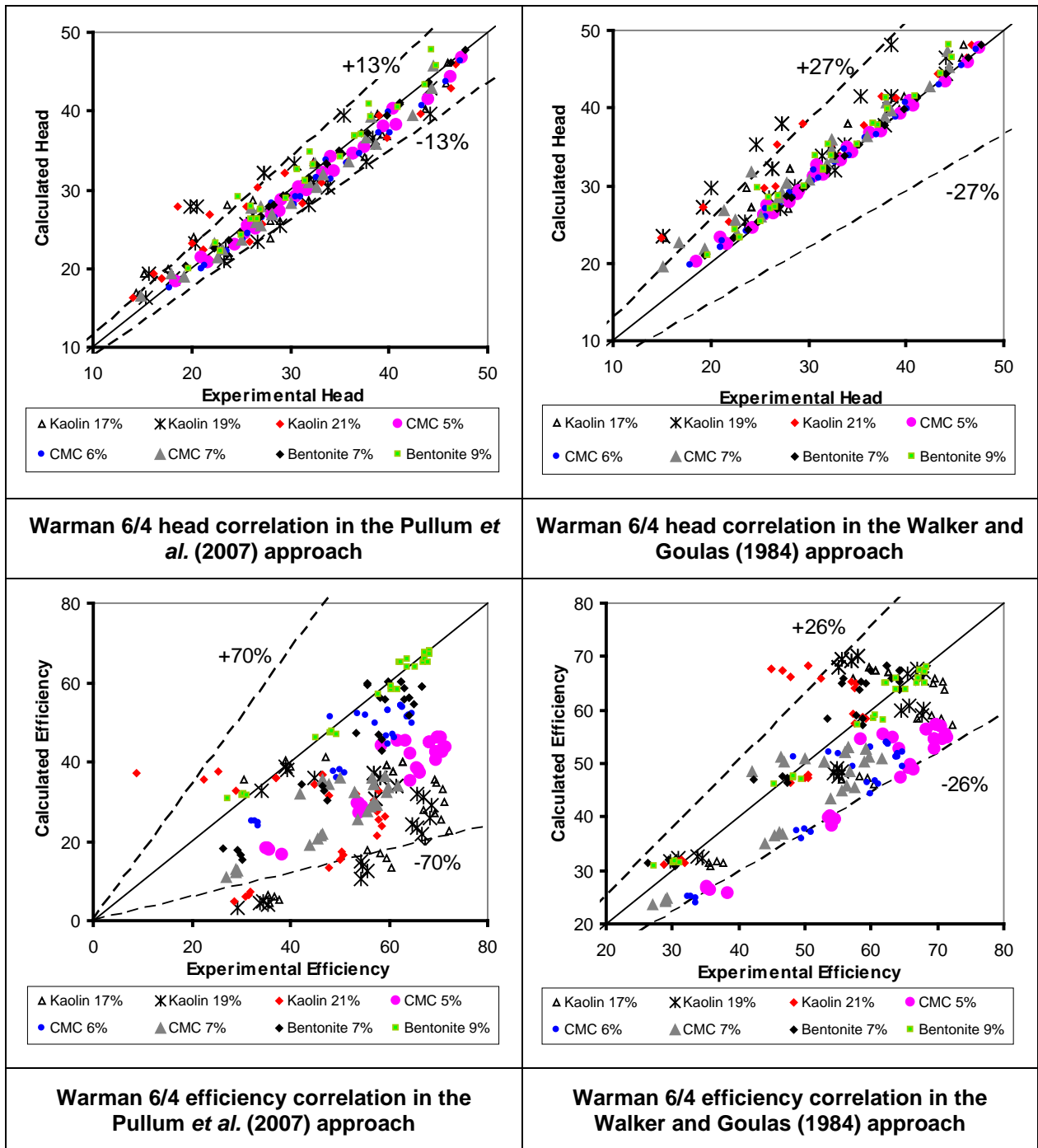


Figure 5.5: Comparison between Pullum *et al.* (2007) approach and Walker and Goulas (1984) approach results obtained using existing data for the Warman 6/4 pump

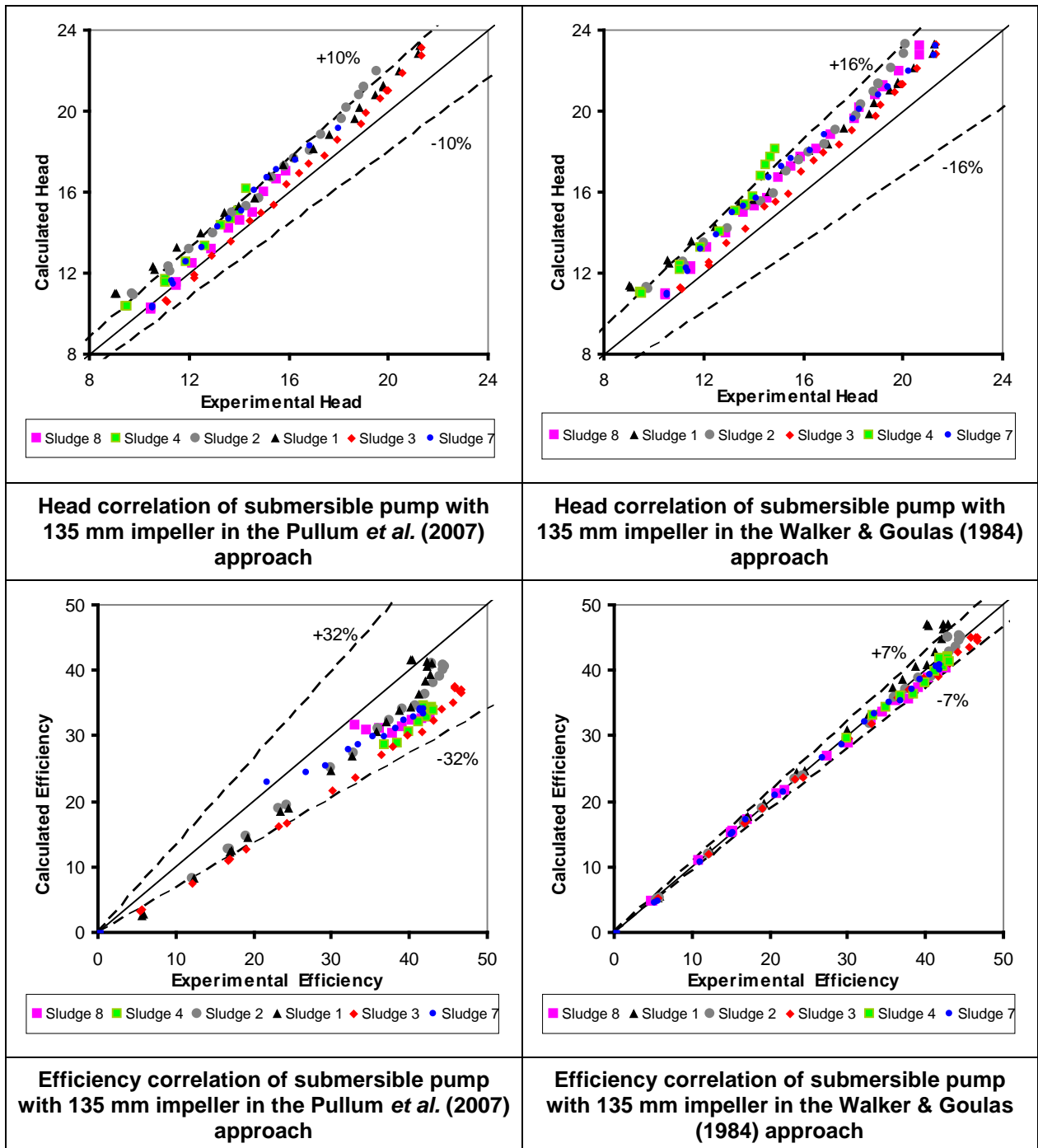


Figure 5.6: Comparison between Pullum *et al.* (2007) approach and Walker and Goulas (1984) approach results obtained using submersible centrifugal pump with 135 mm diameter impeller

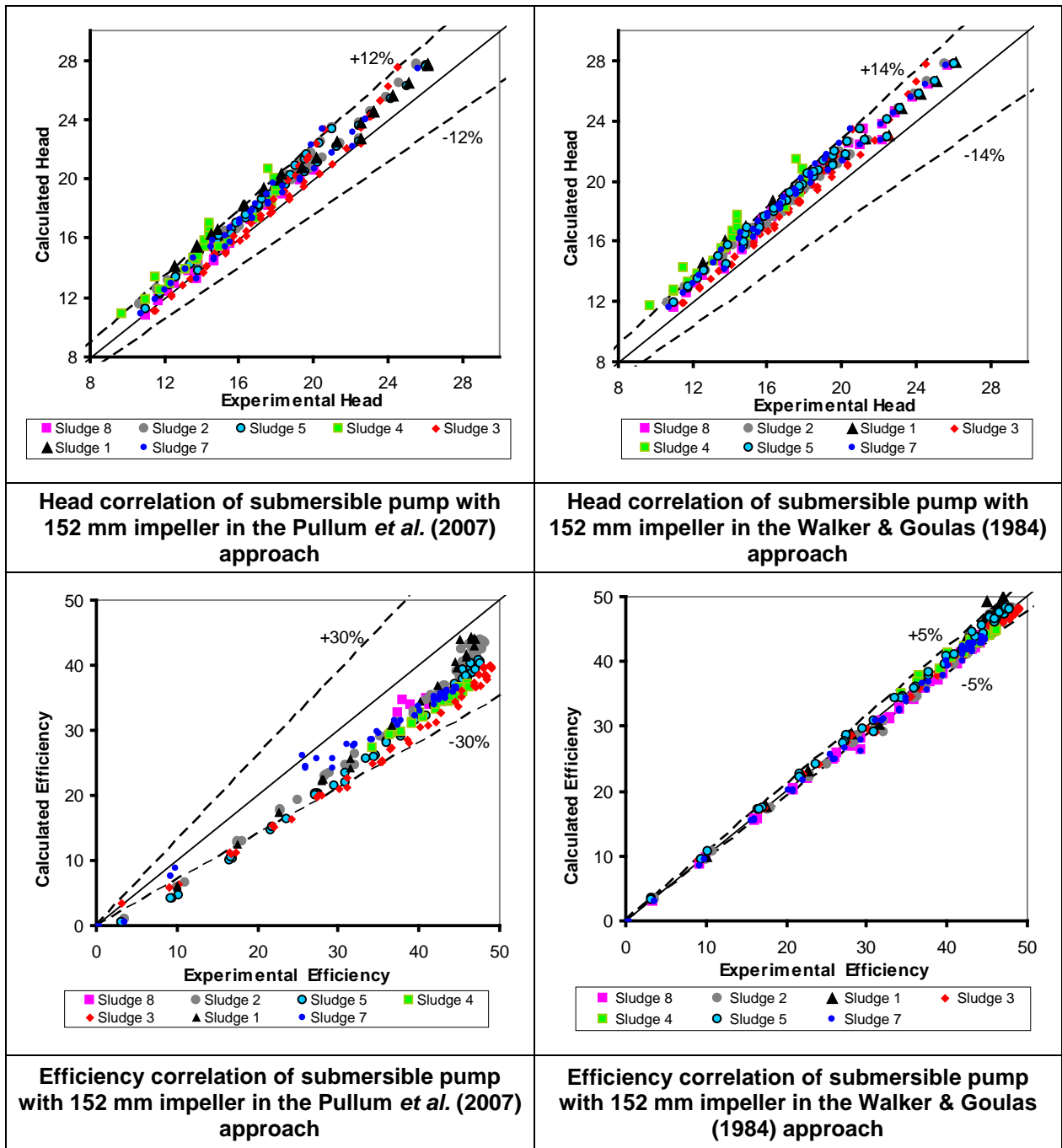


Figure 5.7: Comparison between Pullum *et al.* (2007) approach and Walker and Goulas (1984) approach results obtained using submersible centrifugal pump with 152 mm diameter impeller

The results of this comparative study, between the Walker and Goulas (1984) and the Pullum *et al.* (2007) approaches are summarised in Table 5.3.

Table 5.2: Summary of the results of Walker and Goulas (1984) and Pullum *et al.* (2007) approaches comparison

			Walker & Goulas (1984)			Pullum <i>et al.</i> (2007)		
			Error margin	% Points in error margin	R ²	Error margin	% Points in error margin	R ²
This work data	Warman 4/3	Head	±10%	93	0.9844	±8%	91	0.9905
		Efficiency	±18%	90	0.8688	-20%	92	0.9022
Kabamba (2006) data	GIW 4/3	Head	15%	91	0.9599	±8%	92	0.9880
		Efficiency	±18%	91	0.8524	-	-	0.5945
	Warman 6/4	Head	-3 to 27	90	0.8563	±13%	90	0.9197
		Efficiency	±26%	92	0.6818	-	-	0.5223
Submersible pumps data	135 mm Impeller	Head	16%	92	0.8563	±10%	92	0.9134
		Efficiency	±7%	93	0.9857	-32 to 6	90	0.7570
	152 mm Impeller	Head	14%	94	0.8759	-2 to 12	91	0.9294
		Efficiency	±5%	92	0.9927	-30 to 10	90	0.7502

Both the error margins and R² show that the pump head is reasonably well predicted using the Pullum *et al.* (2007) approach while the efficiency is well predicted using the Walker and Goulas (1984) approach.

Concerning the efficiency prediction, the HI method gives both the head and efficiency correction factors for a given value of viscosity. When applying the Pullum *et al.* (2007) approach to a data set, the same value of w leads to both head and efficiency correction factors which allow both head and efficiency predictions.

As it can be observed from Figures 5.4 to 5.7, the efficiency is poorly predicted using the Pullum *et al.* (2007) approach. This can be explained by the fact that the characteristic dimension was determined essentially by optimisation of the error between calculated and experimental head only.

5.6 ANALYSIS OF VISCOSITY

5.6.1 Bingham plastic viscosity versus apparent viscosity

As stated in Chapter 2, the Bingham plastic viscosity is a constant value for each concentration, while the apparent viscosity depends on the shear rate. For a given concentration of material and pump impeller, the apparent viscosity, as calculated in the Pullum *et al.* (2007) approach, depends exclusively on the motor speed, i.e., each and every motor speed has its own apparent viscosity. The apparent viscosities obtained before applying in the HI method were far higher than the Bingham plastic viscosities for all the pumps except for the Warman 4/3.

5.6.2 Sensitivity of the prediction procedures to a change in viscosity

To study the sensitivity of a prediction procedure, the correlation coefficient R^2 was used. In fact the viscosity was varied and the R^2 calculated for each viscosity variation implemented. This variation was implemented by adding or subtracting 5, 10, 15...% to or from the viscosity value. It was applied for the two procedures for each pump.

For a given pump, the more sensitive procedure was the one for which R^2 would increase (or decrease) more rapidly than the other for the same viscosity variation. To quantify this sensitivity, the following procedure was adopted. If R_1^2 and R_2^2 are the values of R^2 obtained after varying the viscosity by $\% \Delta v_1$ and $\% \Delta v_2$ respectively, the rate ΔR^2 of variation of R^2 is given by Equation 5.3.

$$\Delta R^2 = \frac{R_1^2 - R_2^2}{\% \Delta v_1 - \% \Delta v_2} . \quad \text{Equation 5.3}$$

The method for which the ΔR^2 -values are higher is taken to be more sensitive to a change in viscosity.

Figures 5.8 to 5.12 are the results of ΔR^2 versus $\% \Delta v$ graphs obtained for the different pumps used in this work.

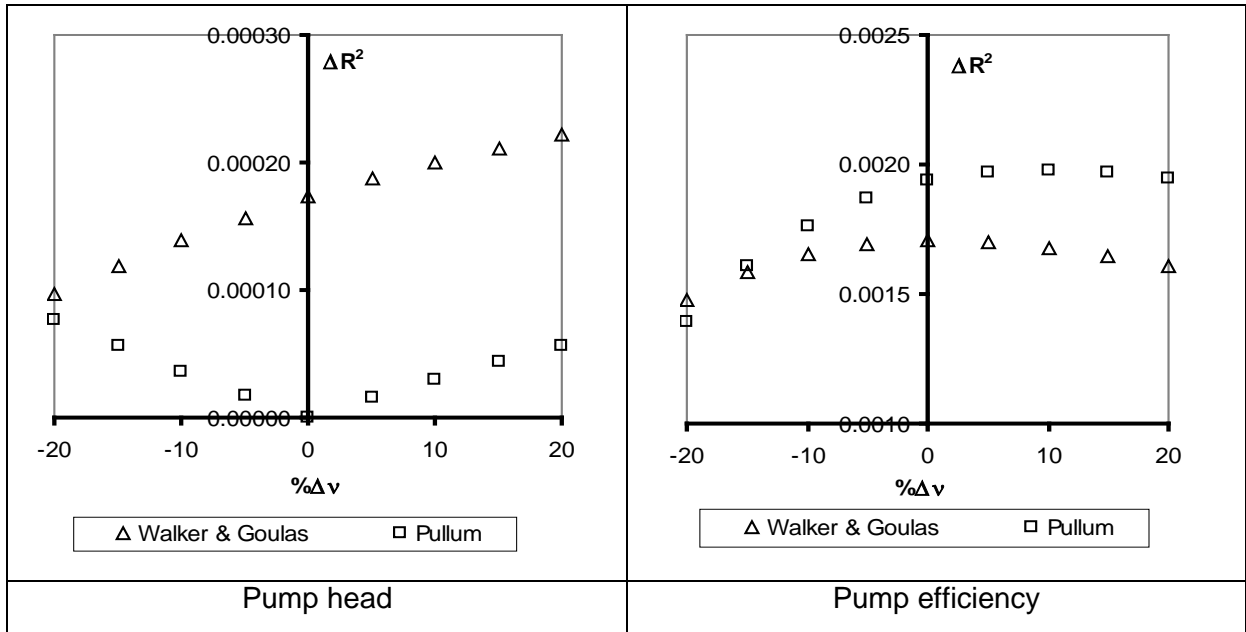


Figure 5.8: Sensitivity of the pump performance prediction procedures to a change in viscosity for the Warman 4/3 pump

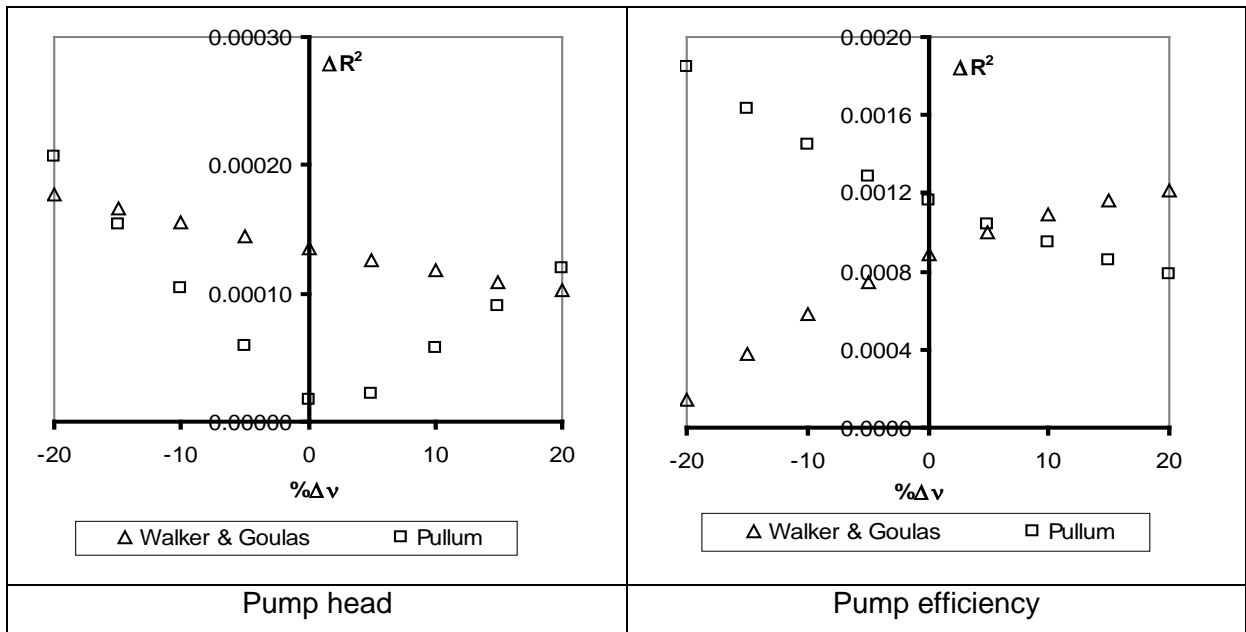


Figure 5.9: Sensitivity of the pump performance prediction procedures to a change in viscosity for the GIW 4/3 pump

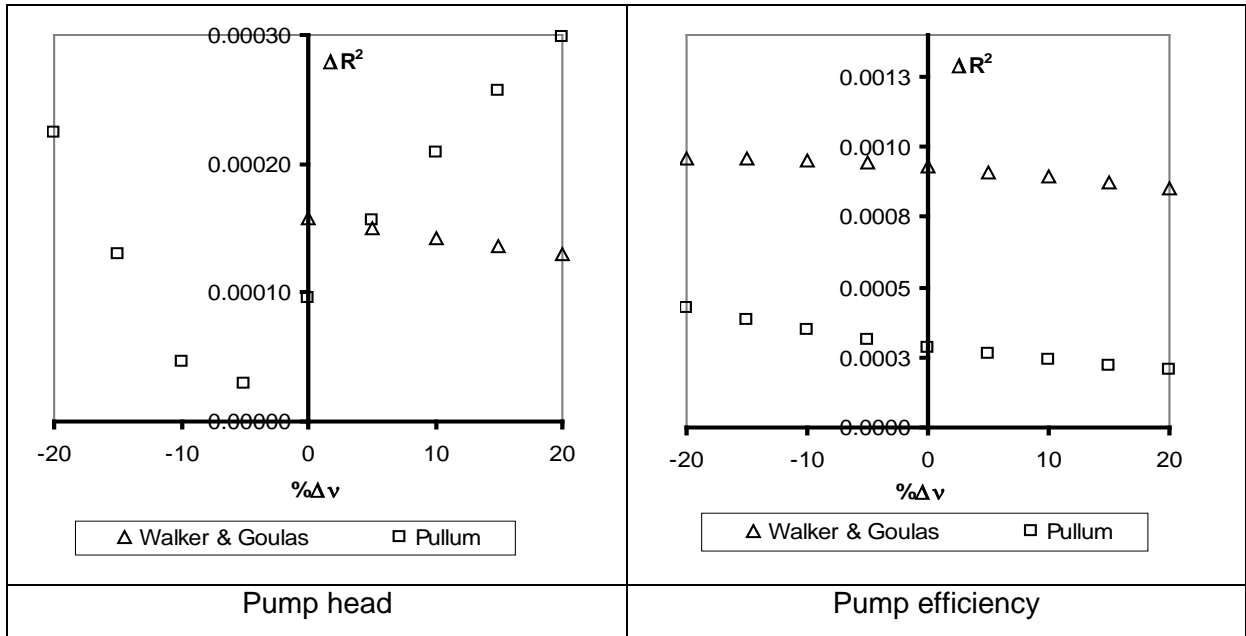


Figure 5.10: Sensitivity of the pump performance prediction procedures to a change in viscosity for the Warman 6/4 pump

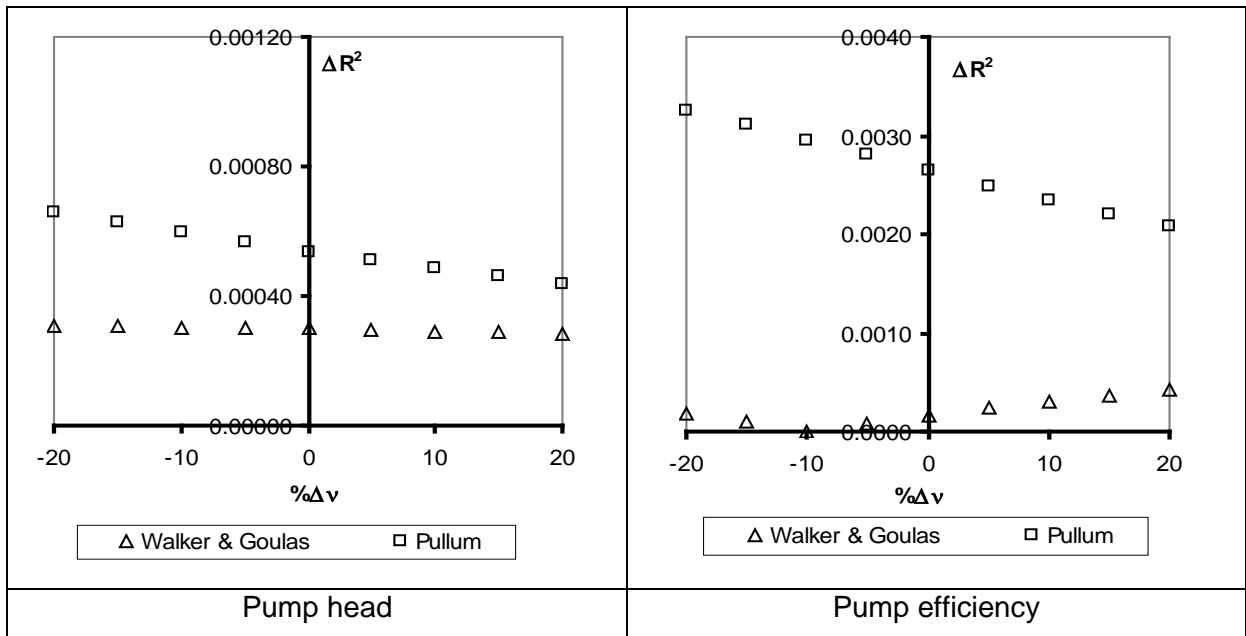


Figure 5.11: Sensitivity of the pump performance prediction procedures to a change in viscosity for the 135 mm impeller submersible pump

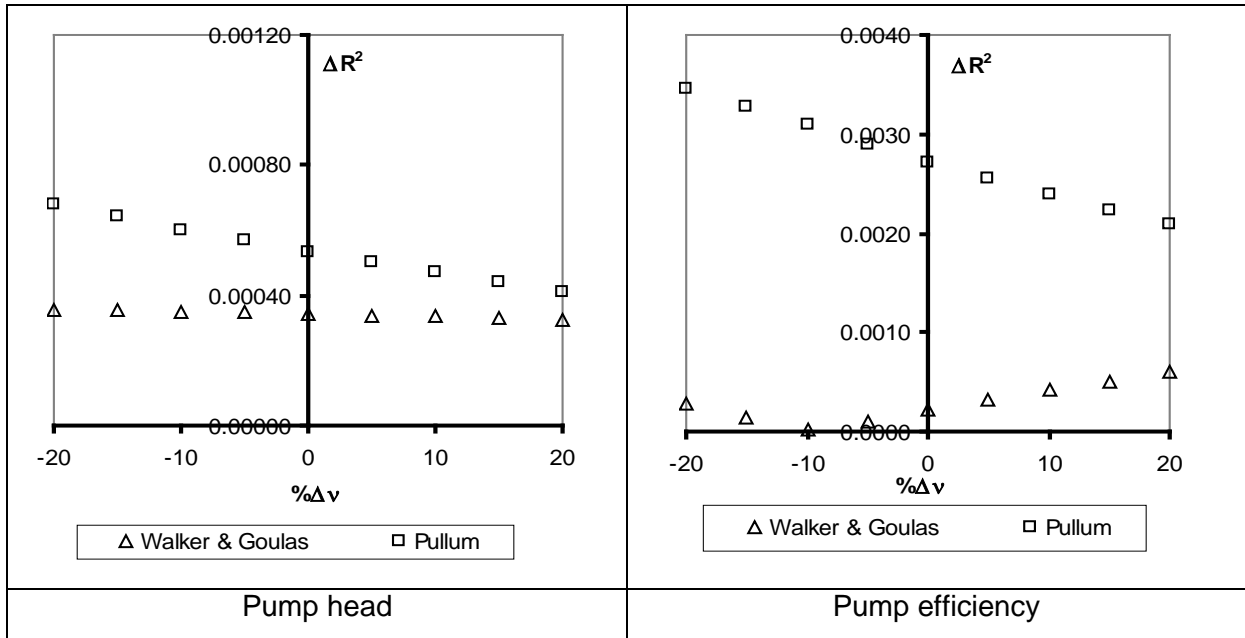


Figure 5.12: Sensitivity of the pump performance prediction procedures to a change in viscosity for the 152 mm impeller submersible pump

Table 5.4 below gives the summary of the sensitivity of the pump performance prediction procedures to a change in viscosity.

Table 5.3: Summary of the pump performance prediction procedures sensitivity to a change in viscosity

Pump	More sensitive pump performance prediction procedure	
	For head	For efficiency
Warman 4/3	Walker & Goulas (1984)	Pullum <i>et al.</i> (2007)
GIW 4/3	Walker & Goulas (1984)	Pullum <i>et al.</i> (2007)
Warman 6/4	Pullum <i>et al.</i> (2007)	Walker & Goulas (1984)
135mm Submersible	Pullum <i>et al.</i> (2007)	Pullum <i>et al.</i> (2007)
152mm Submersible	Pullum <i>et al.</i> (2007)	Pullum <i>et al.</i> (2007)

It can be noticed from this table that the Pullum *et al.* (2007) approach is slightly more sensitive to a change in viscosity than the Walker and Goulas (1984) approach.

5.7 CONCLUSIONS

In this chapter the discussion revolved around comparisons at two levels. From the first level of comparisons the value of the characteristic dimension ($w = 0.085$) close to that of ($w = 0.084$) provided in the Pullum *et al.* (2007) work, for the GIW 4/3 pump, was achieved using the Kabamba (2006) database. This w value led to the better head prediction ($\pm 8\%$) than that obtained in the Pullum *et al.* (2007) work ($\pm 10\%$). On the other hand, for the Warman 4/3 pump the value ($w = 0.059$) provided in the Pullum *et al.* (2007) work did not give satisfactory results. This led to the determination of a new value for the characteristic dimension ($w = 0.023$) which led also to the better prediction of $\pm 8\%$ than the $\pm 10\%$ obtained in the Pullum *et al.* (2007) work.

At the second level of comparisons the following conclusions can be drawn:

- Overall, on one hand the head was better predicted using the Pullum *et al.* (2007) approach for all the pumps used and on the other hand the efficiency was better predicted using the Walker and Goulas (1984) approach for all the pumps except for the Warman 4/3.
- For the Pullum *et al.* (2007) approach, this work achieved better results in two cases than those of $\pm 10\%$ published by Pullum *et al.* (2007) for the head prediction.
- For the Walker and Goulas (1984) approach, this work did not manage to achieve the same accuracies as those published by Walker and Goulas (1984) for both head and efficiency prediction, except for the efficiency of the 152 mm submersible pump.
- The Walker and Goulas (1984) approach for predicting efficiency presented better results. An attempt was made using the Pullum *et al.* (2007) approach with limited success.
- The Pullum *et al.* (2007) approach is more sensitive to a change in viscosity than the Walker and Goulas (1984) approach.

Chapter 6 CONCLUSIONS AND RECOMMENDATIONS

6.1 INTRODUCTION

The lack of agreement between all results obtained by using the HI method to predict the non-Newtonian pump performance has been the rationale for this project.

Experimental work has been conducted and results analysed. Conclusions and recommendations are presented in this chapter.

6.2 SUMMARY

The aim of this work was to evaluate the procedure to determine a representative non-Newtonian viscosity to be used in the HI method for the pump performance prediction. The two main existing approaches (Pullum *et al.* (2007) and Walker and Goulas (1984)) were reviewed and applied to the three sets of data available for this work:

- Kabamba (2006) data obtained by testing kaolin, CMC and bentonite with two centrifugal pumps: a GIW 4/3 and a Warman 6/4.
- New data obtained in this work by testing kaolin and CMC with a Warman 4/3 centrifugal pump.
- Data obtained by testing eight different concentrations of sewage sludge with two submersible centrifugal pumps of same type and different impeller size.

In the Pullum *et al.* (2007) approach, the ranges close to that of the Pullum *et al.* (2007) work were obtained for head prediction for all data sets analysed in this work (even better ranges were obtained in some cases). An attempt at efficiency prediction was made but with limited success, except for kaolin and CMC data where the efficiency was under-predicted by 20%. Using the Walker and Goulas (1984) approach, better pump efficiency prediction results were achieved compare with those obtained using the Pullum *et al.* (2007) approach, but only one pump could reach the same efficiency prediction result as the Walker and Goulas (1984) work.

Table 6.1 below summarises the non-Newtonian pump performance prediction results.

Table 6.1: Summary of the non-Newtonian pump deration results

				Walker & Goulas	Pullum <i>et al.</i>
Walker & Goulas (1984)	Hazleton 3 in	Head	Error margin	±5%	-
		Efficiency	Error margin	±5%	-
	Warman 4/3	Head	Error margin	±5%	-
		Efficiency	Error margin	±5%	-
Sery & Slatter (2002)	Warman 4/3	Head	Error margin	±20%	-
		Efficiency	Error margin	±10%	-
Kabamba (2006)	GIW 4/3	Head	Error margin	±15%	-
		Efficiency	Error margin	±15%	-
	Warman 6/4	Head	Error margin	±10%	-
		Efficiency	Error margin	±20%	-
Pullum <i>et al.</i> (2007)	GIW 4/3	Head	Error margin	-	±10%
		Efficiency	Error margin	-	-
	Warman 4/3	Head	Error margin	-	±10%
		Efficiency	Error margin	-	-
This work data	Warman 4/3	Head	Error margin	±10%	±8%
			R ²	0.9844	0.9905
		Efficiency	Error margin	±18%	-20%
			R ²	0.8688	0.90221
Kabamba (2006) re-evaluated	GIW 4/3	Head	Error margin	+15%	±8%
			R ²	0.9599	0.9880
		Efficiency	Error margin	±18%	-
			R ²	0.8524	0.5945
	Warman 6/4	Head	Error margin	-3 to +27	±13%
			R ²	0.8563	0.9197
		Efficiency	Error margin	±26%	-
			R ²	0.6818	0.5223
Submersible pumps data	135 mm Impeller	Head	Error margin	+16%	±10%
			R ²	0.8563	0.9134
		Efficiency	Error margin	±7%	-32 to +6
			R ²	0.9857	0.7570
	152 mm Impeller	Head	Error margin	+14%	-2 to +12
			R ²	0.8759	0.9294
		Efficiency	Error margin	±5%	-30 to +10
			R ²	0.9927	0.7503

6.3 CONCLUSIONS

- The use of apparent viscosity in the HI method led to the better pump head prediction results, compared with those obtained using the Bingham plastic viscosity. Moreover, the consideration of the flow rate, fluid rheology and pump geometry in the apparent viscosity calculation better describes the fluid behaviour inside the pump. These two reasons have identified the Pullum *et al.* (2007) approach to be a more reliable pump head prediction procedure.
- The use of Bingham plastic viscosity in the HI method led to better efficiency prediction results, compared with those obtained using the apparent viscosity. Even though the accuracies achieved by Walker and Goulas (1984) for pump efficiency prediction were not equalled in this work, their approach is considered to be the more appropriate.
- For the Walker and Goulas (1984) approach, the viscosity depends on the flow curve of a particular concentration of the tested material and remains constant for that concentration in the zone of interest. This is not the case for non-Newtonian fluids. Instead, for the Pullum *et al.* (2007) approach, the viscosity changes with the pump rotational speed.
- The Pullum *et al.* (2007) approach failed to predict the pump efficiency and is more sensitive to a change in viscosity. Therefore the apparent viscosity used in this procedure cannot be the only representative non-Newtonian viscosity to be used in the HI method, though it better predicts the pump head.
- From the results of this work, it is advisable that the pump performance prediction be done using both apparent and Bingham plastic viscosity, the apparent viscosity for the head prediction and the Bingham plastic viscosity for the efficiency prediction.

6.4 CONTRIBUTIONS

- The present work has made available a new database of pump tests for various concentrations of kaolin suspensions, CMC solutions and sewage sludges.
- An attempt has been made to use the Pullum *et al.* (2007) approach to predict pump efficiency.
- The characteristic dimensions have been determined for pumps of other types than those used in the Pullum *et al.* (2007) work.
- The apparent viscosity and the Bingham plastic viscosity can be used in conjunction, depending on whether it is the prediction of the head or the efficiency.

6.5 RECOMMENDATIONS

- As power consumption is very important, more work is required to obtain clarity on the efficiency prediction in the Pullum *et al.* (2007) approach.
- In the Pullum *et al.* (2007) approach there is a need either to include the efficiency aspect in the calculation of the characteristic dimension, or establish two characteristic dimensions for a single pump: one for the head and another for efficiency.
- Pump performance prediction for non-Newtonian fluids is not a solved problem and will require much more research.

REFERENCES

Abulnaga, B.E. 2002. *Slurry systems handbook*. New York: McGraw-Hill.

Al-Fariss, T. & Pinder, K.C. 1987. Flow through porous media of a shear-thinning liquid with yield stress. *Canadian Journal of Engineering*, 65(3):391-405, June.

Angel, T. & Crisswell, J. 1997. *Slurry pump manual*. Salt Lake City, UT: Envirotech Pumpsystems.

ANSI/HI 9.6.7. 2004. *Effects of liquid viscosity on rotodynamic (centrifugal and vertical) pump performance*. Parsippany, NJ: Hydraulic Institute.

Barr, G. 1931. *A monograph of viscometry*. London: Oxford University Press.

Barry, B.A. 1991. *Errors in practical measurement in surveying, engineering, and technology*. Rancho Cordova, CA: Landmark Enterprises.

Benziger, J.B. & Aksay, I.A. 1999. Notes on data analysis: Chemical Engineering 346, Spring Term. Department of Chemical Engineering, Princeton University, Princeton, NJ.

Brinkworth, B.J. 1968. *Introduction to experimentation*. London: English Universities Press.

Brown, N.P. & Heywood, N.I. 1991. *Slurry handling: design of solid liquid systems*. London: Elsevier Applied Science.

Chhabra, R.P. & Richardson, J.F. 1999. *Non-Newtonian flow in the process industries: fundamentals and engineering applications*. Oxford: Butterworth-Heinemann.

Engin, T. & Gur, M. 2003. Comparative evaluation of some existing correlations to predict head degradation of centrifugal slurry pumps. *Journal of Fluids Engineering*, 125(1):149-157, January.

Gandhi, B.K., Singh, S.N. & Seshadri, V. 2000. Improvements in the prediction of performance of centrifugal slurry pumps handling slurries. *Proceedings of the Institution of Mechanical Engineers: Journal of Power and Energy*, 214(A):473-486.

Giles, R.V., Evett, J.B. & Liu, C. 1994. *Schaum's outline of fluid mechanics and hydraulics*. 3rd ed. New York: McGraw-Hill.

Govier, GW & Aziz, K. 1972. *The flow of complex mixtures in pipes*. New York: Van Nostrand Reinhold.

Graham, L.J.W., Pullum, L., Slatter, P., Sery, G. & Rudman, M. 2009. Centrifugal pump performance calculation for homogeneous suspensions. *Canadian Journal of Chemical Engineering*, 87(4):526-533, August.

Haldenwang, R., Fester, V., Sutherland, A., Holm, R. & Du Toit, R. 2010. Design construction, commissioning and testing of a portable tube viscometer and pump rig. 18th International conference on Hydrotransport. Rio De Janeiro, Brazil. 287-298.

Hanks, R.W. & Ricks, B.L. 1975. Transitional and turbulent pipe flow of pseudoplastic fluids. *Journal of Hydronautics*, 9(1):39-44, January.

Hydraulic Institute. 1983. *Hydraulic Institute standards for centrifugal, rotary and reciprocating pumps*. 14th ed. Cleveland, OH: Hydraulic Institute.

International Organization for Standardization. 1999. *ISO 9906: Rotodynamic pumps*. Geneva: ISO.

ISO see International Organization for Standardization.

Kabamba, B.M. 2006. Evolution of centrifugal pump performance derating procedures for non-Newtonian slurries. Unpublished MTech thesis, Cape Peninsula University of Technology, Cape Town.

Lazarus, J.H. & Slatter, P.T. 1988. A method for the rheological characterisation of the tube viscometer data. *Journal of Pipelines*, 7:165-176.

Liu, H. 2003. *Pipeline engineering*. Boca Raton, FL: Lewis Publishers.

Massey, B.S. & Ward-Smith, J. 1998. *Mechanics of fluids*. 7th ed. Cheltenham: Stanley Thornes.

Munson, B.R., Young, D.F., Okiishi, T.H. & Huebsch, W.W. 2010. *Fundamentals of fluid mechanics*. 6th ed. New York: John Wiley.

Paterson, A. & Cooke, R. 1999. The design of slurry pipeline systems. Short course presented at the Cape Technikon, Cape Town, 24 – 26 March, 1999.

Perez, R.X. 2008. *Operator's guide to centrifugal pumps: what every reliability-minded operator needs to know*. Bloomington, IN: Xlibris Corporation.

Pullum, L., Graham, L.J.W. & Rudman, M. 2007. Centrifugal pump performance calculation for homogeneous and complex heterogeneous suspensions. *Journal of the Southern African Institute of Mining and Metallurgy*, 107(6):373-379.

Pullum, L., Graham, L.J.W. & Wu, J. 2011. Centrifugal pump performance with non-Newtonian slurries. Paper presented at the 15th International Conference on Transport and Sedimentation of Solid Particles, Wroclaw, Poland, 6 – 9 September 2011.

Roco, M.C., Marsh, M., Addie, G.R. & Maffett, J.R. 1986. Dredge pump performance prediction. *Journal of Pipelines*, 5:171-190.

SAPMA. 2005 see South African Pump Manufacturers Association.

Sahdev, M. 2007. Centrifugal pumps: basic concepts of operation, maintenance, and troubleshooting (Part 1). The Chemical Engineers' Resource Page.
<http://www.cheresources.com/centrifugalpumps3.shtml> [19 August 2007].

Sellgren, A., Addie, G.R. & Yu, W.C. 1999. Effects of non-Newtonian mineral suspensions on the performance of centrifugal pumps. *Mineral Processing and Extractive Metallurgy Review*, 20:239-249.

Sery, G. & Slatter, P.T. 2002. Centrifugal pump derating for non-Newtonian slurries. In Heywood, N. (ed.) *Proceedings of the 15th International Conference on Slurry Handling and Pipeline Transport: Hydrotransport 15, Banff, Canada, 3 – 5 June 2002*. Cranfield: BHR Group, 2: 679-692.

- Shook, C.A. & Roco, M.C. 1991. *Slurry flow: principles and practice*. Boston, MA: Butterworth-Heinemann.
- Slatter, P.T. 1986. The rheological characterisation of non-Newtonian slurries using a novel balanced beam tube viscometer. Unpublished MSc dissertation, University of Cape Town, South Africa.
- Slatter, P.T. 1994. Transitional and turbulent flow of non-Newtonian slurries in pipes. Unpublished PhD thesis, University of Cape Town, South Africa.
- South African Pump Manufacturers Association. 2005. *Pumps: principles & practice*. 5th ed. Northcliff, Johannesburg: K. Myles and Associates.
- Streeter, V.L. & Wylie, E.B. 1985. *Fluid mechanics*. 8th ed. New York: McGraw-Hill.
- Thomas, A.D. & Wilson, K.C. 1987. New analysis of non-Newtonian flowdashield-power-law fluids. *Canadian Journal of Chemical Engineering*, 65(2):335-338, April.
- Walker, C.I. & Goulas, A. 1984. Performance characteristics of centrifugal pumps when handling non-Newtonian homogeneous slurries. *Proceedings of the Institution of Mechanical Engineers: Journal of Power and Energy*, 198(A):41-49.
- Warman (Africa) (Pty) Ltd. Warman International Pump Curves. Curve book No 1564. Emalaheni: Warman (Africa).
- Wilson, K.C. 1986. Modelling the effects of non-Newtonian and time-dependent slurry behaviour. In Burns, A.P. (ed.). *Proceedings of the 10th International Conference on the Hydraulic Transport of Solids in Pipes: Hydrotransport 10, Innsbruck, Austria, 29 – 31 October 1986*. London: Elsevier Applied Science Publications: BHRA: Paper J1.
- Wilson, K.C., Addie, G.R., Sellgren, A. & Clift, R. 2006. *Slurry transport using centrifugal pumps*. 3rd ed. New York: Springer.
- Wonnacott, G. 1993. The selection of pumps for slurries and pastes. In *BHR Group Conference Series*, 6:91-117. Cranfield: BHR Group.

APPENDICES

LIST OF TABLES

Table A. 1: Water test data in 55.60 mm straight pipe.....	140
Table A. 2: Water test data in 81.20 mm straight pipe.....	140
Table A. 3: Colebrook-White equation solver for the 55.60 mm straight pipe	141
Table A. 4: Colebrook-White equation solver for the 81.20 mm straight pipe	142
Table A. 5: Water pump test results at 1200, 1400 and 1600 rpm.....	143
Table A. 6: Water pump test results at 1800 and 2000 rpm.....	144
Table A. 7:	145
Table A. 8: Warman 4/3 pump test at 1200 and 1400 rpm for CMC 5%.....	145
Table A. 9: 4x3 Warman pump test at 1600, 1800 and 2000 rpm for CMC 5%	146
Table A. 10:	147
Table A. 11: Warman 4/3 pump test at 1200 and 1400 rpm for CMC 8%	147
Table A. 12: 4x3 Warman pump test at 1600, 1800 and 2000 rpm for CMC 8%	148
Table A. 13:	149
Table A. 14: Warman 4/3 pump test at 1200 and 1400 rpm for CMC 9%.....	149
Table A. 15: 4x3 Warman pump test at 1600, 1800 and 2000 rpm for CMC 9%	150
Table A. 16:	151
Table A. 17: Warman 4/3 pump test at 1200 and 1400 rpm for kaolin 21%.....	151
Table A. 18: 4x3 Warman pump test at 1600, 1800 and 2000 rpm for kaolin 21%	152
Table A. 19:	153
Table A. 20: Warman 4/3 pump test at 1200 and 1400 rpm for kaolin 24%.....	153
Table A. 21: 4x3 Warman pump test at 1600, 1800 and 2000 rpm for kaolin 24%	154
Table A. 22:	155
Table A. 23: Warman 4/3 pump test at 1200 and 1400 rpm for kaolin 28%.....	155
Table A. 24: 4x3 Warman pump test at 1600, 1800 and 2000 rpm for kaolin 28%	156
Table A. 25:	157
Table A. 26: Warman 4/3 pump test at 1400 and 1600 rpm for kaolin 30%.....	157
Table A. 27: 4x3 Warman pump test at 1800 and 2000 rpm for kaolin 30%.....	158

Table A. 1: Water test data in 55.60 mm straight pipe

Clear Water Test Analysis					Sum(Diff^2)		31.857										
9-Jun-09					8E-06		8E-06										
D = 55.60 mm k = 08.0 um																	
D =	0.0556		m														
L =	3.00		m														
Temp =	21.00		deg C														
A =	0.002427948		m^2		(fpV^2/2)				DΔP/4L								
V	(sdev)	ρ	D	μ	8V/D	(fpV^2/2)	ΔP (obs)	H,L	Δp Sdev	DΔP/4L	τ _o -τ _{o obs}	Diff	Diff^2	4fLV^2/2Dg	(ρgΔh)	(ΔH/L)	(DΔP/4L)
m/s	m/s	kg/m ³	m	Pa.s	i _m /m	Pa	Pa		Pa	Pa	Pa			m	Pa	i _m	τ _o (calc)
9.046	0.009	998	0.056	0.00098	1.118	152.1	33090	H	0.020	153.3	-1.205	1.452	3.35	32830	1.118	152.1	
8.069	0.008	998	0.056	0.00098	0.898	122.2	26913	H	0.014	124.7	-2.508	6.289	2.69	26372	0.898	122.2	
7.158	0.006	998	0.056	0.00098	0.716	97.4	21538	H	0.011	99.8	-2.363	5.583	2.15	21028	0.716	97.4	
6.207	0.001	998	0.056	0.00098	0.547	74.5	16616	H	0.010	77.0	-2.484	6.171	1.64	16080	0.547	74.5	
5.288	0.003	998	0.056	0.00098	0.405	55.2	12258	H	0.008	56.8	-1.634	2.668	1.22	11906	0.405	55.2	
4.376	0.001	998	0.056	0.00098	0.285	38.7	8686	H	0.006	40.2	-1.500	2.251	0.85	8362	0.285	38.7	
3.488	0.002	998	0.056	0.00098	0.187	25.4	5972	L	0.012	27.7	-2.232	4.980	0.56	5490	0.187	25.4	
2.498	0.001	998	0.056	0.00098	0.101	13.7	3280	L	0.014	15.2	-1.452	2.108	0.30	2966	0.101	13.7	
1.374	0.001	998	0.056	0.00098	0.034	4.6	1126	L	0.040	5.2	-0.596	0.355	0.10	997	0.034	4.6	

Table A. 2: Water test data in 81.20 mm straight pipe

Clear Water Test Analysis					Sum(Diff^2)		1.553										
9-Jul-09					8E-06		8E-06										
D = 81.20 mm k = 08.0 um																	
D =	0.0812		m														
L =	2.50		m														
Temp =	25.85		deg C														
A =	0.005178476		m^2		(fpV^2/2)				DΔP/4L								
V	(sdev)	ρ	D	μ	8V/D	(fpV^2/2)	ΔP (obs)	H,L	Δp Sdev	DΔP/4L	τ _o -τ _{o obs}	Diff	Diff^2	4fLV^2/2Dg	(ρgΔh)	(ΔH/L)	(DΔP/4L)
m/s	m/s	kg/m ³	m	Pa.s	i _m /m	Pa	Pa		Pa	Pa	Pa			m	Pa	i _m	τ _o (calc)
1.627	0.000	997	0.081	0.00088	0.029	5.7	732	L	0.020	5.9	-0.255	0.065	0.07	701	0.029	5.7	
2.258	0.000	997	0.081	0.00088	0.052	10.4	1308	L	0.024	10.6	-0.249	0.062	0.13	1277	0.052	10.4	
2.921	0.000	997	0.081	0.00088	0.084	16.7	2074	L	0.019	16.8	-0.166	0.028	0.21	2054	0.084	16.7	
3.576	0.000	997	0.081	0.00088	0.122	24.3	2998	L	0.027	24.3	-0.072	0.005	0.31	2989	0.122	24.3	
4.235	0.000	997	0.081	0.00088	0.168	33.3	4029	L	0.032	32.7	0.546	0.299	0.42	4097	0.168	33.3	
4.837	0.000	997	0.081	0.00088	0.215	42.6	5137	L	0.021	41.7	0.930	0.865	0.54	5251	0.215	42.6	
5.496	0.000	997	0.081	0.00088	0.273	54.2	6729	H	0.021	54.6	-0.453	0.205	0.68	6673	0.273	54.2	
6.080	0.000	997	0.081	0.00087	0.330	65.5	8075	H	0.033	65.6	-0.070	0.005	0.82	8067	0.330	65.5	
6.834	0.000	997	0.081	0.00087	0.411	81.6	10038	H	0.030	81.5	0.141	0.020	1.03	10055	0.411	81.6	

Table A. 3: Colebrook-White equation solver for the 55.60 mm straight pipe

COLEBROOK-WHITE				Test of sensitivity for Newtonian flow											
Clear Water Test Analysis				COLEBROOK-WHITE EQUATION SOLVER (Newton-Raphson)											
9-Jun-09				k 8E-06											
D = 55.60 mm k = 00.0 um				8V/D (f _p V ² /2) (4fLV ² /2Dg) (ρgΔh) (ΔH/L) DΔP/4L (f)											
D = 0.0556		L(m) = 3.00		(Darcy)											
Vmax = 10.00		Temp = 21.00													
Vstep = 0.40		Vcrit = 0.037													
V	Temp	ρ	D	μ	τ _o (k=0)	ΔH	ΔP		τ _o	f (= f7)	Re	k/D	f1	F(f1)	
m/s	°C	kg/m ³	m	Pa.s	i _m /m	Pa	m	Pa	i _m	Pa					
0.005	21	998	0.056	0.00098	0.667	0.0				0.061	263	0.0000	0.061	Laminar flow	
0.009	21	998	0.056	0.00098	1.335	0.0				0.030	525	0.0000	0.030	Laminar flow	
0.019	21	998	0.056	0.00098	2.670	0.0				0.015	1050	0.0000	0.015	Laminar flow	
0.037	21	998	0.056	0.00098	5.339	0.0				0.008	2100	0.0000	0.008		
0.037	21	998	0.056	0.00098	0.000	0.0	0.00	2	0.000	0.0	0.012	2100	0.0001	0.010	1.124
0.436	21	998	0.056	0.00098	0.004	0.6	0.01	128	0.004	0.6	0.006	24653	0.0001	0.012	-4.145
0.834	21	998	0.056	0.00098	0.014	1.9	0.04	406	0.014	1.9	0.005	47207	0.0001	0.006	-1.047
1.233	21	998	0.056	0.00098	0.028	3.8	0.08	820	0.028	3.8	0.005	69760	0.0001	0.005	-0.607
1.631	21	998	0.056	0.00098	0.046	6.3	0.14	1363	0.046	6.3	0.005	92314	0.0001	0.005	-0.418
2.030	21	998	0.056	0.00098	0.069	9.4	0.21	2030	0.069	9.4	0.005	114867	0.0001	0.005	-0.315
2.428	21	998	0.056	0.00098	0.096	13.1	0.29	2818	0.096	13.1	0.004	137421	0.0001	0.005	-0.249
2.827	21	998	0.056	0.00098	0.127	17.3	0.38	3726	0.127	17.3	0.004	159974	0.0001	0.004	-0.204
3.225	21	998	0.056	0.00098	0.162	22.0	0.49	4752	0.162	22.0	0.004	182527	0.0001	0.004	-0.172
3.624	21	998	0.056	0.00098	0.201	27.3	0.60	5895	0.201	27.3	0.004	205081	0.0001	0.004	-0.147
4.022	21	998	0.056	0.00098	0.244	33.1	0.73	7153	0.244	33.1	0.004	227634	0.0001	0.004	-0.128
4.421	21	998	0.056	0.00098	0.290	39.5	0.87	8527	0.290	39.5	0.004	250188	0.0001	0.004	-0.113
4.819	21	998	0.056	0.00098	0.341	46.4	1.02	10015	0.341	46.4	0.004	272741	0.0001	0.004	-0.100
5.218	21	998	0.056	0.00098	0.396	53.8	1.19	11617	0.396	53.8	0.004	295295	0.0001	0.004	-0.090
5.616	21	998	0.056	0.00098	0.454	61.8	1.36	13333	0.454	61.8	0.004	317848	0.0001	0.004	-0.081
6.015	21	998	0.056	0.00098	0.516	70.3	1.55	15163	0.516	70.3	0.004	340401	0.0001	0.004	-0.074
6.413	21	998	0.056	0.00098	0.582	79.3	1.75	17105	0.582	79.3	0.004	362955	0.0001	0.004	-0.067
6.812	21	998	0.056	0.00098	0.652	88.8	1.96	19159	0.652	88.8	0.004	385508	0.0001	0.004	-0.062
7.210	21	998	0.056	0.00098	0.726	98.8	2.18	21326	0.726	98.8	0.004	408062	0.0001	0.004	-0.057
7.609	21	998	0.056	0.00098	0.804	109.4	2.41	23606	0.804	109.4	0.004	430615	0.0001	0.004	-0.053
8.007	21	998	0.056	0.00098	0.885	120.5	2.66	25997	0.885	120.5	0.004	453169	0.0001	0.004	-0.049
8.406	21	998	0.056	0.00098	0.970	132.0	2.91	28500	0.970	132.0	0.004	475722	0.0001	0.004	-0.045
8.804	21	998	0.056	0.00098	1.059	144.2	3.18	31114	1.059	144.2	0.004	498275	0.0001	0.004	-0.042
9.203	21	998	0.056	0.00098	1.152	156.8	3.46	33841	1.152	156.8	0.004	520829	0.0001	0.004	-0.040
9.601	21	998	0.056	0.00098	1.249	169.9	3.75	36678	1.249	169.9	0.004	543382	0.0001	0.004	-0.037
10.000	21	998	0.056	0.00098	1.349	183.6	4.05	39627	1.349	183.6	0.004	565936	0.0001	0.004	-0.035

Table A. 4: Colebrook-White equation solver for the 81.20 mm straight pipe

COLEBROOK-WHITE					Test of sensitivity for Newtonian flow										
Clear Water Test Analysis					COLEBROOK-WHITE EQUATION SOLVER (Newton-Raphson)										
9-Jun-09					k 8E-06										
D = 81.20 mm k = 00.0 um					8V/D (f _p V ² /2) (4fLV ² /2Dg) (ρgΔh) (ΔH/L) DΔP/4L (f)										
D = 0.0812					(Darcy)										
Vmax = 10.00		L(m) = 2.50													
Vstep = 0.40		Temp = 25.85													
Vcrit = 0.0228															
V	Temp	ρ	D	μ	τ _o (k=0)	ΔH	ΔP		τ _o	f (= f7)	Re	k/D	f1	F(f1)	
m/s	°C	kg/m ³	m	Pa.s	i _m /m	Pa	m	Pa	i _m	Pa					
0.003	26	997	0.081	0.00088	0.281	0.0					0.061	263	0.0000	0.061	Laminar flow
0.006	26	997	0.081	0.00088	0.561	0.0					0.030	525	0.0000	0.030	Laminar flow
0.011	26	997	0.081	0.00088	1.122	0.0					0.015	1050	0.0000	0.015	Laminar flow
0.023	26	997	0.081	0.00088	2.244	0.0					0.008	2100	0.0000	0.008	
0.023	26	997	0.081	0.00088	0.000	0.0	0.00	0.4	0.000	0.0	0.012	2100	0.0001	0.010	1.120
0.422	26	997	0.081	0.00088	0.003	0.5	0.01	61.3	0.003	0.5	0.006	38892	0.0001	0.012	-4.922
0.821	26	997	0.081	0.00088	0.008	1.6	0.02	202.3	0.008	1.6	0.005	75684	0.0001	0.006	-1.063
1.220	26	997	0.081	0.00088	0.017	3.4	0.04	414.2	0.017	3.4	0.005	112476	0.0001	0.005	-0.612
1.619	26	997	0.081	0.00088	0.028	5.6	0.07	693.5	0.028	5.6	0.004	149268	0.0001	0.005	-0.420
2.018	26	997	0.081	0.00088	0.042	8.4	0.11	1038.2	0.042	8.4	0.004	186060	0.0001	0.004	-0.314
2.417	26	997	0.081	0.00088	0.059	11.7	0.15	1446.8	0.059	11.7	0.004	222852	0.0001	0.004	-0.248
2.816	26	997	0.081	0.00088	0.078	15.6	0.20	1918.5	0.078	15.6	0.004	259645	0.0001	0.004	-0.203
3.215	26	997	0.081	0.00088	0.100	19.9	0.25	2452.3	0.100	19.9	0.004	296437	0.0001	0.004	-0.170
3.615	26	997	0.081	0.00088	0.125	24.7	0.31	3047.8	0.125	24.7	0.004	333229	0.0001	0.004	-0.145
4.014	26	997	0.081	0.00088	0.152	30.1	0.38	3704.6	0.152	30.1	0.004	370021	0.0001	0.004	-0.126
4.413	26	997	0.081	0.00088	0.181	35.9	0.45	4422.2	0.181	35.9	0.004	406813	0.0001	0.004	-0.111
4.812	26	997	0.081	0.00088	0.213	42.2	0.53	5200.3	0.213	42.2	0.004	443605	0.0001	0.004	-0.098
5.211	26	997	0.081	0.00088	0.247	49.0	0.62	6038.8	0.247	49.0	0.004	480397	0.0001	0.004	-0.088
5.610	26	997	0.081	0.00088	0.284	56.3	0.71	6937.4	0.284	56.3	0.004	517189	0.0001	0.004	-0.079
6.009	26	997	0.081	0.00088	0.323	64.1	0.81	7895.9	0.323	64.1	0.004	553981	0.0001	0.004	-0.072
6.408	26	997	0.081	0.00088	0.365	72.4	0.91	8914.1	0.365	72.4	0.004	590773	0.0001	0.004	-0.066
6.807	26	997	0.081	0.00088	0.409	81.1	1.02	9992.1	0.409	81.1	0.004	627565	0.0001	0.004	-0.060
7.206	26	997	0.081	0.00088	0.455	90.4	1.14	11129.5	0.455	90.4	0.003	664357	0.0001	0.004	-0.055
7.605	26	997	0.081	0.00088	0.504	100.1	1.26	12326.3	0.504	100.1	0.003	701149	0.0001	0.003	-0.051
8.005	26	997	0.081	0.00088	0.556	110.3	1.39	13582.5	0.556	110.3	0.003	737941	0.0001	0.003	-0.047
8.404	26	997	0.081	0.00088	0.609	121.0	1.52	14898.0	0.609	121.0	0.003	774734	0.0001	0.003	-0.044
8.803	26	997	0.081	0.00088	0.666	132.1	1.66	16272.6	0.666	132.1	0.003	811526	0.0001	0.003	-0.041
9.202	26	997	0.081	0.00088	0.724	143.8	1.81	17706.4	0.724	143.8	0.003	848318	0.0001	0.003	-0.038
9.601	26	997	0.081	0.00088	0.785	155.9	1.96	19199.3	0.785	155.9	0.003	885110	0.0001	0.003	-0.036
10.000	26	997	0.081	0.00088	0.849	168.5	2.12	20751.1	0.849	168.5	0.003	921902	0.0001	0.003	-0.034

Table A. 5: Water pump test results at 1200, 1400 and 1600 rpm

Pump speed rpm	Temperature suction pipe (T1) °c	Temperature discharge pipe (T2) °c	Pump discharge flow l/s	Suction Pressure Adj. (P1) kPa	Discharge Pressure Adj. (P2) kPa	Differential pressure kPa	Pump Suction head m	Pump Discharge head m	Pump head m	Pump power output rho.q.g.H W	Pump shaft torque N.m	Pump power in 2.Pi.n.T W	Pump efficiency %
1203.4	30.7	35.7	28.7	-12.189	85.522	97.711	-0.23	10.93	11.16	3134	42.7	5377	58.3
1203.8	30.7	35.8	24.4	-8.555	104.957	113.512	-0.04	12.36	12.40	2961	39.0	4920	60.2
1205.3	30.7	35.9	20.9	-5.992	118.971	124.963	0.10	13.40	13.30	2715	35.7	4500	60.3
1206.1	30.7	35.9	16.5	-3.373	133.478	136.850	0.24	14.48	14.24	2305	31.2	3947	58.4
1207.5	30.7	35.9	12.1	-1.418	145.462	146.880	0.34	15.40	15.06	1790	26.3	3331	53.7
1208.3	30.7	36.0	8.5	-0.171	152.221	152.392	0.41	15.91	15.49	1290	22.2	2810	45.9
1208.3	30.7	36.0	5.8	0.500	155.140	154.641	0.45	16.11	15.66	890	19.1	2411	36.9
1209.0	30.8	36.1	2.8	0.931	156.898	155.967	0.48	16.23	15.75	437	15.9	2019	21.6
1209.3	31.3	37.0	0.1	2.117	162.360	160.242	0.59	16.76	16.17	13	12.8	1623	0.8
1401.3	32.1	37.6	33.4	-16.661	114.538	131.199	-0.46	14.61	15.07	4926	56.8	8337	59.1
1401.5	32.1	37.9	29.5	-12.895	135.801	148.695	-0.27	16.19	16.45	4753	52.9	7761	61.2
1402.3	32.2	38.0	25.8	-9.561	153.923	163.484	-0.09	17.53	17.62	4451	49.1	7209	61.7
1403.0	32.2	38.0	21.9	-6.711	169.839	176.550	0.06	18.71	18.64	4002	44.6	6546	61.1
1403.8	32.3	38.1	17.6	-3.886	185.753	189.639	0.22	19.91	19.69	3385	39.4	5785	58.5
1405.3	32.3	38.1	13.6	-1.934	198.056	199.990	0.32	20.87	20.55	2744	34.5	5073	54.1
1406.0	32.3	38.2	9.9	-0.498	205.397	205.896	0.40	21.40	21.00	2045	29.5	4348	47.0
1407.9	32.3	38.3	5.6	0.626	210.927	210.301	0.46	21.80	21.34	1163	23.0	3384	34.4
1408.3	32.3	38.3	3.6	0.907	212.410	211.502	0.48	21.91	21.43	757	20.8	3069	24.7
1409.0	33.8	40.1	0.1	2.579	219.042	216.463	0.64	22.55	21.92	17	16.0	2356	0.7
1602.2	32.9	38.3	38.2	-22.214	148.466	170.681	-0.76	18.92	19.68	7361	73.8	12383	59.4
1603.0	32.9	38.4	34.5	-17.847	171.908	189.755	-0.53	20.65	21.18	7149	69.7	11703	61.1
1603.7	33.1	38.5	30.5	-13.818	194.853	208.671	-0.31	22.37	22.68	6783	65.6	11011	61.6
1605.2	33.2	38.6	26.4	-9.998	215.825	225.823	-0.11	23.93	24.04	6204	60.2	10127	61.3
1606.0	33.3	38.7	21.6	-6.490	236.349	242.839	0.07	25.47	25.39	5376	53.6	9012	59.7
1608.1	33.3	38.8	17.4	-3.811	252.249	256.060	0.22	26.69	26.47	4515	48.0	8091	55.8
1608.9	33.4	38.9	13.6	-1.833	264.242	266.075	0.33	27.62	27.29	3621	41.9	7056	51.3
1610.4	33.4	38.9	10.0	-0.467	271.176	271.642	0.40	28.12	27.72	2703	36.5	6158	43.9
1611.2	33.5	39.0	6.7	0.356	275.272	274.916	0.45	28.41	27.96	1844	31.2	5272	35.0
1611.9	33.5	39.2	3.4	1.044	278.766	277.722	0.49	28.68	28.19	935	26.5	4466	20.9
1613.4	35.2	41.3	0.1	3.018	286.193	283.175	0.68	29.41	28.73	27	21.6	3649	0.7

Table A. 6: Water pump test results at 1800 and 2000 rpm

Pump speed rpm	Temperature suction pipe (T1) °C	Temperature discharge pipe (T2) °C	Pump discharge flow l/s	Suction Pressure Adj. (P1) kPa	Discharge Pressure Adj. (P2) kPa	Differential pressure kPa	Pump Suction head m	Pump Discharge head m	Pump head m	Pump power output rho.q.g.H W	Pump shaft torque N.m	Pump power in 2.Pi.n.T W	Pump efficiency %
1802.1	34.9	54.9	43.2	-28.494	181.947	210.440	-1.09	23.34	24.43	10334	93.6	17655	58.5
1802.9	35.0	54.8	40.3	-24.866	203.939	228.805	-0.91	24.99	25.90	10215	90.6	17109	59.7
1803.0	35.2	55.7	36.9	-20.683	228.225	248.908	-0.68	26.83	27.51	9946	86.0	16237	61.3
1804.3	35.3	57.0	33.0	-16.193	253.808	270.001	-0.43	28.78	29.21	9442	81.3	15360	61.5
1805.6	35.4	54.1	29.6	-12.804	272.164	284.968	-0.26	30.12	30.38	8789	76.2	14400	61.0
1807.4	35.5	53.5	23.7	-7.916	301.447	309.363	0.00	32.35	32.34	7498	67.6	12793	58.6
1808.1	35.6	53.5	20.7	-5.796	314.847	320.643	0.11	33.39	33.27	6733	63.3	11983	56.2
1809.6	35.6	53.6	16.9	-3.583	329.115	332.699	0.23	34.50	34.27	5687	56.3	10669	53.3
1811.1	35.7	53.6	12.5	-1.438	340.660	342.098	0.35	35.36	35.01	4299	48.3	9161	46.9
1813.3	35.7	53.7	8.5	-0.202	346.494	346.696	0.41	35.75	35.34	2948	41.1	7799	37.8
1814.1	35.7	53.8	5.1	0.611	350.795	350.184	0.46	36.07	35.62	1766	35.3	6710	26.3
1816.2	37.7	56.8	0.2	3.375	362.233	358.858	0.72	37.18	36.46	65	26.8	5089	1.3
1999.7	29.2	34.2	47.9	-32.263	222.089	254.352	-1.14	28.48	29.63	13887	114.2	23914	58.1
2001.2	29.6	35.0	44.6	-28.212	249.813	278.024	-0.97	30.57	31.53	13766	109.1	22871	60.2
2002.0	30.0	35.0	40.5	-23.434	282.441	305.876	-0.75	33.05	33.80	13399	103.0	21593	62.1
2003.0	30.2	35.6	35.5	-17.872	319.604	337.476	-0.47	35.92	36.39	12655	96.0	20127	62.9
2005.0	30.5	35.8	30.7	-12.846	348.617	361.463	-0.21	38.09	38.30	11503	88.3	18539	62.0
2007.2	30.8	36.1	25.0	-7.817	378.955	386.772	0.06	40.42	40.36	9879	78.3	16456	60.0
2008.7	31.0	36.3	21.2	-5.007	396.272	401.279	0.21	41.76	41.54	8611	71.2	14985	57.5
2010.5	31.2	36.5	16.7	-2.291	412.766	415.057	0.36	43.02	42.67	6970	62.5	13153	53.0
2012.2	31.3	36.7	12.2	-0.118	423.706	423.824	0.48	43.82	43.35	5176	53.2	11219	46.1
2013.9	31.4	36.9	8.3	1.214	430.057	428.843	0.55	44.27	43.72	3535	45.1	9505	37.2
2015.7	31.5	37.1	4.7	1.979	433.935	431.957	0.59	44.56	43.96	2035	38.2	8066	25.2
2017.0	33.6	40.7	0.3	5.129	446.358	441.228	0.90	45.77	44.87	115	30.4	6423	1.8

Table A. 7:

Material type	CMC 5%	
Date	2-Aug-09	
Pump	Warman 4/3	
Water Density	1000.0	Kg/m³
Material Density	1030.3	Kg/m³

Table A. 8: Warman 4/3 pump test at 1200 and 1400 rpm for CMC 5%

Pump speed rpm	Temperature suction pipe (T1) °C	Temperature discharge pipe (T2) °C	Pump discharge flow l/s	Suction Pressure Adj. (P1) kPa	Discharge Pressure Adj. (P2) kPa	Differential pressure kPa	Pump Suction head m	Pump Discharge head m	Pump head m	Pump power output rho.q.g.H W	Pump shaft torque N.m	Pump power in 2.Pi.n.T W	Pump efficiency %
1197.9	41.3	41.5	16.8	-5.317	118.467	123.784	0.07	12.59	12.53	2124	45.2	5669	37.5
1198.2	41.3	41.5	14.2	-3.032	125.279	128.311	0.23	13.07	12.84	1848	43.0	5398	34.2
1199.4	41.3	41.6	11.5	-0.582	131.458	132.041	0.42	13.51	13.09	1515	40.7	5109	29.7
1200.1	41.3	41.7	8.4	1.735	136.650	134.916	0.60	13.87	13.27	1125	37.3	4682	24.0
1200.2	41.3	41.5	5.7	3.817	140.868	137.051	0.78	14.20	13.42	766	34.1	4282	17.9
1201.6	41.2	41.4	2.3	6.144	147.769	141.625	0.99	14.81	13.83	317	30.4	3824	8.3
1202.4	41.1	41.4	0.0	8.480	155.318	146.839	1.21	15.55	14.33	-2	28.1	3533	-0.1
1402.9	40.9	41.0	23.0	-11.822	152.861	164.683	-0.38	16.61	16.99	3957	55.2	8111	48.8
1403.7	41.1	41.4	19.9	-8.578409	164.88858	173.46699	-0.17	17.47	17.64	3555	52.1	7654	46.4
1405.2	41.2	41.3	16.3	-4.925	176.878	181.803	0.09	18.33	18.24	2998	48.9	7191	41.7
1405.9	41.2	41.5	12.5	-1.632	186.086	187.718	0.33	18.98	18.64	2361	45.2	6650	35.5
1407.4	41.2	41.5	8.2	1.806	193.757	191.952	0.61	19.52	18.91	1570	39.8	5860	26.8
1408.2	41.1	41.3	3.9	4.821	202.864	198.044	0.86	20.29	19.43	770	35.6	5253	14.7
1408.9	41.2	41.3	0.0	8.160	216.503	208.343	1.18	21.60	20.42	-2	30.5	4503	0.0

Table A. 9: 4x3 Warman pump test at 1600, 1800 and 2000 rpm for CMC 5%

Pump speed rpm	Temperature suction pipe (T1) °C	Temperature discharge pipe (T2) °C	Pump discharge flow l/s	Suction Pressure Adj. (P1) kPa	Discharge Pressure Adj. (P2) kPa	Differential pressure kPa	Pump Suction head m	Pump Discharge head m	Pump head m	Pump power output rho.q.g.H W	Pump shaft torque N.m	Pump power in 2.Pi.n.T W	Pump efficiency %
1603.7	38.9	39.0	27.9	-18.075	194.633	212.708	-0.81	21.35	22.16	6252	74.0	12429	50.3
1605.1	39.0	39.3	25.4	-14.912	206.611	221.523	-0.60	22.20	22.80	5850	70.2	11801	49.6
1605.6	39.2	39.5	22.4	-11.502	218.958	230.460	-0.37	23.08	23.45	5314	66.3	11152	47.7
1607.1	39.3	39.6	17.7	-5.874	238.208	244.082	0.03	24.51	24.48	4368	59.3	9985	43.7
1607.4	39.4	39.6	14.8	-3.811	244.357	248.169	0.17	24.89	24.72	3687	59.1	9951	37.0
1608.3	39.4	39.7	10.4	-0.002	253.705	253.707	0.46	25.54	25.09	2626	52.4	8822	29.8
1610.4	39.5	39.7	6.5	3.004	262.574	259.570	0.70	26.26	25.56	1670	46.9	7906	21.1
1611.1	39.5	39.7	3.2	5.293	271.086	265.793	0.91	27.03	26.12	841	42.0	7086	11.9
1611.8	40.0	40.3	0.0	8.382	284.255	275.873	1.20	28.30	27.10	-3	37.1	6262	-0.1
1799.9	40.4	40.7	33.6	-25.277	236.506	261.783	-1.25	26.35	27.60	9369	91.8	17294	54.2
1801.4	40.6	40.8	30.6	-20.738	253.710	274.448	-0.95	27.58	28.53	8830	87.6	16523	53.4
1802.6	40.8	41.0	26.2	-15.064	276.595	291.658	-0.59	29.22	29.81	7879	80.7	15228	51.7
1803.3	41.0	41.3	22.3	-10.586	293.103	303.689	-0.29	30.40	30.69	6923	76.5	14440	47.9
1804.3	41.2	41.4	18.0	-6.272	308.649	314.922	0.00	31.51	31.51	5724	71.4	13497	42.4
1805.8	41.3	41.6	14.6	-3.116	318.115	321.231	0.23	32.17	31.94	4703	66.0	12480	37.7
1807.3	41.4	41.7	10.5	0.391	326.747	326.356	0.50	32.78	32.28	3422	60.2	11385	30.1
1808.1	41.5	41.7	6.9	3.088	336.950	333.861	0.72	33.64	32.92	2295	54.7	10361	22.2
1809.3	41.4	41.7	3.4	5.464	345.505	340.041	0.92	34.39	33.47	1135	48.4	9161	12.4
1811.1	43.0	42.9	0.0	8.647	362.158	353.512	1.23	36.01	34.78	-5	41.8	7924	-0.1
2001.5	40.4	40.5	38.9	-33.316	284.272	317.588	-1.75	32.02	33.77	13292	118.4	24810	53.6
2002.8	40.8	40.9	34.9	-27.176	311.347	338.522	-1.37	33.97	35.34	12455	111.7	23424	53.2
2003.6	41.0	41.4	30.5	-20.731	337.400	358.130	-0.95	35.85	36.80	11362	104.7	21973	51.7
2005.2	41.3	41.5	25.5	-14.324	362.805	377.129	-0.54	37.67	38.21	9849	100.1	21024	46.8
2007.4	41.5	41.6	20.3	-8.481	384.656	393.136	-0.14	39.25	39.40	8096	91.5	19237	42.1
2008.8	41.6	41.9	16.0	-4.249	397.910	402.160	0.15	40.18	40.02	6463	83.6	17580	36.8
2011.0	41.8	42.0	11.2	-0.200	409.257	409.457	0.45	40.98	40.53	4580	75.5	15891	28.8
2013.0	41.8	42.0	6.8	3.212	421.958	418.746	0.73	42.04	41.31	2836	66.8	14072	20.2
2014.0	41.8	42.0	3.1	5.733	433.164	427.431	0.95	43.06	42.11	1301	60.2	12700	10.2
2015.4	43.3	43.5	0.0	9.014	449.750	440.736	1.27	44.68	43.41	-4	53.1	11206	0.0

Table A. 10:

Material type	CMC 8%	
Date	22-Aug-09	
Pump	Warman 4/3	
Water Density	1000.0	Kg/m³
Material Density	1046.2	Kg/m³

Table A. 11: Warman 4/3 pump test at 1200 and 1400 rpm for CMC 8%

Pump speed	Temperature suction pipe (T1)	Temperature discharge pipe (T2)	Pump discharge flow	Suction Pressure Adj. (P1)	Discharge Pressure Adj. (P2)	Differential pressure	Pump Suction head	Pump Discharge head	Pump head	Pump power output rho.q.g.H	Pump shaft torque	Pump power in 2.Pi.n.T	Pump efficiency
rpm	°c	°c	l/s	kPa	kPa	kPa	m	m	m	W	N.m	W	%
1205.3	32.8	32.9	0.0	6.986	153.228	146.242	1.05	15.11	14.06	0	30.9	3897	0.0
1203.8	32.7	32.9	2.0	4.288	145.614	141.327	0.80	14.38	13.58	279	33.3	4197	6.6
1203.8	32.9	32.9	3.9	2.676	139.945	137.269	0.65	13.85	13.21	524	34.9	4399	11.9
1203.4	33.1	33.5	6.1	0.757	136.540	135.783	0.48	13.58	13.10	818	36.9	4645	17.6
1203.0	33.4	33.5	8.1	-0.908	133.138	134.046	0.34	13.31	12.98	1080	38.7	4881	22.1
1202.7	33.6	33.8	10.0	-2.745	129.600	132.345	0.18	13.06	12.87	1325	41.2	5192	25.5
1202.3	33.9	33.9	12.2	-4.740	125.379	130.119	0.03	12.76	12.73	1595	42.9	5406	29.5
1202.2	34.0	34.3	14.1	-6.791	120.626	127.417	-0.13	12.42	12.56	1819	45.1	5673	32.1
1405.2	34.2	34.2	0.0	6.912545	210.30367	203.39112	1.05	20.67	19.62	4	36.3	5345	0.1
1404.5	34.1	34.3	2.1	4.316	200.445	196.129	0.80	19.72	18.92	399	39.4	5789	6.9
1403.7	33.9	34.1	4.0	2.603	194.809	192.207	0.64	19.20	18.56	771	41.2	6063	12.7
1403.6	34.0	34.3	6.0	1.121	191.098	189.978	0.51	18.89	18.38	1126	43.4	6375	17.7
1403.0	34.2	34.5	8.1	-0.673	187.182	187.854	0.36	18.58	18.22	1512	46.4	6813	22.2
1402.5	34.5	34.8	10.0	-2.401	183.779	186.181	0.22	18.33	18.12	1864	48.5	7126	26.2
1402.2	34.7	34.8	12.1	-4.219	180.118	184.336	0.08	18.09	18.01	2245	51.0	7483	30.0
1401.5	34.9	35.0	14.0	-6.068	175.904	181.972	-0.07	17.80	17.87	2568	53.3	7823	32.8
1401.5	35.1	35.3	16.2	-8.156	170.335	178.491	-0.22	17.42	17.64	2937	56.1	8229	35.7
1400.0	35.3	35.6	17.9	-10.035	164.971	175.006	-0.35	17.04	17.40	3204	58.1	8523	37.6
1400.0	35.5	35.7	20.1	-12.239	158.222	170.462	-0.50	16.59	17.09	3532	60.5	8863	39.8

Table A. 12: 4x3 Warman pump test at 1600, 1800 and 2000 rpm for CMC 8%

Pump speed rpm	Temperature suction pipe (T1) °c	Temperature discharge pipe (T2) °c	Pump discharge flow l/s	Suction Pressure Adj. (P1) kPa	Discharge Pressure Adj. (P2) kPa	Differential pressure kPa	Pump Suction head m	Pump Discharge head m	Pump head m	Pump power output rho.q.g.H W	Pump shaft torque N.m	Pump power in 2.Pi.n.T W	Pump efficiency %
1610.4	36.1	36.4	0.0	7.151	282.745	275.594	1.07	27.73	26.66	-3	42.0	7075	0.0
1608.9	37.7	37.9	1.9	4.679	269.710	265.030	0.83	26.47	25.64	496	45.9	7738	6.4
1608.5	35.7	35.9	4.5	2.592	261.699	259.108	0.64	25.73	25.09	1149	49.1	8267	13.9
1608.1	35.4	35.7	7.1	0.551	255.467	254.916	0.47	25.20	24.73	1803	52.9	8908	20.2
1607.4	35.5	35.7	9.6	-1.669	249.895	251.564	0.28	24.76	24.47	2422	57.0	9603	25.2
1605.9	35.7	35.8	12.1	-3.785	245.601	249.386	0.12	24.47	24.35	3023	60.6	10199	29.6
1605.3	35.9	35.9	14.7	-6.222	240.285	246.507	-0.06	24.12	24.19	3647	64.1	10781	33.8
1605.0	36.0	36.4	17.2	-8.613	233.741	242.355	-0.24	23.68	23.91	4212	67.9	11412	36.9
1603.7	36.3	36.4	19.6	-11.153	225.919	237.072	-0.41	23.14	23.55	4740	70.9	11910	39.8
1602.9	36.7	36.9	22.2	-14.063	216.358	230.420	-0.61	22.47	23.09	5267	72.8	12218	43.1
1603.0	37.0	37.2	24.0	-16.171	209.337	225.508	-0.75	21.99	22.75	5613	72.6	12182	46.1
1602.9	37.2	37.5	26.5	-19.269	197.894	217.164	-0.96	21.19	22.14	6028	75.6	12693	47.5
1812.9	39.1	39.4	0.0	7.343	362.844	355.500	1.09	35.53	34.44	-4	48.0	9106	0.0
1811.1	37.4	37.6	3.2	3.850	344.431	340.581	0.76	33.77	33.01	1094	55.7	10556	10.4
1809.5	37.1	37.4	6.2	1.606	335.426	333.819	0.56	32.96	32.40	2046	60.0	11371	18.0
1808.8	37.2	37.6	9.0	-0.643	327.895	328.538	0.37	32.33	31.95	2963	64.5	12210	24.3
1808.1	37.4	37.7	12.1	-3.289	320.889	324.178	0.17	31.81	31.64	3930	69.4	13146	29.9
1807.3	37.7	37.9	15.1	-6.206	314.438	320.644	-0.05	31.38	31.43	4886	74.6	14119	34.6
1805.8	38.0	38.1	18.1	-8.725	306.650	315.375	-0.22	30.86	31.08	5770	79.3	14997	38.5
1805.1	38.3	38.4	21.1	-11.982	296.193	308.175	-0.45	30.13	30.58	6629	82.7	15638	42.4
1803.6	38.6	38.8	24.2	-15.451	284.088	299.540	-0.68	29.29	29.97	7433	85.8	16204	45.9
1803.6	38.9	39.1	26.9	-18.780	272.005	290.785	-0.89	28.46	29.36	8118	87.9	16606	48.9
1802.8	39.3	39.4	29.9	-22.246	257.201	279.447	-1.10	27.44	28.54	8768	91.2	17223	50.9
1802.1	39.6	39.8	32.6	-25.682	241.921	267.603	-1.30	26.36	27.66	9264	95.0	17921	51.7
2014.6	41.9	42.1	0.0	7.642	451.567	443.925	1.12	44.18	43.06	-5	55.0	11602	0.0
2013.2	39.3	39.6	4.2	3.453	428.950	425.497	0.72	42.02	41.29	1773	64.9	13677	13.0
2011.3	39.2	39.5	7.9	0.795	418.634	417.839	0.50	41.12	40.62	3277	70.5	14847	22.1
2009.5	39.4	39.6	12.1	-2.646	406.445	409.091	0.23	40.14	39.91	4948	77.8	16376	30.2
2008.0	39.9	40.0	16.2	-6.299	396.757	403.056	-0.04	39.48	39.52	6573	86.4	18162	36.2
2007.0	40.2	40.4	19.9	-9.947	385.778	395.725	-0.29	38.74	39.03	7991	92.0	19340	41.3
2005.1	40.6	40.8	23.9	-14.252	370.111	384.363	-0.57	37.65	38.22	9386	98.1	20597	45.6
2003.6	41.0	41.2	28.0	-19.091	351.393	370.484	-0.88	36.34	37.22	10699	101.8	21363	50.1
2002.8	41.6	41.8	32.2	-23.990	328.924	352.915	-1.16	34.77	35.93	11873	108.3	22711	52.3
2001.3	42.1	42.3	35.9	-29.003	305.849	334.852	-1.45	33.13	34.59	12727	113.9	23866	53.3
1999.8	42.5	42.8	38.5	-32.713	286.929	319.642	-1.66	31.78	33.44	13223	117.7	24659	53.6

Table A. 13:

Material type	CMC 9%	
Date	30-Aug-09	
Pump	Warman 4/3	
Water Density	1000.0	Kg/m³
Material Density	1057.9	Kg/m³

Table A. 14: Warman 4/3 pump test at 1200 and 1400 rpm for CMC 9%

Pump speed rpm	Temperature suction pipe (T1) °c	Temperature discharge pipe (T2) °c	Pump discharge flow l/s	Suction Pressure Adj. (P1) kPa	Discharge Pressure Adj. (P2) kPa	Differential pressure kPa	Pump Suction head m	Pump Discharge head m	Pump head m	Pump power output rho.q.g.H W	Pump shaft torque N.m	Pump power in 2.Pi.n.T W	Pump efficiency %
1209.1	33.4	33.6	0.0	7.739	155.844	148.104	1.12	15.20	14.08	-2	34.3	4342	0.0
1208.8	33.3	33.7	2.2	4.457	145.868	141.411	0.81	14.25	13.44	309	36.9	4676	6.6
1208.3	33.5	33.8	4.1	2.746	140.683	137.937	0.65	13.78	13.13	557	39.2	4958	11.2
1208.3	33.8	34.0	6.1	0.924	137.501	136.577	0.49	13.52	13.03	822	41.0	5187	15.9
1207.6	34.1	34.4	8.0	-0.857	134.179	135.036	0.34	13.27	12.93	1080	43.0	5442	19.8
1207.6	34.3	34.6	10.1	-2.929	130.071	133.000	0.17	12.97	12.79	1345	45.4	5745	23.4
1206.1	34.7	35.0	12.1	-4.659	126.258	130.917	0.04	12.70	12.67	1585	47.7	6028	26.3
1206.1	34.9	36.0	13.6	-6.185	122.893	129.078	-0.08	12.48	12.55	1771	48.9	6182	28.7
1401.5	35.2	35.5	18.8	-11.86091	160.99469	172.8556	-0.49	16.56	17.05	3328	64.9	9525	34.9
1401.6	35.8	36.0	16.8	-9.255	168.078	177.332	-0.30	17.07	17.36	3021	61.6	9034	33.4
1402.3	36.0	36.4	14.7	-6.863	174.098	180.961	-0.12	17.49	17.61	2684	58.3	8566	31.3
1402.6	36.2	36.6	12.6	-4.556	179.615	184.171	0.06	17.87	17.82	2323	55.2	8109	28.6
1403.0	36.4	36.8	10.3	-2.326	184.148	186.474	0.23	18.19	17.95	1927	52.1	7649	25.2
1403.8	36.6	37.0	8.3	-0.355	188.060	188.416	0.39	18.47	18.08	1555	49.6	7296	21.3
1403.8	36.8	36.9	6.3	1.425	191.813	190.389	0.54	18.76	18.22	1186	46.5	6842	17.3
1405.3	36.9	37.0	4.1	3.315	196.626	193.311	0.71	19.17	18.46	789	44.3	6522	12.1
1405.3	36.9	37.2	1.9	5.114	203.631	198.517	0.87	19.81	18.94	376	41.7	6131	6.1
1406.0	37.3	37.6	0.0	7.696	215.031	207.334	1.12	20.90	19.78	-2	37.0	5449	0.0

Table A. 15: 4x3 Warman pump test at 1600, 1800 and 2000 rpm for CMC 9%

Pump speed rpm	Temperature suction pipe (T1) °c	Temperature discharge pipe (T2) °c	Pump discharge flow l/s	Suction Pressure Adj. (P1) kPa	Discharge Pressure Adj. (P2) kPa	Differential pressure kPa	Pump Suction head m	Pump Discharge head m	Pump head m	Pump power output rho.q.g.H W	Pump shaft torque N.m	Pump power in 2.Pi.n.T W	Pump efficiency %
1601.5	36.6	36.8	24.7	-18.640	202.865	221.505	-0.95	21.23	22.18	5696	81.9	13729	41.5
1602.3	36.9	37.0	22.6	-15.497	213.058	228.555	-0.72	21.96	22.68	5308	76.9	12901	41.1
1602.9	37.2	37.4	20.0	-12.524	222.543	235.067	-0.52	22.61	23.13	4805	72.9	12242	39.2
1603.1	37.5	37.8	17.5	-9.326	231.722	241.048	-0.29	23.26	23.55	4288	70.3	11798	36.3
1603.7	37.8	38.0	15.0	-6.370	239.089	245.460	-0.06	23.77	23.84	3716	68.9	11569	32.1
1603.8	38.1	38.3	12.6	-3.879	245.202	249.081	0.12	24.20	24.08	3158	65.9	11062	28.5
1605.2	38.4	38.5	9.9	-1.368	250.833	252.201	0.32	24.59	24.27	2503	60.6	10184	24.6
1606.0	38.6	38.9	7.5	0.844	256.123	255.279	0.50	25.00	24.50	1919	56.6	9526	20.1
1607.5	38.8	39.0	5.0	2.952	262.649	259.697	0.68	25.55	24.87	1300	52.8	8888	14.6
1607.9	38.9	39.0	2.7	4.685	269.710	265.026	0.83	26.19	25.36	712	48.9	8229	8.7
1608.8	39.7	39.9	0.0	7.755	284.928	277.173	1.12	27.64	26.51	-4	44.0	7418	0.0
1805.2	39.1	39.3	30.9	-25.883	249.898	275.780	-1.38	26.60	27.98	8981	101.5	19185	46.8
1806.8	39.3	39.5	28.1	-21.655	265.543	287.198	-1.10	27.70	28.80	8399	96.1	18192	46.2
1808.2	39.6	39.9	23.8	-16.077	285.429	301.507	-0.73	29.08	29.81	7375	89.1	16873	43.7
1808.2	39.7	39.9	23.9	-16.020	285.569	301.589	-0.73	29.09	29.82	7385	89.2	16894	43.7
1808.9	40.0	40.4	21.2	-12.383	297.169	309.552	-0.47	29.92	30.39	6689	84.9	16075	41.6
1809.7	40.4	40.7	18.1	-8.787	308.420	317.207	-0.22	30.70	30.92	5810	79.0	14962	38.8
1811.1	40.7	40.9	15.2	-5.667	317.110	322.777	0.01	31.30	31.29	4928	73.8	14005	35.2
1811.9	41.0	41.3	11.9	-2.407	324.127	326.534	0.25	31.76	31.51	3903	69.6	13200	29.6
1811.9	41.1	41.4	9.1	0.060	330.411	330.351	0.44	32.22	31.78	2995	67.0	12710	23.6
1813.4	41.3	41.6	6.1	2.470	339.485	337.014	0.64	32.98	32.34	2050	63.0	11972	17.1
1814.2	41.4	41.6	3.0	4.769	349.535	344.766	0.84	33.88	33.04	1038	57.7	10966	9.5
1816.4	44.4	44.6	0.0	7.984	368.080	360.096	1.14	35.65	34.50	-5	50.2	9542	0.0
2005.3	39.8	39.9	36.5	-33.284	300.275	333.558	-1.81	32.40	34.21	12930	125.9	26433	48.9
2007.4	40.4	40.5	33.0	-27.546	323.229	350.774	-1.44	34.02	35.46	12134	117.7	24735	49.1
2008.1	41.1	41.4	29.8	-22.532	342.242	364.773	-1.11	35.36	36.47	11252	111.7	23487	47.9
2009.1	41.6	41.8	25.9	-17.116	362.284	379.399	-0.76	36.76	37.52	10063	104.3	21939	45.9
2011.1	42.2	42.3	22.2	-12.637	378.584	391.221	-0.46	37.91	38.37	8848	97.5	20523	43.1
2012.7	42.5	42.8	18.2	-7.999	392.877	400.876	-0.14	38.89	39.03	7372	89.7	18910	39.0
2014.1	42.9	43.2	14.7	-4.401	402.595	406.996	0.12	39.54	39.42	6008	82.4	17384	34.6
2014.8	43.2	43.4	11.2	-1.187	410.919	412.106	0.36	40.12	39.77	4632	77.8	16412	28.2
2016.2	43.4	43.7	7.5	1.861	422.084	420.223	0.60	41.03	40.43	3124	74.6	15747	19.8
2017.1	43.6	43.8	3.6	4.629	435.255	430.627	0.83	42.19	41.36	1560	68.2	14404	10.8
2019.3	47.6	47.9	0.0	8.356	458.355	449.999	1.18	44.39	43.21	-6	58.2	12306	0.0

Table A. 16:

Material type	Kaolin 21%	
Date	12-Sep-09	
Pump	Warman 4/3	
Water Density	1000.0	Kg/m³
Material Density	1348.1	Kg/m³

Table A. 17: Warman 4/3 pump test at 1200 and 1400 rpm for kaolin 21%

Pump speed rpm	Temperature suction pipe (T1) °c	Temperature discharge pipe (T2) °c	Pump discharge flow l/s	Suction Pressure Adj. (P1) kPa	Discharge Pressure Adj. (P2) kPa	Differential pressure kPa	Pump Suction head m	Pump Discharge head m	Pump head m	Pump power output rho.q.g.H W	Pump shaft torque N.m	Pump power in 2.Pi.n.T W	Pump efficiency %
1206.1	36.0	36.2	28.3	-6.569	131.226	137.795	0.50	12.07	11.57	4334	55.4	7000	61.9
1207.5	36.2	36.4	25.3	-3.557	148.830	152.387	0.60	13.00	12.40	4149	51.7	6538	63.5
1208.2	36.4	36.6	22.1	-1.013	165.156	166.169	0.68	13.86	13.19	3851	48.1	6080	63.3
1208.8	36.6	36.9	18.7	1.814	180.737	178.922	0.78	14.70	13.92	3434	43.6	5518	62.2
1209.7	36.8	36.9	15.4	4.094	193.867	189.773	0.87	15.42	14.55	2969	38.7	4903	60.6
1211.2	36.9	37.0	12.0	6.233	205.581	199.348	0.96	16.08	15.12	2400	33.8	4287	56.0
1211.5	37.0	37.2	9.2	7.671	211.449	203.778	1.02	16.38	15.36	1861	29.3	3716	50.1
1212.1	37.1	37.2	6.2	9.107	216.504	207.398	1.09	16.65	15.55	1279	24.8	3154	40.6
1213.5	37.2	37.3	3.0	10.161	220.842	210.681	1.15	16.90	15.75	620	19.9	2534	24.5
1214.3	37.6	37.7	0.0	15.34593	233.11829	217.77237	1.53	17.81	16.27	-6	15.6	1979	-0.3
1401.5	29.3	29.4	33.1	-12.958	171.454	184.412	0.24	15.82	15.58	6814	78.6	11529	59.1
1401.8	29.6	29.7	30.2	-9.169	192.104	201.274	0.39	16.94	16.56	6616	74.4	10923	60.6
1402.2	29.9	29.9	27.0	-5.676	212.555	218.232	0.51	18.04	17.53	6268	69.5	10207	61.4
1402.9	30.1	30.2	24.2	-2.930	228.294	231.225	0.61	18.88	18.27	5850	65.1	9568	61.1
1403.7	30.3	30.6	21.1	-0.640	243.715	244.355	0.67	19.70	19.03	5311	60.5	8888	59.8
1405.1	30.6	30.7	18.2	1.692	257.325	255.633	0.76	20.45	19.69	4738	55.8	8218	57.7
1405.9	30.8	31.0	15.2	3.833	269.790	265.957	0.84	21.15	20.30	4084	50.4	7420	55.0
1407.4	31.0	31.3	12.4	5.644	278.989	273.346	0.92	21.65	20.73	3389	45.3	6671	50.8
1408.1	31.2	31.3	9.2	7.380	285.239	277.859	1.00	21.96	20.96	2554	39.3	5796	44.1
1408.9	31.3	31.6	6.3	8.771	290.612	281.841	1.07	22.25	21.18	1767	34.2	5040	35.1
1410.4	31.4	31.6	2.9	9.918	296.379	286.461	1.13	22.61	21.48	819	28.0	4136	19.8
1411.1	32.4	32.6	0.0	15.216	309.427	294.211	1.52	23.58	22.05	-7	23.3	3438	-0.2

Table A. 18: 4x3 Warman pump test at 1600, 1800 and 2000 rpm for kaolin 21%

Pump speed rpm	Temperature suction pipe (T1) °c	Temperature discharge pipe (T2) °c	Pump discharge flow l/s	Suction Pressure Adj. (P1) kPa	Discharge Pressure Adj. (P2) kPa	Differential pressure kPa	Pump Suction head m	Pump Discharge head m	Pump head m	Pump power output rho.q.g.H W	Pump shaft torque N.m	Pump power in 2.Pi.n.T W	Pump efficiency %
1602.1	32.4	32.6	38.0	-20.051	215.611	235.662	-0.02	20.03	20.05	10087	99.4	16682	60.5
1602.1	32.7	32.8	35.0	-15.412	242.803	258.216	0.16	21.53	21.38	9882	95.8	16072	61.5
1603.0	33.0	33.3	31.5	-10.931	269.591	280.523	0.32	23.00	22.68	9446	90.1	15129	62.4
1603.9	33.4	33.7	28.5	-7.302	289.654	296.956	0.45	24.08	23.62	8914	85.3	14327	62.2
1605.7	33.8	34.0	25.0	-3.867	310.705	314.572	0.57	25.20	24.64	8137	79.2	13319	61.1
1607.2	34.1	34.3	21.8	-1.407	328.293	329.700	0.64	26.17	25.53	7360	73.6	12382	59.4
1608.0	34.4	34.5	18.4	1.359	344.576	343.216	0.74	27.07	26.33	6423	67.0	11285	56.9
1609.3	34.6	34.9	15.2	3.749	358.429	354.680	0.84	27.85	27.02	5448	60.7	10234	53.2
1611.0	34.8	34.9	12.1	5.600	366.778	361.178	0.91	28.27	27.36	4383	53.7	9064	48.4
1611.8	35.0	35.3	9.2	7.155	373.833	366.678	0.98	28.66	27.68	3374	47.9	8084	41.7
1613.3	35.2	35.4	6.2	8.664	378.595	369.931	1.06	28.90	27.84	2268	40.8	6894	32.9
1614.7	35.4	35.7	3.0	9.648	386.669	377.021	1.11	29.44	28.33	1128	34.6	5853	19.3
1616.2	36.5	36.7	0.0	15.721	401.907	386.186	1.56	30.57	29.01	-10	29.0	4916	-0.2
1805.1	36.5	36.7	42.5	-27.277	260.697	287.975	-0.29	24.33	24.61	13841	124.0	23434	59.1
1806.9	37.0	37.2	39.0	-21.578	297.460	319.037	-0.08	26.40	26.48	13664	117.8	22292	61.3
1807.3	37.3	37.4	35.4	-16.073	333.743	349.816	0.13	28.49	28.36	13282	113.7	21521	61.7
1808.7	37.6	37.9	31.9	-11.527	364.102	375.629	0.29	30.21	29.92	12637	107.4	20341	62.1
1809.4	38.0	38.3	28.2	-7.664	390.085	397.748	0.41	31.63	31.21	11640	99.8	18916	61.5
1811.6	38.3	38.4	25.0	-4.636	410.486	415.122	0.51	32.75	32.24	10669	93.5	17728	60.2
1813.2	38.5	38.8	21.6	-1.443	431.033	432.476	0.63	33.92	33.29	9507	86.1	16348	58.2
1814.7	38.8	38.9	18.3	1.217	447.236	446.019	0.72	34.82	34.09	8233	78.5	14925	55.2
1816.9	39.1	39.2	14.7	3.685	461.399	457.714	0.82	35.60	34.78	6776	70.0	13324	50.9
1819.1	39.4	39.5	10.9	5.695	471.468	465.773	0.90	36.12	35.23	5078	61.3	11684	43.5
1820.0	39.5	39.7	7.7	7.524	478.297	470.773	0.99	36.49	35.50	3615	53.6	10207	35.4
1822.1	39.7	39.8	3.8	9.136	487.174	478.038	1.08	37.05	35.98	1832	44.5	8500	21.5
1823.6	41.5	41.6	0.0	16.173	507.302	491.129	1.60	38.54	36.94	-11	36.6	6992	-0.2
2003.4	35.3	35.5	46.5	-34.634	308.480	343.114	-0.57	28.81	29.37	18063	156.2	32761	55.1
2004.8	35.9	36.3	42.7	-27.499	359.878	387.377	-0.29	31.86	32.15	18142	148.0	31070	58.4
2005.8	36.3	36.6	38.3	-20.305	409.787	430.092	-0.03	34.76	34.78	17602	139.8	29356	60.0
2007.2	36.8	36.9	34.2	-14.434	452.159	466.593	0.19	37.24	37.05	16775	134.4	28247	59.4
2008.6	37.4	37.5	30.2	-9.789	484.790	494.578	0.34	39.08	38.73	15482	125.2	26334	58.8
2010.6	37.7	38.0	26.3	-5.919	512.996	518.915	0.46	40.67	40.20	13987	116.0	24417	57.3
2012.1	38.1	38.2	22.6	-2.439	535.718	538.158	0.59	41.95	41.36	12382	106.9	22520	55.0
2014.5	38.3	38.6	18.4	0.990	557.727	556.736	0.71	43.19	42.47	10358	96.1	20274	51.1
2016.8	38.7	38.9	14.4	3.965	573.007	569.042	0.83	44.02	43.18	8215	85.2	18003	45.6
2019.2	38.9	39.2	10.5	6.173	583.597	577.424	0.93	44.58	43.65	6043	74.7	15792	38.3
2022.0	39.2	39.3	6.0	8.126	594.403	586.277	1.02	45.22	44.20	3509	62.8	13289	26.4
2023.1	39.8	39.9	3.2	9.185	601.541	592.355	1.08	45.69	44.61	1868	55.3	11724	15.9
2024.3	42.3	42.6	0.0	15.643	620.008	604.365	1.56	47.06	45.51	9	47.7	10102	0.1

Table A. 19:

Material type	Kaolin 24%	
Date	19-Sep-09	
Pump	Warman 4/3	
Water Density	1000.0	Kg/m³
Material Density	1400.6	Kg/m³

Table A. 20: Warman 4/3 pump test at 1200 and 1400 rpm for kaolin 24%

Pump speed rpm	Temperature suction pipe (T1) °c	Temperature discharge pipe (T2) °c	Pump discharge flow l/s	Suction Pressure Adj. (P1) kPa	Discharge Pressure Adj. (P2) kPa	Differential pressure kPa	Pump Suction head m	Pump Discharge head m	Pump head m	Pump power output rho.q.g.H W	Pump shaft torque N.m	Pump power in 2.Pi.n.T W	Pump efficiency %
1200.9	33.0	33.1	25.8	-9.187	143.183	152.370	0.22	12.23	12.01	4255	56.7	7128	59.7
1201.5	33.4	33.4	22.8	-5.894	160.494	166.389	0.35	13.14	12.79	4008	53.4	6721	59.6
1202.3	33.6	33.8	20.4	-3.729	172.165	175.894	0.42	13.73	13.30	3722	50.4	6344	58.7
1202.9	33.8	34.0	17.7	-1.407	183.910	185.317	0.51	14.33	13.82	3353	46.8	5896	56.9
1203.0	34.1	34.2	15.2	0.498	194.863	194.366	0.59	14.93	14.34	2986	43.3	5458	54.7
1203.8	34.2	34.4	12.5	2.362	204.053	201.691	0.67	15.42	14.75	2537	39.8	5020	50.5
1205.2	34.4	34.5	10.3	3.609	209.808	206.199	0.72	15.71	14.99	2124	36.4	4590	46.3
1206.0	34.6	34.7	7.5	5.179	214.298	209.119	0.79	15.92	15.12	1559	31.6	3992	39.1
1207.3	34.7	34.8	5.0	6.388	218.170	211.782	0.86	16.12	15.26	1048	27.5	3482	30.1
1207.5	34.8	34.9	2.7	7.250716	222.11932	214.86861	0.91	16.37	15.46	580	24.0	3034	19.1
1208.2	34.9	35.3	0.0	14.926	238.319	223.393	1.46	17.53	16.07	-4	20.1	2547	-0.2
1399.9	35.2	35.4	32.0	-16.685	179.349	196.034	-0.05	15.74	15.79	6941	79.0	11581	59.9
1400.0	35.4	35.5	30.0	-14.190	193.390	207.580	0.04	16.47	16.43	6781	76.2	11171	60.7
1401.4	35.6	35.8	27.3	-10.797	212.506	223.303	0.17	17.47	17.31	6486	72.6	10649	60.9
1402.2	35.9	35.9	24.2	-7.546	230.596	238.143	0.28	18.40	18.12	6027	67.8	9949	60.6
1402.9	36.1	36.1	21.1	-4.502	247.391	251.893	0.39	19.28	18.89	5474	63.2	9287	58.9
1403.7	36.3	36.3	18.0	-1.838	262.174	264.012	0.49	20.05	19.56	4834	57.9	8509	56.8
1405.1	36.5	36.6	15.0	0.443	274.891	274.449	0.58	20.74	20.16	4159	53.3	7844	53.0
1405.9	36.8	36.8	12.2	2.348	284.542	282.194	0.66	21.25	20.59	3439	47.9	7048	48.8
1407.5	36.9	37.3	9.4	4.018	289.951	285.933	0.73	21.50	20.76	2673	42.2	6217	43.0
1408.7	37.0	37.2	6.2	5.557	295.612	290.055	0.81	21.79	20.98	1796	36.7	5420	33.1
1410.4	37.1	37.2	3.2	6.893	301.243	294.349	0.88	22.13	21.25	924	31.2	4607	20.1
1411.1	37.8	37.9	0.0	15.311	320.593	305.283	1.49	23.51	22.03	-6	26.3	3889	-0.2

Table A. 21: 4x3 Warman pump test at 1600, 1800 and 2000 rpm for kaolin 24%

Pump speed rpm	Temperature suction pipe (T1) °c	Temperature discharge pipe (T2) °c	Pump discharge flow l/s	Suction Pressure Adj. (P1) kPa	Discharge Pressure Adj. (P2) kPa	Differential pressure kPa	Pump Suction head m	Pump Discharge head m	Pump head m	Pump power output rho.q.g.H W	Pump shaft torque N.m	Pump power in 2.Pi.n.T W	Pump efficiency %
1603.6	36.7	36.9	37.9	-24.817	219.985	244.802	-0.32	19.72	20.03	10440	105.1	17643	59.2
1605.1	36.9	37.2	35.1	-20.879	244.285	265.164	-0.19	20.98	21.17	10210	100.7	16928	60.3
1605.8	37.1	37.2	31.4	-15.942	275.408	291.350	-0.02	22.65	22.67	9791	94.5	15896	61.6
1607.3	37.4	37.5	28.0	-11.892	299.527	311.419	0.12	23.90	23.78	9140	89.2	15021	60.8
1608.7	37.7	37.9	24.5	-8.097	321.119	329.216	0.25	25.03	24.78	8350	83.0	13988	59.7
1610.3	38.0	38.3	21.1	-4.678	341.050	345.728	0.38	26.09	25.72	7456	76.7	12935	57.6
1611.1	38.2	38.2	17.5	-1.693	358.870	360.563	0.49	27.05	26.56	6399	70.3	11868	53.9
1613.3	38.5	38.6	14.2	0.737	371.962	371.225	0.58	27.75	27.16	5309	63.5	10720	49.5
1614.7	38.7	38.9	10.6	3.052	380.485	377.433	0.68	28.15	27.47	4013	54.1	9154	43.8
1616.3	38.9	39.2	7.1	4.906	387.910	383.004	0.77	28.54	27.77	2716	46.7	7902	34.4
1617.8	39.0	39.4	3.6	6.623	395.539	388.915	0.87	29.00	28.13	1378	39.4	6668	20.7
1619.3	40.2	40.2	0.0	15.905	417.285	401.380	1.53	30.55	29.02	-8	32.7	5553	-0.1
1802.8	39.5	39.7	42.8	-32.256	262.062	294.318	-0.56	23.74	24.29	14273	132.0	24926	57.3
1803.6	39.8	39.9	39.4	-27.281	299.464	326.744	-0.41	25.78	26.19	14176	124.7	23545	60.2
1805.8	40.1	40.3	35.3	-21.344	339.268	360.613	-0.21	27.92	28.14	13637	116.3	21985	62.0
1807.3	40.5	40.6	31.4	-16.250	373.304	389.554	-0.04	29.76	29.81	12853	110.4	20887	61.5
1808.8	40.8	40.8	27.3	-10.869	405.657	416.527	0.16	31.53	31.37	11762	102.6	19440	60.5
1811.0	41.1	41.3	23.1	-6.420	433.298	439.718	0.32	33.02	32.70	10376	93.7	17766	58.4
1813.1	41.4	41.6	19.4	-3.052	453.802	456.854	0.44	34.13	33.69	8993	85.9	16302	55.2
1814.4	41.8	41.8	15.4	0.024	471.090	471.066	0.56	35.05	34.49	7314	77.6	14744	49.6
1817.0	42.1	42.2	11.6	2.560	481.470	478.910	0.67	35.56	34.89	5584	66.6	12670	44.1
1819.2	42.4	42.5	7.5	4.893	491.244	486.351	0.77	36.07	35.30	3634	56.2	10697	34.0
1820.7	42.6	42.6	3.7	6.624	501.138	494.514	0.87	36.69	35.82	1816	47.6	9082	20.0
1820.7	42.6	42.6	3.6	6.658	502.341	495.684	0.87	36.77	35.90	1777	46.8	8927	19.9
1822.5	44.4	44.4	0.0	16.934	524.564	507.630	1.61	38.36	36.75	-10	39.3	7495	-0.1
2002.7	42.0	42.2	46.9	-39.089	304.896	343.985	-0.76	27.77	28.53	18398	160.3	33612	54.7
2003.6	42.2	42.2	43.2	-33.016	357.732	390.748	-0.58	30.80	31.38	18634	151.3	31750	58.7
2005.8	42.5	42.5	39.3	-26.946	407.132	434.078	-0.39	33.59	33.98	18331	142.8	29988	61.1
2008.1	42.8	43.0	35.1	-20.999	450.548	471.546	-0.20	35.99	36.19	17449	133.6	28095	62.1
2008.8	43.3	43.5	31.6	-16.398	486.681	503.080	-0.05	38.04	38.09	16519	129.1	27151	60.8
2011.5	43.7	43.8	27.2	-11.316	521.458	532.774	0.12	39.94	39.82	14859	119.6	25188	59.0
2013.9	44.1	44.1	23.5	-7.387	546.938	554.325	0.26	41.34	41.07	13247	110.7	23344	56.7
2016.2	44.5	44.7	19.6	-3.864	569.757	573.621	0.39	42.59	42.20	11342	101.6	21453	52.9
2017.7	44.9	44.9	15.8	-0.224	584.945	585.169	0.55	43.37	42.82	9321	91.4	19310	48.3
2020.6	45.2	45.4	11.3	2.891	600.128	597.237	0.68	44.17	43.49	6729	78.0	16512	40.8
2023.3	45.5	45.6	7.8	4.809	607.742	602.934	0.77	44.56	43.79	4674	68.4	14494	32.3
2025.8	45.7	45.8	3.9	6.479	619.909	613.430	0.86	45.33	44.48	2361	57.6	12220	19.3
2028.1	48.3	48.4	0.0	17.914	645.521	627.606	1.68	47.16	45.48	-12	48.4	10270	-0.1

Table A. 22:

Material type	Kaolin 28%	
Date	30-Sep-09	
Pump	Warman 4/3	
Water Density	1000.0	Kg/m³
Material Density	1461.7	Kg/m³

Table A. 23: Warman 4/3 pump test at 1200 and 1400 rpm for kaolin 28%

Pump speed rpm	Temperature suction pipe (T1) °c	Temperature discharge pipe (T2) °c	Pump discharge flow l/s	Suction Pressure Adj. (P1) kPa	Discharge Pressure Adj. (P2) kPa	Differential pressure kPa	Pump Suction head m	Pump Discharge head m	Pump head m	Pump power output rho.q.g.H W	Pump shaft torque N.m	Pump power in 2.Pi.n.T W	Pump efficiency %
1200.2	53.4	53.5	18.3	-11.249	169.143	180.392	-0.15	12.80	12.95	3393	49.5	6217	54.6
1201.7	53.9	54.0	16.1	-9.519	178.600	188.119	-0.09	13.27	13.36	3079	45.9	5780	53.3
1201.7	54.3	54.3	14.5	-8.190	185.187	193.377	-0.03	13.61	13.64	2832	45.6	5744	49.3
1202.4	54.5	54.7	12.4	-6.933	192.165	199.098	0.01	13.96	13.95	2484	43.1	5428	45.8
1202.4	54.6	54.6	10.3	-5.759	197.654	203.414	0.06	14.23	14.17	2097	39.5	4975	42.2
1203.1	54.6	54.8	8.2	-4.433	201.125	205.558	0.12	14.37	14.25	1672	36.5	4598	36.4
1203.9	54.7	54.9	6.0	-3.306	203.769	207.075	0.17	14.48	14.31	1235	32.6	4110	30.0
1205.0	54.7	54.8	4.2	-2.358	206.858	209.216	0.22	14.65	14.43	879	29.7	3743	23.5
1205.4	54.7	54.7	2.1	-0.816	211.922	212.738	0.32	14.97	14.65	445	27.2	3427	13.0
1206.0	54.5	54.6	0.0	11.41109	237.37486	225.96376	1.17	16.74	15.57	-5	25.4	3212	-0.1
1402.4	51.3	51.5	24.6	-18.633	215.424	234.057	-0.46	16.69	17.14	6052	75.2	11047	54.8
1403.7	51.9	51.9	21.7	-15.358	232.330	247.688	-0.33	17.54	17.87	5572	70.4	10352	53.8
1405.3	52.4	52.5	18.3	-12.392	249.558	261.950	-0.23	18.40	18.63	4881	63.8	9389	52.0
1406.1	52.7	52.8	15.6	-9.354	266.190	275.543	-0.09	19.34	19.43	4344	59.0	8691	50.0
1406.1	52.8	52.9	15.6	-9.368	266.367	275.735	-0.09	19.35	19.44	4341	59.2	8720	49.8
1407.7	53.1	53.2	12.1	-6.853	278.960	285.813	0.01	19.99	19.98	3458	52.0	7665	45.1
1409.0	53.3	53.4	9.1	-5.046	284.603	289.648	0.09	20.23	20.15	2637	47.0	6939	38.0
1410.6	53.4	53.4	6.0	-3.453	289.257	292.710	0.16	20.44	20.28	1751	40.0	5913	29.6
1411.3	53.4	53.5	2.9	-1.634	296.773	298.407	0.27	20.90	20.63	860	35.1	5182	16.6
1412.1	53.2	53.3	0.0	15.999	326.105	310.106	1.49	22.92	21.43	-6	31.1	4597	-0.1

Table A. 24: 4x3 Warman pump test at 1600, 1800 and 2000 rpm for kaolin 28%

Pump speed rpm	Temperature suction pipe (T1) °c	Temperature discharge pipe (T2) °c	Pump discharge flow l/s	Suction Pressure Adj. (P1) kPa	Discharge Pressure Adj. (P2) kPa	Differential pressure kPa	Pump Suction head m	Pump Discharge head m	Pump head m	Pump power output rho.q.g.H W	Pump shaft torque N.m	Pump power in 2.Pi.n.T W	Pump efficiency %
1603.0	52.3	52.3	31.4	-27.216	258.697	285.913	-0.76	20.64	21.40	9630	101.1	16974	56.7
1603.8	52.8	53.0	28.7	-23.545	280.639	304.184	-0.63	21.77	22.40	9211	95.3	16010	57.5
1605.3	53.3	53.4	25.5	-19.583	306.168	325.752	-0.49	23.12	23.61	8630	89.6	15071	57.3
1607.5	53.6	53.6	22.0	-15.755	327.856	343.611	-0.35	24.23	24.58	7742	83.2	14009	55.3
1608.3	53.9	53.9	18.8	-13.125	345.203	358.329	-0.27	25.12	25.39	6826	77.9	13118	52.0
1609.0	54.3	54.4	16.2	-10.653	360.812	371.465	-0.16	25.99	26.15	6080	71.3	12012	50.6
1611.2	54.5	54.6	13.4	-9.342	371.906	381.248	-0.14	26.56	26.70	5141	65.0	10973	46.9
1612.0	54.8	55.0	10.5	-7.888	377.531	385.420	-0.09	26.78	26.87	4057	58.9	9938	40.8
1613.9	55.1	55.2	7.0	-4.310	384.206	388.516	0.11	27.10	26.98	2724	51.3	8675	31.4
1615.0	55.3	55.3	4.1	-2.654	391.286	393.939	0.20	27.51	27.31	1616	45.2	7647	21.1
1617.0	55.2	55.4	0.0	14.493	425.857	411.364	1.38	29.88	28.49	-7	37.5	6342	-0.1
1802.2	44.2	44.3	36.1	-36.439	310.330	346.769	-1.15	25.02	26.18	13562	129.8	24504	55.3
1802.9	44.8	45.0	32.8	-30.954	347.428	378.382	-0.95	27.05	28.00	13166	122.7	23164	56.8
1805.2	45.4	45.5	28.7	-24.955	385.280	410.235	-0.73	29.06	29.79	12248	113.7	21491	57.0
1807.4	46.2	46.4	24.6	-19.727	420.049	439.777	-0.53	30.96	31.49	11126	105.8	20018	55.6
1808.9	46.8	46.9	20.7	-15.439	445.782	461.221	-0.37	32.32	32.69	9712	97.7	18508	52.5
1811.1	47.4	47.5	16.7	-11.476	468.820	480.296	-0.21	33.56	33.77	8071	88.0	16687	48.4
1814.1	48.0	48.2	12.2	-7.959	483.358	491.316	-0.07	34.25	34.32	6009	75.9	14416	41.7
1816.2	48.3	48.5	8.6	-5.866	491.505	497.371	0.02	34.64	34.62	4258	67.4	12828	33.2
1817.9	48.5	48.7	4.3	-3.383	502.441	505.824	0.15	35.27	35.11	2179	56.8	10805	20.2
1820.1	49.6	49.8	0.0	15.322	539.606	524.285	1.44	37.81	36.37	-9	47.6	9065	-0.1
2002.8	48.3	48.3	39.9	-42.896	341.677	384.573	-1.39	27.90	29.29	16740	154.5	32409	51.7
2004.5	48.9	48.9	36.3	-36.955	408.227	445.181	-1.18	31.89	33.07	17229	145.4	30511	56.5
2007.3	49.5	49.7	31.7	-29.013	468.296	497.308	-0.87	35.30	36.17	16438	135.7	28532	57.6
2008.7	50.1	50.1	28.7	-24.970	499.135	524.105	-0.73	37.01	37.73	15518	128.6	27057	57.4
2010.7	50.7	50.7	24.3	-19.444	542.401	561.846	-0.52	39.45	39.98	13923	121.6	25597	54.4
2013.3	51.6	51.7	20.2	-15.362	570.232	585.594	-0.38	40.95	41.33	11975	112.3	23678	50.6
2014.7	52.2	52.3	16.7	-12.131	589.088	601.219	-0.26	41.95	42.20	10111	102.7	21663	46.7
2019.2	52.7	52.7	11.9	-8.072	606.394	614.466	-0.08	42.82	42.90	7325	86.8	18356	39.9
2020.8	53.1	53.2	8.1	-5.910	617.212	623.122	0.01	43.39	43.37	5065	76.9	16284	31.1
2023.7	53.5	53.6	4.1	-3.649	627.536	631.185	0.13	43.99	43.85	2591	64.4	13658	19.0
2026.5	56.8	57.0	0.0	15.509	666.416	650.907	1.46	46.66	45.20	-12	53.7	11389	-0.1

Table A. 25:

Material type	Kaolin 30%	
Date	7-Oct-09	
Pump	Warman 4/3	
Water Density	1000.0	Kg/m³
Material Density	1490.2	Kg/m³

Table A. 26: Warman 4/3 pump test at 1400 and 1600 rpm for kaolin 30%

Pump speed rpm	Temperature suction pipe (T1) °c	Temperature discharge pipe (T2) °c	Pump discharge flow l/s	Suction Pressure Adj. (P1) kPa	Discharge Pressure Adj. (P2) kPa	Differential pressure kPa	Pump Suction head m	Pump Discharge head m	Pump head m	Pump power output rho.q.g.H W	Pump shaft torque N.m	Pump power in 2.Pi.n.T W	Pump efficiency %
1402.3	44.9	44.6	19.8	-25.049	234.022	259.070	-1.04	17.15	18.18	5256	72.5	10641	49.4
1403.0	45.5	45.0	18.3	-20.327	242.117	262.444	-0.76	17.57	18.32	4910	69.3	10178	48.2
1403.7	46.3	46.1	16.4	-18.430	252.354	270.784	-0.68	18.10	18.78	4510	66.2	9737	46.3
1403.8	46.7	46.8	14.4	-16.856	260.180	277.036	-0.62	18.49	19.11	4028	64.2	9442	42.7
1405.2	47.0	47.1	12.2	-15.414	266.993	282.407	-0.56	18.81	19.37	3453	61.0	8974	38.5
1405.9	47.3	47.6	10.1	-14.140	271.206	285.345	-0.51	18.98	19.50	2892	56.7	8353	34.6
1407.4	47.6	47.6	8.1	-12.828	274.326	287.154	-0.45	19.11	19.56	2326	52.4	7727	30.1
1407.7	47.8	47.8	6.3	-11.485	277.554	289.039	-0.38	19.26	19.64	1797	48.6	7169	25.1
1408.4	47.9	47.9	4.1	-10.004	282.924	292.928	-0.30	19.58	19.87	1198	43.6	6435	18.6
1409.0	48.0	48.1	2.1	-8.149577	288.56964	296.71922	-0.18	19.93	20.11	623	40.3	5949	10.5
1410.5	47.9	47.7	0.0	9.638	324.267	314.629	1.03	22.36	21.33	-6	37.5	5534	-0.1
1605.9	43.8	43.3	27.4	3.381	6.011	322.627	-1.32	21.82	23.13	9271	98.7	16601	55.8
1607.4	44.6	44.2	25.0	3.084	5.482	336.353	-1.21	22.65	23.86	8722	93.9	15808	55.2
1608.1	45.3	45.7	22.5	2.774	4.931	347.948	-1.13	23.33	24.46	8040	88.8	14949	53.8
1609.0	45.8	45.8	20.1	2.475	4.399	359.293	-1.03	24.03	25.06	7350	83.3	14031	52.4
1610.4	46.4	46.4	17.5	2.159	3.838	369.375	-0.95	24.64	25.59	6548	79.8	13451	48.7
1611.1	46.7	46.4	15.0	1.854	3.297	377.565	-0.86	25.15	26.01	5717	75.9	12800	44.7
1612.3	47.1	47.2	12.5	1.536	2.731	383.324	-0.80	25.49	26.29	4787	70.9	11966	40.0
1614.1	47.6	47.6	10.0	1.229	2.185	386.208	-0.71	25.68	26.39	3845	64.3	10863	35.4
1614.8	47.9	48.0	7.6	0.936	1.665	389.539	-0.65	25.90	26.55	2946	59.5	10064	29.3
1616.3	48.3	48.2	5.0	0.617	1.097	394.003	-0.53	26.27	26.80	1960	55.7	9430	20.8
1617.2	48.5	48.6	2.4	0.301	0.535	399.558	-0.39	26.76	27.15	969	49.1	8315	11.7
1618.7	48.5	48.8	0.0	-0.002	-0.004	414.907	1.32	29.51	28.19	-8	43.4	7356	-0.1

Table A. 27: 4x3 Warman pump test at 1800 and 2000 rpm for kaolin 30%

Pump speed rpm	Temperature suction pipe (T1) °C	Temperature discharge pipe (T2) °C	Pump discharge flow l/s	Suction Pressure Adj. (P1) kPa	Discharge Pressure Adj. (P2) kPa	Differential pressure kPa	Pump Suction head m	Pump Discharge head m	Pump head m	Pump power output rho.q.g.H W	Pump shaft torque N.m	Pump power in 2.Pi.n.T W	Pump efficiency %
1802.0	45.1	45.1	34.2	-39.731	334.864	374.594	-1.44	25.95	27.38	13671	127.8	24121	56.7
1802.8	45.6	45.5	31.2	-35.929	363.131	399.060	-1.33	27.41	28.73	13102	121.7	22969	57.0
1805.0	46.2	46.5	28.1	-31.804	395.036	426.840	-1.19	29.14	30.33	12469	114.4	21623	57.7
1807.0	46.8	47.0	24.6	-27.702	420.784	448.486	-1.05	30.45	31.50	11333	105.9	20037	56.6
1808.0	47.5	47.7	21.1	-24.109	442.131	466.240	-0.93	31.52	32.45	10028	99.3	18802	53.3
1809.4	48.0	47.9	17.4	-20.832	461.083	481.916	-0.82	32.46	33.28	8457	92.6	17548	48.2
1811.8	48.6	48.7	14.0	-18.068	473.478	491.546	-0.71	33.05	33.76	6888	83.3	15812	43.6
1814.0	49.5	49.6	10.5	-15.727	481.330	497.056	-0.62	33.38	33.99	5229	74.3	14106	37.1
1815.0	49.8	49.9	6.9	-13.384	489.192	502.576	-0.50	33.76	34.27	3473	66.5	12633	27.5
1817.0	50.1	50.3	3.8	-11.131	498.258	509.389	-0.38	34.30	34.68	1932	57.8	11005	17.6
1819.2	50.1	50.2	0.0	7.292	532.840	525.548	0.87	36.63	35.76	-10	49.2	9378	-0.1
2002.7	42.1	42.3	37.4	-45.192	343.305	388.497	-1.63	27.09	28.72	15694	153.2	32125	48.9
2005.9	44.3	44.4	33.0	-38.712	454.924	493.636	-1.43	33.97	35.40	17081	146.2	30705	55.6
2008.0	46.0	46.1	28.9	-33.132	499.596	532.728	-1.25	36.40	37.64	15892	136.2	28637	55.5
2009.5	47.1	47.9	25.1	-28.701	538.932	567.632	-1.10	38.59	39.69	14544	127.9	26916	54.0
2011.0	47.9	47.8	21.2	-24.504	565.088	589.593	-0.95	39.93	40.89	12655	120.9	25463	49.7
2013.2	48.8	49.0	17.4	-20.933	586.170	607.102	-0.82	41.02	41.84	10612	110.4	23268	45.6
2016.2	49.5	49.6	13.2	-17.932	600.615	618.547	-0.72	41.69	42.41	8158	99.5	21008	38.8
2017.7	50.2	50.3	9.2	-15.289	610.959	626.248	-0.61	42.18	42.79	5735	88.9	18784	30.5
2020.7	50.7	50.7	4.9	-12.213	623.394	635.606	-0.44	42.88	43.32	3086	75.7	16018	19.3
2023.5	51.3	51.4	0.0	13.719	672.346	658.627	1.31	46.17	44.86	-14	62.6	13272	-0.1